

**Biopharmaceutical Studies of Slow Release, Subcutaneous Polymeric
Drug Delivery Systems**



Claire Deadman

A Thesis Submitted For the Degree of Doctor of Philosophy

2006

**Department of Pharmaceutics, University of London
School of Pharmacy, 29/39 Brunswick Square, London,
WC1N 1AX, United Kingdom.**



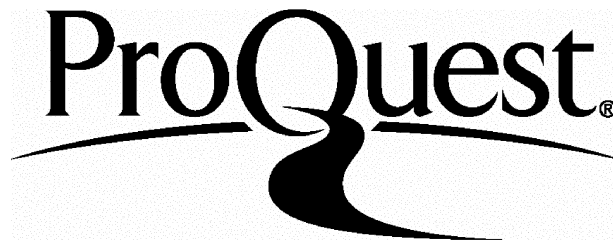
ProQuest Number: 10104241

All rights reserved

INFORMATION TO ALL USERS

The quality of this reproduction is dependent upon the quality of the copy submitted.

In the unlikely event that the author did not send a complete manuscript and there are missing pages, these will be noted. Also, if material had to be removed, a note will indicate the deletion.



ProQuest 10104241

Published by ProQuest LLC(2016). Copyright of the Dissertation is held by the Author.

All rights reserved.

This work is protected against unauthorized copying under Title 17, United States Code.
Microform Edition © ProQuest LLC.

ProQuest LLC
789 East Eisenhower Parkway
P.O. Box 1346
Ann Arbor, MI 48106-1346

Plagiarism Statement

This thesis describes research conducted in the School of Pharmacy, University of London between 2002 and 2006 under the supervision of Professor I.W. Kellaway and Dr. S. Murdan. I certify that the research described is original and that any parts of the work that have been conducted by collaboration are clearly indicated. I also certify that I have written the text herein and have clearly indicated by suitable citation any part of this dissertation that has already appeared in publication.

Signature

Date

Acknowledgements

I would like to sincerely thank my academic supervisors Professor Ian Kellaway and Dr Sudaxshina Murdan for their combined guidance and encouragement throughout the research project. Thanks also to my industrial supervisor Dr Paul Dickinson for his continued support over for the duration of the project and assistance with a number of practical issues. AstraZeneca and the University of London School of Pharmacy are gratefully acknowledged for their financial input.

A very big thank you to Mohammed Yasin at AstraZeneca who developed and validated the LCMSMS method, and helped with the interpretation of the results, and to the rest of the team who made me feel so welcome during my visit(s) to Macclesfield. I am very grateful to the technical staff at the School of Pharmacy, particularly Steve Coppard for his invaluable assistance with the animal work, Dave McCarthy for his 'award winning' microscopy expertise and Keith Barnes MBE for pretty much everything else. Thanks also to Olivia Daleur for her assistance with the stability study.

To my friends and fellow PhD students Matt, Rachel, and Talia, I truly couldn't have done it without you. Thanks to Mum, Dad and my brother Kev for being so supportive, and last but by no means least, Dan for putting up with me through the difficult times (i.e. 7 - 8am!) and for being practically perfect.

Abstract

Subcutaneously injected polymeric dosage forms have been used successfully to achieve sustained release of various drugs and peptides. A complex interplay of factors affect drug release rates from such dosage forms, such as nature of dosage form, drug and polymer properties, formulation variables etc. making the prediction of release characteristics challenging. In this thesis, the effect of drug lipophilicity on absorption rates from PLGA microspheres and *in situ*-forming depots was investigated.

The beta-blockers were chosen as model drug compounds, being a homologous group of drugs having similar molecular weights and pK_a values, yet widely differing lipophilicities. Alprenolol, metoprolol and atenolol were selected to represent the series based on their experimentally determined octanol-buffer partition coefficients.

The first part of the study focused on formulation and characterisation of beta-blocker loaded microspheres with suitable *in vitro* release profiles. Microspheres were prepared by spray drying, and characterised in terms of particle size, surface morphology, drug loading and release. The beta-blockers represented a considerable challenge owing to their surface-active nature and tendency to suffer a large burst release from microspheres. Efforts were therefore directed towards modifying the formulation to improve the drug release profiles, including emulsion spray drying, addition of competing surfactants and hydrophobic ion pairing. The latter was successful in reducing burst and prolonging release, and microspheres were deemed suitable for *in vivo* investigation. *In situ*-forming depot preparations were also formulated with the aim of comparing release profiles and tissue compatibility with the preformed microspheres.

Following initial experiments to ascertain intravenous clearance kinetics, the polymeric dosage forms were injected subcutaneously in rats. Drug plasma concentrations were analysed and absorption profiles were determined by deconvolution. It was found that the nature of the dosage form had a significantly greater impact on the rate and extent of absorption than the lipophilicity of the encapsulated drugs.

Abbreviations/Symbols

ANOVA	Analysis of variance	LLOQ	Lower limit of quantification
AUC	Area under the curve	Mp	Melting point
C_{max}	Maximum plasma concentration	MRM	Multiple reaction monitoring
CAD	Collision activated dissociation	Mw	Molecular weight
CK	Creatine kinase	m/z	Mass/charge ratio
CL	Clearance	NMP	<i>N</i> -methyl-2-pyrrolidone
CMC	Carboxymethylcellulose	NMR	Nuclear magnetic resonance
CV	Coefficient of Variation	<i>P</i>	Partition coefficient
DCM	Dichloromethane	P_{app}	Apparent partition coefficient
DMSO	Dimethyl sulfoxide	PBS	Phosphate buffered saline
DSC	Differential Scanning Calorimetry	PLG	Poly(glycolic acid)
EVA	Ethylene vinylacetate	PLA	Poly(lactic acid)
<i>F</i>	Fraction absorbed	PLGA	Poly(lactide-co-glycolide)
FDA	Food and Drug Administration	PVA	Polyvinyl alcohol
<i>fu</i>	Fraction unionised	QC	Quality control
GBM	Glioblastoma multiforme	RI	Refractive index
GC	Gas chromatography	RPM	Revolutions per minute
GM	Geometric mean	RSD	Relative standard deviation
H & E	Haematoxylin and Eosin	SAIB	Sucrose acetate isobutyrate
HIP	Hydrophobic Ion Pair	SC	Subcutaneous
HPLC	High performance liquid chromatography	SD	Standard deviation
IA	Intra adipose	SEM	Scanning electron microscopy
IM	Intra muscular	SPANOVA	Split plot (repeated measures) ANOVA
IP	Intra peritoneal	SR	Slow/sustained release
IS	Internal Standard	$t_{1/2}$	Half life
ISD	<i>In situ</i> -forming depot	<i>T</i>	Tailing factor
ISM	<i>In situ</i> -forming microspheres	T_g	Glass transition temperature
IV	Intra venous	T_{max}	Time to reach C_{max}
IV	Inherent viscosity	TEA	Triethylamine
IV/IVC	<i>In vitro</i> / <i>in vivo</i> correlation	TLC	Thin layer chromatography
K_{el}	Elimination rate constant	USP	United States Pharmacopoeia
LCMS	Liquid chromatography mass spectrometry	UV	Ultra-violet
LHRH	Luteinising hormone releasing hormone	<i>V</i>	Volume of distribution
		VMD	Volume median diameter

Contents

1	Introduction	17
1.1	Parenteral Drug Delivery.....	17
1.1.1	Intravenous Injection	19
1.1.2	Subcutaneous Injection.....	21
1.1.3	Intramuscular Injection.....	22
1.1.4	Bioavailability of Parenteral Injections	23
1.2	Factors Affecting Drug Absorption from Subcutaneous and Intramuscular Sites	24
1.2.1	Drug Related Factors	25
1.2.2	Formulation Factors.....	26
1.2.3	Physiological Factors.....	28
1.3	Sustained Release Injectable Products	30
1.3.1	Aqueous Suspensions	32
1.3.2	Non-Aqueous Solutions and Suspensions	33
1.3.3	Encapsulation-type Depot Preparations.....	34
1.3.3.1	Non-Biodegradable Polymers	35
1.3.3.2	Biodegradable Materials	39
1.3.3.2.1	Polyanhydrides.....	41
1.3.3.2.2	Polyesters	43
1.3.3.3	Implants.....	50
1.3.3.4	Microspheres	51
1.3.3.5	<i>In Situ</i> -Forming Drug Delivery Systems.....	55
1.4	Research Aims.....	59
2	Beta-Blockers: Suitability as Model Compounds.....	61
2.1	Introduction	61

2.1.1	Structure and Physicochemical Properties of the Beta-Blockers.....	61
2.1.2	Lipophilicity	64
2.1.3	Techniques for the Determination of Partition Coefficient (<i>P</i>)	64
2.1.4	Beta-Blocker Stability	67
2.1.5	Quantification of Beta-Blockers	68
2.2	Materials.....	69
2.3	Methods.....	69
2.3.1	Buffer Preparation	69
2.3.2	Shake Flask Determination of Partition Coefficient (<i>P</i>).....	70
2.3.3	UV Spectroscopy	71
2.3.4	Beta-Blocker Stability Study	72
2.3.5	HPLC	72
2.4	Results and Discussion.....	77
2.4.1	Shake Flask Determination of log <i>P_{app}</i> Values	77
2.4.2	Beta-Blocker Stability	79
2.4.2.1	UV Spectroscopy.....	79
2.4.2.2	HPLC.....	82
2.5	Conclusion.....	86
3	Microsphere Formulation and Characterisation	88
3.1	Introduction	88
3.1.1	Spray Drying as a Method for Microsphere Preparation.....	89
3.1.2	In Vitro Dissolution Testing – Background to Technique.....	94
3.2	Materials.....	95
3.3	Methods.....	97
3.3.1	Preparation of the Feed Solution for Spray Drying	97
3.3.2	Spray Drying.....	101
3.3.3	Surface and Internal Microsphere Morphology.....	101

3.3.4	Particle Size Analysis	102
3.3.5	Drug Loading.....	103
3.3.6	Extraction Efficiency	104
3.3.7	Release Studies	105
3.3.8	Residual Solvent.....	107
3.4	Results and Discussion.....	108
3.4.1	Extraction Efficiency	108
3.4.2	Characterisation of Solution Spray Dried Microspheres	111
3.4.3	Characterisation of Emulsion Spray Dried Microspheres.	118
3.4.4	Emulsion Spray Dried Microspheres with PVA.....	122
3.4.5	Solution Spray Dried Microspheres with Span 60.....	124
3.5	Conclusions	125
4	Hydrophobic Ion Pairing as a Strategy for Achieving Sustained Release of Beta-Blockers from Spray Dried Polymeric Microspheres.....	127
4.1	Introduction	127
4.2	Materials.....	129
4.3	Methods.....	129
4.3.1	HIP Formation and Characterisation	129
4.3.1.1	Transmittance	130
4.3.1.2	Residual drug.....	130
4.3.1.3	HIP Melting Point Determination by DSC.....	131
4.3.2	HIP Partition Coefficients.....	132
4.3.3	Microsphere Formulation and Characterisation	132
4.3.3.1	Injection Formulation.....	133
4.4	Results and Discussion.....	134
4.4.1	HIP Formation	134

4.4.2	HIP Melting Point Determination.....	136
4.4.3	Partition Coefficients.....	137
4.4.4	Microsphere Characterisation.....	138
4.4.5	Microsphere Injectability.....	142
4.5	Conclusion.....	143
5	<i>In Vivo</i> Investigations into the Absorption Profiles of Beta-Blockers from Subcutaneous Formulations	145
5.1	Introduction.....	145
5.1.1	Choice of Animal Model	146
5.2	Materials.....	150
5.3	Methods.....	151
5.3.1	Animal Housing.....	151
5.3.2	Intravenous (IV) Injection of Drug Solutions.....	151
5.3.3	Subcutaneous Injection of Aqueous Solutions of the Hydrophobic Ion Pairs.....	153
5.3.4	Subcutaneous Administration of Microsphere Formulations	154
5.3.5	Subcutaneous Administration of <i>In Situ</i> -Forming Depots.....	154
5.3.6	Blood Sampling	156
5.3.7	Analysis of Plasma Samples.....	157
5.3.7.1	Stock Solutions For Calibration	157
5.3.7.2	Quality control (QC) Stock Solutions	158
5.3.7.3	Preparation of Quality Control Rat Plasma Samples	159
5.3.7.4	Preparation of Plasma Calibration Standards.....	160
5.3.7.5	Assay Validation	161
5.3.7.6	Extraction Procedure	162
5.3.7.7	Chromatographic Conditions	163
5.3.7.8	Mass Spectrometric Conditions.....	164

5.3.8	Pharmacokinetic and Statistical Analysis.....	165
5.3.9	Histology	168
5.4	Results and Discussion.....	170
5.4.1	LC-MS/MS Method Validation.....	170
5.4.2	In Vivo Studies	176
5.4.2.1	Intravenous Administration of Alprenolol and Metoprolol.....	176
5.4.2.2	Subcutaneous Injection of Alprenolol and Metoprolol HIPs in Aqueous Solution	185
5.4.2.3	Microspheres	197
5.4.2.4	<i>In Situ</i> -Forming Depots.....	206
5.4.2.5	Statistical Comparisons of Drug Release from Microspheres and <i>In Situ</i> - Forming Depots.....	215
5.4.3	Histopathology.....	218
5.5	Conclusions	220
6	General Discussion and Future Directions	223
	Appendix	228
	References	230

List of Figures

Figure 1.1: Routes of parenteral drug administration.....	19
Figure 1.2: Absorption of drug substances across the capillary wall	21
Figure 1.3: Schematic representing the plasma concentration versus time profiles of a hypothetical drug following IV and SC/IM administration.....	24
Figure 1.4: Schematic of physical methods used to achieve SR in the SC and IM routes	32
Figure 1.5: Schematic representing (a) reservoir and (b) matrix-type drug delivery devices manufactured from non-biodegradable polymers.....	36
Figure 1.6: Release of a hypothetical drug from a non-biodegradable reservoir	37
Figure 1.7: Release of a hypothetical drug from a non-biodegradable matrix	38
Figure 1.8: Degradation and metabolism of poly[bis(carboxyphenoxy):sebacic acid] copolymer.....	42
Figure 1.9: Synthesis of PLGA via ring-opening condensation polymerisation.....	43
Figure 1.10: Biodegradation and metabolism of PLGA	44
Figure 1.11: Illustration of two mechanisms of polymer degradation	54
Figure 2.1: Structure and physicochemical properties of the 5 shortlisted beta-blockers	63
Figure 2.2: Double equilibrium of a partially ionised solute between two immiscible phases... ..	66
Figure 2.3: Schematic of HPLC set-up	73
Figure 2.4: Schematic representation of the parameters used to calculate HPLC tailing factor. ..	76
Figure 2.5: Correlation between literature and experimentally determined $\log P_{app}$ values.....	78
Figure 2.6: Chemical structures of metoprolol, atenolol and alprenolol	79
Figure 2.7: Stability study of atenolol, metoprolol and alprenolol solutions determined by UV spectroscopy.	80
Figure 2.8: Sample chromatograms from the HPLC analysis of atenolol and metoprolol.....	83
Figure 2.9: Stability study of atenolol, metoprolol and alprenolol solutions determined by HPLC.....	84
Figure 3.1: Schematic and photograph of Buchi Mini Spray Dryer 191	91
Figure 3.2: Liquid-liquid extraction of atenolol, metoprolol tartrate and alprenolol HCl from dichloromethane to deionised water, determined by UV spectroscopy	109
Figure 3.3: SEM images of solution spray dried microspheres (batches 1-4).....	111
Figure 3.4: Representative particle size distributions of solution spray dried microspheres	112

Figure 3.5: Internal morphology of solution spray dried microspheres (batch 2).....	113
Figure 3.6: <i>In vitro</i> drug release profiles from microsphere batches 1 - 3	115
Figure 3.7: NMR of microspheres for the quantitative determination of residual DCM	116
Figure 3.8: SEM of microspheres prepared from a high viscosity feed solution (batch 5).....	117
Figure 3.9: Optical microscopy photographs of the emulsion prepared with alprenolol (a) immediately after preparation, (b) 1 hour post preparation	118
Figure 3.10: SEM images of emulsion spray dried microspheres (batches 7, 8 and 9).....	119
Figure 3.11: <i>In vitro</i> release profiles of emulsion spray dried microspheres (batches 7-9)	121
Figure 3.12: SEM images of (a) blank and (b) atenolol loaded microspheres with PVA.	122
Figure 3.13: Drug release profile of emulsion spray dried microspheres with PVA	123
Figure 3.14: SEM images of microspheres prepared from solutions of drug and Span 60	124
Figure 4.1: a) Structure of sodium octanoate and b) schematic of HIP formation.....	128
Figure 4.2: Transmittance change of the solution during alprenolol HIP formation.....	134
Figure 4.3: The amount of residual alprenolol in the supernatant following HIP formation. ...	135
Figure 4.4: SEM images of alprenolol and metoprolol HIP loaded microspheres.....	138
Figure 4.5: <i>In vitro</i> dissolution profiles of HIP loaded microspheres compared with batches 2 and 3	141
Figure 5.1: Transverse sectional view of the rat tail.....	152
Figure 5.2 : Subcutaneous injection into the scruff of a rat.....	153
Figure 5.3: Schematic for the formulation of <i>in situ</i> -forming depots.....	155
Figure 5.4: Proposed fragmentation pathway of metoprolol and alprenolol.	171
Figure 5.5: A representative LCMSMS alprenolol chromatogram with internal standard.	172
Figure 5.6: A representative LCMSMS metoprolol chromatogram with internal standard.	173
Figure 5.7: Typical LCMSMS calibration plot for alprenolol (2 to 250 ng/mL)	174
Figure 5.8: Typical LCMSMS calibration plot for metoprolol (2 to 250 ng/mL).	175
Figure 5.9: Alprenolol plasma concentration-time curves following a 1 mg IV bolus dose.	180
Figure 5.10: Metoprolol plasma concentration-time curves following a 1 mg IV bolus dose. .	181
Figure 5.11: Non-compartmental modelling of alprenolol IV concentration-time curve.....	182
Figure 5.12: Non-compartmental modelling of metoprolol IV concentration-time curve.	183
Figure 5.13: Alprenolol plasma concentration-time curves following a 1 mg SC dose.....	188
Figure 5.14: Metoprolol plasma concentration-time curves following a 1 mg SC dose.	190
Figure 5.15 : Fraction absorbed vs time curves of aqueous HIP SC injections.....	195

Figure 5.16: Alprenolol plasma concentration vs time curves following SC dosing of microspheres.	200
Figure 5.17: Metoprolol plasma concentration-time curves following SC dosing of microspheres.	202
Figure 5.18: Absorption profiles of metoprolol and alprenolol from SC injected HIP loaded microspheres, generated using Wagner-Nelson deconvolution.	205
Figure 5.19: Alprenolol plasma concentration vs time curves following SC dosing of <i>in situ</i> -forming depots.	209
Figure 5.20: Metoprolol plasma concentration vs time curves following SC dosing of <i>in situ</i> -forming depots.	211
Figure 5.21: Absorption profiles generated using Wagner-Nelson deconvolution.	214
Figure 5.22: Digital photograph illustrating the superficial wound caused by scratching of the injection site	218
Figure 5.23: Digital photograph of the injection site with the skin removed revealing the polymeric mass of (a) microspheres and (b) <i>in situ</i> -forming depot.	219
Figure 5.24: Digital photographs of the excised mass of a) <i>in situ</i> -forming depot and b) microspheres at 10 days post administration.	219
Figure 5.25: Light microscope images of H&E stained sections of <i>in situ</i> -forming depots 10 days post administration.	220
Figure A.1: Plasma alprenolol concentration-time profile for rat A8, illustrating an unsuccessful IV injection.	228
Figure A.2: Representative DSC traces of a) alprenolol HCl, b) alprenolol HIP and c) freeze dried alprenolol HCl.	229

List of Tables

Table 1.1 : Properties of a range of standard grade Medisorb [®] polymers.....	46
Table 1.2: FDA approved biodegradable polymeric slow release dosage forms.	49
Table 2.1: Mobile phase composition for the HPLC analysis of the beta-blockers.	75
Table 2.2: log P_{app} values of the beta-blockers.....	77
Table 2.3: Comparison of drug concentrations measured by UV spectroscopy on day 0 and day 14 of the stability study.....	82
Table 2.4: Comparison of drug concentrations measured by HPLC on day 0 and day 14 of the stability study.....	85
Table 3.1: Process parameters affecting the characteristics of the spray dried product	93
Table 3.2: Physical properties of the Medisorb [®] polymer PLGA DL 2.5A.	96
Table 3.3: Summary of microsphere formulations prepared by spray drying.	100
Table 3.4: Preparation of samples for the determination of extraction efficiency	105
Table 3.5: Calculation of efficiency of extraction.....	110
Table 3.6: Properties of microspheres prepared by solution spray drying.	112
Table 3.7: Percentage drug release from solution spray dried microspheres (batches 1 - 3). ...	114
Table 3.8: Summary of physical characteristics of emulsion spray dried microspheres.....	119
Table 3.9: Percentage drug release from emulsion spray dried microspheres (batches 7-9).....	120
Table 4.1: Onset of HIP melting transitions determined by DSC.	137
Table 4.2: log P_{app} of alprenolol and metoprolol HIPs.....	138
Table 4.3: Cumulative % drug release from HIP loaded microspheres	140
Table 5.1: Inorganic components in the serum of laboratory animals.	148
Table 5.2: Preparation of quality control rat plasma samples.	159
Table 5.3 : Preparation of the plasma calibration standards	160
Table 5.4: Mobile phase gradient for the LC-MS/MS analysis of alprenolol and metoprolol .	163
Table 5.5: Mass spectrometer main working parameters.....	164
Table 5.6 : Alprenolol plasma concentrations following a 1 mg IV bolus dose.	178

Table 5.7: Metoprolol plasma concentrations following a 1 mg IV bolus dose.....	179
Table 5.8: Pharmacokinetic parameters from the non-compartmental analysis of concentration-time profiles following an IV bolus dose of alprenolol.....	184
Table 5.9: Pharmacokinetic parameters from the non-compartmental analysis of concentration-time profiles obtained following an IV bolus dose of metoprolol....	184
Table 5.10 : Alprenolol plasma concentrations following a 1 mg SC dose	187
Table 5.11: Metoprolol plasma concentrations following a 1 mg SC dose.....	189
Table 5.12 : AUC from 0- <i>t</i> following a 1 mg SC dose of alprenolol HIP.....	191
Table 5.13: AUC from 0- <i>t</i> following a 1 mg SC dose of metoprolol HIP.	192
Table 5.14: Wagner-Nelson deconvolution of alprenolol subcutaneous solution data.	193
Table 5.15 : Wagner-Nelson deconvolution of metoprolol subcutaneous solution data.	194
Table 5.16: Absorption rates from SC solutions of alprenolol and metoprolol HIPs.....	196
Table 5.17: Alprenolol plasma concentrations following SC dosing of microspheres.	199
Table 5.18: Metoprolol plasma concentrations following SC dosing of microspheres.....	201
Table 5.19: Wagner-Nelson deconvolution of alprenolol microsphere data.....	203
Table 5.20: Wagner-Nelson deconvolution of metoprolol microsphere data.....	204
Table 5.21: Absorption rate constants over three time intervals of alprenolol and metoprolol HIPs from subcutaneously injected microspheres.....	206
Table 5.22: Alprenolol plasma concentrations following SC dosing of <i>in situ</i> -forming depots.....	208
Table 5.23: Metoprolol plasma concentrations following SC dosing of <i>in situ</i> -forming depots.....	210
Table 5.24: Wagner-Nelson deconvolution of alprenolol <i>in situ</i> -forming depot data.....	212
Table 5.25: Wagner-Nelson deconvolution of metoprolol <i>in situ</i> -forming depot data.	213
Table 5.26: Absorption rate constants over three time intervals of alprenolol and metoprolol HIPs from subcutaneously injected <i>in situ</i> -forming depots.....	215
Table 5.27: Tukey HSD test of fraction absorbed.....	216
Table 5.28: Tukey HSD post hoc comparison of mean absorption rate from <i>in situ</i> -forming depots.....	217

Chapter 1

Introduction

1 Introduction

In this thesis, the effect of drug lipophilicity on absorption rates from slow release subcutaneously injected polymeric dosage forms is investigated. To put the work into context, the concept of parenteral drug delivery, use of the parenteral route for the administration of slow release dosage forms and methods of manufacturing the same are discussed in this introductory chapter.

1.1 Parenteral Drug Delivery

Use of the oral route for drug delivery is by far the most facile, convenient, and acceptable means of delivering medication to the systemic circulation, and is generally considered to be the route of choice for new formulations in development within the pharmaceutical industry. Unfortunately, many occasions arise where the oral route is unsuitable. A number of drugs exhibit poor oral bioavailability, such as those which are digested by gut enzymes (e.g. insulin) or undergo extensive first-pass metabolism (e.g. glyceryl trinitrate), thereby precluding their use as oral agents. In some cases, the gastrointestinal tract may be non-functional or inaccessible e.g. following gastric surgery or in comatose patients. Additionally, the lag time between peroral administration and systemic absorption is unacceptable in certain situations where a rapid onset of action is required. In such cases, drug delivery may be achieved parenterally.

The term 'parenteral' is derived from the Greek 'para' (meaning besides) and 'enteron' (meaning gut) (Avis and Morris 1984). Parenteral drug delivery, therefore, is the

delivery of drug substances by any means other than via the digestive tract, and so encompasses a wide variety of routes including pulmonary, transdermal, nasal, mucosal, intrathecal, intra-arterial, subcutaneous, intramuscular and intravenous delivery. Today the term is usually only applied to injectable formulations targeting the systemic circulation.

Christopher Wren was one of the first to practise parenteral drug administration. In 1656 he injected an extract of opium intravenously into dogs using a sharpened goose quill attached to a pigs bladder. Following the introduction of the hypodermic syringe in the early nineteenth century, parenteral injection has developed into a widely used method of delivering drug substances to the systemic circulation (Avis and Morris 1984). Today sterile injection paraphernalia is widely available. Needles are usually made from stainless steel or plastic, ranging from ¼ inch to 6 inches in length, depending on the required site and depth of injection. The size of the needle bore is termed the gauge (G), ranging from 11 - 32 G, with the largest gauge number referring to the smallest bore needle (Akers 2005).

The most commonly employed routes of parenteral administration are intramuscular (IM), subcutaneous (SC) and intravenous (IV) injections (see Fig. 1.1). It was initially believed that subcutaneous and intramuscular injections could be used only to provide local action at the site of injection, until 1858 when Benjamin Bell noted the absorption of subcutaneously injected drugs into the systemic circulation (Florence and Attwood 2005). Subcutaneous and intramuscular injections have since become widely used routes of systemic drug administration.

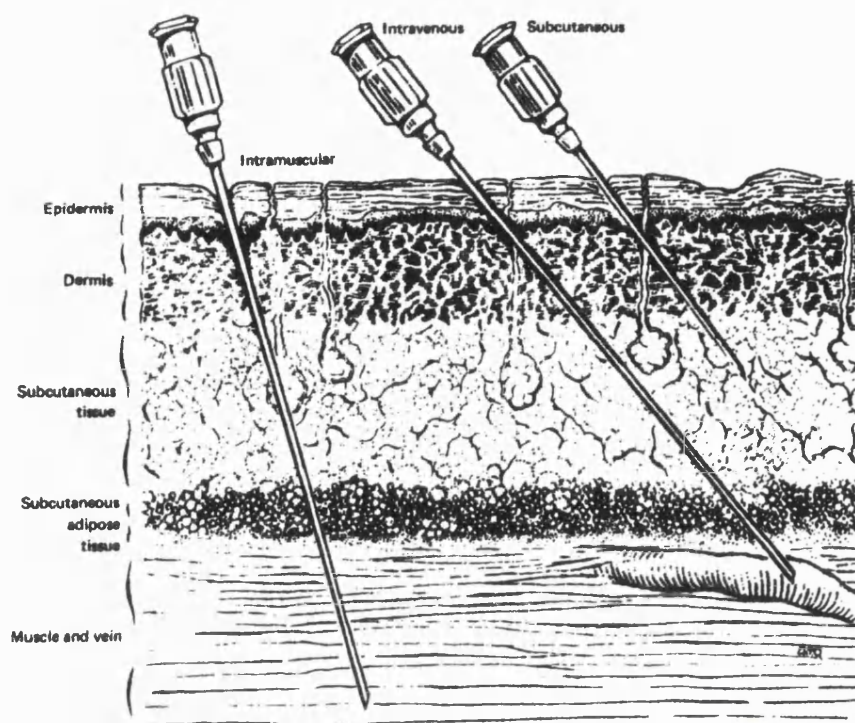


Figure 1.1: Routes of parenteral drug administration showing intramuscular, intravenous and subcutaneous injection (adapted from Florence and Attwood 2005).

The parenteral administration of drugs by its very nature bypasses many of the natural protective barriers of the body. All parenterally administered formulations must therefore meet strict requirements of sterility and apyrogenicity to reduce the risks of infection and other adverse events (Akers 1985; USP 2000).

1.1.1 Intravenous Injection

Intravenous administration involves injection of the formulation directly into the venous circulation (see Fig. 1.1), thereby avoiding first pass metabolism. Drug is delivered to the tissues with 100% bioavailability and an almost immediate pharmacological effect (see Section 1.1.4). This rapid onset of action allows the dose to be tailored to

therapeutic response (e.g. in patient controlled analgesia), and enables plasma drug concentration to be maintained at a therapeutic level (as discussed in Section 1.3).

Intravenous injections must be formulated as sterile, apyrogenic solutions*, which must be free from particulates ($> 5 \mu\text{m}$) to reduce the risk of infusion phlebitis, vasoocclusion and potentially fatal pulmonary embolism. This particle size cut-off is based on the fact that erythrocytes measure $4.5 \mu\text{m}$ in diameter (Akers 2005). Injection is usually through a 1 - 2 inch needle, 15 - 25 G depending on the nature and volume of injection.

Volumes $> 100 \text{ mL}$ may be administered via this route (termed large volume parenterals) (USP 1994) e.g. for parenteral nutrition or in fluid replacement therapy. These require slow infusion through an indwelling catheter, and must be isotonic and at physiological pH to avoid adverse reactions caused by hyper/hypotonicity or acid/alkalosis. Slightly larger variations in pH and tonicity can be tolerated if the injection volume is small (1 - 50 mL) and is administered slowly (over 1 - 5 min), since it will be diluted by the systemic circulation.

The obvious advantage of this route is the direct administration of a known concentration of drug into the systemic circulation. However, in terms of patient acceptability the use of needles and the need for a trained medical professional to administer the injection make this undesirable as a route for frequent drug administration. Additionally, repeated injection may cause vascular damage and there is a substantial risk of infection. From an industrial perspective, the sterile production

* suspensions are also permissible if particle size is significantly $< 5 \mu\text{m}$.

facilities required to manufacture parenteral formulations are expensive to build and maintain.

1.1.2 Subcutaneous Injection

The formulation is injected into the layer of tissue beneath the skin's surface (see Fig. 1.1) through which the drug solute diffuses to the capillaries, where it is absorbed into the systemic circulation (by partitioning across the endothelium or diffusing through pores in the capillary wall) (see Fig. 1.2). This region consists of loose connective tissue with a good supply of capillary and lymphatic vessels, making it an attractive site for drug administration. Absorption from this route can be rapid, but is not instantaneous as in intravenous injection (see Fig. 1.3), as processes such as partitioning and dissolution and can be rate limiting. The factors affecting the rate of absorption from this site are discussed in detail in Section 1.2.

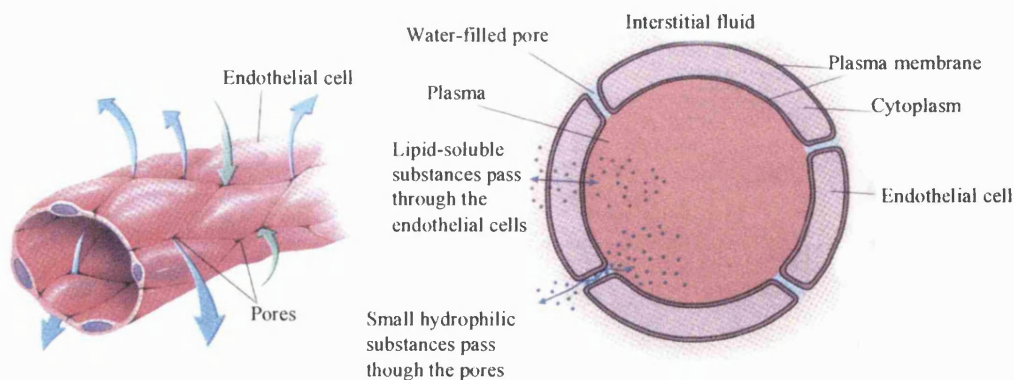


Figure 1.2: Absorption of hydrophilic and lipophilic substances across the capillary wall (adapted from Sherwood 1996).

In man, injection volume is limited to 0.5 – 2.0 mL, and common sites of injection include the arms, legs and abdomen (Kadir 1990). A range of pH and tonicity can be

tolerated, but due to the sensory nerve innervation in this area, the further these values deviate from physiological conditions, the more painful the injection tends to be. Like intravenous injections, formulations administered at this site must be sterile and apyrogenic, but particulates can be tolerated, and depending on their nature would be degraded or phagocytosed. Since large particles do not enter the systemic circulation from this site, there is no danger of embolism, but a foreign body response may be elicited (see Section 5.3.9). As a parenteral route, subcutaneous administration is simple and accessible, and more patient acceptable than other routes e.g. intravenous or intrathecal. In fact, patients often learn to self-administer injections via this route which is particularly useful when frequent injection is required (e.g. for multiple daily injections in insulin dependent diabetes mellitus). Subcutaneous injections are usually administered through a short needle ($\frac{1}{4}$ to $\frac{5}{8}$ inch) to avoid penetration into the deeper adipose fat layer. Usually 24 - 25 G needles are used although larger sizes can be used if the formulation so requires (e.g. for viscous solutions, suspensions or implants) (Akers 2005).

1.1.3 Intramuscular Injection

Intramuscular injections are injected directly into the skeletal muscle, beneath the subcutaneous adipose layer (see Fig. 1.1). This is achieved using a longer needle than for subcutaneous injection (1 - 2 inches), and tends to be in the range of 19 - 22 G depending on the formulation. Muscle tissue has a rich supply of capillaries, but few, if any, lymph vessels. Common sites for intramuscular injection in man are the deltoid (upper arm), vastus lateralis (lateral thigh) and gluteus maximus (buttocks). Blood flow to different muscle groups varies widely. The deltoid region has approximately 20%

greater resting blood flow than the gluteus maximus muscle, with vastus lateralis being intermediate (Kadir 1990). This can have profound effects on drug absorption from the intramuscular site, as discussed in Section 1.2.3. Volumes injected intramuscularly are generally in the region of 1 – 6 mL, although volumes of up to 10 mL may be injected into the larger gluteal muscle (Kadir 1990).

1.1.4 Bioavailability of Parenteral Injections

The bioavailability (F) of a drug administered via any route is its plasma level profile (AUC) compared to that following intravenous administration (Florence and Attwood 2005). For example, bioavailability of a subcutaneously administered compound would be calculated according to Equation 1.1.

$$F_{sc} = \frac{AUC_{sc}}{AUC_{iv}}$$

Equation 1.1: Calculation of the subcutaneous bioavailability (F_{sc}) of a compound where AUC_{sc} and AUC_{iv} are the area under the plasma concentration versus time profiles of the compound following subcutaneous and intravenous administration respectively.

Since intravenous injections are administered directly into the circulation, peak plasma concentration levels (C_{max}) are reached almost instantaneously, following which the drug is cleared from the circulation by metabolism and elimination. Following subcutaneous or intramuscular administration, an absorption phase precedes C_{max} , the duration of which is determined by the factors discussed in Section 1.2. Typical plasma drug concentration profiles following injections via these routes are represented graphically in Fig. 1.3.

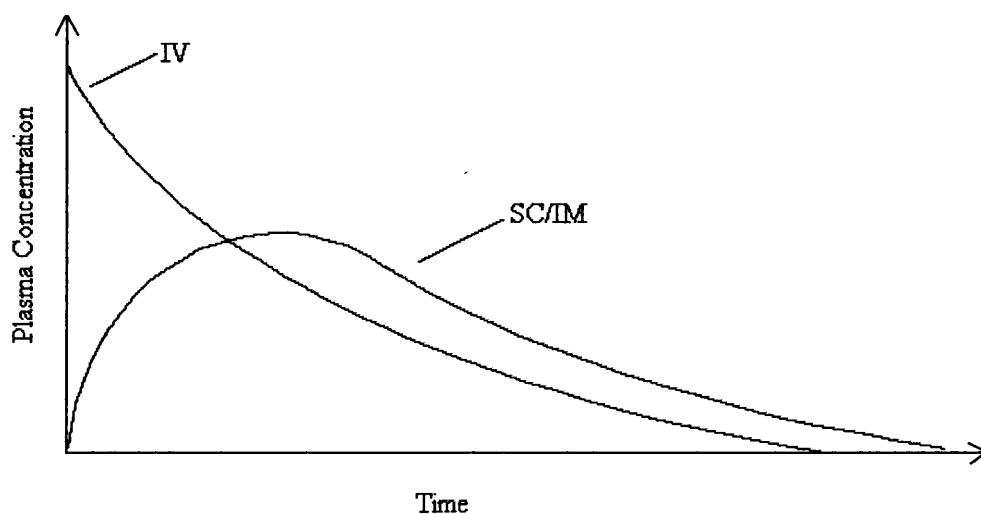


Figure 1.3: Schematic representing the plasma concentration versus time profiles of a hypothetical drug following intravenous (IV) and subcutaneous/intramuscular (SC/IM) administration.

1.2 Factors Affecting Drug Absorption from Subcutaneous and Intramuscular Sites

The rate and extent of drug absorption from both the intramuscular and subcutaneous sites are affected by a large number of inter-related factors. Knowledge of these properties can be utilised to predict, or manipulated to control drug absorption rates from such formulations.

Drug absorption from the intramuscular or subcutaneous site appears to be largely similar, resulting in similar plasma concentration profiles. A study into the effect of the route of administration of insulin in children highlighted differences between anatomical regions, but no differences between intramuscular and subcutaneous absorption rates at any given anatomical site were observed (Ballard 1968). The points discussed herein can therefore be applied to both sites, unless otherwise stated.

The factors affecting drug absorption rates from subcutaneous and intramuscular sites have been extensively investigated and reviewed (Zuidema et al. 1988; Zuidema et al. 1994; MacDiarmid 1983; Ballard 1968) although due to the complexity of the process some uncertainty remains. The factors affecting absorption can be grouped into three broad categories, based on the physicochemical properties of the drug, the nature of the formulation and the anatomical and physiological attributes of the injection site, each of which are described briefly below.

1.2.1 Drug Related Factors

Molecular weight has been shown to influence the clearance rate of some macromolecular compounds from intramuscular sites, with larger molecules undergoing slower diffusion through the connective tissue and pores in the capillary wall. However, for drugs which fall into the molecular weight range of 100 - 1000, absorption across capillary walls is independent of molecular size (MacDiarmid 1983).

The rate of dissolution of drug within the vehicle, partitioning from the vehicle and into the interstitium, the extent of tissue binding and the diffusion of drugs across biological membranes are all controlled by the **lipophilicity** of the drug substance (MacDiarmid 1983). Generally, the more lipophilic the drug, the more rapidly it will partition from the aqueous tissue fluids into and across the capillary wall. When a drug is injected in an oily vehicle, however, the partition coefficient of the drug between the vehicle and the aqueous tissue fluids governs release, and can result in significant retardation. This ploy has been successfully used to achieve sustained release from this site (see Section 1.3.2).

A compound with low **solubility** in the aqueous tissue fluids may precipitate out of solution following injection, resulting in the formation of a crystalline deposit at the drug site. Absorption will therefore be dissolution rate limited. Absorption rates of injected suspensions are also governed by the rate of dissolution of drug within the vehicle and tissue fluids.

1.2.2 Formulation Factors

General aspects relating to the injection formulation and vehicle are discussed here. More complex formulation issues such as encapsulation and depot formulations are discussed in detail in Section 1.3.3.

Findings are contradictory as to whether **injection volume** has a positive or negative effect on drug absorption rate. Larger injection volumes are reported to increase absorption rates by maintaining the drugs in solution for longer time periods, and reducing the likelihood of drug precipitation post administration as a crystalline deposit with a slower dissolution rate (Murdan and Florence 2000). In addition, the larger volume gives a larger absorption surface and variation in depot shape, although this is dependent on the extent of the spread of the vehicle. If the spread of the formulation is limited, the effect is opposite as the drug has an increased diffusional pathlength before reaching the absorption site.

Vehicle viscosity affects the spread of the formulation following injection, thereby influencing the available absorption surface and diffusion pathlength of drug solutes.

The extent to which the viscosity of a formulation can be increased is limited by the syringeability of the formulation.

Vehicle lipophilicity affects the rate of partitioning of drug solute from the vehicle to the aqueous interstitium. Lipophilic drug compounds will partition from a lipophilic vehicle to a lesser extent, hence absorption will be slowed.

Many studies have reported the effects of **injection depth** on the absorption rates of intramuscular and subcutaneous injections (reviewed by Zuidema et al. 1994). The differences are thought to result from the often inadvertent injection into the adipose layer (termed intra-adipose injection), following either too shallow an intramuscular injection, or a subcutaneous formulation injected too deeply. This can significantly retard drug absorption, particularly for lipophilic drugs or those in oily vehicles, which tend to be retained in the fatty tissue. This phenomenon may also explain the reported sex differences in drug absorption following intended intramuscular injections into the gluteus maximus. The rate and extent of absorption of dapsone from such an intramuscular injection was significantly lower in women than in men, attributed to the fact that on average, women tend to have a thicker gluteal fat layer (Kadir 1990). Injection technique and use of needles of appropriate lengths are therefore also important considerations.

The effect of **drug concentration** on absorption rate is dependent upon the nature of the drug itself. For water soluble, neutral, inert substances such as sucrose, absorption is independent of concentration (MacDiarmid 1983). However, absorption rates of drugs which have local pharmacological action are often concentration dependent. For

example, atropine reduces blood flow at the injection site, thereby reducing drug absorption rate. In this case, absorption rate is inversely proportional to drug concentration.

1.2.3 Physiological Factors

The greater the degree of **blood perfusion** to the injection site, the faster the rate of drug absorption into the systemic circulation. Different sites around the body are perfused to varying degrees. As mentioned earlier, the deltoid (upper arm) region has significantly greater resting blood flow than the gluteus maximus muscle (buttock), with vastus lateralis (lateral thigh) being intermediate (Kadir 1990). It follows therefore that peak plasma concentration (C_{max}) is achieved faster following subcutaneous or intramuscular injection into the deltoid region compared with the gluteal region. This effect was noted in a study investigating the effect of route of administration on insulin absorption in children (Ballard 1968). The mean absorption half life of insulin following intramuscular and subcutaneous arm injections was 224 and 232 min respectively, while intramuscular and subcutaneous injection into the thigh resulted in increased absorption half lives of 314 min and 310 min respectively. Reported differences due to anatomical site can be largely explained by the differences in blood perfusion, together with the increased likelihood of inadvertent administration of intra-adipose injection in areas where this layer is thickest (e.g. the gluteus maximus).

Rubbing the injection site serves to increase the blood flow to the region, thereby increasing absorption rate. It also aids the spread of the vehicle, providing a larger surface area for more rapid absorption.

Body movement has a profound effect especially if the drug is absorbed primarily via the lymphatic system. In a non-active animal, there is little or no lymph flow around the body, hence drug absorption is significantly decreased. This was demonstrated by the administration of snake venom (mw > 20,000) to rabbits (MacDiarmid 1983). Control animals died within 150 minutes, whereas animals whose hind limb was immobilised using a plaster cast survived for up to 8 hours. Increased body movement and exercise also serves to increase blood flow to the areas in use, providing a second mechanistic explanation for the observed increase in drug uptake.

Some factors that have a retarding effect on drug absorption include poor tissue condition and scarring, which reduce vascularity and therefore blood flow to the region. Certain disease states such as cardiac failure, peripheral vascular disease and myxodoema can also contribute to this effect.

1.3 Sustained Release Injectable Products

A major drawback of the aforementioned routes of parenteral drug administration is the use of needles. Injections are perceived as painful and inconvenient for the patient*, particularly if repeated drug administration is required, often making patient compliance problematic. Repeated injection may also cause tissue damage, altering tissue vascularity, which may in turn affect the absorption profile of the drug from these areas (Senior and Radomsky 2000). An added inconvenience and expense is the need for specially trained staff to administer such injections (although subcutaneous injections can be self-administered).

Needle-less injection systems have been developed to circumvent some of these issues e.g. Bioject[®], AdvantaJet[®], Medi-Jector[®]. Unfortunately these systems are generally more expensive, can still produce pain on injection, are potentially a greater source of contamination and may not be as efficient in dose delivery (Akers 2005).

An important rationale for developing sustained release injectables is therefore to maintain therapeutic plasma concentrations of the drug for as long as possible (days to months) thereby reducing dosing frequency. This serves to improve patient compliance and acceptability. High peak plasma levels and associated increased toxicity can also be avoided by administering drugs in a sustained release formulation, which is particularly advantageous for drugs with a narrow therapeutic range (Zuidema et al. 1994).

* The strength of this argument is of course dependent upon the severity (or perceived severity) of the condition being treated, patients being more tolerant of invasive and unpleasant anticancer therapy, for example, than of antihypertensives or contraceptives.

Prolonged drug action of parenteral products can be achieved simply by using continuous intravenous infusion, without the need for complex formulations. This however requires the use of an indwelling catheter, which increases the risk of infection and compromises the mobility of the patient. This route is normally reserved for use in hospitalised patients (Senior and Radomsky 2000). A clear need therefore exists for subcutaneous or intramuscular formulations, which can deliver the drug at the desired plasma concentration for a prolonged period of time.

Sustained release following intramuscular or subcutaneous injection may be achieved by various formulations including the use of aqueous and non-aqueous solutions and suspensions, liposomes and polymeric drug delivery devices, depending on the nature and solubility of the drug in question. Therapeutic areas where such sustained release technology has been successfully employed to date include antipsychotic agents (risperidone in Risperdal Consta[®]), insulin (Hypurin[®] Bovine Lente) and other hormone treatments (leuprolide in Lupron[®]), hormonal contraceptives (etonogestrel in Implanon[®]) and anticancer agents (goserelin in Zoladex[®]).

In order for absorption into the systemic circulation to occur, the drug must first be in solution in the interstitial fluid. The rationale behind all subcutaneous and intramuscular slow release technology is therefore to slow down the rate at which the drug solution is formed. Physical methods of achieving this and the rate limiting processes involved are illustrated in Figure 1.4 and described in detail in the following sections.

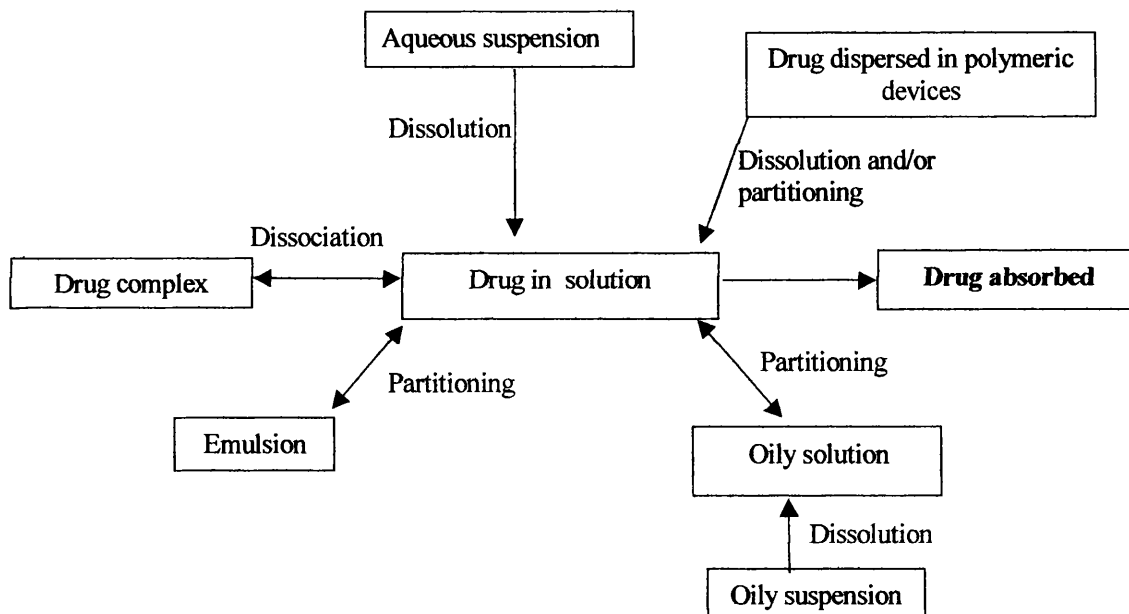


Figure 1.4: Schematic of physical methods used to achieve sustained release in the subcutaneous and intramuscular routes (Lee and Robinson 1978).

1.3.1 Aqueous Suspensions

Drugs with high aqueous solubility may be formulated as aqueous solutions, although following intramuscular or subcutaneous injection, aqueous vehicles are cleared rapidly and drug absorption is rarely prolonged. Intramuscularly or subcutaneously administered suspensions, however, have been used to achieve sustained release. Once injected, the dissolved drug diffuses into the interstitium, from where it is absorbed via the capillaries into the systemic circulation. The suspended drug particles continuously dissolve within the aqueous vehicle to replenish what is being lost, and a slow release profile can be achieved. The rate of dissolution is described by the Noyes-Whitney equation (Equation 1.2).

$$\frac{dm}{dt} = k \cdot A \cdot (C_s - C)$$

Equation 1.2: Noyes-Whitney equation where dm/dt is the dissolution rate of the drug, k is the dissolution rate constant, A is the particle surface area, C_s is the saturation solubility of the solvate in the diffusion layer and C is the solute concentration.

Where sink conditions apply, C can be approximated to zero and Equation 1.2 can be simplified to:

$$\frac{dm}{dt} = k \cdot A \cdot C_s$$

Equation 1.3: Simplified Noyes-Whitney equation.

From this equation, it can be seen that dissolution rate is proportional to drug surface area and the saturation solubility of the drug in the diffusion layer. Since only drug in solution can be absorbed, it follows that reducing dissolution rate will consequently reduce drug absorption rate. Sustained release can therefore be achieved by increasing particle size or reducing the solubility of the drug in the dissolution medium (injection vehicle), for example by altering drug salt or crystal form. Insulin zinc suspension USP is an example of a commercially available aqueous suspension, which employs crystallinity to achieve sustained release.

1.3.2 Non-Aqueous Solutions and Suspensions

Oily vehicles may be used to prolong release of certain drugs following intramuscular injection. Therapeutic areas in which they have been successfully employed include contraception, hormone replacement therapy and depot neuroleptics. Examples of oils approved for use in this field include sesame oil, olive oil, arachis oil, maize oil, almond oil, cottonseed oil and castor oil (Lee and Robinson 1978). Non-aqueous preparations

are not normally injected subcutaneously due to the pain and irritation caused at the injection site, and volumes injected intramuscularly are usually limited to 2 mL to reduce tissue damage (Murdan and Florence 2000).

Following intramuscular injection of a drug in an oily vehicle, a localised depot forms at the injection site. Dissolved drug then partitions from the oily vehicle to the aqueous interstitial fluid, from where it enters the circulation. As discussed in Sections 1.2.1 and 1.2.2, the more lipophilic the drug and the vehicle, the slower the rate of partitioning. The oily vehicle remains at the site of injection as a drug reservoir until it is cleared via absorption through the capillaries, lymph, phagocytosis or *in situ* metabolism (Murdan and Florence 2000). In practice, this approach is limited to drugs which are sufficiently oil-soluble and have the optimum partition coefficient (Lee and Robinson 1978). There is also the potential for the lipophilic drug to precipitate out of solution following injection and subsequent dissipation of the vehicle, significantly altering the absorption profile. A formulation in which the drug is suspended in the oily vehicle utilises both dissolution and partitioning as the rate limiting steps to retard absorption.

1.3.3 Encapsulation-type Depot Preparations

Sustained release of drugs may be achieved by incorporation of the drug into a polymeric matrix. The delivery system physically entraps the active, controlling the release rate by diffusion and/or matrix erosion, depending on the nature of the polymer used. The influence of biological variables on absorption rate is therefore greatly reduced, theoretically minimising *inter-* and *intra-*patient variability (Radomsky et al. 2000). Other advantages of this type of delivery system include improved drug stability

as the polymeric delivery system can provide protection from the *in vivo* environment (Senior and Radomsky 2000). A variety of therapeutic agents can be delivered in this manner, from small hydrophilic or hydrophobic molecules to peptides and proteins, and the extent and rate of drug release can be carefully controlled by manipulation of the polymer characteristics.

Materials used can be biodegradable or non-biodegradable, but all must be biocompatible. The delivery system may take on a multitude of forms, ranging from preformed systems such as microspheres (Okada et al. 1994), wafers (Dang et al. 1996) or implants (Negrin et al. 2001), or those formed *in situ* (Dunn 2003; Jain et al. 2000a). The relative merits of each formulation type are discussed in the following sections. Implantable pumps, driven by osmotic or mechanical pressure gradients, and bioresponsive devices are outside the remit of this work, and are therefore not discussed in this introductory chapter.

1.3.3.1 Non-Biodegradable Polymers

Non-biodegradable materials such as silicone elastomers or ethylene vinylacetate copolymers (EVA) have been used in the manufacture of sustained release dosage forms (Sah and Chien 2001). The encapsulating material remains unchanged for the duration of therapy, undergoing no degradation in the biological environment, whether hydrolytic or enzymatic. The devices may be described as ‘reservoir’-type, where the drug is surrounded by a rate controlling polymer membrane, or as a ‘matrix’, where the drug is distributed evenly throughout the polymeric material (see Fig. 1.5). Drug release

is diffusion rate limited in both cases, and is initiated by water penetration and subsequent solubilisation of the active (Sah and Chien 2001).

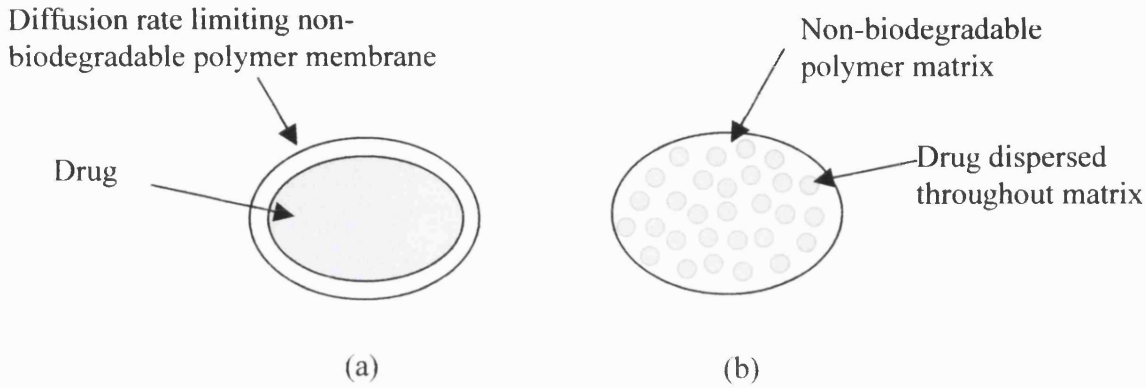


Figure 1.5: Schematic representing (a) reservoir and (b) matrix-type drug delivery devices manufactured from non-biodegradable polymers (adapted from Sah and Chien 2001).

Drug molecules from within the **reservoir** partition into the membrane, diffuse through it, then partition into the implant site. The rate of diffusion through the membrane can be described by Fick's law of diffusion (see Equation 1.4). This equation can be simplified to zero order release kinetics since sink conditions are applicable, whereby drug release rate is independent of time (see Fig. 1.6).

$$\frac{dm}{dt} = \frac{D \cdot k \cdot A \cdot \Delta C}{h}$$

Equation 1.4 : Fick's law of diffusion, where dm/dt is the diffusion rate, D is the diffusion coefficient of the drug in the membrane, k is the partition coefficient of the drug into the membrane, h is the membrane thickness, A is the available surface area, and ΔC is the concentration gradient across the membrane (i.e. $C_r - C_i$ where C_r and C_i denote drug concentrations in the reservoir and at the site of implantation respectively).

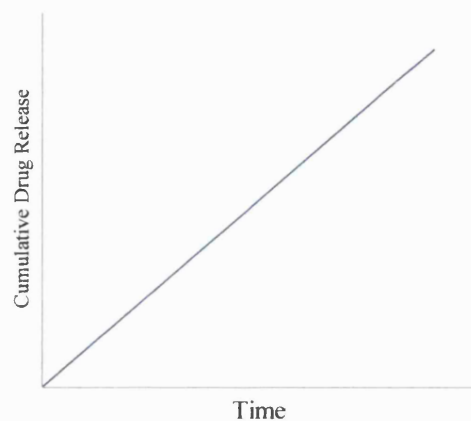


Figure 1.6: Release of a hypothetical drug from a non-biodegradable polymer reservoir (zero order release kinetics).

When the rate controlling membrane is porous, tortuosity (τ) and porosity (ϵ) must also be factored in to the equation. Again, zero order release can be achieved since the membrane surface area and the drug concentration in the reservoir compartment remain effectively unchanged (Sah and Chien 2001).

$$\frac{dm}{dt} = \frac{D_s \cdot A \cdot C_s \cdot \epsilon}{\tau \cdot h}$$

Equation 1.5: For porous membranes C_s and D_s are the drug solubility and the drug diffusion coefficient in the ingressing solvent respectively (Sah and Chien 2001).

Matrix systems are prepared by dissolving or suspending the drug in a polymeric solution, which can then be fashioned into a suitable geometry (e.g. rods, cylinders, films) using techniques such as solvent casting, compression/injection moulding and screw extrusion. Unlike the reservoir systems, where zero order release kinetics apply, drug diffusion from non-biodegradable polymer matrices decreases with respect to time. As time progresses, drug near the surface is released and the remaining drug must then travel further through the matrix in order to reach the exterior. The initial release rate (i.e. the first 50 - 60% of the total drug content) decreases proportionally to the square

root of time, and is described by Equation 1.6. Thereafter, release rate usually declines exponentially with time (Sah and Chien 2001). A graphical representation of drug release from non-biodegradable polymer matrices is shown in Figure 1.7.

$$\frac{dm}{dt} = \frac{k_d}{\sqrt{t}}$$

Equation 1.6: Initial drug diffusion rate (dm/dt) from non-biodegradable polymer matrices where k_d is a proportionality constant dependent upon the properties of the implant and t is time.

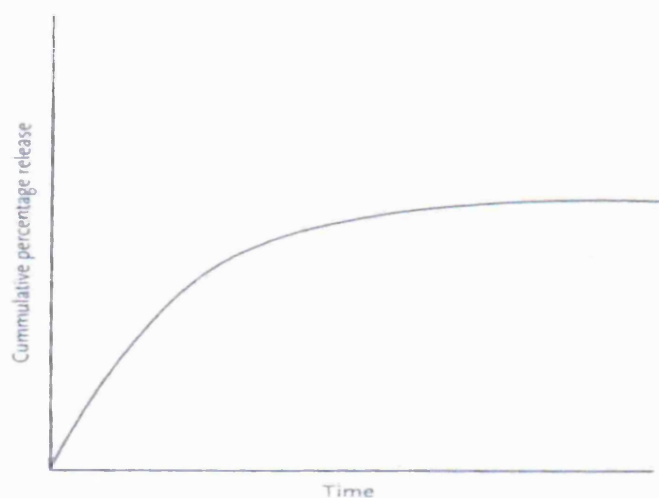


Figure 1.7: Release of a hypothetical drug from a non-biodegradable polymer matrix (Sah and Chien 2001).

This decreasing release rate with time can be partially offset by utilising a reservoir/matrix hybrid system. Organon's Implanon[®] is a commercially available device which employs this technology. It is comprised of a single polymeric rod which is subdermally inserted into the lower surface of the upper arm, and delivers etonogestrel at a rate of $> 30 \mu\text{g/day}$ for 3 years as a hormonal contraceptive. The drug is dispersed in an ethylene vinylacetate (EVA) copolymer matrix, which is extruded into a rod and then coated with an EVA copolymer layer, serving as a rate controlling membrane, thereby combining the matrix and reservoir technology.

The main disadvantage of these non-biodegradable systems is the fact that they must be surgically removed at the end of their therapeutic life. Irritation at the site of implantation has been reported, and water soluble or highly ionised drugs and macromolecules have negligible diffusivity through dense hydrophobic matrices so the number of therapeutic agents which can be incorporated within these devices is limited (Sah and Chien 2001). A more patient acceptable and widely applicable alternative is the use of biodegradable materials, as described in the following section.

1.3.3.2 Biodegradable Materials

Biodegradable polymers are natural or synthetic in origin and are degraded *in vivo*, to produce biocompatible, non-toxic by-products which are eliminated by the normal metabolic pathways (Jain 2000). Some macromolecular, naturally occurring **biopolymers** have been considered for the sustained release of polypeptides and other drugs. These have included various proteins (e.g. albumin, casein, collagen, gelatin) and polysaccharides (cellulose derivatives, chitin derivatives, dextran, hyaluronic acids, inulin and starch). However, their use is said to be limited by their high cost, the difficulty in achieving batch-to-batch reproducibility, their questionable purity and the fact that these materials can be immunogenic when cross-linked (Whateley 1993).

The most promising and commercially viable technology in this category is the Saber™ platform (sucrose acetate isobutyrate extended release) (Tipton 2003). It is based on Sucrose Acetate Isobutyrate (SAIB), a fully esterified sucrose derivative at a nominal ratio of six isobutyrate to two acetates. It exists as a highly viscous, hydrophobic liquid, and as such has been successfully used to achieve sustained drug delivery of a

range of compounds over a period of a few hours to several weeks. The active moiety is dispersed within a solution of SAIB and suitable solvent, such as ethanol or benzyl benzoate, which is then injected intramuscularly or subcutaneously. The solvent then dissipates leaving a viscous depot of SAIB and drug at the injection site from which the drug is released gradually by diffusion from the depot, followed by complete biodegradation of the device. This system works on the same principle as the *in situ*-forming depot systems fabricated from the synthetic polyester copolymer poly(lactide-co-glycolide) described in Section 1.3.3.5. Compared with the non-biodegradable implants described in the previous section, the Saber™ technology has several advantages. The solution can be injected through a narrow bore needle, it is much easier to formulate and a high drug loading can be achieved. Some claimed advantages over PLGA depots include lower solvent content, easier injectability, lower cost and higher hydrophobicity (therefore better protection of certain drugs). This system has been investigated for use with a number of drug compounds, but no products are as yet commercially available (Tipton 2003).

Two classes of **synthetic** biodegradable polymers are currently used in U.S. Food and Drug Administration (FDA) approved products; the aliphatic polyesters (e.g. poly(lactic acid) (PLA), poly(glycolic acid) (PLG) and the copolymer poly(lactide-co-glycolide) (PLGA)), and the polyanhydrides. The characteristics of each class, and examples of drug delivery devices that they are used to fabricate, are discussed in the following sections. The reader is referred to the following references for more detailed reviews of the use of synthetic polymers in controlled release parenteral products (Okada and Toguchi 1995; Radomsky et al. 2000).

1.3.3.2.1 Polyanhydrides

Biodegradable polyanhydrides such as the poly(carboxyphenoxy propane:sebacic acid) copolymer have been approved for use in drug delivery devices. This polymer undergoes ester hydrolysis to yield biscarboxyphenoxy propane and sebacic acid, which are subsequently excreted from the body as illustrated in Figure 1.8. The rate of degradation can be controlled by adjusting the polymer molecular weight and monomer ratio. Increasing the sebacic acid content increases the absorption rate of drugs incorporated in the device, which has been reported to vary from 1 day to 3 years (Sah and Chien 2001).

The Gliadel[®] system consists of the anticancer agent carmustine in a polyanhydride copolymer matrix (poly(carboxyphenoxypropane:sebacicacid) in a 20:80 ratio). The polymer and drug are dissolved in dichloromethane, which is spray dried to form microspheres, which are then compressed into a disk-shaped wafer, 14 mm in diameter and 1 mm thick. Up to 8 wafers are implanted into the brain following tumour resection for the treatment of recurrent glioblastoma multiforme (GBM). The polymer protects the carmustine from degradation and enables the local drug concentration in the brain to be log orders higher than when delivered systemically, with minimal systemic toxicity (Brem and Gabikian 2001).

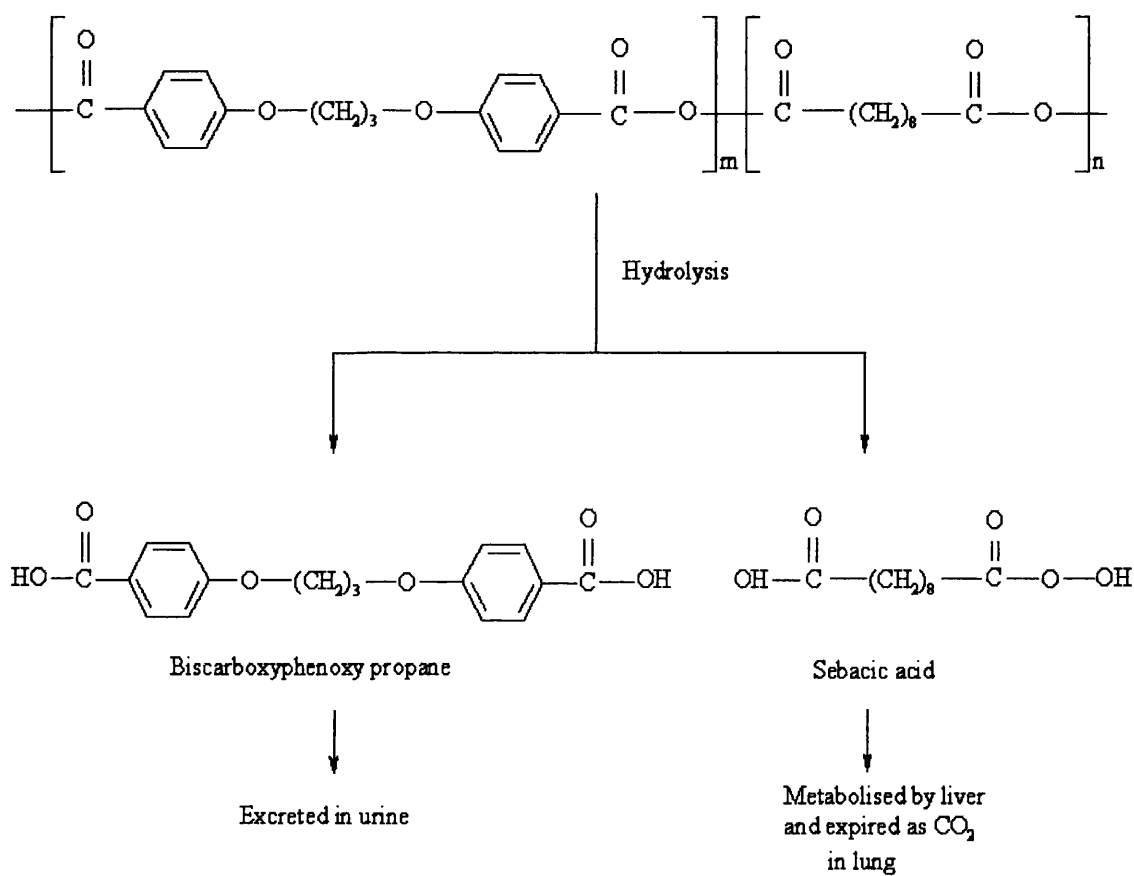


Figure 1.8: Degradation and metabolism of poly[bis(carboxyphenoxy):sebacic acid] copolymer (Sah and Chien 2001).

1.3.3.2.2 Polyesters

The lactide/glycolide homopolymers (PLA and PLG) or the co-polymer (PLGA) have been used for decades (> 30 years) in medical products (e.g. sutures, pins, rods, staples and surgical meshes) and are the most common type of synthetic bioerodible polymer used within the pharmaceutical industry (Okada and Toguchi 1995).

PLGA copolymers are typically synthesised by a ring-opening condensation reaction of their cyclic dimers (Radomsky et al. 2000) (see Fig. 1.9).

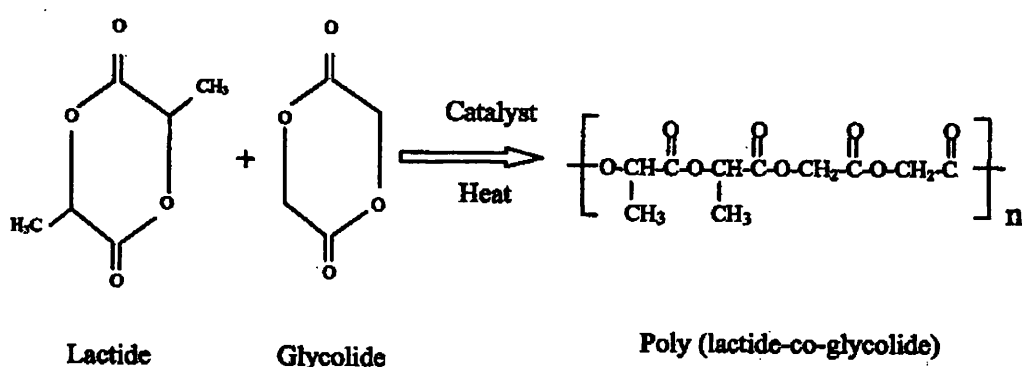


Figure 1.9: Synthesis of poly(lactide-co-glycolide) (PLGA) via a ring-opening condensation polymerisation reaction.

Degradation of PLGA occurs via hydrolysis of the ester linkages, leading to gradual erosion of the device as the polymer backbone degrades. The final products are lactic acid and glycolic acid which are water soluble, non-toxic products of normal metabolism that are either excreted or further metabolised to carbon dioxide and water (Anderson and Shive 1997) as illustrated in Fig. 1.10.

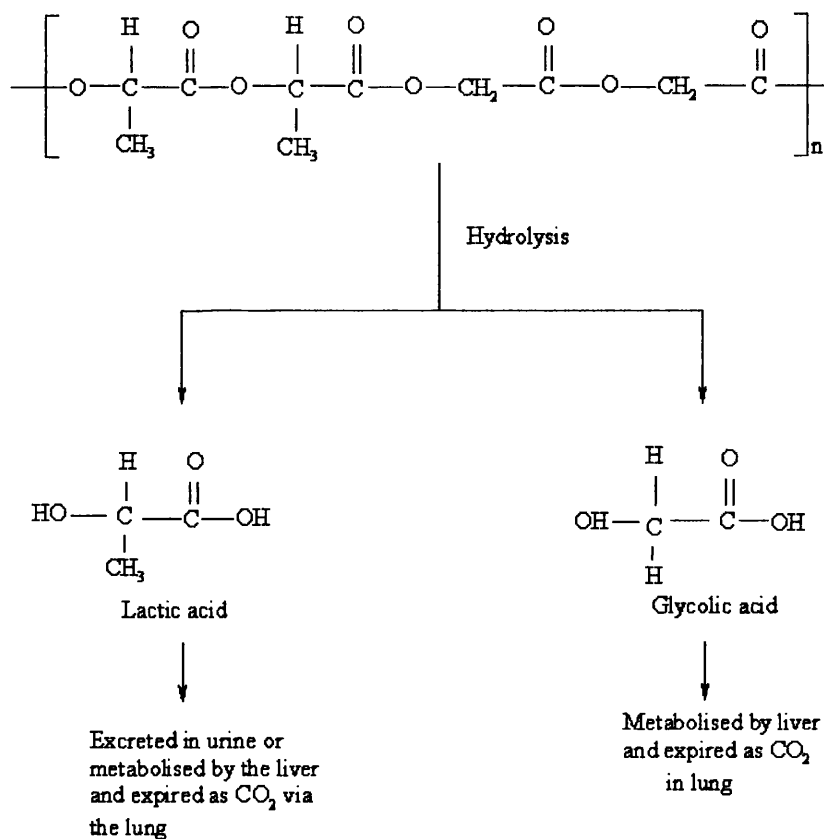


Figure 1.10: Biodegradation and metabolism of poly(lactide-co-glycolide) (PLGA) (Sah and Chien 2001).

The rate of polymer degradation can be controlled by manipulation of the ratio and stereochemistry of the monomer units, the polymer molecular weight and the molecular weight distribution of the polymer chains. The factors affecting the degradation rate of PLGA have been reviewed by numerous research groups (Anderson and Shive 1997; Hasirci et al. 2001; Miller-Chou and Koenig 2003), and are summarised briefly below.

PLA is more hydrophobic than PGA due to the methyl group on its β carbon (see Fig. 1.9). Increasing the **lactide:glycolide ratio** therefore decreases the rate of water uptake, thereby reducing degradation rate (Anderson and Shive 1997). In terms of **stereochemistry**, PLA can exist in the stereoregular L-PLA form or as the racemic DL-PLA. Polymer chains synthesised from the latter are more amorphous in nature due

to the irregularities in its polymer chain structure. DL-PLA therefore tends to degrade more rapidly than the semicrystalline L-PLA (Jain 2000). Increasing polymer **molecular weight** tends to reduce degradation rate since more hydrolytic chain scissions are required to break the polymer into soluble oligomers (Tracy et al. 1999). Conversely, increased **polydispersity** results in faster hydrolysis due to the increased availability of carboxylic acid chain ends which autocatalyse the hydrolytic degradation. Uncapped polymers (i.e. those with free carboxylic end groups) degrade more rapidly than those synthesised with methyl ester capped polymer chains for the same reason (Tracy et al. 1999).

Polymers of varying compositions can be purchased commercially (e.g. Resomer[®] from Boehringer-Ingelheim, Purasorb[®] from PURAC, Lactel[®] from Absorbable Polymers International and Medisorb[®] from Alkermes Inc.). The latter was the company from which the polymeric material was sourced for the work described in this thesis. Biodegradation kinetics of Medisorb[®] polymers vary from weeks to over one year depending on lactide:glycolide ratio, porosity, molecular weight, inherent viscosity, polymer end groups, and crystallinity, as previously discussed. For Medisorb[®] polymers the standard end group is lauryl ester (capped). Polymers denoted 'A' contain a free carboxyl end group (uncapped) and 'M' polymers contain a methyl ester end group (capped). Table 1.1 is a list of the standard grade Medisorb[®] polymers available, and illustrates the effect of polymer ratio and inherent viscosity* on degradation rate. The estimated degradation time of PLGA 50:50 DL 2.5A** for example is 2 - 4 weeks.

* Inherent viscosity is directly related to polymer molecular weight.

** Nomenclature refers to a PLGA copolymer with a 50:50 lactide:glycolide ratio, DL-poly(lactic acid), inherent viscosity *ca* 2.5 dL/g, uncapped (A).

Table 1.1 : Properties of a range of standard grade Medisorb[®] polymers, illustrating the effect of lactide:glycolide ratio and inherent viscosity on degradation rate and glass transition temperature (T_g) (adapted from Alkermes 2001).

Polymer	Inherent viscosity (dL/g)	Lactide:glycolide mole ratio	Approximate glass transition temperature (T_g) (°C)	Degradation time
100 DL	0.66 - 0.80	100:0	50 - 55	12 - 16 months
85:15 DL	0.66 - 0.8	85:15	50 - 55	5 - 6 months
75:25 DL	0.66 - 0.8	75:25	48 - 53	4 - 5 months
65:35 DL	0.66 - 0.8	65:35	45 - 50	3 - 4 months
50:50 DL	0.66 - 0.8	50:50	43 - 48	1 - 2 months
50:50 DL 1A	0.08 - 0.12	50:50	25	1 - 2 weeks
50:50 DL 2A	0.13 - 0.20	50:50	40	2 - 3 weeks
50:50 DL 2.5A	0.21 - 0.31	50:50	44	2 - 4 weeks
50:50 DL 3A	0.25 - 0.43	50:50	45 - 46	3 - 4 weeks
50:50 DL 4A	0.38 - 0.48	50:50	47	3 - 4 weeks

The degradation times listed above are purely approximations, since a multitude of factors affect the polymer degradation time once incorporated within a drug delivery device. The nature of the entrapped drug is one such factor. A study by Giunchedi et al. (1998) revealed that diazepam increased the polymer degradation rate significantly, with the percentage of glycolic acid monomers released from the matrix in 20 days increasing from 8% (blank microspheres) to 35% (diazepam-loaded microspheres). The group reported that basic drugs may either catalyse the hydrolysis of ester linkages and thus increase the degradation rate, or conversely may neutralise carboxyl end groups having the opposite effect. The method of device manufacture is also known to affect

the degradation kinetics, for example spray dried microspheres were shown to have a higher monomer release rate than those produced by solvent evaporation (Giunchedi et al. 1998).

Potential disadvantages of using biodegradable polymers in drug delivery devices include the requirement for an aseptic manufacturing process, since terminal sterilisation is often not feasible due to degradation of the polymer and/or the incorporated drug (e.g. proteins) (Athanasίου et al. 1996). Due to the hydrophobic nature of the polymers used, potentially toxic organic solvents (such as dichloromethane, ethyl acetate or *N*-methyl-2-pyrrolidone) are often utilised during the manufacturing process. Levels of residual solvent in the final product must therefore be carefully controlled. Polymeric drug delivery devices must be supplied as solid dosage forms due to the susceptibility of the polymers to hydrolysis of the ester linkages, and may therefore require reconstitution prior to administration. Readily available diluents such as water for injections, saline and dextrose are rarely suitable for reconstitution of the lyophilised powder as they often lead to aggregation. Suitable diluents must therefore be supplied by the manufacturer.

From a purely commercial perspective, substantial 'R and D' investment is required in terms of time, effort and cost if a new biomaterial is proposed. Safety and biocompatibility must be thoroughly evaluated to secure approval of the regulatory authorities, leading to a delay in development and marketing which has considerable financial implications (Sah and Chien 2001). The industry has recognised the need for guidance on the qualification of new biopolymers to overcome this issue which may

significantly limit the types of sustained release products that could be developed (Burgess et al. 2002).

Despite the aforementioned challenges, biodegradable polymers have shown great potential for application in the field of slow release parenterals. Devices can be formulated as implants, microspheres or as *in situ*-forming depots and the relative merits of each are described in the following sections. Table 1.2 details a range of FDA approved biodegradable polymeric slow release dosage forms, classified according to formulation type.

Table 1.2: Some FDA approved biodegradable polymeric slow release dosage forms.

Trade name	Active ingredient	Distributor	Drug release, months	Indications	Material
Microspheres					
Lupron Depot®	leuprolide	TAP	1, 3, 4	Prostate cancer, endometriosis	PLGA
Nutropin Depot®	somatropin	Genetech	0.5, 1	Growth hormone deficiency	PLGA
Trelstar™ Depot	triptorelin	Pfizer	1	Prostate cancer	PLGA
Sandostatin LAR®	octreotide	Novartis	1	Acromegally, neuroendocrine tumour	PLGA
Risperdal Consta®	risperidone	Janssen-Cilag	0.5	Schizophrenia, psychoses	PLGA
Implants					
Gliadel®	carmustine	Link		Glioblastoma multiforme	Poly(carboxyphenoxypropane :sebacic acid)
Zoladex®	goserelin	AstraZeneca	1, 3	Endometriosis, prostate cancer breast cancer	PLGA
<i>In Situ</i>-forming depots					
Atridox®	doxycycline	Collagenex	7 days	Chronic peridontitis	PLA
Eligard®	leuprolide	Sanofi-Aventis	1	Advanced prostate cancer	PLGA

1.3.3.3 Implants

Implants are single unit drug delivery systems formulated to deliver drug at a desired rate over a prolonged period of time. They are implanted subcutaneously into the loose interstitial tissues of the outer surface of the upper arm, anterior surface of the thigh or the lower portion of the abdomen. This can be achieved with either a large bore needle (16 G) which requires the use of a local anaesthetic, or by surgical implantation, depending on the size and shape of the device. Implants can be formulated in various geometries, including rods, cylinders, rings and films, depending on the desired release characteristics, and are manufactured by melt extrusion, injection moulding or compression moulding (Sah and Chien 2001).

Implants are convenient and have a low risk of infection compared with indwelling catheters, minimal medical surveillance is required post administration, and patient compliance is greatly improved due to the low patient involvement required. Also, this type of implant can be easily removed to stop drug exposure if required. Disadvantages include invasive insertion, scarring, reported discomfort, and adverse reactions caused by local high drug concentrations. They are generally limited to potent drugs as the implant is small, and the fact that they contain a fixed dose of drug in a fixed volume renders implants unsuitable for drugs requiring dosing based on weight or body surface area e.g. for children. A longer duration of drug release (> 3 months) is therefore desirable to improve patient acceptability of this formulation type. Unfortunately, it seems that the use of implants will always be limited due to the invasive nature of this therapy (Sah and Chien 2001).

Zoladex[®] from AstraZeneca consists of PLGA rods loaded with gosereline acetate (a synthetic luteinising hormone releasing hormone (LHRH) analogue) which inhibits pituitary gonadotrophin secretion. The rod is implanted via subcutaneous injection into the anterior abdominal wall through a 16 G hypodermic needle for the treatment of prostate cancer, breast cancer and endometriosis (BNF 2006). The absorption profile from this device is typically characterised by an initial burst followed by a lag period of 4 days representing the time taken for polymer degradation to be initiated by solvent ingress and resultant ester hydrolysis. Pores or microchannels then develop throughout the polymer matrix and a phase of sustained drug release over a 1 or 3 month period follows (RxList 2004).

1.3.3.4 Microspheres

Microspheres are monolithic spherical structures in the 1 - 500 μm size range with a therapeutic agent distributed throughout the polymeric matrix (Whateley 1993). Microspheres are suspended in a suitable vehicle and injected through a narrow bore needle into the subcutaneous or intramuscular tissue, from where sustained release can be achieved. The two most commonly used methods of microsphere preparation are solvent evaporation and spray drying, which are described briefly below.

Solvent evaporation is the most widely used technique for the preparation of PLGA microspheres (Pavanetto et al. 1992). The polymer is dissolved in a suitable water immiscible solvent, into which the active drug is dispersed or dissolved. The resultant solution or dispersion is then emulsified in an aqueous continuous phase containing a suitable emulsifier. The organic solvent diffuses into the aqueous phase and subsequent

evaporation of the solvent leads to the formation of hardened, drug loaded microspheres in the aqueous phase. These are harvested by filtration and then dried thoroughly. This simple process is most successful when the active is insoluble, or poorly soluble, in the aqueous medium. Hydrophilic drugs have a tendency to partition from the organic phase into the aqueous phase, resulting in microspheres with little or no drug loading, i.e. a very poor encapsulation efficiency. Process parameters can be adjusted to alter microsphere properties. Increasing the stirrer speed results in high shear, resulting in a product with a much smaller particle size. The effect of surfactant concentration, disperse phase to continuous phase ratio, and solvent choice have been reviewed. More complex multiple emulsion techniques have been developed to protect proteins from the polymer solution preventing denaturisation (O'Donnell and McGinity 1997).

Spray drying represents a rapid, convenient and easy to scale up alternative method to solvent evaporation for microsphere preparation. The process is described in detail in Section 3.1.1. Briefly, a solution of polymer and drug is sprayed through a nozzle, into the drying chamber, where it comes into contact with the drying medium (air in most cases). Here, the solvent rapidly evaporates due to the large surface area of the droplets, leaving solid microparticles suspended in the drying medium (Masters 1991). The spray drying process is suitable for use with many drugs, even those which are heat labile, due to the mild processing conditions involved in the technique (Jain 2000). Much of the solvent evaporation takes place when the surface is saturated and cool, therefore the product is unlikely to be damaged by heat (Masters 1991).

The techniques for fabricating microspheres were compared by Pavanetto et al. (1992). The authors deemed spray drying to be the most favourable technique based on the narrow particle size distribution, improved morphology, highest encapsulation efficiency and shortest preparation time. The process parameters can also be readily adjusted to alter the characteristics of the product. Spray drying was therefore used for microsphere fabrication throughout this study.

The rate of drug release from microsphere systems is a complex interplay of a multitude of factors. In addition to the factors already discussed pertaining to the nature of the polymer and the drug, additional considerations include the manufacturing method and associated process parameters, percentage drug loading, microsphere size and residual solvent. These formulation related factors are discussed in Chapter 3. Drug release profiles from biodegradable microspheres typically follow a triphasic pattern. There is often an initial phase of rapid drug release associated with the release of surface drug. This phenomenon is known as the burst effect, and is often observed when high drug loading is attempted (Benoit et al. 1984), or when the incorporated drugs are surface active. Following the initial burst of drug release, a slower release phase is observed, resulting from the gradual degradation of the polymer, or diffusion of the drug through the polymer matrix, or indeed a combination of the two processes (Anderson and Shive 1997). A third phase is sometimes seen as a period of rapid drug release, termed the secondary burst, and is attributed to the collapse of the polymer matrix (Sturesson et al. 1993; Nakano et al. 1984). This triphasic behaviour results in a sigmoidal release profile.

For microspheres of less than 300 μm in diameter, degradation is thought to be homogenous, whereby the rate of degradation at the core is equal to the rate at the surface (Anderson and Shive 1997). Larger microparticles, however, are thought to undergo heterogenous degradation (see Fig. 1.11).

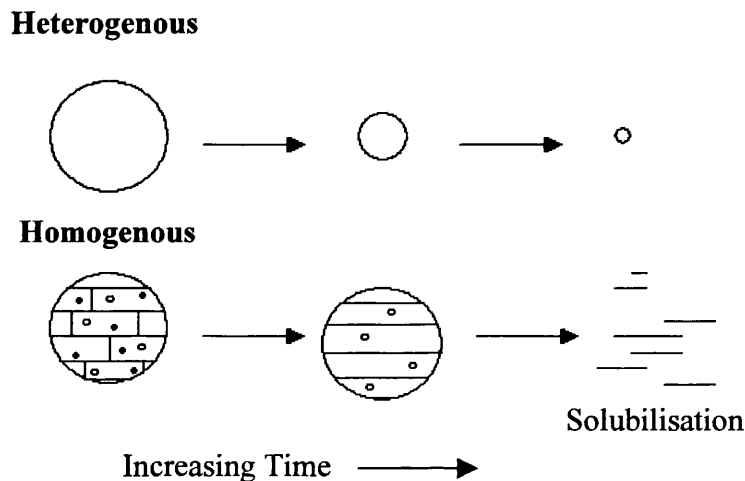


Figure 1.11: Illustration of two mechanisms of polymer degradation (adapted from Hausberger and DeLuca 1995).

Leuprolide is one of the drug substances that is currently available as a sustained release microsphere-based injectable product (Lupron Depot[®]). Leuprolide acetate is a synthetic nonapeptide analogue of leuteinising hormone-releasing hormone (LHRH). Lupron Depot[®] is commercially available as sterile lyophilised microspheres which, when mixed with the supplied diluent, becomes a suspension intended as a monthly intramuscular injection for the palliative treatment of advanced prostatic cancer (BNF 2006). The drug is incorporated within PLGA and PLA microspheres, which prolong the release of drug for one, three and six months, depending on the polymer used (Okada 1997).

Unlike implants, microspheres do not require surgical implantation but, due to their small size, can be simply suspended in a suitable vehicle and injected into the desired site. The less invasive nature of this procedure gives microsphere formulations a significant advantage over implantable devices in terms of patient acceptability and cost. Modification of the polymer characteristics and other processing variables enables drug release to be carefully controlled over a period of months to years. Furthermore, microspheres manufactured from PLGA demonstrate good biocompatibility and complete biodegradability, negating the need for the removal of empty remnants. However, microspheres have several inherent disadvantages including the need for reconstitution prior to injection, and the greater difficulty associated with removal of the device after administration if exposure to the drug needs to be terminated. Additionally, the manufacturing procedures required to produce a sterile, stable and reproducible microsphere product are relatively complicated compared with other similar drug delivery devices (Lambert and Peck 1995). Nonetheless, microsphere products have shown considerable potential in the field of sustained release parenterals.

1.3.3.5 *In Situ*-Forming Drug Delivery Systems

In situ-forming drug delivery systems represent an attractive alternative to microspheres and implants as parenteral depot systems (Packhaeuser et al. 2004). The technology is based on the principle of polymer precipitation. Quite simply, the active drug substance is dispersed or dissolved in a solution of polymer in a biocompatible water-miscible solvent such as *N*-methyl-2-pyrrolidone (NMP) or dimethyl sulfoxide (DMSO) at polymer concentrations ranging from 10 - 80% w/v. The resultant viscous but syringeable solution/suspension is then injected subcutaneously or intramuscularly by conventional syringe and needle. Once injected, the solvent dissipates and the aqueous

tissue fluids penetrate into the organic phase. This leads to phase separation and precipitation of the polymer and concurrent entrapment of the drug, leaving a semi-solid bolus at the injection site (Packhaeuser et al. 2004). Drug release then proceeds by a combination of diffusion and matrix degradation, the rate of which depends on various drug, polymer, solvent and formulation characteristics. The water miscibility of the organic solvent (Brodbeck et al. 1999b) and the polymer concentration (Lambert and Peck 1995) are reported as the most influential factors in terms of their effects on burst release.

In situ-forming depots (ISDs) have a number of advantages over preformed systems. Compared with microspheres ISDs are relatively simple to formulate, thus lowering investment and manufacturing costs, and are much easier to remove in the event of an adverse drug reaction. Additionally, there is no need for surgical implantation or the use of wide bore needles associated with implants. As such, ISD systems have recently been the subject of much research activity (Dunn et al. 1990; Lambert and Peck 1995; Chandrashekar and Udupa 1996; Ravivarapu et al. 2000a; Eliaz et al. 2000), and have had some commercial success. The Atrigel[®] system was developed by Dunn and co-workers in 1987 (Dunn et al. 1990), and is a proprietary delivery system which consists of biodegradable polymers dissolved in a biocompatible carrier. The Atrigel[®] technology was licensed to Atrix Laboratories, where its use has been extended to a number of medical device and drug delivery applications, an example of the latter being the Eligard[®] system, which comprises leuprolide acetate in a PLGA/NMP mixture, for the treatment of prostate cancer. The manufacturing process is very simple. The drug and polymer solutions are filled into separate syringes. The two syringes are coupled together and the contents mixed thoroughly to form a homogenous solution. This solution is then drawn into one syringe, the syringes de-coupled and a needle attached

for injection (Dunn 2003). The active drug substance is then delivered over 1, 3, 4 or 6 months depending on polymer content and drug loading (Ravivarapu et al. 2000a).

The SaberTM platform described in Section 1.3.3.2 is another application of this technology which utilises the naturally occurring biopolymer sucrose acetate isobutyrate (SAIB). Other *in situ*-forming implant systems in development include thermoplastic pastes, *in situ* cross-linking polymer systems and thermally induced gelation. The reader is referred to a review by Packheuser et al. for details of these systems (2004).

The main disadvantage associated with *in situ*-forming depots is the potential toxicity of the organic solvents (e.g. NMP) used to formulate these systems. Administration of Atrigel[®] to Rhesus monkeys revealed only a mild local tissue response with no visual inflammatory effects such as swelling, redness and irritation (Royals et al. 1999). This was in contrast to a study by Kranz et al. (2001) who assessed the myotoxicity of a similar formulation in rats by measuring plasma creatine kinase (CK) concentrations. Injection of 0.3 mL of the formulation (40% w/v PLA in NMP) exhibited a high myotoxic potential similar to the positive control, phenytoin. Unpublished results of a study by Matshke et al. (2002) reported a severe pain reaction during the administration of an NMP based ISD formulation to dogs and cats, leading the authors to question the suitability of this formulation for veterinary use. Alternative solvents have been investigated, of which benzyl alcohol appears the most promising due to its local anaesthetic effects (Packhaeuser et al. 2004). Other drawbacks include the variability of the surface area of the depot formed, which has been shown to result in variable and unpredictable drug release profiles (Jain et al. 2000b). There have also been reports of high burst release compared with preformed microspheres, associated with the lag

period between administration and phase inversion/bolus solidification, particularly when highly water miscible solvents such as NMP are used (Brodbeck et al. 1999a).

To address some of these drawbacks, *in situ*-forming microsphere (ISM) systems have been developed (Luan and Bodmeier 2006). The formulation is comprised of an emulsion of an internal drug-containing polymer solution (e.g. PLGA in NMP) and a continuous oil phase (e.g. peanut oil). Upon injection, the aqueous tissue fluids penetrate and cause phase inversion of the disperse phase, which hardens and results in the formation of discrete polymeric microparticles. This formulation is less viscous than polymer solutions, therefore easier and less painful injection can be expected, and the burst release was reportedly lower owing to the presence of the external oil phase. Additionally, the size of the microparticles is predetermined by the emulsion droplet size, so theoretically drug release is less variable compared with *in situ*-forming depots. The release profile of a leuprolide loaded ISM system compared favourably with conventional microspheres (Lupron depot[®]) and was deemed a good candidate for further study (Luan and Bodmeier 2006).

Due to the complexity and cost of microsphere manufacture and problems associated with the reconstitution and injection of particulates, the *in situ*-forming systems have shown considerable promise as simple alternatives to microspheres as slow release drug delivery devices. The decision was therefore taken to extend the scope of the thesis and include a comparative study of the effect of beta-blocker lipophilicity on release from an *in situ*-forming depot (ISD) formulation, together with the studies on absorption rates from conventionally prepared microspheres.

1.4 Research Aims

Despite the disadvantages of the parenteral route for drug administration, i.e. the use of needles, the risk of infection, and the resultant reduced patient acceptability, injectable formulations are still desirable, particularly in the field of slow release drug delivery. Drugs (including peptides/proteins) can be encapsulated in polymeric matrices and administered as long-term depots, greatly improving therapeutic outcomes as well as increasing patient compliance. However, there is a complex interplay between the factors affecting drug release rates from such delivery systems, such that each drug and delivery system must currently be considered individually on its own merits. The aim of this work was to explore the area further. Specifically in this thesis, the effect of drug lipophilicity on release rates from two polymeric dosage forms (microspheres and *in situ*-forming depots) was investigated.

Objectives were therefore to develop, optimise and characterise microspheres for the sustained release of a range of model drug compounds. The beta-blockers were selected as model drugs as a homologous series with similar molecular weight and pK_a , but widely varying lipophilicity. *In situ*-forming depot preparations were also formulated with the aim of comparing release profiles and tissue compatibility of the two formulation types. Once sustained release profiles were achieved from microspheres *in vitro*, the formulations were tested *in vivo* in rats, the absorption profiles were determined, and the effect of drug lipophilicity on absorption rate was assessed. An improved understanding of the biopharmaceutical aspects of subcutaneously injected microspheres for the sustained release of drugs will be invaluable in the future development of depot formulations.

Chapter 2

Beta-Blockers: Suitability as Model Compounds

2 Beta-Blockers: Suitability as Model Compounds

2.1 Introduction

The beta-blockers are a homologous series of drugs with similar molecular weights and pK_a values, but widely varying lipophilicities. These compounds are therefore potential candidates for the study of the effect of drug lipophilicity on release rates from subcutaneously injected formulations. This chapter explores the suitability of the beta-blockers as model compounds, and the selection of three candidates to be taken forward for development into slow-release formulations based on the experimental determination of $\log P$. The 14-day stability of the three short-listed beta-blockers in solution was also assessed to ensure their suitability for use in long-term dissolution studies.

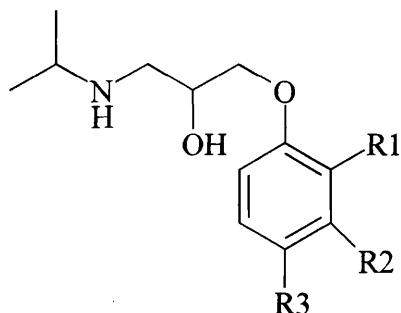
2.1.1 Structure and Physicochemical Properties of the Beta-Blockers

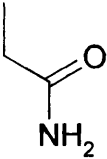
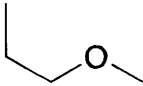
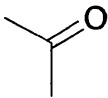
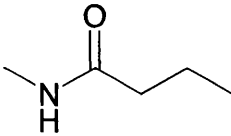
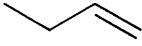
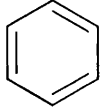
Beta-adrenoceptor blocking agents, or ‘beta-blockers’ as they are more commonly known, are competitive inhibitors of catecholamines at beta-adrenergic receptor sites, derived from the endogenous adrenergic agonist isoprenaline (Davies 1990). The principal effect of beta-blockade is reduced cardiac activity, causing a reduction in the rate and force of contraction of the heart (Martindale 2004). The search for a synthetic adrenoceptor antagonist for the treatment of angina pectoris led to the development of propranolol, first approved for clinical use in 1965. Refinement of the pharmacological properties of propranolol led to the development of a series of more than 50 beta-blockers, all based around an aryloxypropanolamine structure (Davies 1990).

Five beta-blockers were shortlisted for inclusion in this study based on literature lipophilicity values and commercial availability, with the aim of selecting three compounds for further study that would span the log *P* range of the group. The five shortlisted compounds were propranolol, alprenolol, metoprolol, atenolol and acebutolol. Figure 2.1 illustrates the chemical structure common to these 5 compounds and the various ring substitutions that confer different degrees of beta-receptor affinity, partial agonist activity and physicochemical properties (e.g. lipophilicity and stereospecificity) on the molecule.

The variation in lipophilicity affects the duration of beta-blockade, metabolism, elimination, tissue concentration and diffusion through biological barriers to a clinically significant extent. For example, hydrophilic beta-blockers, such as atenolol, are advantageous in that they have a lesser tendency to cross the blood brain barrier, causing fewer central nervous side effects such as sleep disturbances, psychosis, depression and hallucination (Borchard 1998).

Figure 2.1: Structure and physicochemical properties of the 5 shortlisted beta-blockers (adapted from Palm et al. 1996; * Clinical pharmacokinetics 1998; ** Cruickshank 1980).



Compound	R ₁	R ₂	R ₃	Mw	pK _a [*]	log P ^{**}
Atenolol	H	H		266	9.55	0.23
Metoprolol	H	H		267	9.7	2.15
Acebutolol		H		336	9.67	1.87
Alprenolol		H	H	249	9.7	2.61
Propranolol		H	H	259	9.45	3.65

2.1.2 Lipophilicity

The lipophilicity of a drug has been shown to significantly affect its bioavailability following subcutaneous administration as discussed in Section 1.2.1. One of the aims of the thesis is to investigate the relationship between drug lipophilicity and drug absorption rate following subcutaneous administration of polymeric sustained release dosage forms.

The partition coefficient (P) of a substance is defined as the ratio of its concentration in an organic phase ($[C]_{org}$) to its concentration in an aqueous phase ($[C]_{aq}$) at equilibrium (Equation 2.1) (Florence and Attwood 2005). The greater the value of P , the higher the lipophilicity of the solute.

$$P = \frac{[C]_{org}}{[C]_{aq}}$$

Equation 2.1: Calculation of partition coefficient based on the ratio of its concentration in an organic phase ($[C]_{org}$) to its concentration in an aqueous phase ($[C]_{aq}$) at equilibrium.

2.1.3 Techniques for the Determination of Partition Coefficient (P)

Since partition coefficient (P) values may range several orders of magnitude, the logarithm ($\log P$) is commonly used for convenience and will be used throughout this thesis.

Various methods are available for the determination of partition coefficient. Methods for the direct experimental determination of partition coefficient include the filter probe, filter chamber, stir flask, centrifugal partition chromatography and dual-phase potentiometric methods. Chromatographic techniques such as high performance liquid chromatography (HPLC), thin layer chromatography (TLC) and gas chromatography (GC) serve as indirect methods of partition coefficient determination by measuring the hydrophobicity parameter, which shows a good correlation with the partition coefficient (Purcell et al. 1973). Alternatively, methods to estimate partition coefficient based on the fragment contribution method have been developed (Leo et al. 1971), whereby the structure is divided into fragments and the P values of each group are summated. Numerous software packages utilising this technique e.g. ClogP, LogKow (Meylan and Howard 1995) are commercially available. Despite these developments in methodology, the simple and reliable 'shake-flask' technique remains generally accepted as the industrial standard for $\log P$ determination (Takács-Novák and Avdeef 1996).

The shake flask technique involves measurement of the distribution of the drug between two mutually saturated immiscible phases (aqueous and organic). Briefly, the solute is dissolved in either the aqueous or organic phase (the phase in which it is most soluble), the second phase is added and the two are shaken together until equilibrium is reached. The concentration of drug in one or both phases is then determined by UV spectroscopy or other suitable method. $\log P$ may then be calculated using Equation 2.1. *n*-octanol is often chosen as an appropriate organic phase because it mimics biological membranes in several aspects: *n*-octanol has a saturated alkyl chain, it dissolves water to the extent of 1.7 M, and its solubility parameter ($\delta_{\text{octanol}} = 10$) is close to that of biological membranes, for example skin (Panchagnula and Thomas 2000). *n*-octanol is not

completely non-polar and contains a significant amount of water in a stable hydrogen bonded complex. This mimics the situation in biomembranes which are associated with significant amounts of water held by the polar and/or ionic macromolecules that comprise them (PC 1979).

Measured $\log P$ values are affected by a large number of factors including temperature, ionic strength of the aqueous phase, solute and solvent purity and non-equilibrium conditions. As a result, literature values from different sources can vary widely, and experimental conditions are often incompletely specified. The partition coefficient of each compound was therefore determined experimentally under the same conditions, to enable direct comparisons to be made.

Equation 2.1 assumes the compound is fully unionised. For basic compounds with $pK_a > 9$ (such as the beta-blockers), the pH of the aqueous phase would need to be > 11 to achieve this. For the purposes of this study, it was deemed more appropriate to carry out all partitioning experiments at $37\text{ }^\circ\text{C}$, in phosphate buffer pH 7.4 for a better simulation of *in vivo* conditions. At this pH, the beta-blockers are partially ionised and a double equilibrium will exist between the ionised and non-ionised species in the aqueous phase, and between the non-ionised species in both phases (Fig. 2.2).

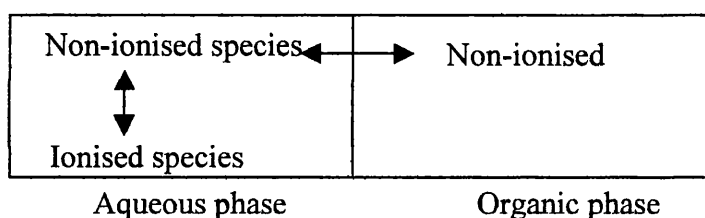


Figure 2.2: Double equilibrium of a partially ionised solute between two immiscible phases.

Thus, the values are reported as apparent partition coefficients (P_{app}) or distribution coefficient (D). Equation 2.2 shows the relationship between the two parameters, allowing calculation of the apparent partition coefficient at any given pH if the pK_a (and therefore fraction unionised) of the compound is known.

$$P_{app} = P \cdot fu$$

Equation 2.2: The Relationship between apparent partition coefficient (P_{app}) and partition coefficient (P) where fu is the fraction of molecules present in the unionised form.

2.1.4 Beta-Blocker Stability

It is imperative that the actives used remain stable under the test conditions employed throughout the duration of study to qualify as suitable model compounds for these sustained release experiments. Attempts to account for drug degradation during dissolution can be made (Kim and Burgess 2002), but this would complicate matters unnecessarily. Stability data for the three compounds was obtained by personal communication with Vivek Chand, Medicines Information Advisor, AstraZeneca Ltd. AstraZeneca routine production stability reports demonstrated a 2 year stability of 1 mg/mL aqueous metoprolol solutions when stored at 25 °C. Similarly, a 0.1% w/v solution of alprenolol in 0.9% w/v NaCl also demonstrated at least a 2 year shelf life at room temperature. Commercially available Tenormin Injection (atenolol 0.05% w/v in normal saline) remains stable for at least a period of 3 years when stored at 25 °C and protected from light. The potential for the three shortlisted beta-blockers to undergo photolytic or hydrolytic degradation under the dissolution conditions employed in this

study (phosphate buffered saline, pH 7.4, 37 °C) was investigated by carrying out a 14-day stability study (see Section 2.3.4).

2.1.5 Quantification of Beta-Blockers

Detection at low concentrations is an essential attribute of the chosen model compounds to allow accurate quantification following slow release dissolution studies, and particularly for use in the *in vivo* experiments.

Methods for the quantification of various beta-blockers by HPLC have been published (Modamio et al. 1996; Basci et al. 1998; Patel et al. 1981), and were used to develop the UV and HPLC assay methods for use in the dissolution and partitioning experiments herein (see Sections 2.3.3 and 2.3.5 respectively). Methods for the extraction and analysis of a range of beta-blockers from biological matrices including plasma and urine are also available (Braza et al. 2000; Kim et al. 2001; Soltés 1989), facilitating the development of the biological assay for use in the *in vivo* studies.

2.2 Materials

The beta-blockers (propranolol hydrochloride, alprenolol hydrochloride, acebutolol hydrochloride, metoprolol tartrate and atenolol) and *n*-octanol (min. 99% purity, glass distilled) were all purchased from Sigma-Aldrich Co. (Poole, Dorset, UK). Acetonitrile, orthophosphoric acid and triethylamine used in mobile phase preparation were all HPLC grade and were obtained from VWR International Ltd. (Poole, Dorset, UK). Potassium dihydrogen orthophosphate, disodium hydrogen orthophosphate, sodium hydroxide and sodium chloride used in buffer preparation were all analytical grade and purchased from BDH. Deionised water was obtained from an Option 4 water purification system (Elga Ltd., High Wycombe, Buckinghamshire, UK). All chemicals and solvents were used as purchased unless otherwise stated.

2.3 Methods

2.3.1 Buffer Preparation

Phosphate buffer solution pH 7.4 for use in the partitioning studies was prepared by adding 250 mL of 0.2 M potassium dihydrogen orthophosphate to 393.4 mL of 0.1 M sodium hydroxide and making up to 1000 mL with deionised water (BP 2003). The pH was determined using a pH meter (model pH 211, Hannah Instruments Ltd., Leighton Buzzard, Bedfordshire, UK), and adjusted with sodium hydroxide when necessary. The pH meter was calibrated using pH 4 and pH 7 buffers prior to each use.

Phosphate buffered saline (PBS) used in the stability studies was prepared by dissolving the following solids in approximately 800 mL deionised water (BP 2003).

- Disodium hydrogen orthophosphate 2.38 g
- Potassium dihydrogen orthophosphate 0.19 g
- Sodium chloride 8.0 g

The resultant solution was then adjusted to pH 7.4 with 1 M HCl if necessary, before being made up to 1000 mL with deionised water.

2.3.2 Shake Flask Determination of Partition Coefficient (*P*)

The two phases (*n*-octanol and phosphate buffer pH 7.4) were mutually saturated by the addition of approximately 5% v/v of each phase to the other, shaking vigorously and leaving to stand overnight. Any excess was then removed using a separating funnel. This phase saturation enables equilibrium conditions to be established faster during the partitioning experiments. Partition coefficients for each drug were determined in triplicate, at two different volume ratios (*n*-octanol:buffer being 20:20 and 5:35), to determine any dependence on phase concentration of partition coefficient (PC 1979). 10 mg of each beta-blocker was accurately weighed and dissolved in phosphate buffer (20 or 35 mL) in 40 mL Teflon[®] centrifuge tubes (Nalgene). The required amount of *n*-octanol was then added to give a total volume of 40 mL (20 and 5 mL respectively). The centrifuge tubes were shaken in a waterbath at 37 °C for 2 hours (gently, so as not to emulsify the mixture). The water bath serves to maintain a constant temperature since partitioning behaviour of substances is dependent upon temperature by approximately 0.01 log unit per °C (Leo et al. 1971), and also represents *in vivo* conditions. The samples were then centrifuged for 10 minutes at 10,000 rpm, 37 °C (3K30 Refrigerated

centrifuge, Sigma Laborzentrifuges GmbH, Osterode am Harz, Germany) to separate the phases. The aqueous phase was sampled carefully to minimise contamination with *n*-octanol (the supernatant phase). A syringe with a disposable needle was partially filled with air. Light positive pressure was applied to gently expel the air whilst inserting the needle through the organic layer. A 5 mL aliquot of the aqueous phase was withdrawn, the syringe quickly removed and the needle detached. Drug concentration in the aqueous phase was then determined using UV spectroscopy (see Section 2.3.3). The concentration of drug in the organic layer was determined by difference, and the apparent partition coefficient was calculated according to Equation 2.1.

2.3.3 UV Spectroscopy

Calibration curves were constructed by preparing solutions of each beta-blocker in phosphate buffer (previously saturated with *n*-octanol) over the concentration range 0.05 – 0.25 mg/mL. Absorbance was measured at the corresponding λ_{\max} of each compound (290, 273, 269, 273 and 233 nm for propranolol, metoprolol, alprenolol, atenolol and acebutolol respectively) against a phosphate buffer blank, and in triplicate. The calibration curves were used to calculate the concentration of drug in the aqueous phase, in the determination of $\log P_{app}$. Calibration curves for use in the stability study were prepared from solutions of beta-blockers in PBS, over the concentration range 3.125 – 100 $\mu\text{g/mL}$.

2.3.4 Beta-Blocker Stability Study

Stability studies were carried out on the three beta-blockers selected for further study based on the results of the shake flask determination of $\log P_{app}$ (see Section 2.4.1). Solutions of alprenolol, metoprolol and atenolol each in PBS (0.1 mg/mL) were stored in both amber and clear glass jars at each of three different temperatures (room temperature, 37 °C and 5 °C). 5 mL aliquots of each sample were removed and analysed by both UV spectroscopy (as detailed in Section 2.3.3) and HPLC (as detailed in Section 2.3.5) on a daily basis for five days, then three times weekly thereafter for a 14-day period to determine drug concentration. A significant reduction in UV absorbance or peak area would indicate drug degradation, while the appearance of extra peaks on the HPLC chromatogram would suggest the presence of degradation products. Either outcome would potentially render the beta-blockers unsuitable candidates for use in this work. The results were analysed using the Mann-Whitney U-Test to determine whether the concentration of drug had changed significantly over the period of study.

2.3.5 HPLC

The beta-blockers under study have a wide range of polarity (the partition coefficients of alprenolol and atenolol differ by 6 orders of magnitude) (Davies 1990), therefore different chromatographic conditions were required to achieve adequate separation and resolution. This was achieved using the same reversed-phase column and mobile phase, with alterations of the mobile phase polarity via the use of a step gradient. The method was adapted from a previously developed HPLC assay of several beta-blockers (Modamio et al. 1996).

A Hewlett-Packard 1050 series HPLC system (Agilent Technologies UK Ltd.) was used, equipped with a 1050 series autosampler, quaternary pump, UV-visible detector (variable wavelength) and online degasser (see Fig. 2.3). The chromatograms obtained were integrated using PC/Chrom⁺ software (H&A Scientific Inc., USA). A 5 μm C₁₈ Nucleosil column (150 x 4 mm i.d.) (Jones Chromatography, Hengoed) was used at ambient temperature, in conjunction with a pre-column of the same material.

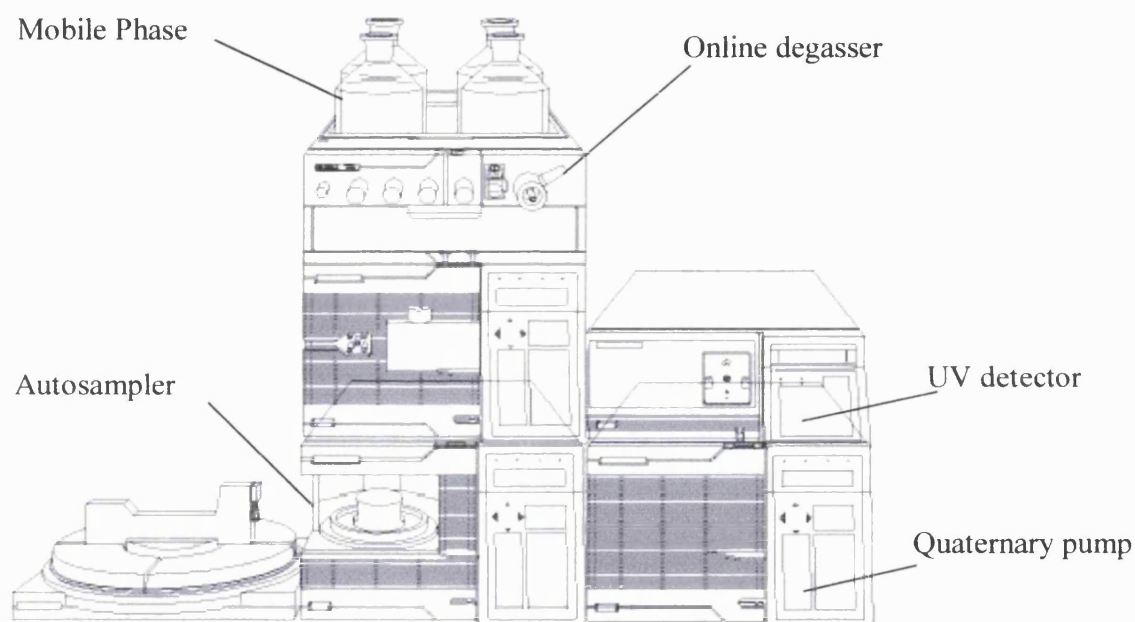


Figure 2.3: Schematic of HPLC set-up, adapted from HP1050 User Manual (Agilent Technologies).

Internal standards were employed to minimise random errors in quantification caused by daily variations in experimental conditions. In this study, one of the other beta-blockers was used as the internal standard due to their chemical similarity (see Table 2.1). Both compounds tend to be equally affected by such changes, therefore the ratio of the two peak areas should remain unchanged. Internal standard (IS) solutions were freshly prepared daily at a concentration of 0.1 mg/mL in HPLC grade water. 1 mL of

the IS solution was added to 1 mL of the sample and vortexed prior to analysis. Calculations were performed to adjust the peak area ratio for the slight daily variation in IS concentration.

The mobile phase comprised a 0.2% w/v solution of triethylamine in water (adjusted to pH 3 with orthophosphoric acid) (solvent A) and acetonitrile (solvent B). Triethylamine (TEA) was used to act as a competing base, to reduce peak tailing caused by the interaction of unbonded surface silanol groups on the silica column with the beta-blockers (Basci et al. 1998). Both solvents A and B were individually filtered through a 0.2 μm nylon filter membrane (Whatman International Ltd., Maidstone, Kent, UK) under vacuum, and sparged with helium using the online degasser prior to use. The relative percentage composition of solvents A and B in the mobile phase was controlled using the quaternary pump over the course of each run. In order to achieve adequate resolution of the drug from its associated internal standard, a step gradient was employed, i.e. the mobile phase composition was adjusted abruptly at a given time point in the run to alter its polarity. The samples were analysed using an injection volume of 50 μL and a mobile phase flow rate of 1.5 mL/min throughout. The chromatographic conditions employed for each compound are summarised in Table 2.1. A post-run time of 2 minutes was included between injections to allow the mobile phase composition to return to its starting value.

All measurements were taken at a wavelength of 273 nm, corresponding to the λ_{max} of metoprolol, which was employed in each run as either sample or internal standard.

Table 2.1: Mobile phase composition for the HPLC analysis of alprenolol, metoprolol and atenolol, detailing the relative % composition of solvent A (water with 0.2% w/v TEA) and solvent B (acetonitrile). The polarity of the mobile phase was decreased 2 minutes into the run by reducing the % of solvent A. The total run time was 6 minutes.

Sample	Internal standard (IS)	% Mobile phase composition			
		$t = 0 - 2 \text{ min}$		$t = 2 - 6 \text{ min}$	
		A	B	A	B
alprenolol	metoprolol	75	25	70	30
metoprolol	alprenolol	75	25	70	30
atenolol	metoprolol	90	10	75	25

The HPLC method was optimised to meet the following system suitability requirements (based on the AstraZeneca Standard Operating Procedure entitled System Suitability Testing for Chromatographic Analyses).

- **Repeatability of injection:** The coefficient of variation (CV) of the peak area of five replicate injections must be < 2.0%.
- **Tailing factor (T):** T is a measure of peak symmetry and is calculated according to Equation 2.3 and Fig. 2.4. A T value > 2 would indicate peak asymmetry, leading to inaccurate peak integration.
- Appropriate **retention times** and adequate **resolution** between drug peak, internal standard and solvent fronts were also required.

$$T = W_{0.05} / 2f$$

Equation 2.3: Calculation of peak tailing factor (T) where $W_{0.05}$ is the peak width at 5% height and f is the width between the start of the peak and the peak maximum at 5% height (see also Fig. 2.4).

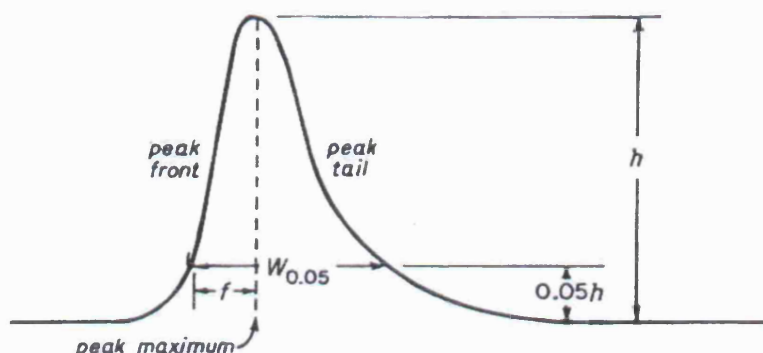


Figure 2.4: Schematic representation of the parameters $W_{0.05}$ and f used to calculate tailing factor (T).

Calibration curves were constructed from solutions of the beta-blockers in PBS over the concentration range 3.125 - 100 $\mu\text{g}/\text{mL}$. 1 mL internal standard was added to 1 mL of each standard solution and vortexed for 1 minute. 50 μL of each sample was then injected in triplicate, the mean peak area ratio (sample/IS) was plotted against standard concentration, and then used to calculate drug concentration in the stability study samples.


2.4 Results and Discussion

2.4.1 Shake Flask Determination of $\log P_{app}$ Values

The mean apparent partition coefficients (P_{app}) calculated according to Equation 2.1 are listed in Table 2.2. P_{app} values were independent of *n*-octanol:buffer volume ratio.

Table 2.2: $\log P_{app}$ values of the beta-blockers as determined by the shake flask technique at 37 °C at two different *n*-octanol:buffer (pH 7.4) volume ratios (20:20 and 5:35) ($n = 6 \pm SD$).

Drug	$\log P_{app} \pm SD$
Propranolol	1.37 ± 0.02
Alprenolol	1.20 ± 0.03
Metoprolol	0.04 ± 0.05
Acebutolol	-0.10 ± 0.04
Atenolol	-1.14 ± 0.10



Lipophilicity

As predicted, propranolol and alprenolol were the most lipophilic species, atenolol the most hydrophilic, and metoprolol and acebutolol exhibiting intermediate values. Good correlation ($R^2 = 0.9831$) was obtained between the experimentally determined $\log P_{app}$ values and those obtained from a literature source (Gulyaeva et al. 2002) (measured in *n*-octanol-buffer systems at pH 7.4, temperature not stated) (Fig. 2.5).

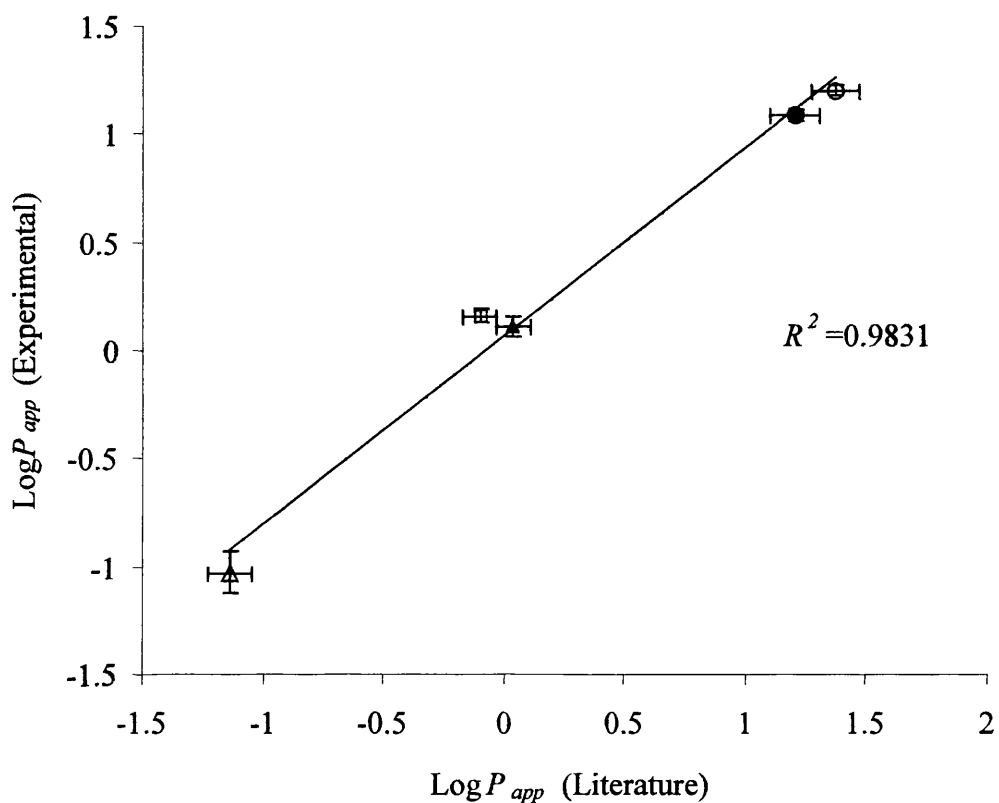


Figure 2.5: Correlation between literature (Gulyaeva et al. 2002) and experimentally determined $\log P_{app}$ values (Δ atenolol, \blacktriangle metoprolol, \square acebutolol, \bullet alprenolol, \circ propranolol).

Three compounds, alprenolol, metoprolol, and atenolol (structures shown in Fig. 2.6) were selected to be taken forward for further studies as they displayed a sufficiently wide range of $\log P_{app}$ values. Propranolol and acebutolol were used no further in this study.

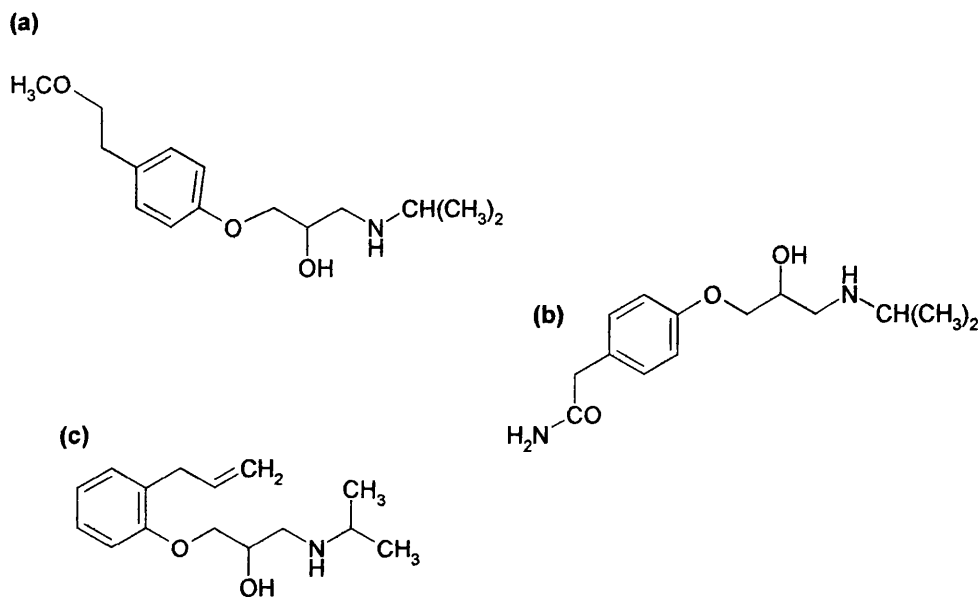


Figure 2.6: Chemical structures of (a) metoprolol, (b) atenolol and (c) alprenolol

2.4.2 Beta-Blocker Stability

For the stability study, drug concentrations were measured by two different methods, UV spectroscopy and HPLC for the reasons outlined in Section 2.3.4. Results from each method are described in turn.

2.4.2.1 UV Spectroscopy

Calibration curves of the three beta-blockers in PBS were generated as previously described. Again, excellent linearity was observed ($R^2 > 0.998$). The concentration of drug in each sample was analysed at predetermined time intervals and was expressed as a percentage of initial drug concentration (Fig.2.7a-c).

a)

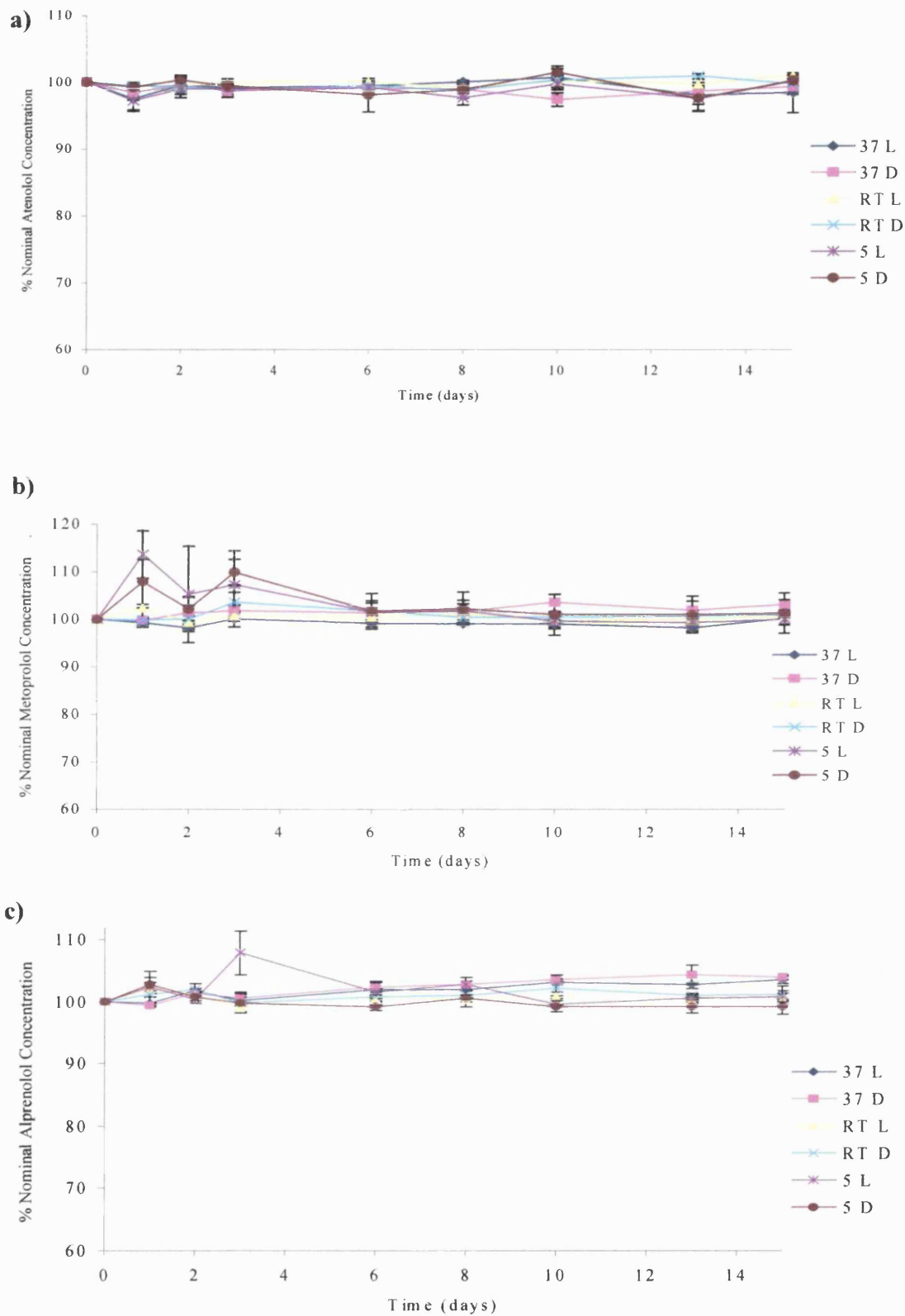


Figure 2.7: Mean % nominal concentrations of a) atenolol, b) metoprolol and c) alprenolol solutions as determined by UV spectroscopy. Solutions were stored at 37 °C, room temperature (RT) and 5 °C, under both light (L) and dark (D) conditions ($n = 3$).

Unexpectedly high absorbance values of drug from samples stored at 5 °C on days 1 – 3 for metoprolol and day 3 for alprenolol were probably due to the formation of condensation on the cuvette wall during analysis which would result in an increased measured drug concentration. In subsequent measurements, samples were allowed to reach room temperature prior to measurement. No downward trend in drug concentration was evident from the concentration/time profiles for any of the three compounds (Fig 2.7).

The Mann-Whitney U test (one-tailed, $n = 3$) was applied to initial (day 0) and final (day 14) drug concentrations to determine whether any significant change in concentration could be detected (see Table 2.3). The results denoted * in Table 2.3 show that initial and final concentrations were significantly different. This was observed in three of the six samples stored at 37 °C. The difference results from a slight increase in mean drug concentration, suggesting an alternative reason such as bacterial growth in the solution, as opposed to drug degradation. These results indicate that no significant degradation of the beta-blockers in solution occurred over the 14-day test period, but suggest that it may be prudent to include an antimicrobial agent such as sodium azide in the dissolution medium for the *in vitro* drug release studies.

Table 2.3: *p* values generated by application of the Mann-Whitney U-test (exact sig., one-tailed) to drug concentrations measured by UV spectroscopy on day 0 and day 14 of the stability study. * $p \leq 0.05$ indicates a significant difference in concentration.

	Probability (<i>p</i>) (<i>n</i> =3)		
	Atenolol	Metoprolol	Alprenolol
37 L	0.25	0.35	0.05*
37 D	0.20	0.05*	0.05*
RT L	0.10	0.20	0.10
RT D	0.30	0.35	0.20
5 L	0.40	0.35	0.35
5 D	0.50	0.50	0.15

2.4.2.2 HPLC

Validation of the HPLC method was successful. A stable baseline could be achieved and no sample carry over was experienced. Tailing factors were < 2 for both sample and IS peaks, and good peak resolution was achieved. Figures 2.8 (a) and (b) are sample chromatograms from the HPLC analysis of atenolol and metoprolol respectively, showing the solvent fronts, drug peaks and IS peaks.

HPLC calibration curves for each of the three beta-blockers were generated over the concentration range 3.125 – 100 $\mu\text{g/mL}$, with R^2 values > 0.997 for each compound. Drug content in the samples was calculated using the relevant calibration curve and expressed as a percentage of original drug concentration.

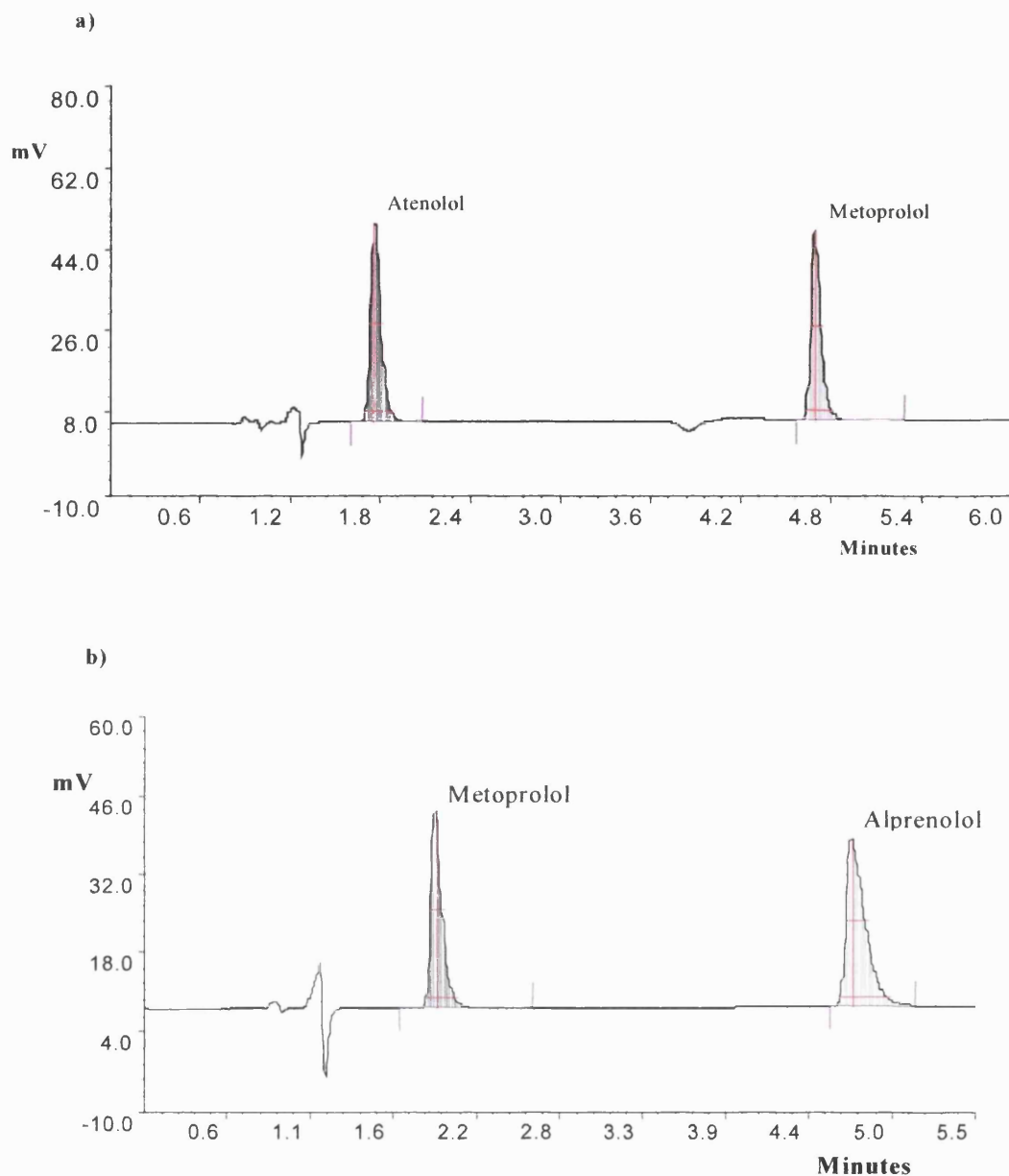


Figure 2.8: Sample chromatograms from the HPLC analysis of a) atenolol (metoprolol IS) and b) metoprolol (alprenolol IS)

In this case, drug peak area was used as opposed to peak area ratio as an overlay of the concentration profiles for atenolol and alprenolol (for which the same internal standard solution was used) revealed a trend in high/low values, indicating possible inaccuracies in IS preparation (data not shown). Figure 2.9 (a)-(c) illustrates the drug concentration profiles of the stability samples as measured by HPLC (IS excluded).

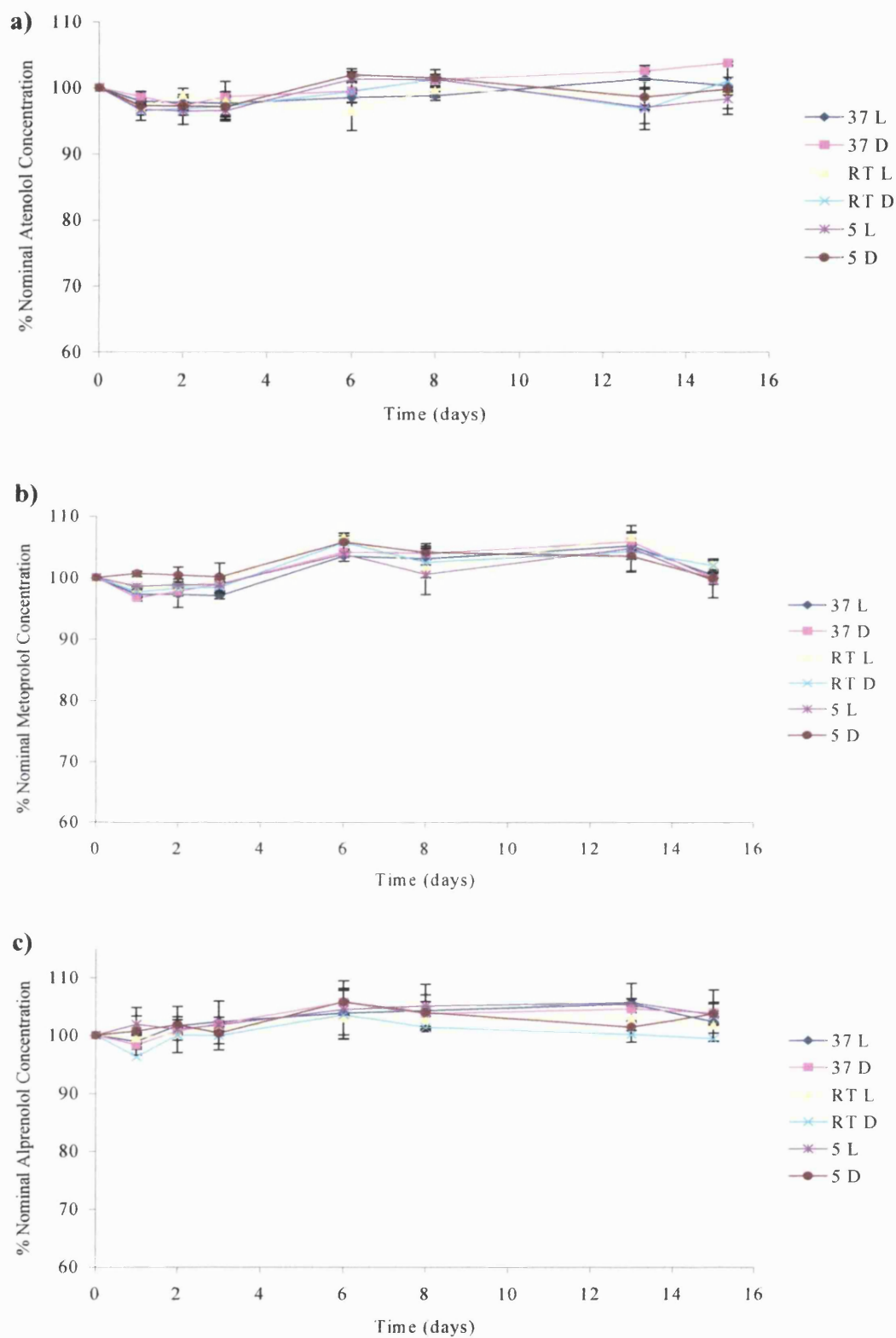


Figure 2.9: Mean % nominal concentrations of a) atenolol, b) metoprolol and c) alprenolol solutions as determined by HPLC. Solutions were stored at 37 °C, room temperature (RT) and 5 °C, under both light (L) and dark (D) conditions ($n = 3$).

Chromatograms from day 0 and day 14 for each compound are the same i.e. no peak broadening or splitting had occurred, and the appearance of no additional peaks indicates that no breakdown products were formed over the duration of the study period. Table 2.4 shows the results of the application of the Mann-Whitney U-test to initial and final drug concentrations ($n = 3$). p values > 0.05 indicate no significant difference between initial drug concentration and that following 14 days storage under the specified conditions. Once again, the differences observed were as a result of slight increases in measured drug concentration, suggestive of inter-day variability of the assay, which was less controlled owing to the absence of internal standard. There was no obvious correlation between the significantly different results from the UV and the HPLC analyses.

Table 2.4: p values generated by application of a Mann-Whitney U-test to drug concentrations measured by HPLC on day 0 and day 14 of the stability study. * $p \leq 0.05$ indicates a significant difference in concentration.

	Probability (p) ($n = 3$)		
	Atenolol	Metoprolol	Alprenolol
37 L	0.45	0.25	0.25
37 D	0.05*	0.03*	0.05*
RT L	0.35	0.05*	0.10
RT D	0.10	0.05*	0.35
5 L	0.15	0.35	0.20
5 D	0.40	0.50	0.05*

2.5 Conclusion

The beta-blockers appear to be suitable for use as model compounds, being a homologous group with similar molecular weight and pK_a but a wide variation in lipophilicity. They are easily detected at low concentrations by UV spectroscopy, and a validated HPLC method has been developed for their quantification. Apparent partition coefficients of 5 compounds were measured experimentally, and used to shortlist three beta-blockers (atenolol, metoprolol and alprenolol) to be taken forward for development into polymeric slow release dosage forms. The stability of these three compounds in the dissolution test conditions over a 14-day period was demonstrated by the fact that no significant reduction in concentration was detected by either HPLC or UV spectroscopy.

Chapter 3

Microsphere Formulation and Characterisation

3 Microsphere Formulation and Characterisation

3.1 Introduction

Polymeric microsphere drug delivery systems by definition are drug-loaded polymeric particles in the micron size range, which can be dispersed in an aqueous vehicle for subcutaneous or intramuscular injection. As discussed in the introductory chapter (Section 1.3.3.4), they have shown great promise as slow release delivery devices due to their ease of administration compared with implants, and the potential for tailoring of the drug release profile by manipulation of various formulation parameters.

A complex array of interacting factors affect drug release rates from microspheres, making the prediction of release characteristics a difficult task. One aim of this thesis was to study the effect of drug lipophilicity on absorption rates from subcutaneously injected polymeric microspheres. The beta-blockers were identified as a suitable group of model compounds (as discussed in Chapter 2) having similar molecular weights and pKa values, but varying lipophilicity. The purpose of this chapter was to formulate and characterise beta-blocker loaded microspheres with suitable *in vitro* drug release profiles to be taken forward for study *in vivo*. Gradual release over a 1 - 2 week period was deemed sufficient to be classed as sustained release, and to allow the study of the effects of drug lipophilicity, but not too long to compromise time management of the study and to enable sufficient *in vivo* experiments to be carried out within the allotted time frame.

Pertaining to the **formulation** aspect of this chapter, various methods of microsphere preparation are at our disposal, with procedures based on solvent evaporation/extraction and spray drying being the most commonly encountered (see Section 1.3.3.4). The reduced reliance on the solubility properties of the drugs used makes spray drying the preferred method for microsphere fabrication in this study. The background to this technique and factors affecting the characteristics of the spray dried product are discussed in the following section (Section 3.1.1).

In terms of **characterisation** of the spray dried microspheres, particle size analysis (by laser diffraction), visualisation of surface morphology (by scanning electron microscopy, SEM), residual solvent determination (by NMR), and *in vitro* dissolution testing of the spray dried microspheres were performed.

3.1.1 Spray Drying as a Method for Microsphere Preparation

By definition, spray drying is the transformation of feed from a fluid state into a dried particulate form by spraying the feed into a hot drying medium (Masters 1991). A schematic diagram and digital photograph of the spray dryer used in this work (Buchi 191) is shown in Figure 3.1.

The feed solution is first atomised by spraying under pressure through a nozzle (C)*, into the drying chamber (D), where it comes into contact with the drying medium (hot air in most cases). Here, the solvent rapidly evaporates due to the large surface area of

* The bracketed letters (A-H) refer to the schematic diagram in Fig. 3.1.

the droplets, leaving solid microparticles suspended in the drying medium. Drying takes place in two stages. First there is enough moisture within the droplet to replace that lost at the surface. This is the constant rate period or first period of drying. Diffusion of moisture from within the droplet maintains surface saturated conditions, and evaporation takes place at a constant rate. When moisture content becomes too low, the critical point is reached and a dried shell forms around the surface. Evaporation then depends on the rate of moisture diffusion through the dried shell. The thickness increases with time causing a decrease in the rate of evaporation. This is the falling rate period or the second period of drying. After a residence time of a few seconds within the drying chamber (dependent on the aspiration setting), the solid microspheres are separated from the air in the cyclone (G) and can be recovered from the collecting vessel (H) (Masters 1991).

For preparation of the feed solution, it is often desirable for the drug and polymer to be dissolved in a common solvent. Since PLGA is insoluble in aqueous media, we have little choice but to use potentially toxic organic solvents such as dichloromethane (DCM). Dichloromethane has been described as the solvent of choice for spray drying of PLGA microspheres based on particle morphology and release characteristics (Bain et al. 1999; Bitz and Doelker 1996), and was therefore used throughout this study.

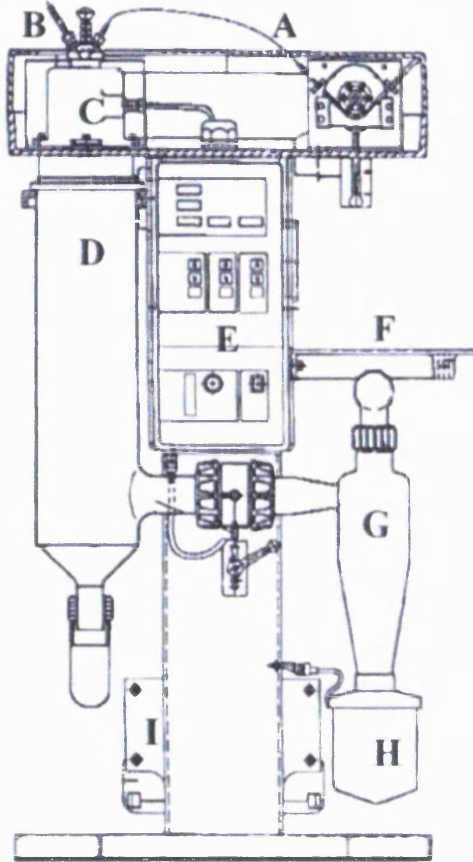


Figure 3.1: Schematic and photograph of Buchi Mini Spray Dryer 191, where A = feed pump tubing, B = compressed air inlet, C = pneumatic nozzle, D = drying chamber, E = control panel, F = sample feed holder, G = cyclone, H = collection vessel and I = aspirator (Buchi, 2002).

In Europe there are no general guidelines for residual organic solvent content with products being assessed on an individual basis, however the USP XXIV gives general guidelines that residual dichloromethane concentration must be less than 500 ppm (USP 2000). However, owing to the low boiling point (40 °C) and high volatility of this solvent, residual dichloromethane in spray dried microspheres is usually minimal (Wang and Wang 2002a). High residual solvent does not only have potential toxicity implications, but may also cause increased burst release (Blanco-Prieto et al. 2000). A NMR method to quantify the residual solvent was used in this study, and is described in Section 3.3.8.

The effects of various spray drying process parameters on the product characteristics are outlined below, and summarised in Table 3.1:

- **Droplet size:** Increasing the nozzle pressure, or decreasing the nozzle size serves to decrease the mean droplet size, leading to microspheres of smaller mean diameter.
- **Feed viscosity:** Increasing the concentration of polymer within the feed solution, or reducing the feed temperature results in coarser sprays, with larger liquid droplets and higher polydispersity (Wang and Wang 2002b)
- **Feed rate:** Increasing the feed rate reduces the outlet temperature since more energy is required to evaporate the higher solvent throughput. This can result in larger particles with higher residual moisture content (Buchi 2002).
- **Aspiration:** Low aspiration settings (i.e. low air flow rates) increase the residence time of the product within the dryer, leading to lower residual moisture content. Increased aspiration leads to higher yields due to improved separation of the product from the drying air in the cyclone (Buchi 2002).

- **Inlet temperature:** Increasing the inlet temperature reduces bulk density as evaporation rates are faster and particles are more porous and fragmented.
- **Outlet temperature:** Lower outlet temperatures result in microspheres with higher residual moisture and more agglomerates (Masters 1991), although this is relative to the boiling point of the solvent used. Outlet temperatures greater than the glass transition temperature or melting point of the polymer used cause melting and agglomeration.
- **Solvent:** The solvent used affects the matrix architecture and density of the microspheres (Baras et al. 2000). For example, acetone was shown to produce more porous microspheres than those spray dried from a dichloromethane based feed solution (Bain et al. 1999).

Table 3.1: Summary of process parameters affecting the characteristics of the spray dried product (adapted from Buchi 2002). 0 indicates no effect, + is an increase, - is a decrease.

	Aspirator rate ↑	Inlet temp. ↑	Spray air flow ↑	Feed rate ↑	Feed solution polymer concentration ↑
Particle size	0	0	---	+	+++
Residual Solvent	++	--	0	++	-
Yield	++	-	0	+/-	+

No examples of spray dried beta-blocker loaded microspheres were found in the literature. The spray drying process parameters employed were therefore based on those used for the encapsulation of low molecular weight, water soluble compounds such as

etanidazole and rifampicin within PLGA microspheres (Bain et al. 1999; Wang and Wang 2002b), and then optimised according to morphology and yield. The aim was for the drug to be distributed evenly throughout the polymer matrix to achieve a sustained release profile over a time period of 7 - 14 days. The product would preferably be comprised of discreet, smooth and spherical microspheres, to facilitate injectability and syringeability, and reproducibility of release profiles.

3.1.2 *In Vitro* Dissolution Testing – Background to Technique

Current USP dissolution apparatus is designed for oral and transdermal products (USP 2000) so the choice of an appropriate method for microspheres is challenging. Problems such as sample containment and large dissolution medium volume make many of the methods unsuitable for use with microspheres. Strategies to overcome these issues can often introduce further problems, such as the use of dialysis tubing to contain the microspheres causing aggregation and violation of sink conditions (Burgess et al. 2002). For the purposes of this study, a simple alternative apparatus was used, employing a 'sample and separate' technique, which is currently used for preliminary studies within the pharmaceutical industry. This technique has been deemed sufficient to allow differentiation between products, but not necessarily to obtain meaningful *in vitro/in vivo* correlation (IV/IVC) (Burgess, 2004). The technique involves shaking tubes containing the test sample in a suitable volume of relevant media. At each test time-point, the tubes are centrifuged to separate the free drug in solution from the undissolved material, and a portion of supernatant is assayed for drug content. The supernatant removed is then replaced with an equal volume of fresh dissolution medium, the tubes are then vortexed to resuspend the particles and returned to the study.

Phosphate buffered saline, at physiological pH (7.4) and temperature (37 °C) was used, with the addition of a surfactant (Tween 80, 0.1% w/v) to aid wetting and sample dispersion, and sodium azide (0.01% v/v) as a bacteriostatic agent to control microbiological growth. The required volume of dissolution medium was calculated so that once all drug was released, the solution was < 33% w/v of the saturation concentration so as not to inhibit ongoing release (i.e. sink conditions were achieved).

Burst release does not have an official definition, but depends on the total duration of release (Burgess et al. 2004). In the case of microspheres which release over weeks to months, it is often described as the amount of active drug substance released in the first 1.5 days. Burst release is a common phenomenon with PLGA microspheres. It can be advantageous if it acts as a loading dose, enabling therapeutic drug levels to be attained rapidly. However, dumping of a high percentage of the dose initially could cause toxicity issues, as well as the resultant depletion of the drug reservoir, potentially compromising the sustained release nature of the product. Simple formulation approaches to reduce burst release, such as emulsion spray drying and surfactant incorporation were investigated in this study.

3.2 Materials

The beta-blockers (alprenolol, metoprolol and atenolol) were purchased from Sigma-Aldrich (Poole, UK) and were used without further purification. The emulsifiers polyvinyl alcohol (PVA, medium viscosity), polysorbate 80 (Tween 80) and sorbitan monostearate (Span 60) and the antimicrobial agent sodium azide were also purchased from Sigma-Aldrich. Potassium dihydrogen orthophosphate, disodium hydrogen

orthophosphate, sodium hydroxide and sodium chloride used in buffer preparation were all analytical grade and purchased from VWR International Ltd. (Poole, Dorset, UK), as was the spray drying solvent, dichloromethane (DCM). Water where used was deionised, and was obtained from an Option 4 water purification system (Elga Ltd., High Wycombe, Buckinghamshire, UK). For NMR studies, sodium formate was purchased from Sigma-Aldrich, and *d*₄-acetic acid was obtained from Cambridge Isotope Laboratories Inc. (Andover, USA).

The poly(lactide-co-glycolide) polymer Medisorb[®] 50:50 DL 2.5A (mw 24 000 Da) was purchased from Alkermes Inc. (Cincinnati Ohio, USA). This polymer has a 50:50 lactide:glycolide ratio with a free carboxylic acid end group (i.e. uncapped), and was chosen for its suitable degradation time of approximately 2 - 4 weeks, and relatively high glass transition temperature (*T*_g) to facilitate spray drying. The physical properties of this polymer are summarised in Table 3.2. The polymer was stored frozen and desiccated, and was allowed to reach room temperature prior to opening to prevent condensation.

Table 3.2: Physical properties of the Medisorb[®] polymer utilised to prepare microspheres (data obtained from Certificate of Analysis, Alkermes Inc.).

Polymer	Inherent viscosity (dL/g)	Glass transition temp. (<i>T</i> _g , °C)	Mw (kDa)	Polydispersity
50:50 DL 2.5A	0.26	43.6	24	1.78

3.3 Methods

3.3.1 Preparation of the Feed Solution for Spray Drying

The simplest method of spray drying is solution spray drying, where the drug and polymer are simply dissolved in a common solvent (dichloromethane (DCM) in this case) and spray dried directly according to the process parameters outlined in the following section (Section 3.3.2). The target drug loading was 20% w/w (with respect to the total weight of drug and polymer) to facilitate detection in subsequent *in vivo* studies. The polymer (PLGA 50:50 DL 2.5A) was dissolved in 50 mL DCM to give a concentration of 3% w/v. The relevant beta-blocker was then dissolved in the polymeric solution to give a nominal microsphere loading of 20% w/w*. These batches were denoted **batches 1 - 3**. The feed solution for the preparation of blank microspheres was prepared in the same way, with the omission of the active drug substance (denoted **batch 4**). Solutions were stirred with a magnetic stirrer bar during spray drying, and covered with foil throughout to prevent solvent evaporation and to protect the potentially photosensitive actives. Some additional batches were spray dried using *i*) higher feed solution viscosity (17% w/v PLGA) (**batch 5**) and *ii*) lower drug loading (6% w/w) (**batch 6**) for comparison of morphology and/or release profile with the microspheres prepared as described above.

* Atenolol is only slightly soluble in DCM and as such, the maximum concentration achieved was 1 mg/mL. The PLGA content was reduced accordingly (to 0.4% w/v) to maintain a nominal drug loading of 20% w/w.

Since burst release is a common phenomenon (as discussed in Section 3.1.2), a number of additional formulation approaches were explored, namely *i*) emulsion spray drying *ii*) emulsion spray drying with additional stabilising agent (PVA) and *iii*) the addition of a competing surfactant (Span 60) to the drug/polymer solution. Each of these is described in turn below.

It was hypothesised that the formation of a w/o emulsion would alter the distribution of drug within the polymer matrix, and potentially reduce the amount of surface associated drug. The beta-blockers, being surface active agents (Attwood and Agarwal 1979), are capable of stabilising the emulsion. The aim was to prepare an emulsion with the beta-blocker oriented at the boundaries of the internal aqueous phase in the atomised droplets during spray drying. The active drug substance (66 mg^{*}) was dissolved in 2.5 mL deionised water to comprise the aqueous disperse phase. PLGA (264 mg^{**}) was dissolved in 50 mL DCM (0.53% w/v). The aqueous phase was then added dropwise to the organic solution and was homogenised using an Ultra Turrax T25 homogeniser (IKA-Werke GmbH, Staufen, Germany) at 24 000 rpm for 5 minutes. The resultant emulsion was examined by optical microscopy to investigate its stability immediately after preparation and after standing for 1 hour (approximate time taken to spray dry 50 mL feed solution at a pump rate of 4%). The emulsion was then spray dried according to the appropriate process parameters (see Section 3.3.2), and denoted **batches 7 - 9**. Blank microspheres could not be prepared by this method due to absence of the active, which also acted as the emulsifying agent.

* Limited by the lowest aqueous solubility of the three compounds (atenolol, 26.5 mg/mL).

** To give a theoretical loading of 20% w/w with respect to the total weight of drug and polymer.

In a different set of experiments, polyvinyl alcohol (PVA), a non-ionic macromolecular stabilising agent was added to the emulsion with the aim of competing with, and displacing the drug molecules from the oil/water interface, favouring their accumulation within the aqueous disperse phase. 5 mL of the aqueous phase, comprising of PVA 0.5% w/v in deionised water, and 50 mL of the organic phase (PLGA 1.5% w/v in DCM), were homogenised at 24 000 rpm for 5 min. 130 mg of the active drug substance (atenolol, metoprolol or alprenolol) was then added to the resulting emulsion, to give a theoretical microsphere loading of 15% w/w, and then stirred magnetically for 1 hour before spray drying. The emulsions became completely destabilised upon addition of alprenolol and metoprolol, and an insoluble white precipitate formed. Alprenolol and metoprolol could not therefore be incorporated in this formulation, as a result of the complexation reaction between the drugs and the PVA. The feed solution for the blank microspheres was prepared in the same way, minus the active drug substance. The atenolol and blank emulsions were spray dried, and the harvested microspheres were stored desiccated and protected from light (**batches 10 and 11**).

An alternative method to emulsion formation was to incorporate a suitable surfactant within the organic drug/polymer solution to compete with, and displace the beta-blockers from the droplet surface during spray drying. Sorbitan monostearate (Span 60), a lipophilic nonionic surfactant, was selected. Solutions comprising 2% w/v Span 60, 3% w/v PLGA 50:50 2.5A and drug (equivalent to 20% w/w nominal loading), along with a blank solution prepared in the same way, were spray dried as described in Section 3.3.2, and denoted **batches 12 - 15**.

The composition of each of the batches prepared as described above are summarised in Table 3.3.

Table 3.3: Summary of formulation variables for microsphere preparation by spray drying.

Batch	Drug	Theoretical drug loading (% w/w)	PLGA conc. (% w/v)	Feed type
1	Atenolol	20	0.4	Solution
2	Metoprolol	20	3	Solution
3	Alprenolol	20	3	Solution
4	Blank	N/A	3	Solution
5	Metoprolol	20	17	Solution
6	Alprenolol	6	3	Solution
7	Atenolol	20	0.53	Emulsion
8	Metoprolol	20	0.53	Emulsion
9	Alprenolol	20	0.53	Emulsion
10	Atenolol	15	1.5	Emulsion + PVA
11	Blank	N/A	1.5	Emulsion + PVA
12	Atenolol	20	3	Solution + Span 60
13	Metoprolol	20	3	Solution + Span 60
14	Alprenolol	20	3	Solution + Span 60
15	Blank	N/A	3	Solution + Span 60

3.3.2 Spray Drying

A Büchi B-191 Mini Spray Dryer was used (Büchi Laboratories, Flawil, Switzerland) (see Fig 3.1) with a 0.5 mm nozzle fitted. The various feed solutions were spray dried using the following process parameters unless otherwise stated: inlet temperature 45 °C, outlet temperature 36 - 40 °C, polymer solution feed rate 4%, aspiration ratio 65% and compressed air flow 800 L/h. Yield was calculated as the ratio of the weight of the microspheres obtained relative to the total weight of the drug and polymer used. Where yields were extremely low, additional material was retrieved from the cyclone wall using a plastic spatula to enable characterisation. Microspheres were stored refrigerated and desiccated until further use.

3.3.3 Surface and Internal Microsphere Morphology

The surface morphologies of the microspheres were examined by scanning electron microscopy (SEM). SEM analysis was performed by Mr. D. McCarthy of the SEM service at the University of London, School of Pharmacy. Samples were immobilised on metal stubs by brushing the microspheres over a piece of double sided adhesive carbon tape. The sample was then sputter-coated with gold atoms using a K550 machine (Emitech Ltd., Ashford, Kent, UK) and then visualised using a XL20 electron microscope (Philips, Eindhoven, Netherlands). Microspheres were typically imaged within 24 h of preparation unless otherwise stated.

For visualisation of the internal structure of the microspheres, the samples were first embedded in resin, frozen in liquid nitrogen, sectioned using a microtome, then examined by SEM as described above.

3.3.4 Particle Size Analysis

Particle size analysis of the spray dried microspheres was performed by laser diffraction, using a Malvern Mastersizer X (Malvern Ltd., Worcestershire, UK). The instrument is equipped with a He-Ne 632.8 nm laser diffraction source and operates over a 0.5 - 900 μm particle size range. A Malvern MS7 magnetically stirred small volume (15 mL) diffraction cell was used.

The following method was used, based on the guidance given in the standard operating procedure for particle size analysis by laser diffraction (ISO 13320-1 1999). Approximately 10 mg microspheres were added to approximately 1 mL of 0.5% w/v Tween 80 in deionised water then sonicated briefly (XB6 Ultrasonic Bath, Grant Instruments Ltd., Royston, Herts, UK) to aid dispersion. Brief sonication was used to assist dispersion of the samples, bearing in mind that too much ultrasound may fracture friable particles, or cause agglomeration due to the increased rate of particle-particle collision (Ward-Smith et al. 2002). The sample was then pipetted dropwise into the cell until a suitable obscuration value was achieved (10 - 15%). The stir speed was chosen so as to effectively suspend all the material without causing air entrainment. Each sample was read in triplicate and the mean $D(v,0.5)$ value, also known as the volume median diameter (VMD) was reported ($n = 3$).

The particle size distributions are calculated from the analysis of the intensity of scattered light at various angles, with the angle of diffraction being inversely proportional to particle diameter. The Mie theory was used to generate a particle size distribution from the diffraction data, which required the input of the refractive indices

(RI) of the suspending medium and of the particles (real and imaginary components). The RI of water is known (1.33), but since the microspheres are composite particles, no literature RI value was available. Owing to the sphericity and transparency of the spray dried microspheres prepared, values of 1.6 and 0.00 (real and imaginary components respectively) were chosen.

3.3.5 Drug Loading

The amount of drug recovered from the spray dried microspheres was determined using a simple liquid-liquid extraction technique. Approximately 10 mg microspheres (accurately weighed) were dissolved in 1 mL DCM within a 15 mL centrifuge tube (Corning). 10 mL deionised water was then added and the tubes were shaken in a shaking water bath (Clifton Shaking Bath, Nickel Electro Ltd., England) at 37 °C for 2 hours, a time previously shown to be adequate for the drug to partition into the aqueous phase. The two phases were then separated by centrifugation (3K30 Refrigerated centrifuge, Sigma Laborzentrifuges GmbH, Osterode am Harz, Germany) (10 min, 10 000 rpm) after which the aqueous phase was sampled, filtered through a 0.2 µm syringe filter (Millex GV) and analysed by UV spectroscopy. The blank sample was prepared as above, using blank microspheres (batch 4). Measured drug concentrations were adjusted using the extraction efficiency factor described in the following section (Section 3.3.6), and encapsulation efficiency was calculated as the ratio of the actual to the theoretical loading of the drug in the microspheres. Each determination was carried out in triplicate (i.e. 3 samples from the same batch) and reported as the mean value. It is noteworthy that this method does not discriminate between encapsulated and surface associated drug.

3.3.6 Extraction Efficiency

In order to calculate the actual loading, the efficiency of the extraction procedure was determined. This was achieved by extracting known concentrations of drug from equivalent solutions of drug and polymer in dichloromethane over the appropriate concentration range, and under the same conditions. This figure was then used to adjust the encapsulation efficiency and loading calculations.

Stock solutions of active drug substance (Stock A) and PLGA (Stock B) in DCM were prepared, each at a concentration of 10 mg/mL. Appropriate volumes of each stock solution were pipetted into centrifuge tubes to represent 10 mg microspheres (with nominal loading 0 - 25% w/w) dissolved in 1 mL DCM (see Table 3.4). 10 mL water was then added. Samples were shaken at 37 °C for 2 hr, then centrifuged at 10 000 rpm for 10 minutes to separate the phases. Samples were analysed at the corresponding λ_{max} , against the 0% nominal loading blank. Standard solutions of 0.1 mg/mL active in deionised water were prepared and were used to calculate the concentration of drug in the aqueous phase, and expressed as a percentage of the nominal concentration to give extraction efficiency.

Table 3.4: Preparation of samples for the determination of extraction efficiency, where Stock A and Stock B are 10 mg/mL solutions of active and PLGA respectively in DCM.

Nominal loading (% w/w)	Vol. stock A (mL)	Vol. stock B (mL)
0	0	1
5	0.05	0.95
10	0.10	0.90
15	0.15	0.85
20	0.20	0.80
25	0.25	0.75

3.3.7 Release Studies

Phosphate buffered saline (PBS) pH 7.4 used in the dissolution studies was prepared by dissolving the following solids in approximately 800 mL deionised water (BP 2003).

- Disodium hydrogen orthophosphate 2.38 g
- Potassium dihydrogen orthophosphate 0.19 g
- Sodium chloride 8.0 g

The resultant solution was then adjusted to pH 7.4 with 1 M HCl if necessary, before being made up to 1000 mL with deionised water. 1 g Tween 80 (i.e. 0.1% w/v) was then added to aid wetting and dispersion of the microspheres, and 0.1 g sodium azide (0.01% w/v) was added as a bacteriostatic agent.

In vitro dissolution testing was carried out in triplicate at 37 °C. 5 - 10 mg microspheres (accurately weighed) were suspended in a 15 mL Corning centrifuge tube containing 10 mL of the dissolution medium. The samples were placed in a shaking water bath maintained at 37 °C. Sample tubes were removed at predetermined time intervals and centrifuged for 30 s at 15 000 rpm to cause sedimentation of the microspheres. 1 mL of

the supernatant was removed using a Gilson pipette and was passed through a 0.2 μm syringe filter (Millex GV) in preparation for UV analysis. The sample volume was replaced with 1 mL of fresh dissolution medium (pre-warmed to 37 $^{\circ}\text{C}$), the microspheres were resuspended by brief sonication, and the sample tubes were returned to the waterbath.

The assay was carried out as follows: Working standard solutions of each drug were prepared in duplicate, by accurately weighing 10 mg drug into a 100 mL volumetric flask and making up to volume with dissolution medium (PBS pH 7.4 with Tween 80 0.1% w/v and sodium azide 0.01% w/v). This solution was then diluted 1 in 10 to give a solution of 0.1 mg/mL. These working standard solutions were assayed prior to each run and used to calculate the concentration of drug in the dissolution medium. Linearity of the assay of the beta-blockers in PBS has been previously demonstrated (see Section 2.4.2.1). Absorbance was measured at the corresponding λ_{max} of each compound (273 nm for atenolol and metoprolol, 269 nm for alprenolol) against a blank of fresh dissolution medium, and in triplicate. Samples from the dissolution studies were diluted to within this concentration range with fresh dissolution medium when necessary.

The cumulative amount of drug released was calculated according to Equation 3.1, which takes into consideration the dilutions caused by sample volume replacement, and expressed as a percentage of the mean amount recovered in the drug loading study (see Section 3.3.5).

$$R_n = 100 \cdot \left\{ \left[\frac{C_n V + C_{n-1} V_s}{V} \right] / D \right\}$$

Equation 3.1: Calculation of the cumulative % drug released during the *in vitro* dissolution studies, where R_n is the % cumulative release at time-point n , C_n is the concentration at time-point n , V is the volume of dissolution medium, V_s is the volume of supernatant medium withdrawn at each time point and D is the drug content of the sample (as determined in the drug loading study) (adapted from Clarke et al. 2005).

3.3.8 Residual Solvent

Residual solvent for a selection of solution spray dried batches was determined approximately two weeks post preparation (equivalent to the approximate time between spray drying and *in vitro* dissolution testing). A nuclear magnetic resonance (NMR) spectroscopy method for quantifying residual dichloromethane in PLGA microspheres was employed (obtained by personal communication from Jonathan Booth, AstraZeneca, Macclesfield, UK). 30 mg of sample and 20 mg of sodium formate (as the reference standard) were accurately weighed into the same vessel. 1 mL of d_4 -acetic acid was added, and the sample was sonicated for 15 min to ensure the sample and standard were completely dissolved. The solution was then transferred into a 5 mm NMR tube. High field proton NMR was recorded on a Bruker Avance 400 MHz NMR spectrometer (Bruker, Karlsruhe, Germany) using a 45 degree pulse and a 60 second pulse repetition time.

The spectrum was referenced by setting the chemical shift of the methyl signals due to residual acetic acid to 2.03 ppm. Accurate integrals for the sodium formate singlet absorption at 8.2 ppm and residual dichloromethane (at 5.4 ppm) were obtained using the MestRe-C NMR data processing software (Mestrelab Research, Spain).

The strength of the DCM signal was calculated using Equation 3.2:

$$S_s = (I_s \times W_r \times M_s \times N_r \times S_r) / (I_r \times W_s \times M_r \times N_s)$$

Equation 3.2: Calculation of residual solvent where S = strength N = number of protons, M = molecular weight, W = weight and I = integral, of the sample (s) and reference standard, sodium formate (r).

3.4 Results and Discussion

3.4.1 Extraction Efficiency

The mean absorbance values obtained from the UV analysis of the extraction efficiency samples were plotted against nominal percentage drug concentration, as illustrated in Figure 3.2. The assay showed excellent linearity over the 0 - 25% w/w loading range, with R^2 values of 0.999, 0.999 and 0.997 for alprenolol, metoprolol and atenolol respectively.

Calculated extraction efficiencies approximated to 100% for all three compounds over the nominal loading range of 5% to 25% (Table 3.5) therefore no adjustment to drug loading calculations was required.

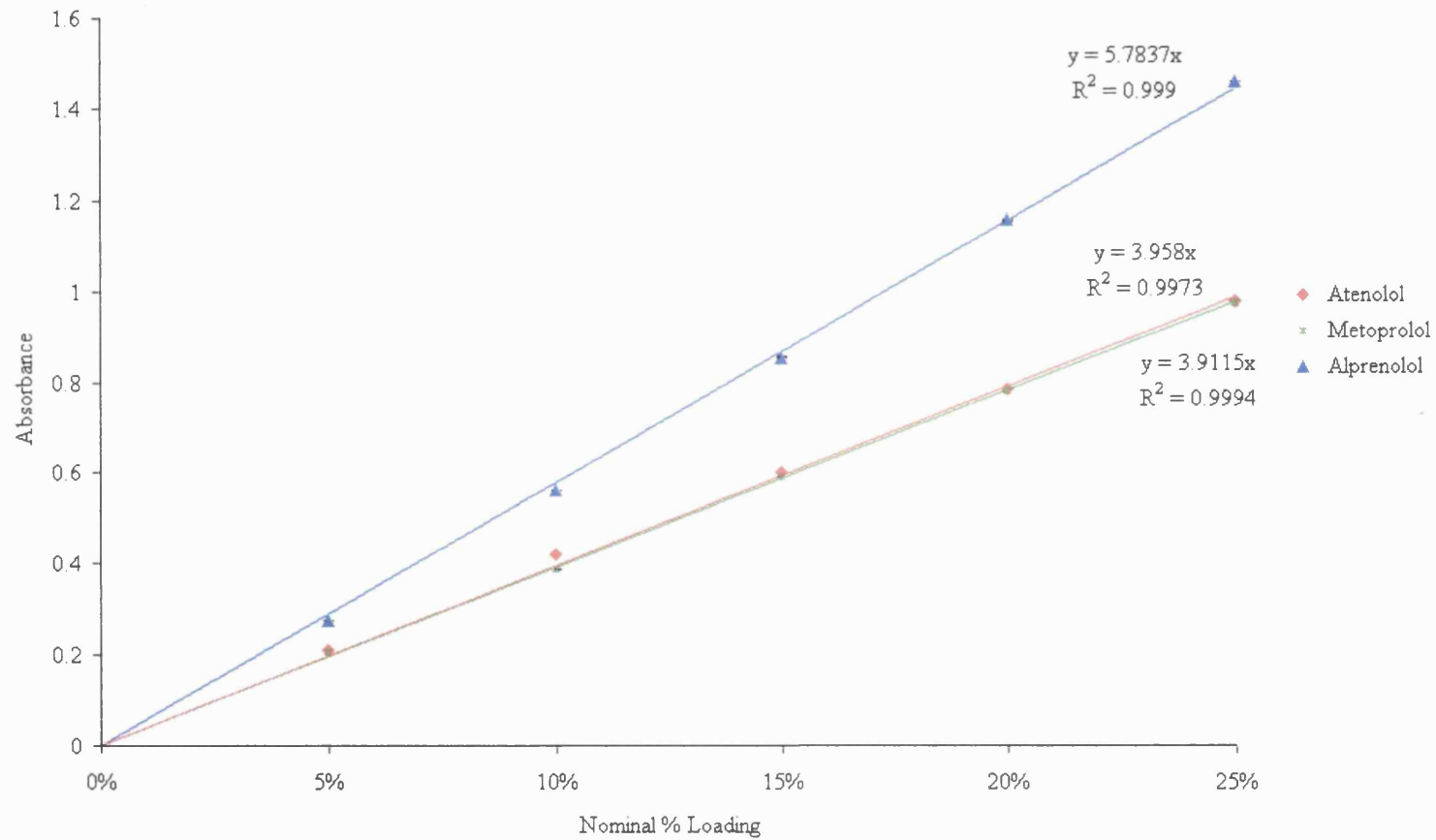


Figure 3.2: Liquid-liquid extraction of atenolol, metoprolol tartrate and alprenolol HCl from dichloromethane to deionised water, determined by UV spectroscopy at 273 nm for atenolol and metoprolol, and 269 nm for alprenolol.

Table 3.5: Calculation of efficiency of extraction of each drug substance from a solution of drug and polymer in 1 mL DCM, into 10 mL deionised water, over the range of 0 - 25% theoretical loading.

		Atenolol		Metoprolol		Alprenolol	
Nominal loading (%)	Nominal drug conc. in aq. phase (mg/mL)	Measured conc. (mg/mL)	Extraction efficiency (%)	Measured conc. (mg/mL)	Extraction efficiency (%)	Measured conc. (mg/mL)	Extraction efficiency (%)
5	0.045	0.048	104.69	0.047	104.12	0.043	94.47
10	0.091	0.095	104.82	0.088	96.62	0.087	96.17
15	0.136	0.136	99.58	0.134	98.46	0.133	97.68
20	0.182	0.178	97.68	0.178	97.65	0.180	99.19
25	0.227	0.222	97.48	0.221	97.38	0.228	100.13
Mean % extraction efficiency ± SD (n = 5)		100.85 ± 3.66		98.84 ± 3.02		97.53 ± 2.28	

3.4.2 Characterisation of Solution Spray Dried Microspheres

Microspheres were successfully spray dried from solutions of polymer and drug (20% w/w nominal loading), with yields of 18.6%, 29.8% and 27.7% for atenolol, metoprolol and alprenolol respectively. SEM images are shown in Figure 3.3. Figures 3.3 b-d, prepared from solutions with 3% w/v PLGA in the feed solution reveal products with smooth and spherical surface morphology and in the approximate size range of < 1 – 10 μm diameter. The atenolol loaded spheres with 0.4% w/v PLGA were irregular in shape with a ‘deflated’ appearance (Fig. 3.3a). This has been previously observed with microspheres spray dried using a low polymer content, where significant deformation of the shape of droplets occurs during solvent evaporation and microsphere hardening (Wang and Wang 2002a).

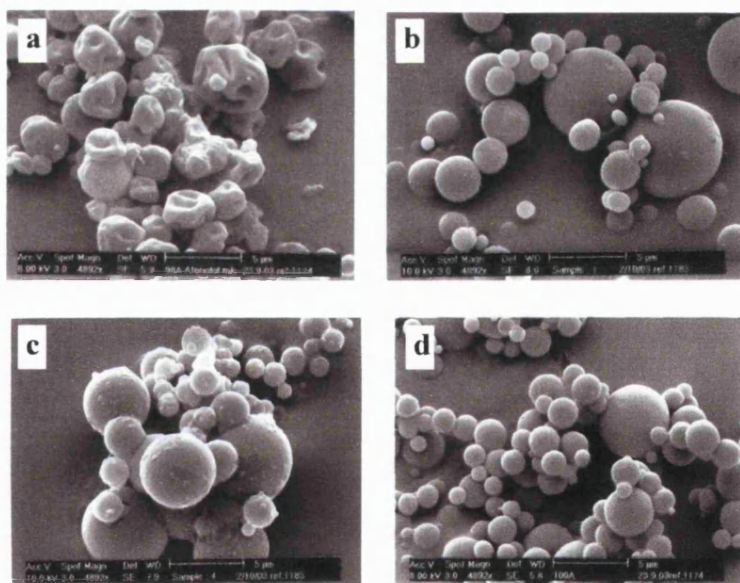


Figure 3.3: SEM images of solution spray dried microspheres loaded with a) atenolol, b) metoprolol c) alprenolol and d) blank (batches 1 - 4, 5 μm scale bar).

The properties of the microspheres prepared by this method are given in Table 3.6. Representative particle size distributions of the three drug loaded microsphere batches are illustrated in Fig.3.4.

Table 3.6: Properties of microspheres prepared by solution spray drying. *Cross reference batch numbers with Table 3.3 for feed solution properties.

Batch *	Drug	Yield (%)	Mean % loading \pm SD ($n = 3$)	Mean encapsulation efficiency (%)	Mean D(v,0.5) \pm SD ($n = 3$, μm)
1	Atenolol	18.6	18.0 \pm 0.36	89.9	3.4 \pm 0.1
2	Metoprolol	29.8	12.1 \pm 0.11	60.5	5.9 \pm 0.0
3	Alprenolol	27.7	12.7 \pm 0.42	63.3	6.2 \pm 0.0
4	N/A	5.2	N/A	N/A	5.4 \pm 0.0

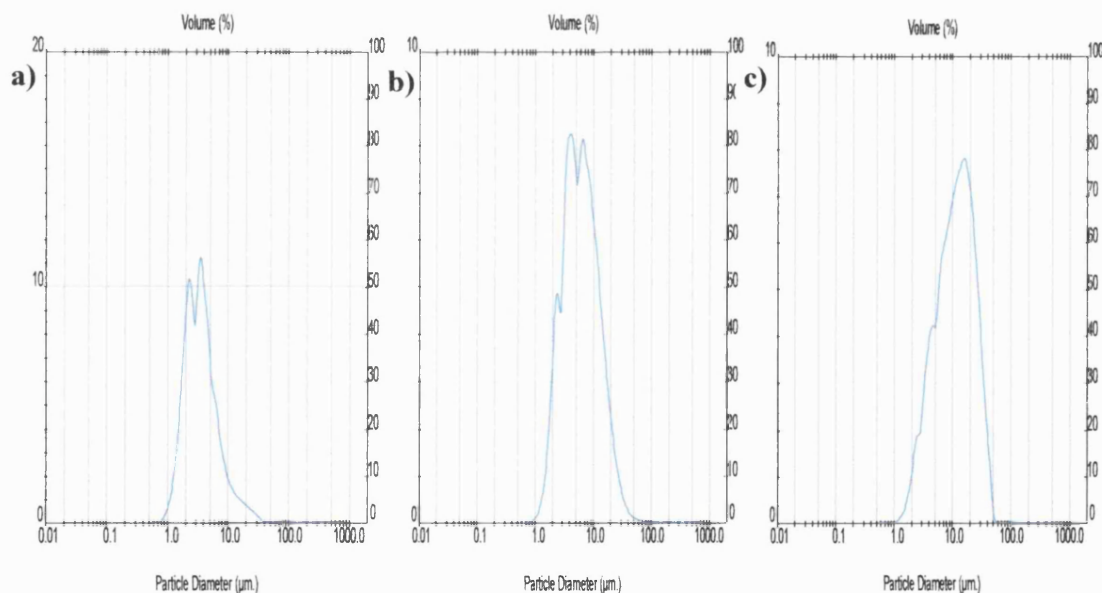


Figure 3.4: Representative particle size distributions of a) atenolol, b) metoprolol and c) alprenolol loaded solution spray dried microspheres determined by laser diffraction.

Attempts were made to view the internal morphology of the solution spray dried microspheres by SEM. However, they proved difficult to section using the equipment available due to their small size and malleable nature. Also, owing to the relatively low glass transition temperature of the PLGA (43.6 °C), the samples were subject to deformation upon focusing of the electron beam during SEM. By embedding the samples in resin, freezing in liquid nitrogen and sectioning using a microtome, the images shown in Figure 3.5 were obtained. The microspheres appear to be slightly porous, or ‘honeycomb’ in nature, but not hollow. This indicates that under the process conditions employed, a polymeric matrix is formed suitable for the entrapment of drug.

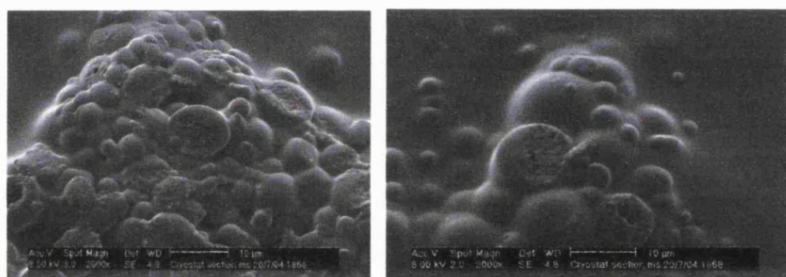


Figure 3.5: SEM images of metoprolol loaded solution spray dried microspheres (batch 2) showing internal morphology.

The cumulative percentage drug release-time profiles from batches 1 - 3 are shown in Table 3.7 and illustrated in Figure 3.6. Very high burst release was recorded, with 61.9, 76.0 and 87.5% of the encapsulated metoprolol, alprenolol and atenolol respectively released by the time of the first measurement (0.1 hr). Due to the near total release of entrapped active within the first 4 hours, studies were terminated prematurely. Repeated measures ANOVA revealed a statistically significant difference ($F(2,6) = 137.3$, $p < 0.05$) between the three groups. Atenolol, the most hydrophilic of the compounds was released significantly faster and more extensively than either metoprolol or alprenolol.

This is in agreement with the hypothesis that hydrophilic compounds partition more readily from the lipophilic environment of the polymeric matrix into the aqueous dissolution medium. The other two compounds, however, did not follow this hypothesised trend, possibly indicating a more complex interaction between the drug and polymer. However, care must be taken when drawing conclusions from these data owing to the fact that the atenolol loaded microspheres were prepared from a lower viscosity feed solution than the metoprolol and alprenolol formulations (0.4% w/v *cf* 3% w/v). This resulted in smaller particles with irregular morphology, which could also account for the comparative rapidity of release. The high initial release suggests that none of the compounds were sufficiently entrapped within the matrix, and release was by rapid diffusion from the microsphere surface and/or pores within the polymer matrix. This formulation does not provide sustained release *in vitro*, and was therefore deemed unsuitable to be studied *in vivo*.

Table 3.7: Cumulative % drug release from solution spray dried microspheres (batches 1 - 3).

Mean cumulative % release \pm SD ($n = 3$)			
Time (hr)	Atenolol	Metoprolol	Alprenolol
0	0.0	0.0	0.0
0.1	87.5 \pm 2.3	61.9 \pm 0.3	76.0 \pm 2.3
0.5	92.9 \pm 2.4	68.5 \pm 0.6	80.2 \pm 1.8
1	94.6 \pm 1.1	72.7 \pm 1.3	80.1 \pm 1.9
2	97.0 \pm 1.0	78.7 \pm 1.6	85.0 \pm 1.8
3	99.7 \pm 1.9	80.9 \pm 2.0	88.2 \pm 3.1
4	102.0 \pm 2.0	81.7 \pm 2.2	89.5 \pm 2.7

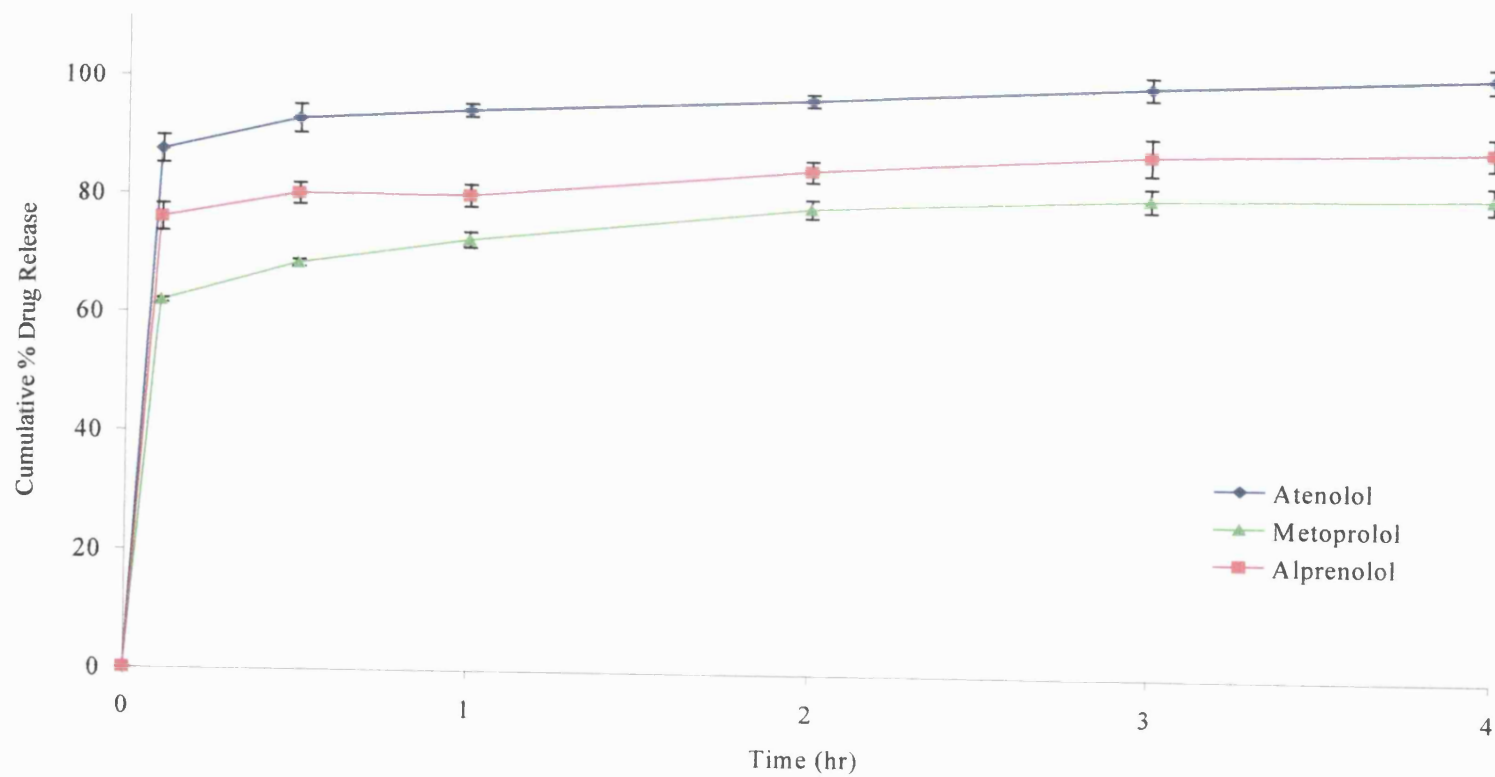


Figure 3.6: *In vitro* drug release profiles from solution spray dried microspheres, batches 1 - 3 ($n = 3 \pm SD$).

The residual solvent of a selection of solution spray dried batches was measured by NMR (see Fig. 3.7). Figure 3.7c is the trace obtained from spiking a sample with approximately 0.1 mL DCM, resulting in a peak at 5.4 ppm. No detectable peak at 5.4 ppm was seen in any of the other runs, indicating that none of the batches tested had any residual DCM detectable by this method. High residual solvent can therefore be excluded as a factor contributing to the high burst release from these formulations.

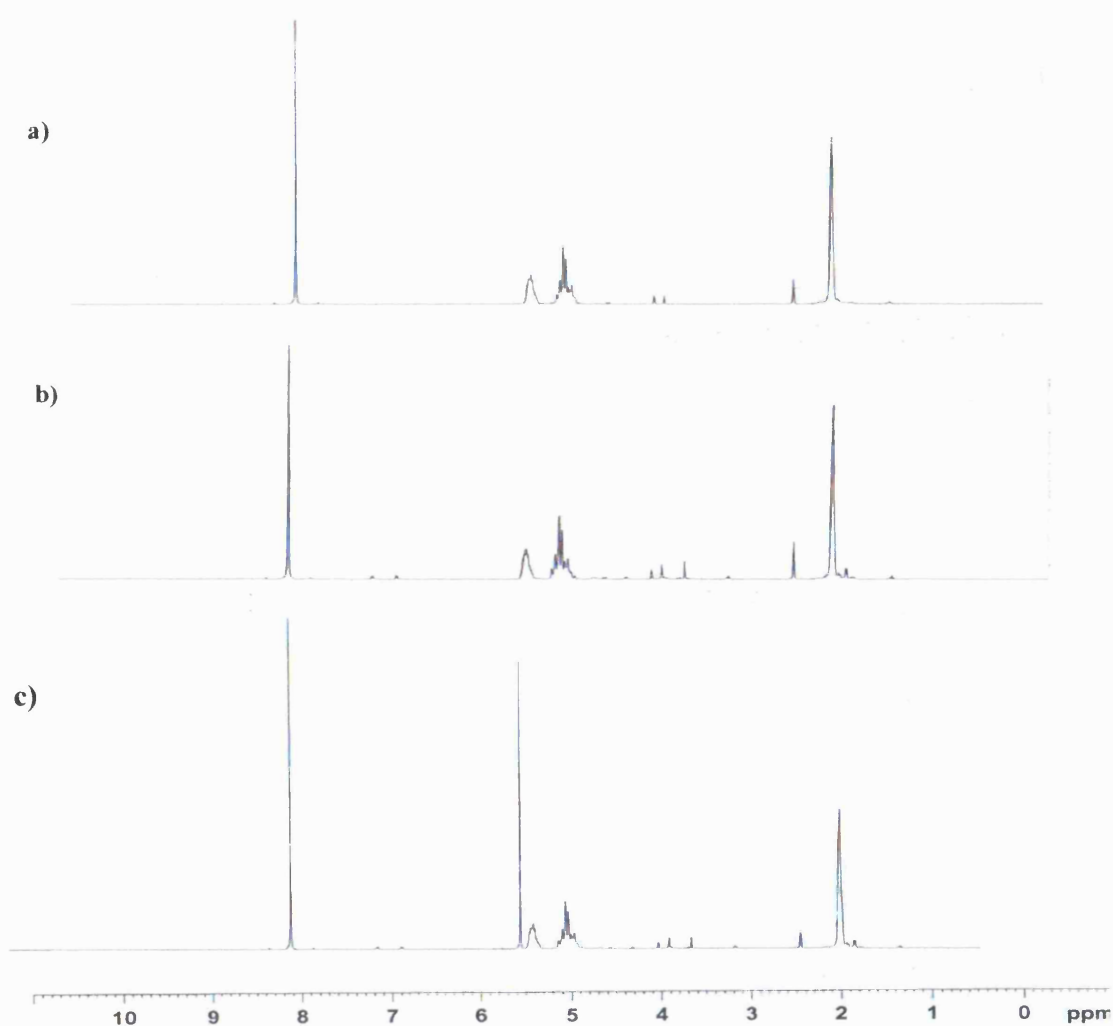


Figure 3.7: NMR of microspheres from (a) blank (batch 4), (b) metoprolol loaded (batch 2), (c) metoprolol loaded (batch 2) spiked with approx. 0.1 mL DCM for the quantitative determination of residual DCM, showing the acetic acid peak at 2.03 ppm, sodium formate (standard) at 8.2 ppm and DCM at 5.4 ppm

In an attempt to improve the drug release profile, a metoprolol loaded (20% w/w) batch was prepared from a feed solution high in PLGA content (17% w/v), with the aim of increasing microsphere size (batch 5). From the SEM micrograph (Fig. 3.8), the particles do indeed appear larger in size, but were agglomerated, incompletely formed and contained polymeric threads. The higher viscosity of the feed solution is thought to lead to poorer atomisation in the spray dryer, resulting in the observed morphology (Wang and Wang 2002b). This morphology could lead to syringeability and injectability problems. No further characterisation of this batch was therefore carried out.

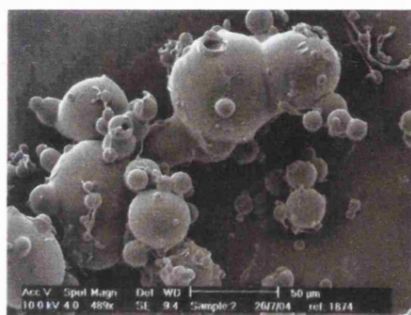


Figure 3.8: SEM of microspheres prepared from a high viscosity feed solution, comprising metoprolol (20% w/w) and PLGA 17% w/v (batch 5).

Another formulation approach employed in an attempt to reduce burst release was a reduction in drug loading, from 20% w/w to 6% w/w. High drug loading has been cited as a cause of dose dumping due to increased osmotic pressure and channel formation (Blanco-Prieto et al. 2000). However, alprenolol loaded microspheres prepared with a lower nominal percentage drug loading (6% w/w, batch 6) also exhibited a very high burst, with approximately 100 % drug release within the first 4 hours (data not shown).

These simple modifications to the solution spray drying process failed to produce an acceptable product. Emulsion spray drying was therefore explored, the outcome of which is described in the following sections.

3.4.3 Characterisation of Emulsion Spray Dried Microspheres.

Optical microscopy photographs of the emulsion prepared with alprenolol, chosen as an example, are shown in Figure 3.9. Figure 3.9a shows the emulsion approximately 5 minutes post preparation, and reveals a dispersed phase composed of droplets of regular shape and uniform size. Figure 3.9b shows the same emulsion 1 hour later. No detectable changes in dispersed phase droplet size were seen, indicating the absence of coalescence over this time interval. The emulsion was therefore deemed sufficiently stable for spray drying. Product yields were 31.5%, 24.9% and 26.9% for atenolol, metoprolol and alprenolol respectively. The characteristics of the emulsion spray dried microspheres are summarised in Table 3.8.

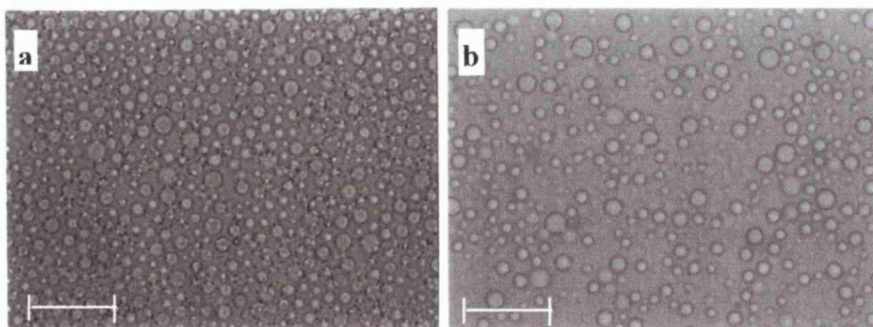


Figure 3.9: Optical microscopy photographs of the emulsion prepared with alprenolol (a) immediately after preparation, (b) 1 hour after preparation (scale bar represents 10 μm).

Table 3.8: Summary of physical characteristics of emulsion spray dried microspheres.

Batch	Drug	Yield (%)	Mean % loading \pm SD ($n = 3$)	Mean encapsulation efficiency (%)	Mean D(v, 0.5) (μm) \pm SD ($n = 3$)
7	Atenolol	31.5	12.1 \pm 0.1	72.9	5.0 \pm 0.03
8	Metoprolol	24.9	11.8 \pm 0.2	70.7	4.3 \pm 0.03
9	Alprenolol	26.9	8.3 \pm 0.2	49.4	5.5 \pm 0.02

SEM images of the microspheres prepared by emulsion spray drying (Fig. 3.10) revealed irregular, non-spherical particles, attributable to the deformation of the shape of droplets during the spray drying of a low viscosity feed solution (0.53% w/v PLGA) at a slow pump rate.

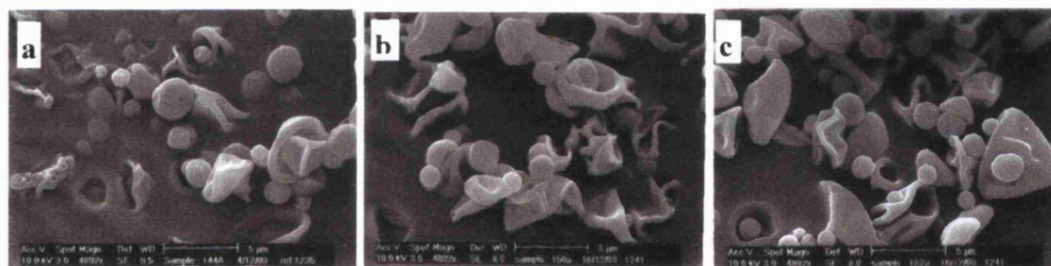


Figure 3.10: SEM images of emulsion spray dried a) atenolol, b) metoprolol and c) alprenolol loaded microspheres (batches 7, 8 and 9).

The cumulative percentage release of active from these emulsion spray dried microspheres is reported in Table 3.9, and is illustrated in Fig 3.11. Once again drug release was rapid and extensive within the 21 hr observation period, rendering this formulation unsuitable for *in vivo* studies.

Table 3.9: Mean cumulative % drug release from emulsion spray dried microspheres (batches 7, 8 and 9).

Mean cumulative % release \pm SD ($n = 3$)			
Time (hr)	Atenolol	Metoprolol	Alprenolol
0	0.00	0.00	0.00
0.1	67.05 \pm 1.7	64.97 \pm 2.1	54.47 \pm 8.0
0.5	71.22 \pm 1.2	71.57 \pm 1.1	62.13 \pm 5.8
1	77.87 \pm 3.9	73.93 \pm 1.0	65.53 \pm 5.5
2	80.88 \pm 3.2	77.77 \pm 0.8	68.83 \pm 5.4
21	93.60 \pm 2.9	92.90 \pm 1.7	84.73 \pm 4.0

The high burst release observed suggests that drug remained accumulated at the microsphere surface, despite attempting to redistribute it by emulsification of the feed solution. It was hypothesised that the use of a stabilising agent (polyvinyl alcohol, PVA) to displace the beta-blockers from the oil/water interface, encouraging their accumulation within the internal aqueous phase, could reduce the initial burst release. The result of the incorporation of PVA within the emulsified feed solution is discussed in the following section (Section 3.4.4).

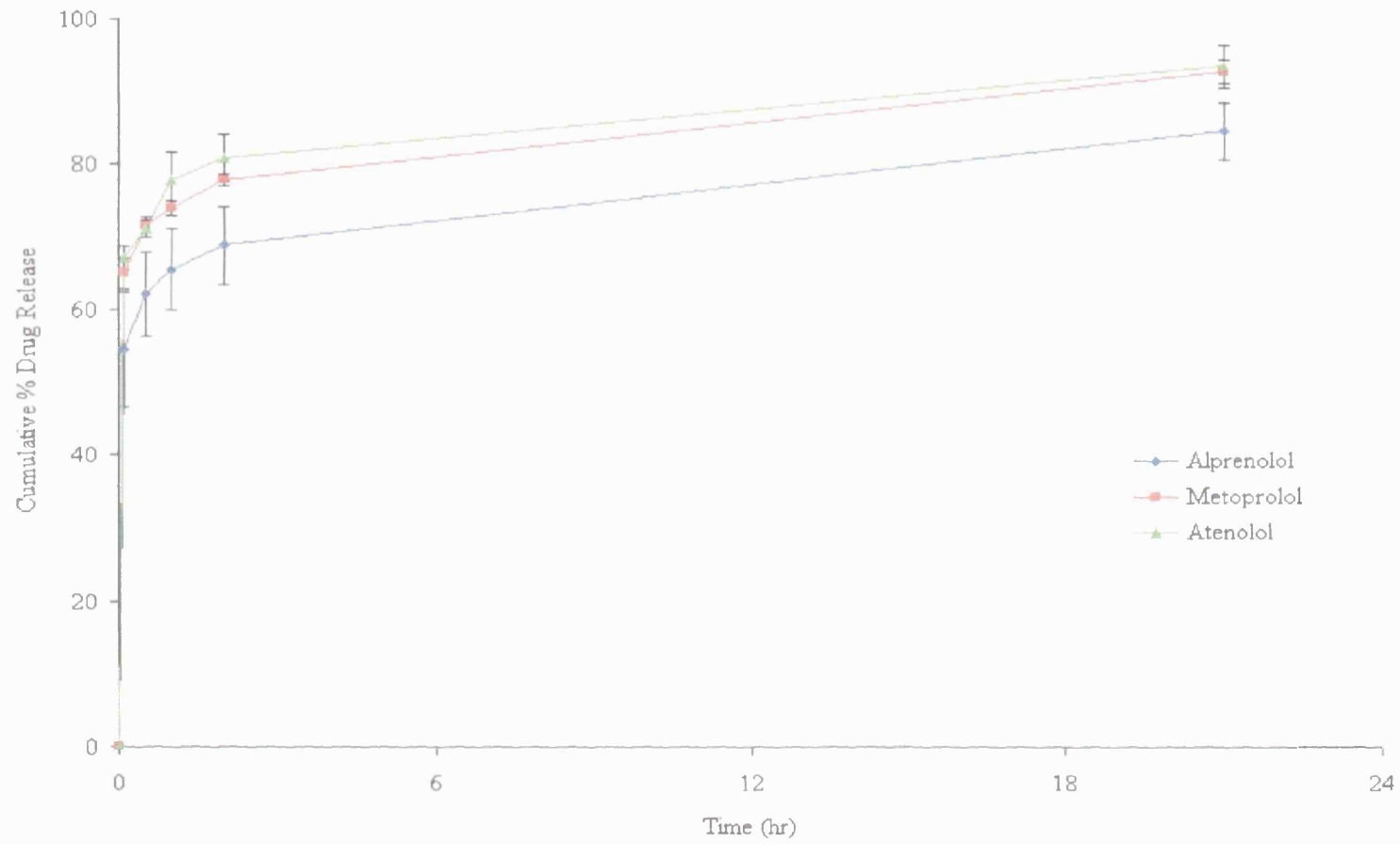


Figure 3.11: *In vitro* drug release profiles from emulsion spray dried microspheres, batches 7 - 9 ($n = 3 \pm SD$).

3.4.4 Emulsion Spray Dried Microspheres with PVA

As discussed in Section 3.3.1, alprenolol and metoprolol underwent a complexation reaction with the PVA, leading to emulsion destabilisation and salt precipitation. In contrast, the blank and atenolol containing emulsions appeared stable under optical microscopy and were spray dried successfully (batches 10 and 11), with yields of 14.8% and 24.8% respectively. SEM images reveal a mixture of spherical and irregular shaped particles, possibly attributable to the intermediate concentration of PLGA used (1.5% w/v), or as a consequence of emulsification or PVA addition (see Fig. 3.12).

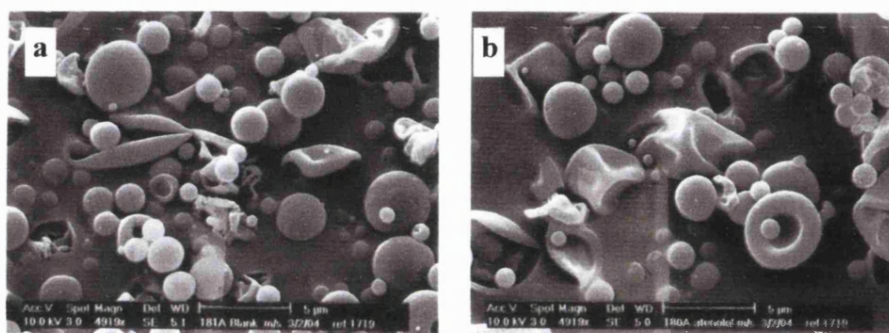
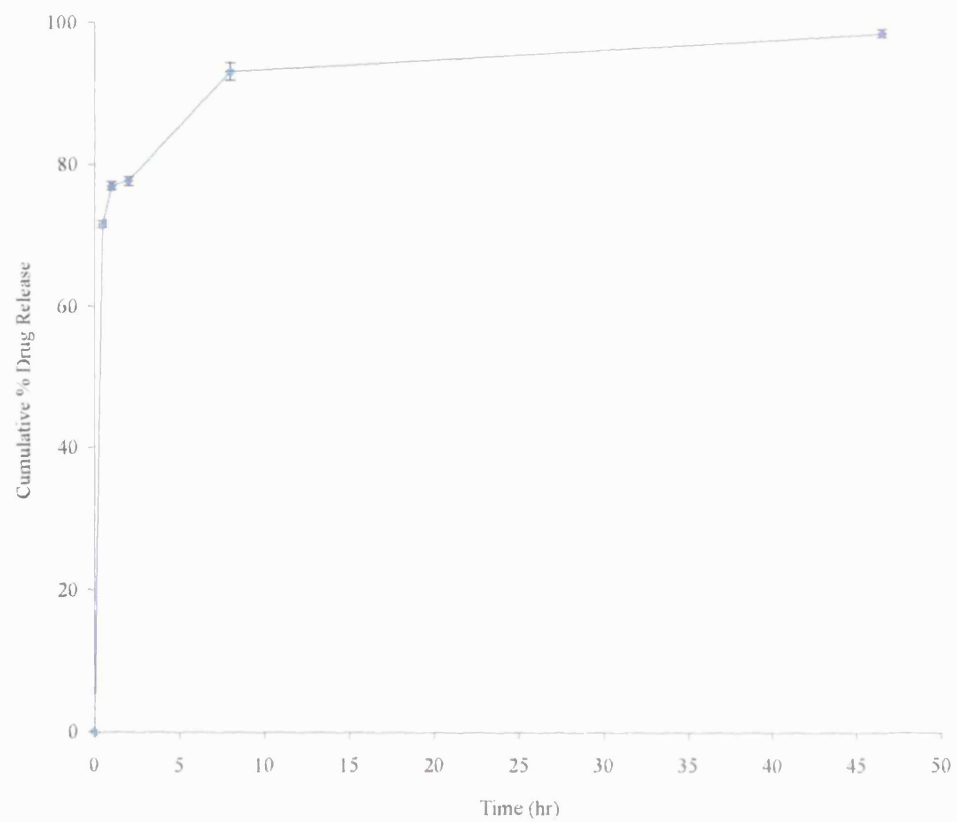


Figure 3.12: SEM images of (a) blank and (b) atenolol loaded microspheres with PVA.

A mean drug loading of $12.1\% \pm 3.5$ ($n = 3$), i.e. a mean loading efficiency of 82.2% was achieved. Drug release data is illustrated in Fig. 3.13. Once again, a very high burst release was observed, with approximately 77% of the encapsulated drug being released within the first hour of the study, and 93% released after just 8 hours incubation. This attempt to modify the release profile was therefore deemed unsuccessful.

The following section describes the results of the addition of a competing surfactant (Span 60) to the drug/polymer solution, aiming to displace the beta-blockers from the air/solvent interface of the atomised droplet during spray drying, thereby reducing surface associated drug and burst release.



Time (hr)	Mean cumulative % atenolol release ± SD (n=3)
0	0.00
0.5	71.58 ± 0.50
1	76.95 ± 0.58
2	77.63 ± 0.59
8	93.14 ± 1.26
46.5	98.63 ± 0.54
76	100.40 ± 0.41

Figure 3.13: *In vitro* release profile of atenolol from emulsion spray dried microspheres with PVA, batch 10 ($n = 3 \pm SD$).

3.4.5 Solution Spray Dried Microspheres with Span 60

During the spray drying of feed solutions containing Span 60 2% w/v, a large amount of 'sticky' product was observed to deposit on the walls of the drying apparatus. SEM pictures reveal that the spray dried products did not consist of discrete spheres, but appeared as agglomerates of irregularly shaped particles (Fig. 3.14), and some fractured, hollow shells were apparent (Fig. 3.14 b). Since the outlet temperature was not observed to exceed 42 °C, the glass transition temperature (T_g) of the polymer was not exceeded. It is possible that the surfactant plasticised the PLGA, thereby lowering the T_g of the polymer. This formulation was deemed unsuitable for further characterisation.

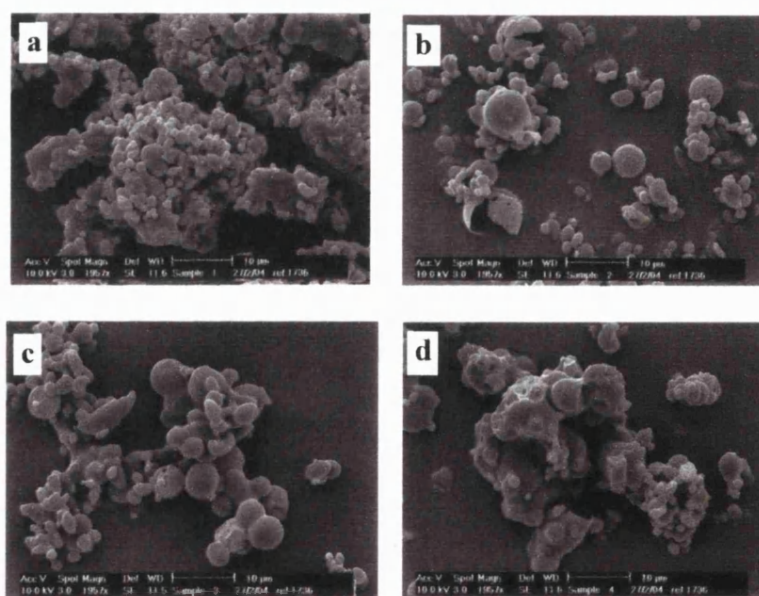


Figure 3.14: SEM images of a) atenolol b) metoprolol and c) alprenolol loaded microspheres spray dried from solutions of drug (20% w/w loading), PLGA (3% w/v) and Span 60 (2% w/v). Figure d) shows blank microspheres (10 µm scale bar).

3.5 Conclusions

Beta-blocker loaded microspheres spray dried from a solution of drug and polymer in dichloromethane under the conditions employed in this study did not act as slow release drug delivery devices. The formulations suffered from a very high initial burst, with the majority of the contents released within the first few hours of the study. This remained the case despite attempts at emulsion spray drying and the incorporation of Span 60 and PVA as molecules competing for the droplet surface.

Beta-blockers are known to be surface active (Attwood and Agarwal 1979), as exemplified by their membrane stabilising actions and local anaesthetic effects (Florence and Attwood 2005). Their amphiphilic structure may result in orientation of the active at the solvent/air interface during spray drying, causing drug accumulation at the droplet surface. Subsequently, drug would be concentrated at the dried microsphere surface, offering a possible explanation for the immediate release seen.

In the next chapter, the attempts to overcome the immediate release, based on the surface activity hypothesis, using hydrophobic ion pairing, are discussed.

Chapter 4

Hydrophobic Ion Pairing as a Strategy for Achieving Sustained Release of Beta-Blockers from Spray Dried Polymeric Microspheres

4 Hydrophobic Ion Pairing as a Strategy for Achieving Sustained Release of Beta-Blockers from Spray Dried Polymeric Microspheres

4.1 Introduction

As discussed in the previous chapter, beta-blocker loaded microspheres suffered very high burst release and near-total release of active within the first few hours of incubation, despite numerous attempts to modify the release profile. Hydrophobic ion pairing has been highlighted as a potential strategy for improving the incorporation of ionic compounds within the non-aqueous environment of polymeric microspheres (Falk et al. 1997; Choi and Park 2000). The technique has also been shown to reduce burst release from spray dried microspheres, exemplified by the ion pairing of leuprolide acetate with sodium oleate (Alcock et al. 2002). Hydrophobic ion pairing involves the stoichiometric replacement of the polar counterions (e.g. chloride and tartrate) with a more hydrophobic moiety, and has the combined effect of reducing aqueous solubility and increasing the solubility of the compound in organic solvents (Meyer and Manning 1998). In this chapter, ion pairing of the beta blockers was attempted with the aim of altering the distribution of the drug within the polymer matrix, through a combination of altering solubility properties and surface activity, to reduce burst effect and achieve slow release of the actives.

The three beta-blockers (atenolol, metoprolol and alprenolol) possess an ionisable secondary amine functionality ($pK_a \sim 9.6, 9.7$ and 9.7 for atenolol, metoprolol and alprenolol respectively). A weakly acidic amphiphilic molecule (sodium octanoate) was

therefore chosen as an appropriate ion pairing agent*. The structure of sodium octanoate and a schematic diagram describing the ion pairing process is illustrated in Fig 4.1 below.

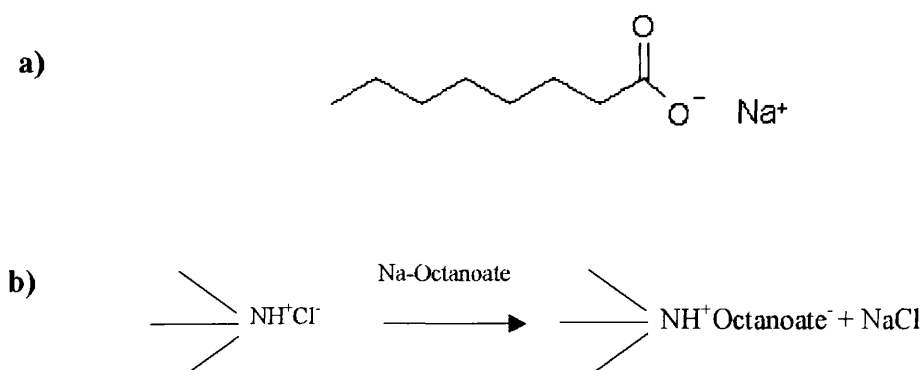


Figure 4.1: a) Structure of sodium octanoate ($C_8H_{15}O_2Na$)
 b) Scheme for the formation of a hydrophobic ion paired complex between a beta-blocker ($R-NHCl$) and sodium octanoate.

Ion pair formation between the beta-blockers and octanoate in aqueous solution was investigated by measuring changes in *i*) the concentration of beta-blocker remaining in solution and *ii*) solution turbidity, as a function of drug:octanoate molar ratio. After optimisation of the ion pairing process, the resultant ion pair complex was harvested and freeze dried. Melting points of the hydrophobic ion pairs (HIPs) were measured to confirm complex formation and apparent octanol/buffer partition coefficients (P_{app}) were determined. The HIPs were then encapsulated within PLGA microspheres by spray drying, and the microspheres were subsequently characterised by scanning electron microscopy (SEM), laser diffraction and *in vitro* dissolution testing as previously described. Successful formulations were formulated into suspensions for subcutaneous injection for *in vivo* investigation.

* The sodium salt was used since octanoic acid is immiscible with water.

4.2 Materials

The beta-blockers (atenolol (as free base), metoprolol tartrate and alprenolol hydrochloride) and the ion pairing agent sodium octanoate were purchased from Sigma-Aldrich Co. (Poole, Dorset, UK). Sodium carboxymethylcellulose (CMC) used in injection vehicle preparation was also purchased from Sigma-Aldrich. All other materials were obtained as described in previous chapters.

4.3 Methods

4.3.1 HIP Formation and Characterisation

The following investigation was performed to optimise the conditions for HIP preparation:

Solutions of sodium octanoate in deionised water at varying concentrations were added in a dropwise manner into 5 mL of 20 mg/mL of each beta blocker in deionised water, which corresponded to the sodium octanoate/beta blocker molar ratio range from 0.5 to 4.0. This was carried out in 15 mL centrifuge tubes (Corning) on ice, with the purpose of reducing the ion pair solubility and thereby encouraging precipitation. The ion pairing was carried out in deionised water (pH 5 - 6) to eliminate the effect of buffer salt ions on the ionic interactions between the two species (Choi and Park 2000). Formation of a white precipitate indicated ion pair formation. The percentage transmittance of the resultant mixtures was monitored as described in Section 4.3.1.1. The tubes were then centrifuged at 10 000 rpm for 10 min at 4 °C (3K30 Refrigerated centrifuge, Sigma Laborzentrifuges GmbH, Osterode am Harz, Germany). The supernatant was analysed

for % residual drug concentration as described in Section 4.3.1.2. The pellet was snap frozen in liquid nitrogen and freeze-dried (Drywinner 110, Heto-Holten A/S, Gydevang, Denmark) for a minimum of 12 h. In cases where no precipitate formed, the solution itself was frozen in liquid nitrogen and lyophilised directly. The freeze drying process removes residual solvent (water in this case) by vacuum sublimation, to yield a solid product.

4.3.1.1 Transmittance

In some cases, the dropwise addition of the sodium octanoate solutions to the drug solutions resulted in the spontaneous formation of a cloudy solution, indicating the formation of the ion pair complex. As the complex forms, it aggregates, forming light scattering particles, reducing the transmittance of visible light through the solution. The turbidity of the solution/suspension at each molar ratio was quantified by monitoring the percentage transmittance of the mixture at 500 nm using a UV spectrophotometer (Varian), where 0% transmittance would be opaque and impervious to visible light and 100% indicates complete transparency.

4.3.1.2 Residual drug

Following centrifugation to precipitate the water insoluble ion pair complex, the supernatant was filtered through a 0.22 μm syringe filter (Millex GV) and assayed for drug content by UV spectroscopy. This technique provided an indirect measure of the amount of drug that had formed the complex and precipitated. Values were expressed as a percentage of the starting concentration of drug remaining in solution. The beta-

blocker concentration was determined by measuring UV absorbance compared with a 0.1 mg/mL calibration standard as previously described.

4.3.1.3 HIP Melting Point Determination by DSC

Differential scanning calorimetry (DSC) provides quantitative information about exothermic, endothermic and heat capacity changes as a function of temperature and time (Clas et al. 1999). The calorimeter measures the differential amount of energy required to maintain a sample and reference chamber at the same temperature over a heating or cooling cycle. Thermal transitions, such as melting and glass transitions can be accurately determined in this manner. Owing to the fact that different salt forms of a compound have different melting points, this technique was used to compare the melting points of the freeze dried HIPs and freeze dried original salt forms (HCl and tartrate) of the beta-blockers. Non-freeze dried samples of the original salt forms were also tested to investigate the effect of lyophilisation on melting point. The freeze dried samples of the original salt forms were prepared by dissolving approximately 15 mg of each beta blocker in 0.5 mL deionised water, which was then frozen in liquid nitrogen and freeze-dried overnight. Thermal analysis was carried out using a Pyris 1 differential scanning calorimeter (DSC, Perkin Elmer, Perkin Elmer Corporation, Norwalk, CT, USA). Samples of known mass (approximately 5 mg) were loaded into aluminium sample pans and crimp sealed. An empty crimped pan was used as a reference. Samples were loaded at 25 °C and allowed to reach thermal equilibrium prior to each run. The samples were cooled to 0 °C at a rate of 10 °C per min, then heated under nitrogen purge (at a flow rate of 20 mL/min) at a rate of 10 °C per min over a temperature range of 0 - 200 °C. Power time curves were recorded throughout, and the melting point onset

of each sample was determined in triplicate, using three separately weighed samples. The DSC was calibrated on a regular basis using indium and lead standards.

4.3.2 HIP Partition Coefficients

Apparent octanol/buffer partition coefficients of the successfully formed HIPs were determined as described in Section 2.3.2. Determinations were carried out in triplicate at two different octanol:buffer volume ratios (20:20 and 5:35).

4.3.3 Microsphere Formulation and Characterisation

Microspheres were prepared by spray drying. The feed solution was prepared by dissolving 150 mg freeze dried HIP and 1.5 g PLGA in 50 mL dichloromethane (DCM, 3% w/v), giving a nominal loading of 9.1% w/w HIP (approximately equivalent to 6% w/w free base). This solution was spray dried using a Buchi Mini spray dryer 191 as described in Section 3.3.2 under the same processing conditions, with the exception of the use of a high performance cyclone (Büchi Laboratories, Flawil, Switzerland) which has been found to significantly increase yield, particularly for small particle sizes (Brandenberger 2003). The spray dried microspheres were collected in a glass vial and stored under desiccation and protected from light. Microspheres were then characterised by SEM and particle size analysis, drug loading and *in vitro* dissolution testing as described in the previous chapter, using calibration curves constructed from standard solutions of HIP in phosphate buffered saline (PBS, pH 7.4).

4.3.3.1 Injection Formulation

Some preliminary studies to determine a suitable injection formulation for use *in vivo* were carried out. The injection vehicle was based on the Lupron Depot[®] formulation, containing Tween 80 (0.1% w/v), CMC sodium (0.5% w/v) and PBS pH 7.4. The three month Lupron Depot[®] formulation comprises 15% w/v solids. However, the highest percentage solids content of the HIP loaded microspheres injectable through a 25 G needle without clogging was 10% w/v.

The injectability of a sample metoprolol HIP loaded formulation containing 10% w/v microspheres was determined by measuring the percentage of nominal dose delivered over ten injections, by the following method:

800 mg microspheres were suspended in 8 mL of the injection vehicle and sonicated for approximately 30 s to disperse the particles. 0.5 mL of the suspension was drawn up into a 1 mL syringe (without needle), then injected into a 15 mL centrifuge tube containing 1 mL DCM through a 25 G needle (the largest permissible bore size for subcutaneous injection in rats). The centrifuge tube was then sonicated for approximately 5 min to dissolve the microspheres, before 10 mL of water was added and the mixture shaken for 2 hr at 37 °C to perform a liquid-liquid extraction. The samples were then centrifuged to separate the phases. The aqueous phase was filtered, and the beta-blocker content determined by UV spectroscopy as previously described and expressed as a % of the nominal dose. This process was repeated ten times.

4.4 Results and Discussion

4.4.1 HIP Formation

For alprenolol, a cloudy suspension was formed spontaneously upon addition of the sodium octanoate solutions to the drug solutions, attributed to the formation of the water insoluble ion pair complex. Fig 4.2 shows the transmittance change of the mixture as a function of molar ratio between sodium octanoate and alprenolol HCl. The percentage transmittance sharply decreased at the molar ratio of 0.5, reaching a minimum at a molar ratio of 1.5, and remained at this minimum thereafter.

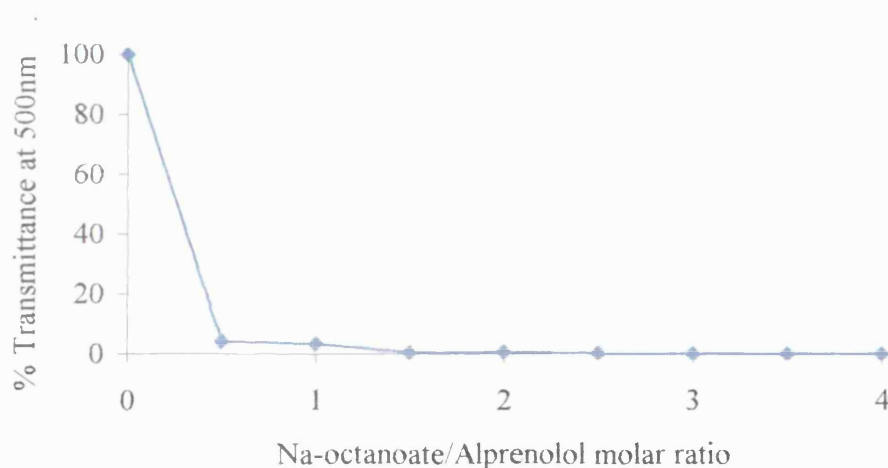


Figure 4.2: Transmittance change of the solution in which the alprenolol: Na-octanoate complex was formed.

Following centrifugation to sediment the solid precipitate, the amount of alprenolol remaining in solution as a function of octanoate/alprenolol molar ratio was measured (see Fig. 4.3). A gradual decrease in residual alprenolol concentration was seen with increasing sodium octanoate added, indicative of complexation between the alprenolol

and octanoate and the formation of the hydrophobic ion pair. It was predicted that the ion pairing would occur at a sodium octanoate/alprenolol molar ratio of 1, although approximately 25% of the alprenolol remained either uncomplexed or the complex was water soluble at this ratio. At a molar ratio of 1.5, 85% of the alprenolol was complexed with the octanoate. Further increase in the molar ratio reduced residual alprenolol in the supernatant, but such an excess of free sodium octanoate was deemed undesirable for microsphere preparation. The freeze dried pellet prepared at a molar ratio of 1.5 was therefore selected for further characterisation.

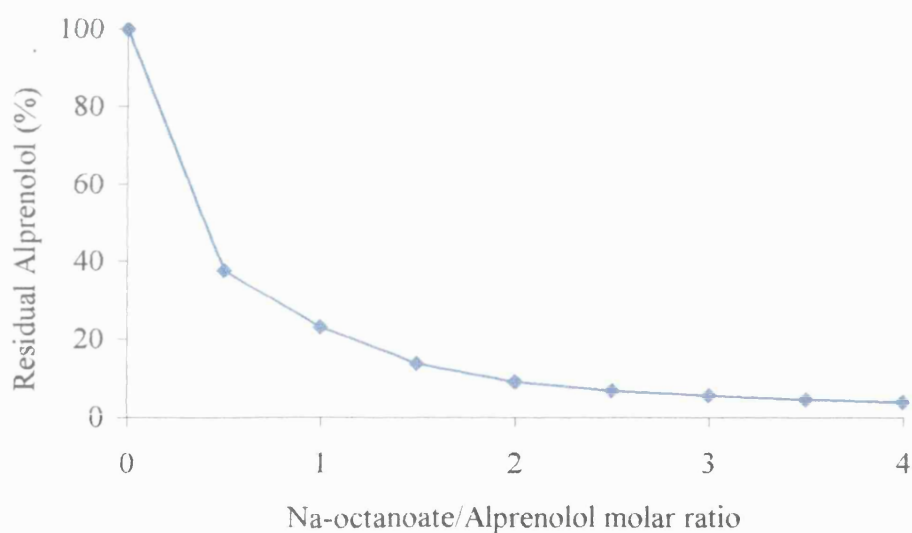


Figure 4.3: The amount of free alprenolol hydrochloride which was not hydrophobically ion paired with Na-octanoate with increasing molar ratios.

For metoprolol, addition of the sodium octanoate solution caused a transient cloudiness which spontaneously clarified, regardless of octanoate/metoprolol molar ratio. This indicated possible HIP formation, but suggested the complex was sufficiently water

soluble such that precipitation did not occur under these conditions. Residual metoprolol could therefore not be measured since a soluble product cannot be separated via this method. The solution (also prepared at a molar ratio of 1.5) was therefore freeze dried directly, and the melting point of the lyophilised product was measured as described in Section 4.3.1.3 to ascertain whether any change in salt form had occurred.

Upon addition of the sodium octanoate solution to the atenolol solutions, no cloudiness was seen no matter how transient. The solution was freeze dried directly, but a physical mixture of the two compounds (atenolol and sodium octanoate) persisted (demonstrated by melting point determination by DSC). Atenolol was therefore dropped and experiments proceeded with alprenolol and metoprolol HIPs.

4.4.2 HIP Melting Point Determination

The melting points of the different compounds are shown in Table 4.1. The melting point onset of drugs was unaffected by freeze drying (ANOVA, posthoc Tukey HSD, $p > 0.05$). However, the formation of the HIP complex significantly altered the melting point (from 106 °C to 70.4 °C, and from 120 °C to 50 °C for alprenolol and metoprolol respectively), confirming the formation of alternative salt forms of the two beta-blockers. Representative DSC traces of alprenolol HCl, alprenolol HIP and freeze dried alprenolol HCl are illustrated in Appendix Fig. A2.

Table 4.1: Onset of melting transitions determined by DSC. 'HIP' refers to the freeze dried product of the combined drug and sodium octanoate solutions. *Indicates a significant difference (ANOVA, posthoc Tukey HSD $p < 0.05$).

Sample	Mean melt onset temperature (°C) ($n = 3$)	SD ($n = 3$)
Alprenolol HCl (as purchased)	106.1	0.25
Freeze dried alprenolol HCl	106.0	0.33
Alprenolol 'HIP'	70.4*	0.06
Metoprolol tartrate (as purchased)	120.0	0.35
Freeze dried metoprolol tartrate	120.1	0.62
Metoprolol 'HIP'	50.1*	2.63
Atenolol (as purchased)	145.8	0.43
Freeze dried atenolol	145.9	1.2
Atenolol 'HIP'	145.9	0.82

4.4.3 Partition Coefficients

The mean apparent partition coefficients ($\log P_{app}$) determined between octanol and phosphate buffer (pH 7.4) at 37 °C are shown in Table 4.2. There is a clear dependence of partition coefficient on phase volume ratio, suggestive of ionisation and/or self-association of the solute, and the existence of a multi-way equilibrium (Leo et al. 1971).

Table 4.2: Octanol/buffer apparent partition coefficients ($\log P_{app}$) of alprenolol and metoprolol HIPs, determined by the shake flask method at pH 7.4, 37 °C, at two different volume ratios.

Drug	Phase volume ratio (organic:aqueous)	Mean $\log P_{app} \pm SD$ ($n = 3$)
Metoprolol HIP	20:20	0.20 ± 0.23
Metoprolol HIP	5:35	0.60 ± 0.05
Alprenolol HIP	20:20	0.95 ± 0.03
Alprenolol HIP	5:35	1.25 ± 0.03

4.4.4 Microsphere Characterisation

The HIP loaded microspheres had similar surface morphology to the solution spray dried microspheres (shown in Fig. 4.4) in that they were smooth and spherical, and appeared to be of a similar size range of 1 - 5 μm . Laser diffraction particle size analysis revealed volume median diameters of $4.8 \pm 0.2 \mu\text{m}$ and $6.1 \pm 0.1 \mu\text{m}$ for alprenolol and metoprolol HIP loaded microspheres respectively ($n = 3$).

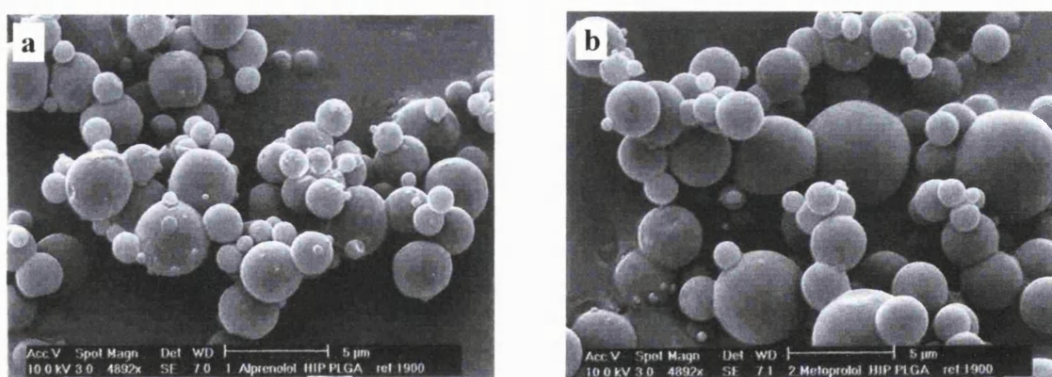


Figure 4.4: SEM images of a) alprenolol and b) metoprolol HIP loaded microspheres.

Data from *in vitro* dissolution studies of the HIP loaded microspheres are listed in Table 4.3 and illustrated graphically in Figure 4.5. The burst release (i.e. the cumulative % drug released within the first hour) was $15.0 \pm 1.7\%$ and $14.9 \pm 1.3\%$ for alprenolol and metoprolol respectively. This constitutes a significant reduction in burst release compared with solution spray dried microspheres loaded with the original drug salts (batches 2 and 3 of Table 3.3) (Mann-Whitney U-test, $p < 0.05$). Comparison of the release profiles of the two sets of microspheres reveal a great improvement, with the gradual release of drug from the HIP loaded microspheres over 7 days.

Table 4.3: Cumulative % drug release from HIP loaded microspheres.

Mean cumulative % release \pm SD ($n = 3$)		
Time (hr)	Alprenolol	Metoprolol
0	0.0	0.0
0.1	3.8 \pm 1.7	12.4 \pm 4.5
0.5	10.1 \pm 1.8	13.6 \pm 1.7
1	15.0 \pm 1.7	14.9 \pm 1.3
2	23.5 \pm 1.3	20.8 \pm 3.4
5	33.4 \pm 2.8	29.2 \pm 5.1
8	37.6 \pm 3.0	34.0 \pm 5.5
24	46.1 \pm 2.2	40.6 \pm 6.3
48	55.8 \pm 3.2	46.3 \pm 5.6
120	72.1 \pm 5.8	56.7 \pm 5.6
168	77.5 \pm 5.1	64.0 \pm 4.0

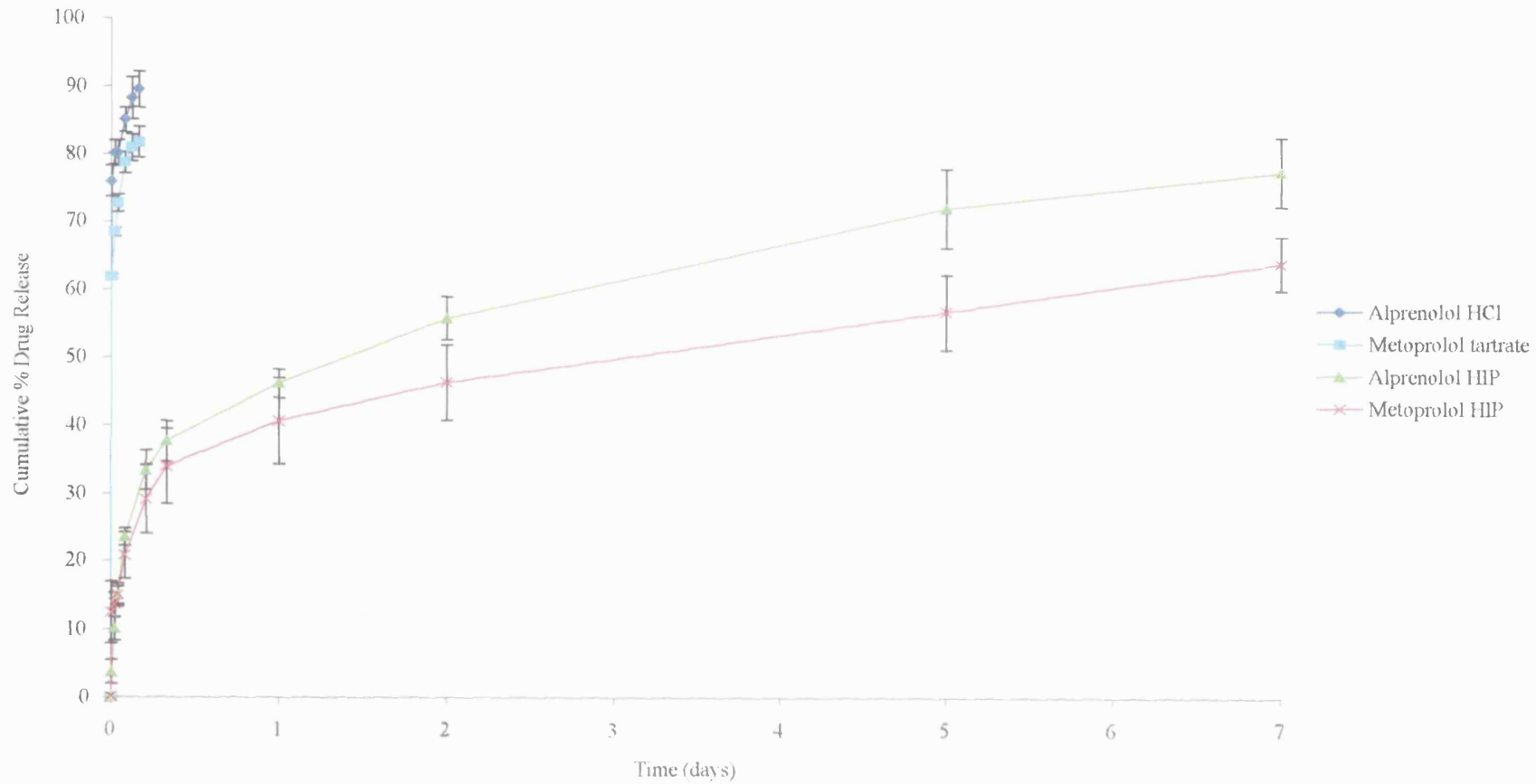


Figure 4.5: *In vitro* dissolution profiles of alprenolol and metoprolol HIP loaded microspheres compared with microspheres loaded with the HCl and tartrate salts, batches 2 and 3 ($n = 3 \pm SD$).

As the aqueous dissolution medium penetrates the polymeric microspheres, the ion pairs are likely to dissolve and partition from the hydrophobic polymer matrix into the aqueous dissolution medium. One would hypothesise that the more hydrophilic of the two compounds (i.e. metoprolol) would partition more readily into the dissolution medium, and therefore be released more rapidly. However, repeated measures analysis of variance (SPANOVA) comparing the release profiles of the alprenolol and metoprolol HIPs, revealed no significant difference *in vitro*, at the $p < 0.05$ level ($F(1,4) = 1.997, p = 0.231$).

The low burst release and slow release profile of these HIP loaded microspheres made them suitable for *in vivo* study. Studies to determine a suitable injection formulation, in terms of vehicle and solids content to enable reproducible injection of the nominal dose were carried out, the results of which are described in the following section.

4.4.5 Microsphere Injectability

The mean % nominal dose delivered when 0.5 mL microsphere suspension was injected into 1 mL DCM and extracted into water was $95.93 \pm 1.85\%$ ($n = 10$). The reproducibility of injection was deemed acceptable for this formulation and no problems with needle clogging were encountered at this solids content (10% w/v).

4.5 Conclusion

Hydrophobic ion pairs of alprenolol octanoate and metoprolol octanoate were successfully prepared and characterised. The differences in aqueous solubility and melting point between the precipitated material and the original drug salts confirmed formation of the ion pairs of metoprolol and alprenolol octanoate. An ion pair of atenolol could not be made under these conditions and atenolol was therefore dropped from the study. Spray dried microspheres containing the ion pairs of alprenolol and metoprolol, of suitable size and morphology, were prepared at a loading of 9.1% w/w. They demonstrated significantly reduced burst compared with microspheres loaded with the original drug salts and release was prolonged over 7 days *in vitro*. The mechanism of this altered dissolution profile is thought to arise from the alteration of the solubility of the drugs in the polymer matrix, and reduced surface activity of the encapsulated drugs, resulting in a more even distribution of drug throughout the microspheres, and the concomitant reduction in surface associated drug. An injection formulation was prepared which gave reproducible delivery of the nominal microsphere dose, and was deemed suitable to be taken forward for *in vivo* testing.

Chapter 5

***In Vivo* Investigations into the Absorption Profiles of Beta-Blockers from Subcutaneous Formulations**

5 *In Vivo* Investigations into the Absorption Profiles of Beta-Blockers from Subcutaneous Formulations

5.1 Introduction

Microspheres loaded with hydrophobic ion pairs (HIPs) of alprenolol and metoprolol demonstrated sustained release *in vitro*, as described in the previous chapter (Chapter 4). In *situ*-forming depot systems (described in Section 1.3.3.5) have been identified as a simple alternative to microspheres, being easily formulated from a solution of drug and polymer in a suitable organic solvent, and are more easily administered through a narrow bore needle. Associated disadvantages include the use of toxic organic solvents (e.g. NMP), and pain on injection. Alprenolol and metoprolol HIP loaded *in situ*-forming depots were formulated (as described in Section 5.3.5), to enable the comparison of the two formulation types. The phase inversion kinetics governing the formation of the *in situ*-forming depot, and thereby determining the drug release profile, are difficult to replicate *in vitro*. This is due to differences in solvent volume (sink conditions of the *in vitro* dissolution medium *cf* interstitial fluid *in vivo*) and the absence of the restrictive architecture of the injection site. The *in situ*-forming depots were not therefore tested *in vitro*.

The aim of this chapter was to evaluate these formulations *in vivo* following subcutaneous administration into a suitable animal model. The effect of *i*) drug lipophilicity and *ii*) nature of the depot (pre-formed microspheres *vs in situ*-forming depot) on absorption rate were investigated. Subcutaneously administered aqueous solutions of each HIP were also administered to study the absorption characteristics of

the HIPs independently of the polymer matrices, i.e. serving as a control. The tissue reactions to the polymeric dosage forms (microspheres and *in situ*-forming depots) were also examined.

In order to obtain the absorption profiles of metoprolol and alprenolol from the different formulation types, the Wagner-Nelson method of deconvolution was employed. This required prior knowledge of the clearance kinetics (namely volume of distribution at steady state (V_{ss}) and clearance rate (CL)) of the two compounds, which were determined experimentally following intravenous administration to rats. Drug absorption profiles from the three types of dosage form could then be assessed. Plasma drug concentration was determined by high performance liquid chromatography coupled with electrospray ionisation tandem mass spectrometry (LC-MS/MS), chosen for its sensitivity and specificity. Histopathology was performed to compare the tissue reactions to the formulations at the injection sites.

5.1.1 Choice of Animal Model

Extensive research has been carried out to determine the physiological differences between the gastro-intestinal tract and surrounding vasculature of animals and man, and the effects these differences have on the bioavailability of orally administered drugs. Informed decisions concerning the suitability of different animal models can therefore be made when choosing a suitable species in which to test oral formulations. However, little such work has been carried out in relation to the parenteral administration of drugs, in fact it has been recommended that research in this area should be initiated (Burgess et al. 2002).

Release from encapsulation-type drug delivery systems, such as microspheres and *in situ*-forming devices, is predominantly controlled by the polymeric matrix (as discussed in Section 1.3.3). It has therefore been concluded that as far as these delivery systems are concerned, provided **biochemistry** and **tissue reaction** at the site of the injection are similar, then release profiles are likely to be comparable across species (Dickinson et al. 2003). In terms of **biochemistry**, the interstitial fluid acts as the dissolution medium for intramuscular and subcutaneously injected pharmaceuticals. Differences in composition may therefore have a dramatic effect on absorption rates. Interstitial fluid is in equilibrium with plasma/serum, and plasma composition data are available for a selection of small laboratory animals and man (shown in Table 5.1). Values are broadly similar across species.

Table 5.1: Mean and range of values of the inorganic components in the serum of the male of each species listed (adapted from Mitruka and Rawnsley 1977).

	Mice (Albino)	Rat (Albino)	Rabbit	Dog	Man
Sodium (mEq/L)	138 (128 - 145)	147 (143 - 156)	146 (138 - 155)	147 (139 - 153)	141 (135 - 155)
Potassium (mEq/L)	5.25 (4.89 - 5.9)	5.82 (5.4 - 7.0)	5.75 (3.7 - 6.8)	4.54 (3.6 - 5.2)	4.1 (3.6 - 5.5)
Chloride (mEq/L)	108 (105 - 110)	102 (100 - 110)	101 (92 - 112)	114 (103 - 121)	104 (98 - 109)
Bicarbonate (mEq/L)	26.2 (20 - 32)	24 (13 - 32)	24.2 (16 - 32)	21.8 (15 - 29)	27 (22 - 33)
Phosphorous (mg/dL)	5.6 (2.3 - 9.2)	7.56 (3.1 - 11.0)	4.82 (2.3 - 6.9)	4.4 (2.7 - 5.7)	3.5 (2.5 - 4.8)
Calcium (mg/dL)	5.6 (3.2 - 8.5)	12.2 (7.2 - 13.9)	10 (5.6 - 12.1)	10.2 (9.3 - 11.7)	9.8 (8.5 - 10.7)
Magnesium (mg/dL)	3.11 (0.8 - 3.9)	3.12 (1.6 - 4.4)	2.52 (2 - 5.4)	2.1 (1.5 - 2.8)	2.12 (1.8 - 2.9)

The body temperature of rabbits is high compared with that of other small laboratory animals (38.5 - 39.5 °C in rabbits compared with 35.9 - 37.5 °C in rats). Temperature has a significant effect on solubility, and may therefore affect the partitioning of drugs from the parenteral formulation to the tissues. Temperature may also be a consideration for formulations whose glass transition temperature (T_g) is close to body temperature (Dickinson et al. 2003).

In terms of **tissue reaction**, the foreign body reaction to injected polymeric devices is said to be identical at subcutaneous and intramuscular injection sites, and is very similar across species including rats, mice, and primates (Dickinson et al. 2003). The nature of this reaction is discussed in further detail in Section 5.3.9.

It can therefore be deduced that the absorption environment is sufficiently similar across species, particularly for pre-formed PLA/PLGA delivery systems (Dickinson et al. 2003). A study in which leuprolide acetate loaded PLGA microspheres were administered subcutaneously or intramuscularly indicated that release rates were the same in dogs and rats. In addition, the species of rat used (Sprague-Dawley versus Wistar) did not have an effect on release rates (Okada et al. 1991). There is a greater potential for variation in systems in which the release rate limiting structure is formed *in vivo* (e.g. *in situ*-forming depots) (Dickinson et al. 2003), although testosterone suppression from an *in situ*-forming depot of leuprolide was found to be similar in both rats and dogs (Ravivarapu et al. 2000b).

Ethically, it is important to use the animal with the lowest neurophysiological sensitivity to meet the experimental objectives, and to adhere to European good practice guidelines

on dosing and sampling volumes (Diehl et al. 2001) whilst achieving quantifiable systemic plasma drug concentrations.

The rat was chosen as an appropriate model for use in these experiments based on the foregoing information and logistic factors.

5.2 Materials

The beta-blockers (propranolol hydrochloride, alprenolol hydrochloride and metoprolol tartrate) were purchased from Sigma-Aldrich (Poole, UK). The Medisorb[®] polymer PLGA 5050 DL 2.5A was purchased from Alkermes Inc. (Ohio, USA). Hydrophobic ion pair (HIP) complexes (alprenolol octanoate and metoprolol octanoate) and the HIP loaded microspheres were prepared as described in Sections 4.3.1 and 4.3.3 respectively. Disodium hydrogen orthophosphate, potassium dihydrogen orthophosphate and sodium chloride used in injection vehicle preparation were all analytical grade and purchased from VWR International Ltd. (Poole, Dorset, UK). Tween 80, *N*-methyl-2-pyrrolidone (NMP) and formaldehyde 37 - 40% (molecular biology grade) were obtained from Sigma-Aldrich (Poole, UK). Deionised water was obtained from an Option 4 water purification system (Elga Ltd., Buckinghamshire, UK). Male Wistar rats weighing 162 - 265 g were purchased from Harlan UK, and the anaesthetic Hypnorm[™] was supplied by Janssen Pharmaceutical (Oxford, UK).

Materials employed in the LC-MS/MS analysis of the plasma samples included control rat plasma (from male Wistar rats, pre-treated with EDTA anticoagulant) obtained from AstraZeneca, Macclesfield. The mobile phase solvents acetonitrile (HPLC grade),

methanol (HPLC grade) and formic acid were purchased from Fisher Scientific (Loughborough, UK), and deionised water was obtained from a Milli Q system (18.2 M Ω) (Millipore Ltd., UK). All chemicals and reagents were used as purchased.

5.3 Methods

5.3.1 Animal Housing

The rats were caged in groups of five and were allowed to move freely before and during the experimental period. They were kept on a light-dark cycle of 12 h at a room temperature of 25 °C, and provided with food and water *ad libitum*. All animals were allowed to acclimatise for a minimum of 7 days prior to experimentation.

5.3.2 Intravenous (IV) Injection of Drug Solutions

The beta-blockers were injected intravenously to establish pharmacokinetic parameters for use in the deconvolution calculations. Sites of intravenous injection in the rat include the dorsal and lateral tail veins (see Fig. 5.1b, d and f), the lateral marginal vein, and the dorsal metatarsal vein in conscious animals, or the sublingual or penile veins in anaesthetised animals (Nebendahl 2000). The lateral tail veins were chosen in this study. The skin on the tails of older rats is tough and covered by scales, making it difficult to pierce and enter the vessels (Nebendahl 2000). For this reason, rats weighing < 260 g were used throughout this study.

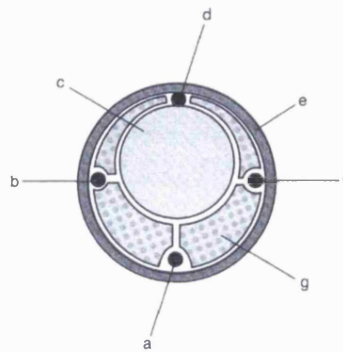


Figure 5.1: Transverse sectional view of the rat tail; ventral artery (a), the lateral veins (b,f), vertebra (c), dorsal vein (d), skin (e), and tendon bundles (g) (Nebendahl 2000).

Rats were lightly anaesthetised with Hypnorm™ (fentanyl citrate 0.315 mg and fluanisone 10 mg) prior to the experiment to facilitate intravenous injection. 0.2 mL Hypnorm™ was administered by intraperitoneal injection into the lower left quadrant of the abdomen.

Solutions of alprenolol HCl and metoprolol tartrate for intravenous injection were prepared by dissolving 22.92 mg and 25.61 mg respectively in 10 mL phosphate buffered saline (PBS) pH 7.4, equivalent to 1 mg (free base)/0.5 mL. These solutions were filtered through 0.22 µm syringe filters (Millex GV) to remove any particulates. Once anaesthetised, the rat's tail was immersed in warm water for 1 - 2 minutes to dilate the blood vessels and thereby facilitate injection. 0.5 mL of the appropriate solution was then injected into the dorsal or lateral tail vein through a 25 G needle. Incorrect needle placement was identifiable by swelling of the tail or blanching of the skin, indicating that the solution was being injected extravascularly into the surrounding skin (Nebendahl 2000). In this event, the needle was repositioned and the dose correctly administered. Blood was sampled from the tail vein over a 3 hour period (at approximately 1, 8, 15, 30, 60, 90, 120 and 180 minutes post administration) as

described in Section 5.3.6, ensuring that samples were taken from a different vein to that into which the dose was administered.

5.3.3 Subcutaneous Injection of Aqueous Solutions of the Hydrophobic Ion Pairs

Alprenolol octanoate HIP (10.8 mg) and metoprolol octanoate HIP (10.24 mg) were each dissolved in 10 mL PBS to give solutions equivalent to 1 mg (free base)/1.5 mL. Unit doses of 1.5 mL were drawn up into 2 mL disposable syringes and 25 G needles attached. The dose was then injected subcutaneously into the dorsolateral area of the neck (scruff) by lifting the fold of loose skin between the thumb and forefinger, and passing the needle in an anterior direction through the skin, parallel to the body (see Fig. 5.2). Leakback and hence loss of fluid was minimised by changing the needle path after the needle had been pushed in half way. Blood was sampled over a 6-hour period (at 5, 15, 30, 60, 90, 120, 240 and 360 minutes post administration) as described in Section 5.3.6.



Figure 5.2 : Subcutaneous injection into the dorsolateral area of the neck (scruff) of a rat (Nebendahl 2000).

5.3.4 Subcutaneous Administration of Microsphere Formulations

Microspheres loaded with the hydrophobic ion pairs (HIPs) (alprenolol octanoate and metoprolol octanoate) were prepared by spray drying as described in Section 4.3.3. 180 mg aliquots of the microspheres were accurately weighed into individual glass vials in advance, ready for reconstitution immediately prior to administration. 1.8 mL of vehicle (PBS pH 7.4 with 0.1% w/v Tween 80 as a suspending agent) was added, giving an injection comprising 10% w/v solids. The vials were then shaken and sonicated for 30 s (Grant Ultrasonic Bath XB6, Grant Instruments, Cambridge, England) to break up any agglomerates and suspend the microspheres. 1.5 mL of this suspension was then drawn up into a 2 mL disposable syringe, to which a 25 G needle was subsequently attached, and the suspension was injected subcutaneously into the scruff. On occasions, the needle became blocked partway through dosing. In this event, the needle was withdrawn and replaced with a new needle, and injection recommenced. The dose was adjusted in subsequent calculations to account for the slight loss of volume. Blood was sampled over a 10-day period (at 30 min, 1 h, 2 h, 4 h, 8 h, 24 h, daily for 7 days and a final sample on day 10) as described in Section 5.3.6.

5.3.5 Subcutaneous Administration of *In Situ*-Forming Depots

The *in situ*-forming depot systems were prepared as follows:

The plunger from a 1 mL disposable syringe (Syringe A) was removed, and 30 mg of the lyophilised HIP (alprenolol octanoate or metoprolol octanoate) was loaded into the barrel. The plunger was then carefully replaced. A 50% w/w solution of polymer in *N*-methyl-2-pyrrolidone (NMP) was prepared in a glass vial, 0.3 mL of which was drawn

up into a second syringe (Syringe B). Both syringes (A and B) were then capped until required. Immediately prior to administration, the syringes were coupled together via a male-male Luer Lock[®] connector (kindly donated by Atrix Laboratories) as illustrated in Fig. 5.3. The contents of the syringes were then mixed thoroughly by alternately depressing the plungers for 50 cycles, or until a homogenous solution was formed. The syringes were then uncoupled and any excess solution was discarded, leaving 0.15 mL of the polymer/drug solution (i.e. 15 mg HIP) in Syringe A. A 25 G needle was attached, any air bubbles removed, and the formulation was injected subcutaneously into the scruff of rats as previously described. No injectability problems were encountered with this formulation type. Blood samples were then taken as per the microsphere study. It is noteworthy that the drug loading of the *in situ*-forming depots was double that of the microspheres (i.e. 20% w/w *cf* 10% w/w), which was deemed necessary to minimise the volume of NMP injected. Despite having a subcutaneous LD₅₀ > 2 g/Kg in rats, injection of 0.3 mL was judged to cause significant discomfort to the animal. Drug loading was therefore doubled to enable an equivalent dose to be given (15 mg HIP) in half the volume of polymer solution (75 mg PLGA in 0.15 mL NMP).

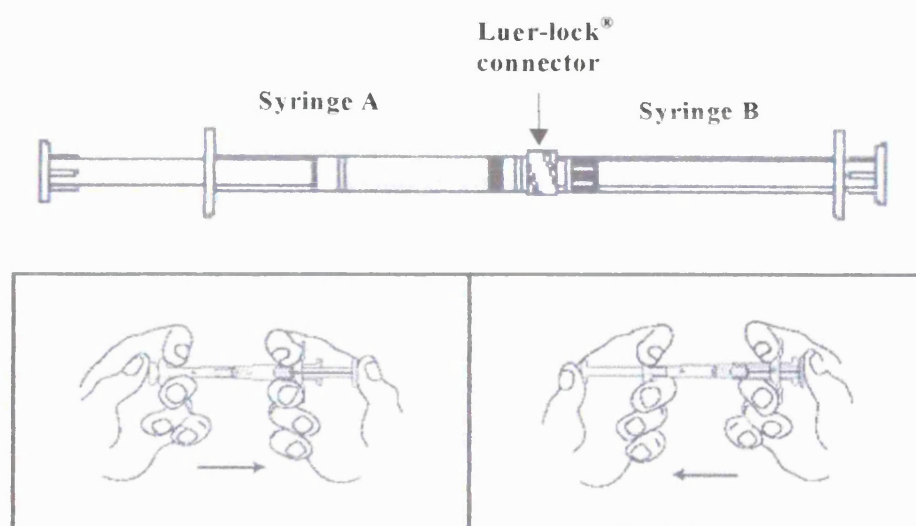


Figure 5.3: Schematics of syringe coupling and mixing procedure for the formulation of the *in situ*-forming depot system (Sanofi-Aventis 2005).

5.3.6 Blood Sampling

The animals were placed in a plastic restraining device and the tail dipped in warm water to increase blood flow to the tail for approximately 1 minute prior to the sampling time (Weiss et al. 2000). A small incision was then made in the tail vein with a scalpel blade and approximately 150 - 200 μ l of blood was collected into anticoagulant (EDTA) coated centrifuge tubes, (Microvette CB300, Sarstedt, UK) which were stored on ice. Further bleeding was stopped by the application of light finger pressure on the blood vessel. Subsequent samples were taken from the same site by removal of the clot with a damp cloth to re-open the wound. If bleeding would not recommence, a fresh incision was made in the tail either in a different vein, or at a more proximal site to the body along the same vein. The capillary tubes containing the blood samples were centrifuged for 10 minutes at 3000 rpm (Eppendorf Centrifuge 5415D, Eppendorf AG, Hamburg, Germany), and the plasma (supernatant) was then transferred to a 1.5 mL Eppendorf tube and frozen (*ca* -20 °C) until analysis. In the case of the intravenous injections, blood was sampled from a different vein to the one in which the drug was administered to avoid contamination of the sample. For collection of the final sample, animals were sacrificed by a Schedule 1 method (CO₂ euthanasia chamber) and blood was obtained by cardiac puncture.

Blood volumes taken were in accordance with the project license criteria that for multiple blood samples, not more than 10% and 15% of the circulating blood volume can be removed in any 24 h or 28 day period respectively.

5.3.7 Analysis of Plasma Samples

The quantification of alprenolol and metoprolol in rat plasma was achieved using HPLC with electrospray ionisation tandem mass spectrometry (LC-MS/MS) using propranolol as an internal standard. The analytical method was developed and validated by Mohammed Yasin (Senior Analyst, AstraZeneca, Macclesfield).

Samples were shipped to AstraZeneca Macclesfield on dry ice overnight, ensuring they remained frozen during transit, and were stored in a freezer (-20 °C) until analysis. The frozen samples were thawed by standing at room temperature for 1.5 hr prior to analysis. The internal standard was added and samples were prepared for analysis as described in Section 5.3.7.6. Briefly, the analyte and the internal standard were extracted from plasma using a protein precipitation procedure, and were injected onto a SCIEX API 4000 LC-MS/MS (ESI positive ion mode) equipped with a C₁₈ HPLC column. Multiple Reaction Monitoring (MRM) mode of mass spectrometry was used for selectivity.

The following sections describe the preparation of standard solutions of alprenolol, metoprolol and the internal standard (propranolol) for construction of the calibration curves, and for quality controls and spiking solutions required during sample analysis.

5.3.7.1 Stock Solutions For Calibration

- **Alprenolol calibration stock solution (500 µg/mL)** – 5.75 mg of alprenolol HCl (5 mg free base equivalent) was accurately weighed into a 10 mL volumetric flask,

dissolved and made up to volume with methanol to yield a 500 µg/mL calibration stock solution.

- **Metoprolol calibration stock solution (500 µg/mL)** – 6.47 mg of metoprolol tartrate (5 mg free base equivalent) was accurately weighed into a 10 mL volumetric flask, dissolved in and made up to volume with methanol to yield a 500 µg/mL calibration stock solution.
- **Composite analytes standard (2.5 µg/mL)** – 50 µL of each stock (alprenolol and metoprolol) were dispensed into a 10 mL volumetric flask and made up to volume with acetonitrile:water (1:1 v/v) to yield a 2.5 µg/mL composite standard solution.
- **Spiking standard A (250 ng/mL)** – 1 mL of the composite analyte standard (2.5 µg/mL) was diluted to 10 mL with acetonitrile:water (1:1 v/v).
- **Spiking standard B (50 ng/mL)** – 200 µL of composite analyte standard (2.5 µg/mL) was diluted to 10 mL with acetonitrile:water (1:1 v/v).
- **Spiking standard C (10 ng/mL)** – 40 µL of composite analyte standard (2.5 µg/mL) was diluted to 10 mL with acetonitrile:water (1:1 v/v).

5.3.7.2 Quality Control (QC) Stock Solutions

- **Alprenolol and metoprolol QC stock (500 µg/mL)** – Prepared individually as for the calibration stock solutions.
- **QC A (2.5 µg/mL)** - 50 µL of each (alprenolol and metoprolol) QC Stock solution (500 µg/mL) was diluted to 10 mL with acetonitrile:water (3:7 v/v).
- **QC B (500 ng/mL)** - 1 mL of QC A (2.5 µg/mL) solution was diluted to 5 mL with acetonitrile:water (3:7 v/v).

- **QC C (50 ng/mL)** - 100 μL of QC A (2.5 $\mu\text{g}/\text{mL}$) solution was diluted to 5 mL with acetonitrile:water (3:7 v/v).

5.3.7.3 Preparation of Quality Control Rat Plasma Samples

Quality control rat plasma samples were prepared by spiking the analytes into control rat plasma. 200 μL of the QC working solutions QC A, QC B and QC C were spiked into 1.8 mL of control rat plasma to give QC rat plasma samples at concentrations of 250, 50 and 5 ng/mL respectively, as shown in Table 5.2.

Aliquots (50 μL) at each of the three concentrations of QC were dispensed in glass tubes and stored frozen at *ca* -20 $^{\circ}\text{C}$ until required.

Table 5.2: Preparation of quality control rat plasma samples.

Nominal QC concentration (ng/mL)	QC spiking solution used	Volume of QC solution spiked into control rat plasma (μL)	Final plasma volume (mL)
5	QC C (50 ng/mL)	200	2
50	QC B (500 ng/mL)	200	2
250	QC A (2500 ng/mL)	200	2

- **Internal standard stock solution (500 $\mu\text{g}/\text{mL}$)** - A stock solution of propranolol internal standard was prepared at a concentration of 500 $\mu\text{g}/\text{mL}$ in methanol. 50 μL of this stock solution was further diluted to 5 mL to produce an intermediate internal standard solution at the concentration of 5 $\mu\text{g}/\text{mL}$.

- **Internal standard spiking solution (50 ng/mL)** – 200 µL of intermediate internal standard solution (5 µg/mL) was diluted to 20 mL with acetonitrile/water (1:1 v/v).

5.3.7.4 Preparation of Plasma Calibration Standards

Calibration standards were prepared individually for each assay batch by adding spiking standard solution to 50 µL aliquots of control rat plasma as indicated in the Table 5.3.

Table 5.3 : Preparation of the plasma calibration standards in the 2 - 250 ng/mL concentration range, derived from working QC standard solutions QC A, B and C.

Nominal standard concentration (ng/mL)	Spiking standard solution used	Volume of analyte working solution, spiked (µL)	Volume of (1:1) acetonitrile/water (µL)
0	-	0	50
2	C (10 ng/mL)	10	40
5	C (10 ng/mL)	25	25
10	B (50 ng/mL)	10	40
20	B (50 ng/mL)	20	30
50	B (50 ng/mL)	50	0
100	A (250 ng/mL)	20	30
250	A (250 ng/mL)	50	0

5.3.7.5 Assay Validation

The linearity of the matrix standard curve was determined by plotting the area ratios of analyte to internal standard against the actual concentration using 1/x weighted least squares regression over a calibration range 2 - 250 ng/mL.

Six quality control standards (2 each of low, medium and high QC concentrations) were analysed before, during and after each batch of test samples. The acceptability of each batch of test samples depended upon the data from the calibration standards and the QC samples, fulfilling the following requirements:

- A minimum of four out of six QC's being within $\pm 15\%$ of their respective calculated concentrations. (No more than one QC may be greater than $\pm 15\%$ at any one concentration).
- At least 5 calibration samples being within $\pm 15\%$ ($\pm 20\%$ at the lower limit of quantification (LLOQ)) of their respective target concentrations.

In order to minimise the possibility of carry over effects, mobile phase injections were run between samples when it was necessary to follow a high concentration sample with a low concentration sample.

5.3.7.6 Extraction Procedure

Calibration Standards

- 1 To 50 μL of control rat plasma, 50 μL of the appropriate volume of Analyte Spiking solution was added.
- 2 Go to 5

Test Samples

- 3 50 μL of each test sample was transferred to borosilicate glass tubes (Fisher Scientific, UK). In cases where the test sample volume was $< 50 \mu\text{L}$, an appropriate volume of blank plasma was added to make up to volume (factored in as a dilution factor).
- 4 50 μL of acetonitrile:water (1:1 v/v) was added to all test samples using a repeater pipette (Multipette, Eppendorf, Hamburg, Germany).
- 5 425 μL of 50 ng/mL internal standard spiking solution was added to all standards and test samples (Multipette).
- 6 300 μL of acetonitrile was added to all samples (Multipette) as the crash solvent, and the solutions mixed vigorously on multi-vortexer for 2 minutes.
- 7 The tubes were centrifuged at approximately 4500 rpm for 10 minutes at 4 $^{\circ}\text{C}$ (Mistral 3000I, MSE, Leicester, UK).
- 8 The supernatant extracts were transferred to 2 mL amberglass auto-injector vials (Crawford Scientific UK) containing 100 μL glass vial inserts (Varian Ltd., UK), the vials capped and an aliquot of 10 μL analysed by LC-MS/MS.

5.3.7.7 Chromatographic Conditions

An Agilent Series 1100 HPLC system (Agilent Technologies, Germany) was employed, equipped with a HTC PAL autoinjector (Leap Technologies, France). A 3 μm C₁₈ ACE column (50 x 4.6 mm i.d., HiChrom Ltd, UK) was used in conjunction with a Phenomenex MAX RP guard column (4 x 3 mm) at a temperature of 35 °C. The mobile phase comprised of water (solvent A), acetonitrile (solvent B) and a 2.5% v/v aqueous formic acid solution. The relative percentage composition of solvents A, B and C was controlled using the quaternary pump over the course of each run as detailed in Table 5.4. The samples were analysed using an injection volume of 10 μL and a mobile phase flow rate of 1.0 mL/min with a total run time of 4.5 min. The column was conditioned by pumping mobile phase through for approximately 30 min prior to use.

Table 5.4: Mobile phase gradient for the LC-MS/MS analysis of alprenolol and metoprolol where A = water, B = acetonitrile, C = 2.5% v/v formic acid aqueous.

Step	Total time (min)	A (%)	B (%)	C (%)
0	0.0	88	10	2
1	0.5	88	10	2
2	2.5	8	90	2
3	3	3	95	2
4	3.5	88	10	2
5	4.5	88	10	2

5.3.7.8 Mass Spectrometric Conditions

Data were collected using a PE SCIEX API 4000 triple quadrupole mass spectrometer (ABI-SCIEX, Toronto, Canada) operated in Multiple Reaction monitoring (MRM) mode. Atmospheric pressure chemical ionisation was performed, using a Turbo Spray ion source, in the positive ion mode. The working parameters of the mass spectrometer are listed in Table 5.5.

Ions monitored: alprenolol m/z 250.3 → 116.2
 metoprolol m/z 268.3 → 116.3
 propranolol m/z 260.38 → 116.3

Table 5.5: Mass spectrometer main working parameters

Parameter	Value
Source temperature (°C)	700
Dwell time per transition (ms)	150
Ion source gas (Gas1) (psi)	50
Ion source gas (Gas2)(psi)	55
CUR (psi)	10
Ion spray voltage (V)	3500
Entrance potential (V)	10
Collision energy (V)	27
Declustering potential (DP) (V)	81
Collision cell exit potential (V)	10
CAD	5
Ihe	ON
CEM	2000
DF	-250

5.3.8 Pharmacokinetic and Statistical Analysis

Plasma drug concentration data were processed using Microsoft® Excel and a nonlinear regression analysis programme WinNonlin® version 4.1 (Pharsight Corporation, USA). Statistical operations were carried out using SPSS 14.0 for Windows (SPSS Inc.). This section describes the statistical treatment of the data, including the calculation of pharmacokinetic parameters from the intravenous data and use of these parameters in subsequent deconvolution calculations to determine the absorption profiles of alprenolol and metoprolol from the subcutaneously injected formulations (aqueous solutions, microspheres and *in situ*-forming depots).

Initially, all plasma drug concentration values were normalised to a rat weight of 250 g by application of Equation 5.1 to correct for differences in rat body weight.

$$\text{Weight normalised plasma conc. (ng/mL)} = \frac{\text{Rat weight (g)}}{250 \text{ g}} \times \text{Plasma conc. (ng/mL)}$$

Equation 5.1: Weight normalisation of plasma drug concentrations to 250 g.

When the drug plasma concentration was below the lower limit of quantification (LLOQ) it was considered to be 0 ng/mL in animals from which a full sample volume of 50 µL was obtained, and for those in which dilutions were required, the data point was removed. To enable zero values to be plotted on a semi-log scale, these values were designated 0.01 ng/mL. Samples with insufficient volume for extraction were omitted from calculations. The plasma concentration data obtained following intravenous dosing

were fitted to an unweighted non-compartmental model using WinNonlin[®]. The following pharmacokinetic parameters were then generated for each animal:

$AUC_{(0-\infty)}$: Area under the plasma drug concentration-time curve from time $t = 0$ to infinity (min.ng/mL).

V_{ss} : The apparent volume of distribution at steady state (mL).

$t_{1/2}$: The elimination half life (i.e. the time taken for the plasma concentration to fall by one-half (min).

CL : The rate of clearance of drug from the plasma (mL/min).

The geometric means of each parameter were calculated according to Equation 5.2, and these values were used for subsequent deconvolution calculations.

$$GM_{\bar{y}} = \sqrt[n]{(y_1, y_2, y_3, \dots, y_n)}$$

Equation 5.2: Calculation of the geometric mean.

Data from the subcutaneous administration of aqueous solutions of each beta-blocker were processed in a similar fashion. All concentrations were weight normalised to 250 g, and fitted to an unweighted non-compartmental model for a single extravascular input using WinNonlin[®]. Partial AUC s were generated from $t = 0$ to each time point using the linear trapezoidal method. The geometric mean of each AUC value was used, along with the mean pharmacokinetic parameters derived from the intravenous data, in Wagner-Nelson deconvolution calculations. Deconvolution allows the study of the absorption process by effectively removing the distribution and elimination phases from

the plasma concentration-time curve. The Wagner-Nelson is based on the basic principles of mass balance, whereby the amount absorbed (A_{ab}) is equal to the sum of the amount of drug in the body (A) and the amount eliminated (A_{el}) (as described in Equation 5.3) (Rowland and Tozer 1995).

$$A_{ab} = A + A_{el}$$

Equation 5.3: Mass balance equation, where A_{ab} is the amount of drug absorbed, A is the amount in the body and A_{el} is the amount eliminated.

Since from first principles $A = V.C$ and $A_{el} = CL.AUC_{(0-t)}$, substitution into Equation 5.3 gives Equation 5.4 which can be used to calculate the fraction of the dose absorbed with respect to time.

$$\text{Fraction Absorbed} = \frac{V \cdot C + (CL \cdot AUC_{(0-t)})}{\text{Dose}}$$

Equation 5.4: Wagner-Nelson method for calculation of fraction absorbed where V = Volume of distribution (from intravenous data) (mL), C = Plasma concentration at time t (from subcutaneous data) (ng/mL), CL = Clearance (from intravenous data) (mL/min) and $AUC_{(0-t)}$ = Area under the curve from $t = 0$ to time t (from subcutaneous data) (min.ng/mL).

The calculated fraction absorbed was then plotted against time to give the absorption profile of each compound from the subcutaneous site. Data from the subcutaneous injection of alprenolol and metoprolol microspheres and *in situ*-forming depots were treated in the same manner. The cumulative absorption profiles of each formulation were then characterised by calculating and comparing absorption rate constants at different time intervals from the slope of the curve.

5.3.9 Histology

At the end of each experiment animals were sacrificed by CO₂ inhalation. The injection site was exposed and inspected for macroscopic changes, and digital photographs taken. The tissue and polymeric mass was then excised and fixed in formaldehyde (10% v/v dilution of 37 - 40%), 20 x sample volume in a glass vial. The samples were then processed by Stephen Davison of the Histopathology Department, Royal Free Hospital, London. The tissues were dehydrated, cleared and embedded in paraffin. The samples were then sectioned using a microtome, stained (haematoxylin and eosin, H&E) and examined by light microscopy (Phillips) to evaluate the local reactions at the injection site.

The tissue reaction to biocompatible and biodegradable microspheres has been recently reviewed (Anderson and Shive 1997), and is said to occur in three phases. The first phase of the response occurring within the first few days to weeks and is characterised by mechanical injury to the injection site and acute and chronic inflammation involving the accumulation of polymorphonuclear leukocytes, lymphocytes, plasma cells and monocytes, which begin to differentiate into macrophages. The second phase involves the fusion of macrophages into giant cells, visible at the tissue/microsphere interface. Within two to three weeks of implantation, fibrous capsule development is initiated by collagen secreted from fibroblasts, and neoangiogenesis begins (Anderson and Shive 1997). This foreign body reaction persists until the device degrades to less than 10 µm in diameter, at which point the remainder of the device is phagocytosed by macrophages and foreign body giant cells, comprising the third phase of the tissue reaction. After the

polymeric mass has been completely degraded, the size of the fibrous capsule is reduced, leaving minimal scarring (Anderson and Shive 1997).

Due to the relatively short duration of this study (10 days), significant degradation of the polymer matrix is unlikely to be observed. The expected response following 10 days *in situ* is the acute and chronic inflammatory response of phase I, with the possible initiation of fibrous capsule formation.

5.4 Results and Discussion

5.4.1 LC-MS/MS Method Validation

Using a Turbo Ion Spray ionisation interface, alprenolol, metoprolol and the internal standard (propranolol) gave protonated molecular ions at m/z 250, 268 and 260 respectively. Fragmentation of these ions using collision activated dissociation (CAD) and a collision energy of *ca* 27 eV in the Q2 region of the mass spectrometer resulted in strong product ions for the analytes and the internal standard. The predominant ion observed from the fragmentation was at m/z 116 for all three compounds. The proposed fragmentation pathway of the analytes is illustrated in Figure 5.4. The product ions were monitored using multiple reaction monitoring (MRM) from the quasi-molecular ions.

The liquid chromatography-tandem mass spectrometry method developed gave good levels of specificity and sensitivity for the quantitative determination of analytes and internal standard in 50 μ L of rat plasma. Retention times for alprenolol and metoprolol were *ca* 2.7 and 2.47 minutes respectively and no interference from the rat plasma matrix was observed. Sample chromatograms for alprenolol and metoprolol, together with the internal standard propranolol, are illustrated in Figures 5.5 and 5.6 respectively. The assay showed excellent linearity as illustrated by the calibration curves shown in Figures 5.7 and 5.8, which had regression coefficients of 0.9992 and 0.9994 respectively. The lower limit of quantification (LLOQ) of this assay was 2 ng/mL, while the lower limit of detection was in the region of 0.2 ng/mL.

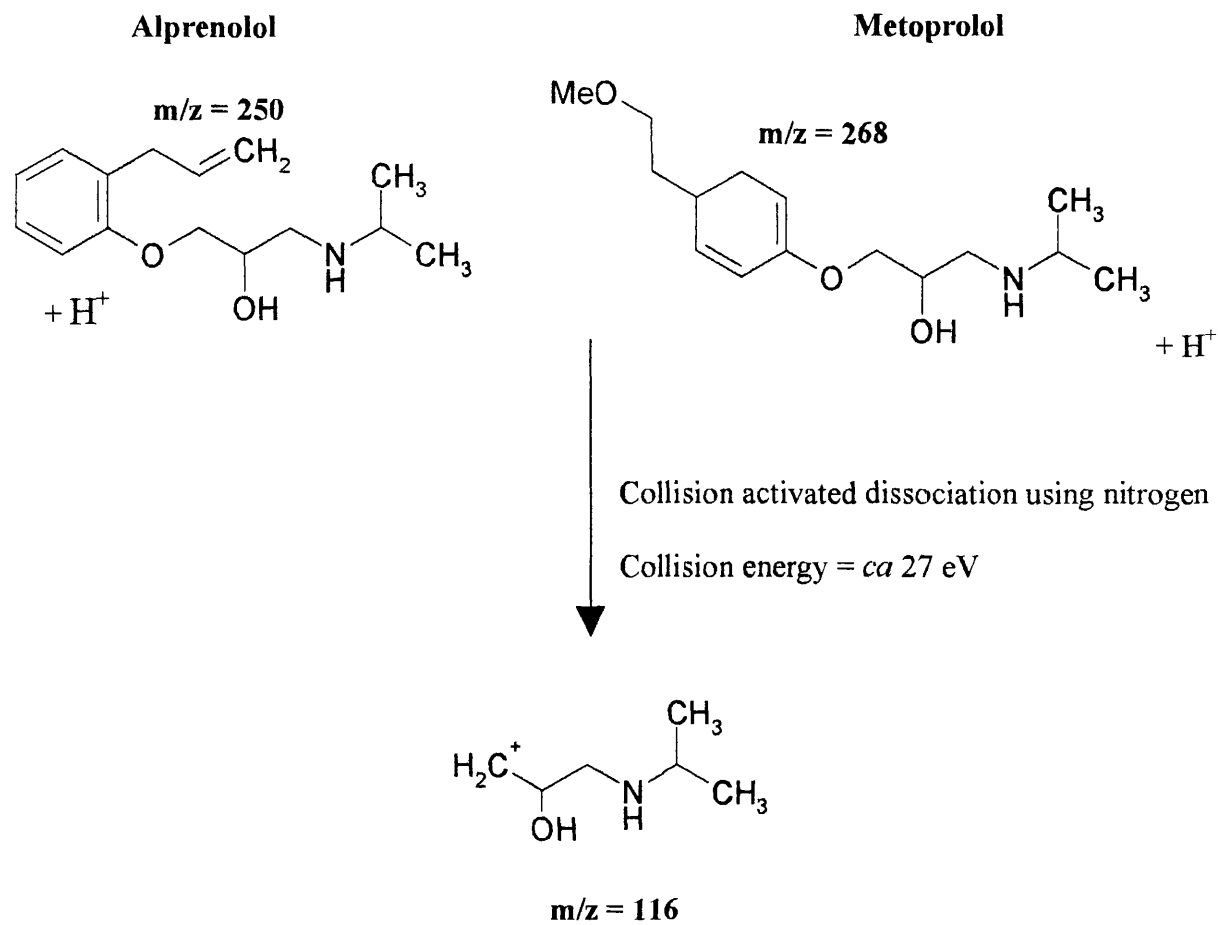


Figure 5.4: Proposed fragmentation pathway of the analytes (metoprolol and alprenolol).

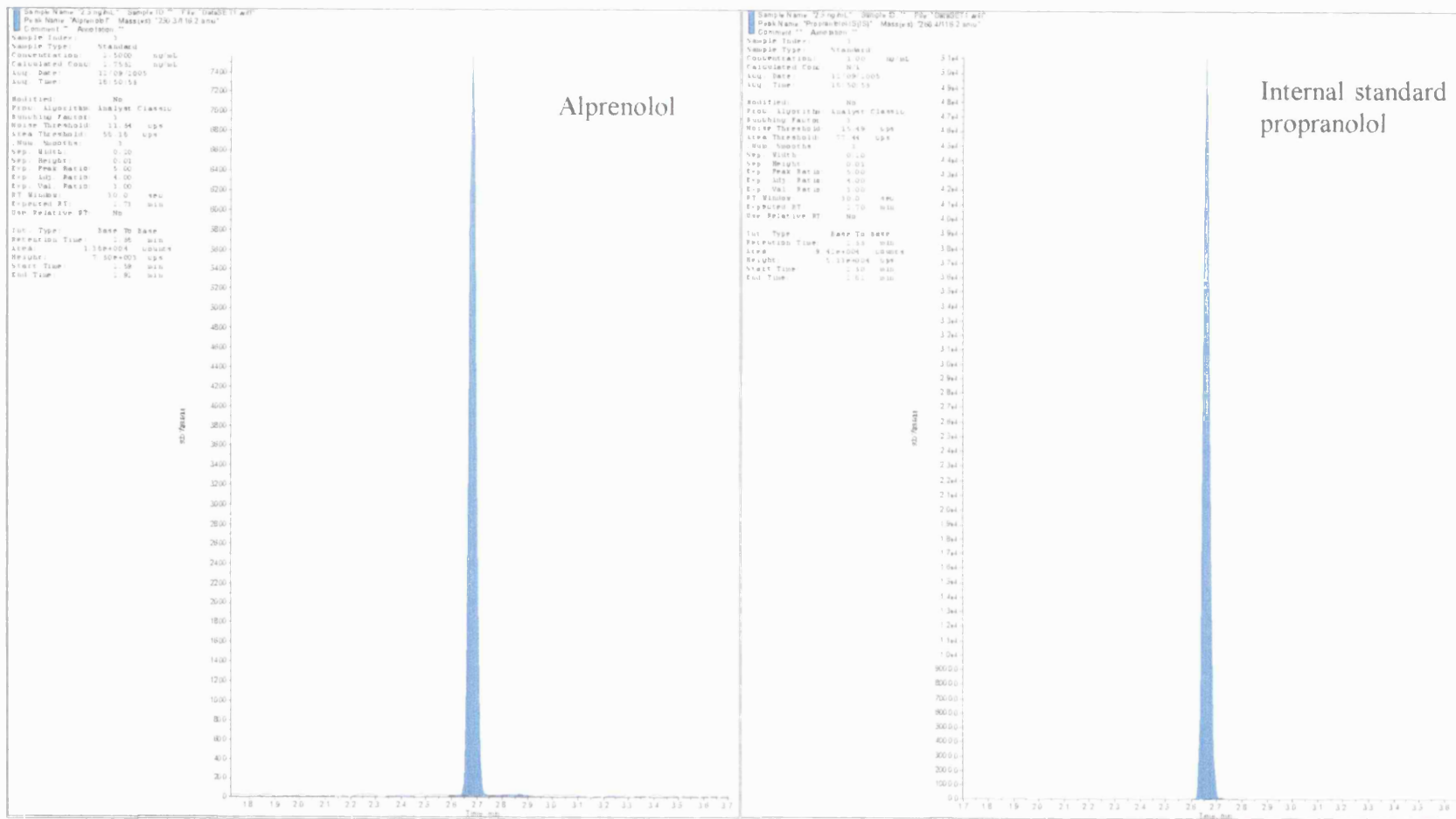


Figure 5.5: A representative alprenolol chromatogram for plasma extracted 2 ng/mL calibration standard, and the internal standard propranolol.

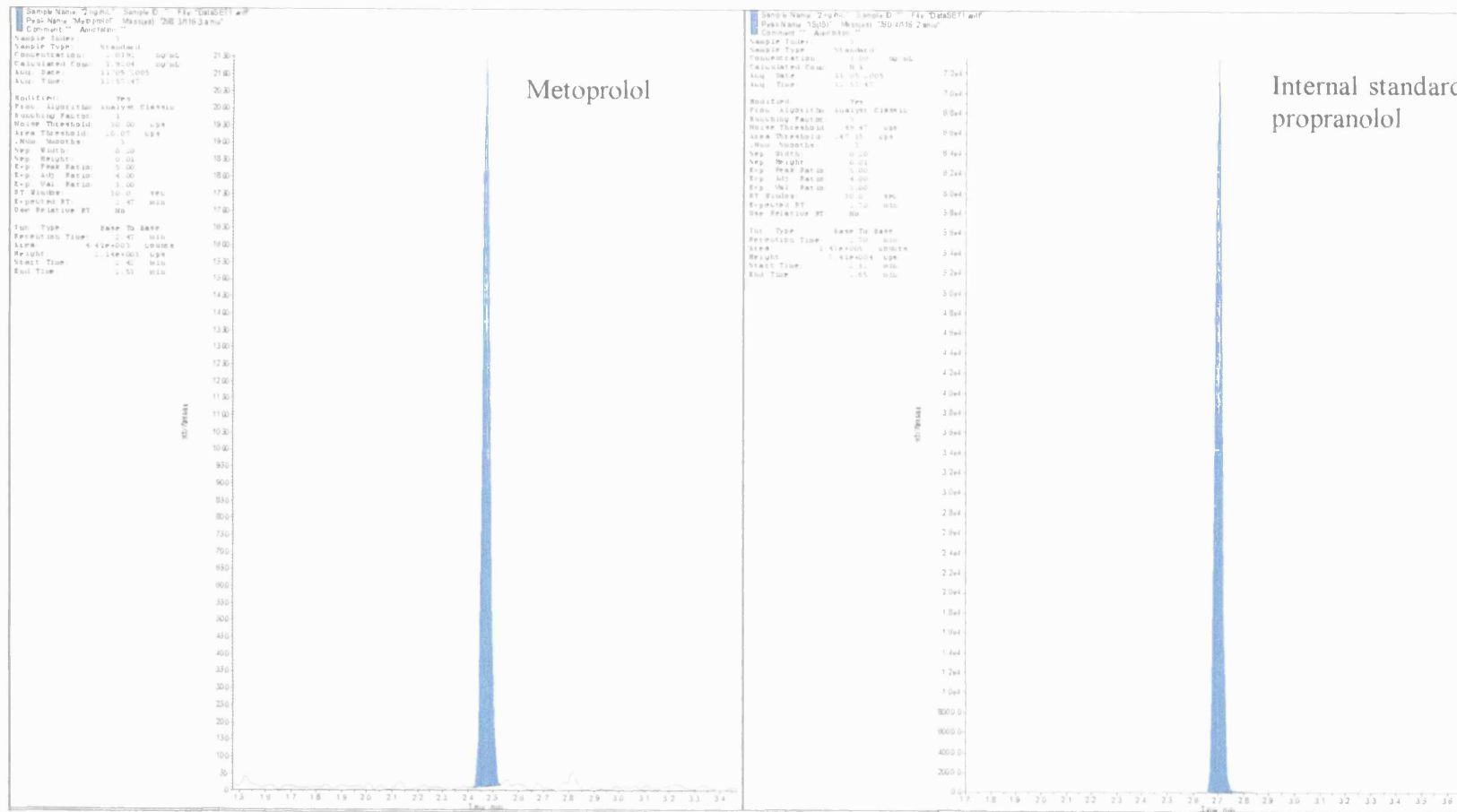


Figure 5.6: A representative metoprolol chromatogram for plasma extracted 2 ng/mL calibration standard, and the internal standard propranolol.

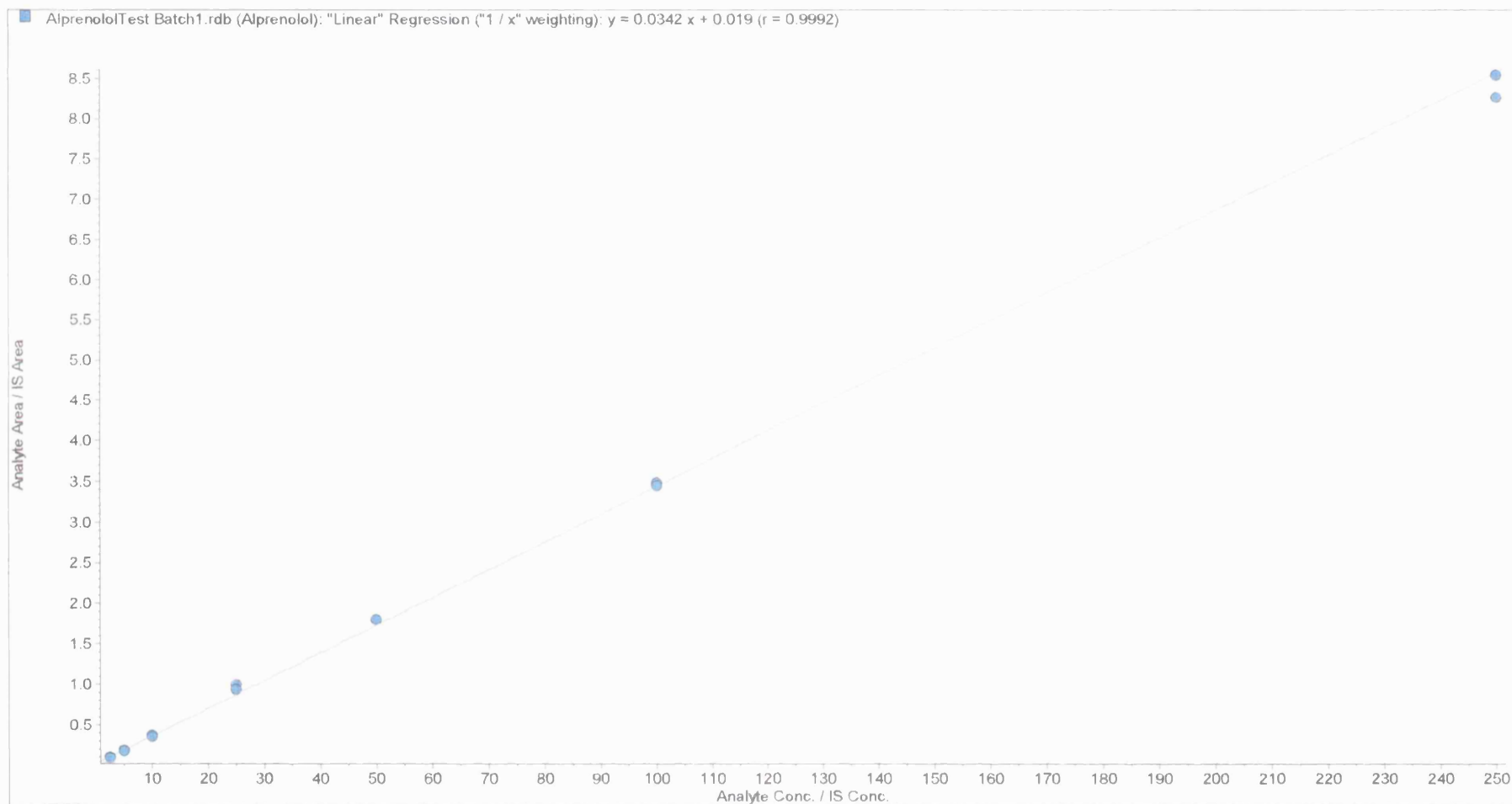


Figure 5.7: Typical calibration plot obtained from rat plasma spiked with 2 to 250 ng/mL alprenolol and the internal standard.

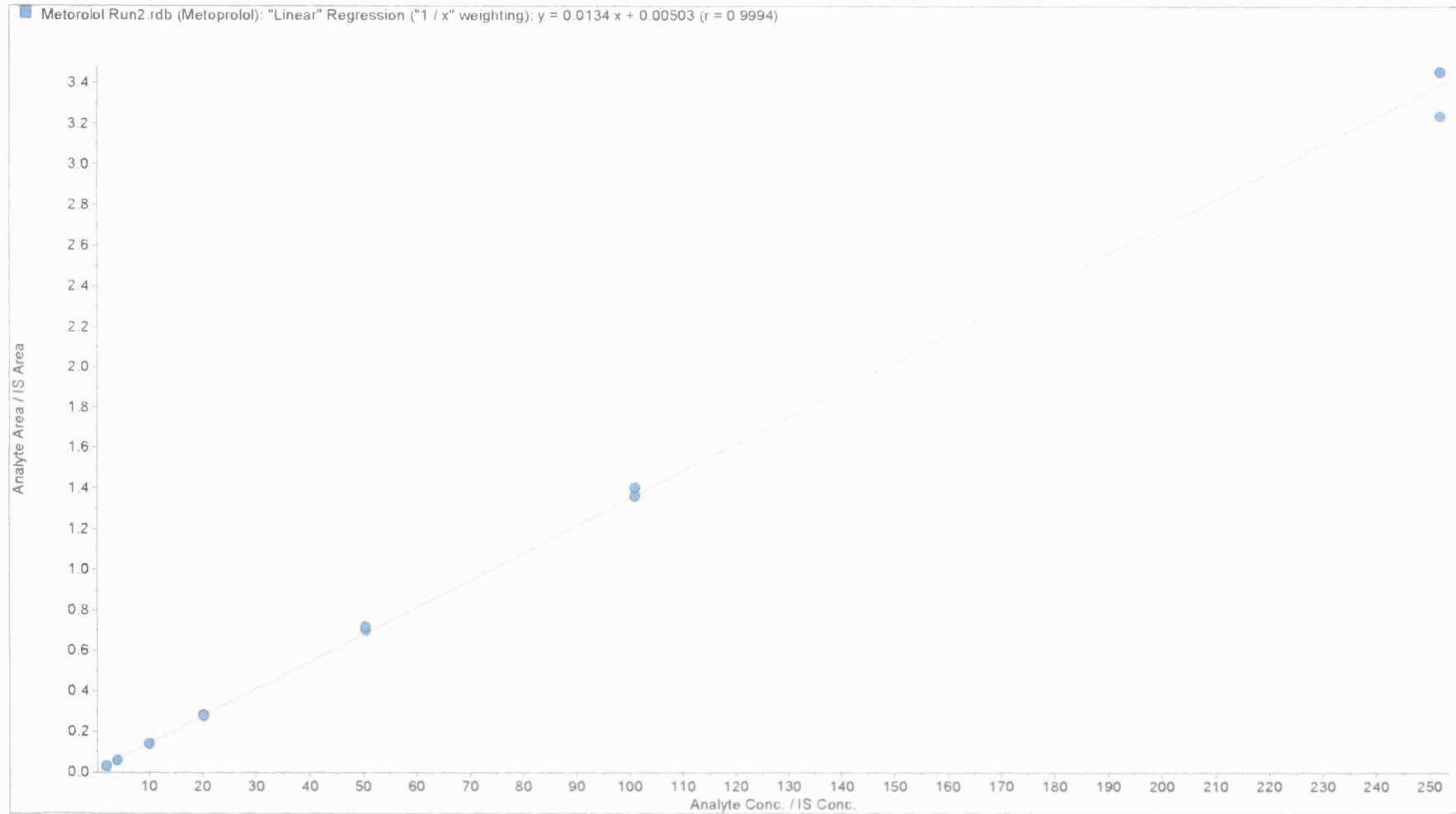


Figure 5.8: Typical calibration plot obtained from rat plasma spiked with 2 to 250 ng/ml metoprolol and the internal standard.

5.4.2 *In Vivo* Studies

5.4.2.1 Intravenous Administration of Alprenolol and Metoprolol

Weight normalised drug plasma concentrations for intravenously administered alprenolol and metoprolol are reported in Tables 5.6 and 5.7 respectively. In retrospect, the 1 minute time point was inappropriate for this study since insufficient time had elapsed to allow arterial-venous mixing, potentially resulting in inaccurate drug plasma concentrations at this time point. Any samples taken before 2 minutes were therefore excluded from the data set, and from further calculations (applicable to rats A7, A10 and M1). Plasma concentration data from rat A8 were also excluded from calculations since the concentration-time profile indicates that the intravenous injection was unsuccessful, i.e. that the drug was inadvertently administered extravascularly (see Appendix Fig. A1). Data from rats A1 and A6 were deemed to be statistical outliers (i.e. were more than ± 2 SD) and were also therefore excluded. The relatively high number of exclusions and hence the higher number of animals used in the alprenolol study was due to initial inexperience in this experimental technique.

Semi-log plots of weight normalised plasma drug concentration values against time for each sample set are depicted in Figures 5.9 and 5.10. Both drugs underwent rapid distribution, which had occurred significantly by the time of the first measurement, hence the apparently low C_{max} values and the rapid initial decline in plasma drug concentration. Consequently, there was a large variability in the first measurement. However, since it is the terminal elimination rate which is of interest in this study, this variability is of little consequence. Improvements in the dosing technique and sampling at a more appropriate time interval (e.g. 5 min post dose) could reduce this variability in future work.

The intravenous plasma concentration-time data were fitted to a non-compartmental model using WinNonlin[®]. Representative curves for the alprenolol and metoprolol intravenous data are shown in Figures 5.11 and 5.12 respectively. Non-compartmental analysis was deemed the most appropriate method for these data since not all the curves could be adequately described by either a one- or two-compartmental model. Errors were encountered during curve stripping due to the rapid change in slope caused by insufficient data points to describe the rapid distribution and subsequent equilibration phases. The two-compartment model was therefore unsuitable in most cases. Additionally, fitting the data to a one-compartment model often resulted in too great a weighting on the highly variable initial data points on the plasma concentration-time curve. With non-compartmental analysis, calculations are based on the area under the plasma concentration versus time curve (*AUC*) and the first moment curve (*AUMC*), and therefore gave a better fit for the terminal elimination phase. Regression coefficients of the sample curves illustrated in Figures 5.11 and 5.12 for rats A10 and M5 were 0.9905 and 1.0 respectively.

The relevant pharmacokinetic parameters were then calculated using WinNonlin[®], and are summarised in Table 5.8 and 5.9. Metoprolol was cleared from the body at a significantly faster rate than alprenolol (108 mL/min *cf* 14 mL/min), and consequently had a significantly shorter half-life ($t_{1/2}$) (20 and 91 min respectively) (*t*-Test, $p < 0.05$). The experimentally determined metoprolol clearance value was considerably higher than rat hepatic blood flow (13.8 mL/min (Davies, 1993)). This phenomenon was also observed by Belpaire et al. (1990) who recorded a metoprolol clearance rate of 292 mL/min/kg in 3 month old animals. The geometric mean values for the steady state volume of distribution (V_{ss}) and clearance rate (*CL*) of each compound were then used in Wagner-Nelson deconvolution calculations as described in the following sections.

Table 5.6 : Weight normalised alprenolol plasma concentrations following a 1 mg (free base equivalent) intravenous bolus dose. *Values omitted from calculations since $t < 2$ min.

Rat weight (g)	227		230		175		178		218		219		221	
Rat no.	A2		A3		A4		A5		A7		A9		A10	
Approx. time (min)	Time (min)	Conc. (ng/mL)	Time (min)	Conc. (ng/mL)	Time (min)	Conc. (ng/mL)	Time (min)	Conc. (ng/mL)	Time (min)	Conc. (ng/mL)	Time (min)	Conc. (ng/mL)	Time (min)	Conc. (ng/mL)
2	2.5	619.365	3.5	226.743	3	2005.990	3.5	4273.210	1	174.330*	4	2421.790	1	681.157*
8	9	332.782	10	299.561	9	237.594	9	314.989	8	314.051	8	248.591	8	457.293
15	17.5	314.704	18	279.340	17.5	204.533	16	287.627	15	242.538	15	248.223	15	520.791
30	33	303.862	34.5	226.642	31.5	215.341	32	300.229	30	240.655	30	247.742	30	409.875
60	63	280.590	64.5	279.560	63	190.820	62.5	226.736	60	249.200	60	216.030	60	296.299
90	93	265.145	99.5	192.749	92	149.184	101	184.543	90	238.248	90	193.149	90	257.836
120	125	224.884	137.5	178.949	127.5	124.607	123	152.439	120	202.313	135	176.838	120	208.695
180	187.5	167.063	190	63.419	191	36.889	184.5	35.846	195	130.591	185	139.161	200	79.543

Table 5.7: Weight normalised metoprolol plasma concentrations following a 1 mg (free base equivalent) intravenous bolus injection. *Insufficient sample volume, **This value was deemed an outlier and was therefore excluded from calculations. Rat M1 was excluded from further calculations due to an insufficient number of data points.

Rat weight (g)	212		184		172		170		162	
Rat no.	M1		M2		M3		M4		M5	
Approx time. (min)	Time (min)	Conc (ng/mL)	Time (min)	Conc (ng/mL)	Time (min)	Conc (ng/mL)	Time (min)	Conc (ng/mL)	Time (min)	Conc (ng/mL)
2	*		2.5	103.047	3	85.849	3.5	227.698	2	664.200
8	8	60.13	10.5	21.84**	10	61.823	9.5	216.179	8.5	474.880
15	17.5	30.07	19.5	82.410	21	57.551	16	204.326	16	424.557
30	34	22.02	32.5	68.037	32.5	46.339	31	93.765	31	297.924
60	*		62	22.418	68.5	33.967	62.5	43.470	64.5	194.432
90	*		96.5	3.073	93	20.023	94.5	38.655	92.5	73.490
120	*		121.5	1.141	122.5	12.743	124.5	12.889	122.5	33.989
180	*		187	0.000	188	0.696	192.5	1.186	183.5	7.204

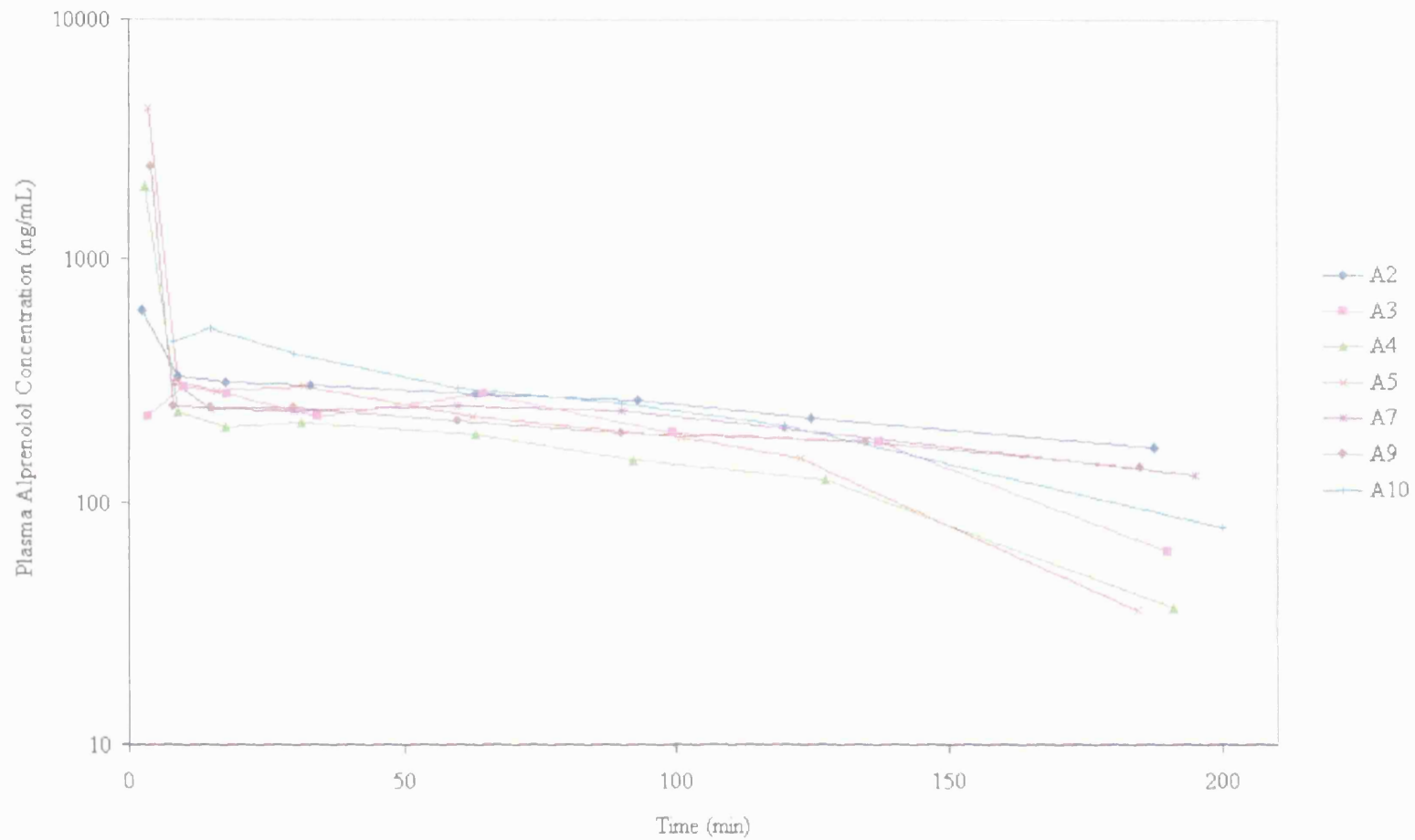


Figure 5.9: Semi-logarithmic plot of weight normalised alprenolol plasma concentration-time curves following a 1 mg (free base equivalent) intravenous bolus dose.

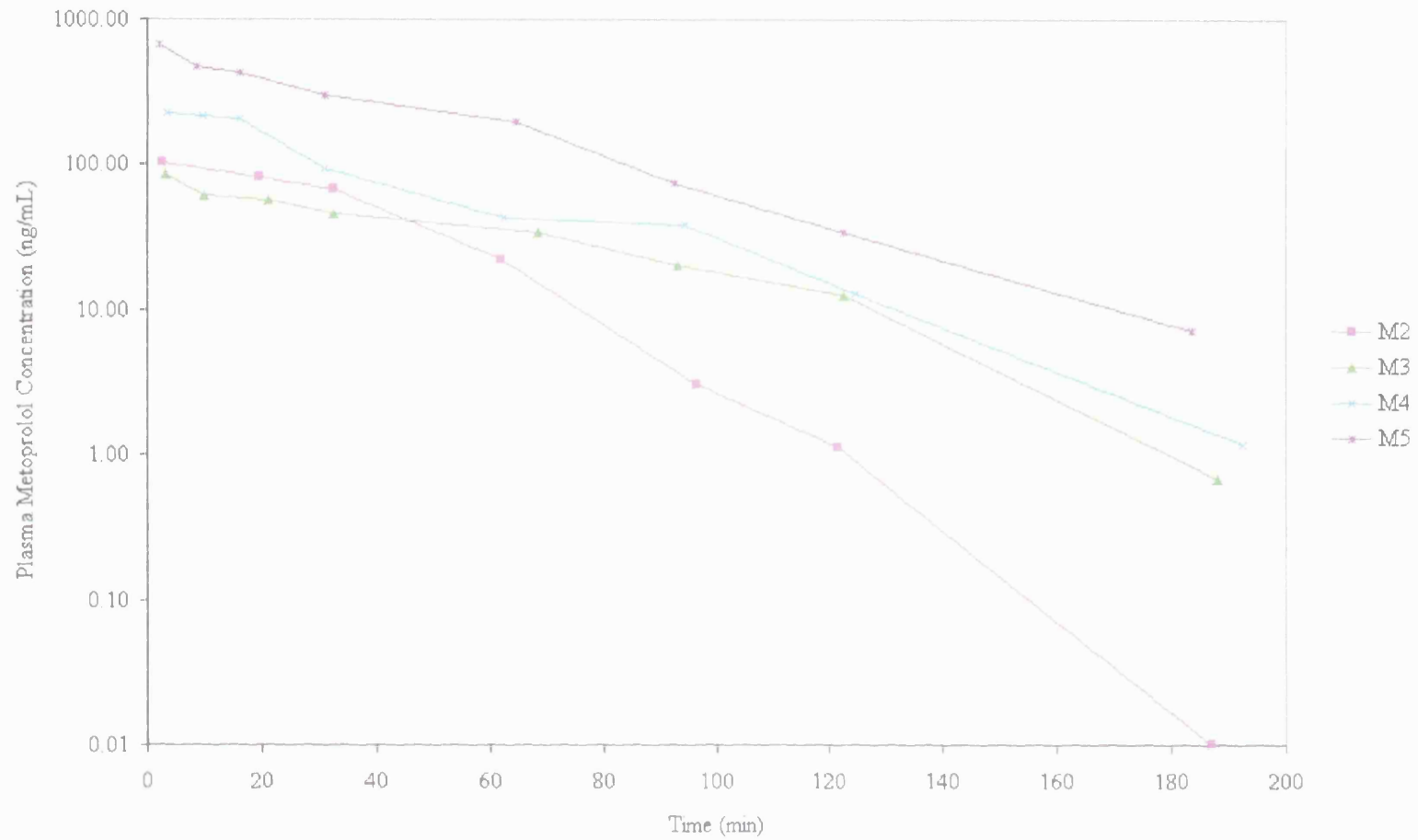


Figure 5.10: Semi-logarithmic plot of weight normalised metoprolol plasma concentration-time curves following a 1 mg (free base equivalent) intravenous bolus dose.

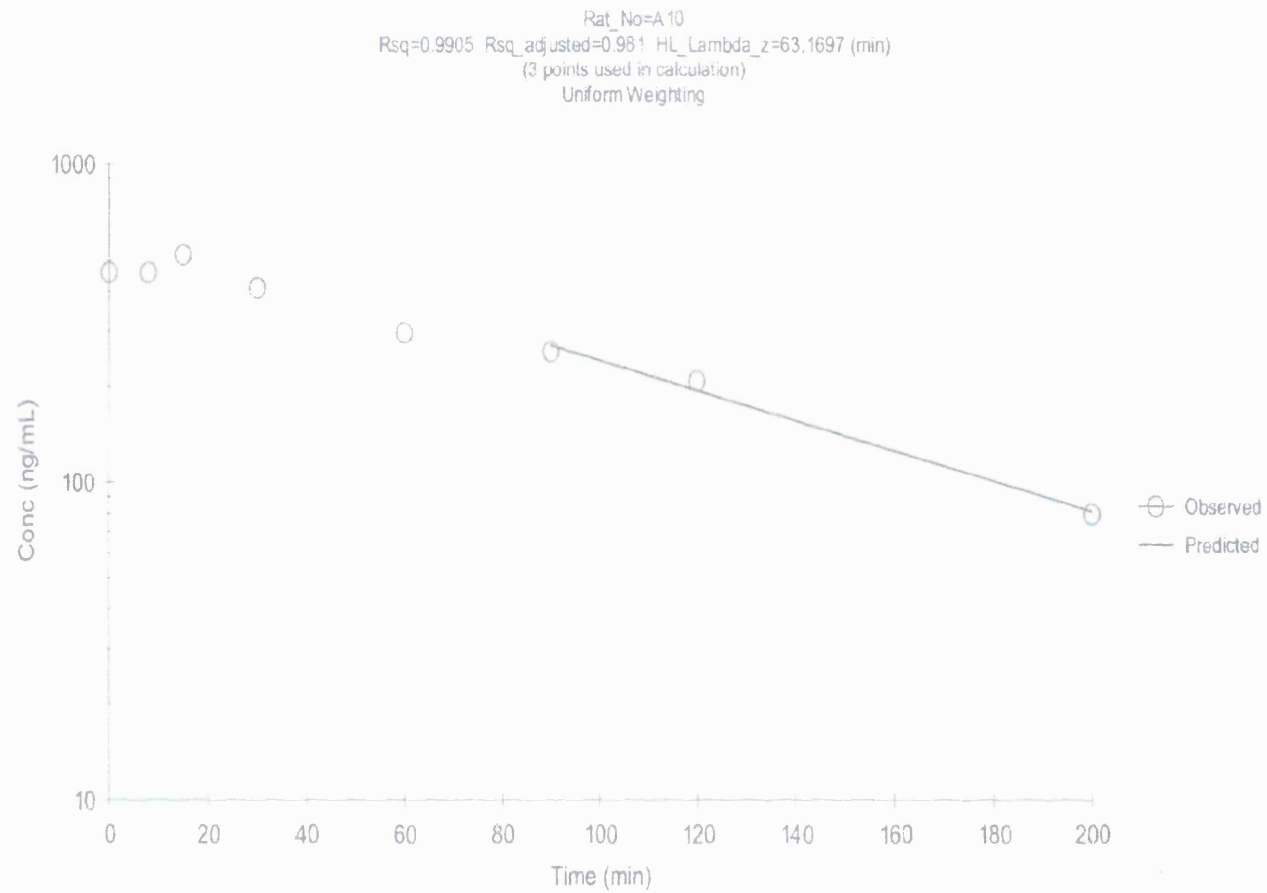


Figure 5.11: Example of fitting of alprenolol intravenous plasma concentration-time profile to a non-compartmental model by WinNonlin[®] (rat A10).

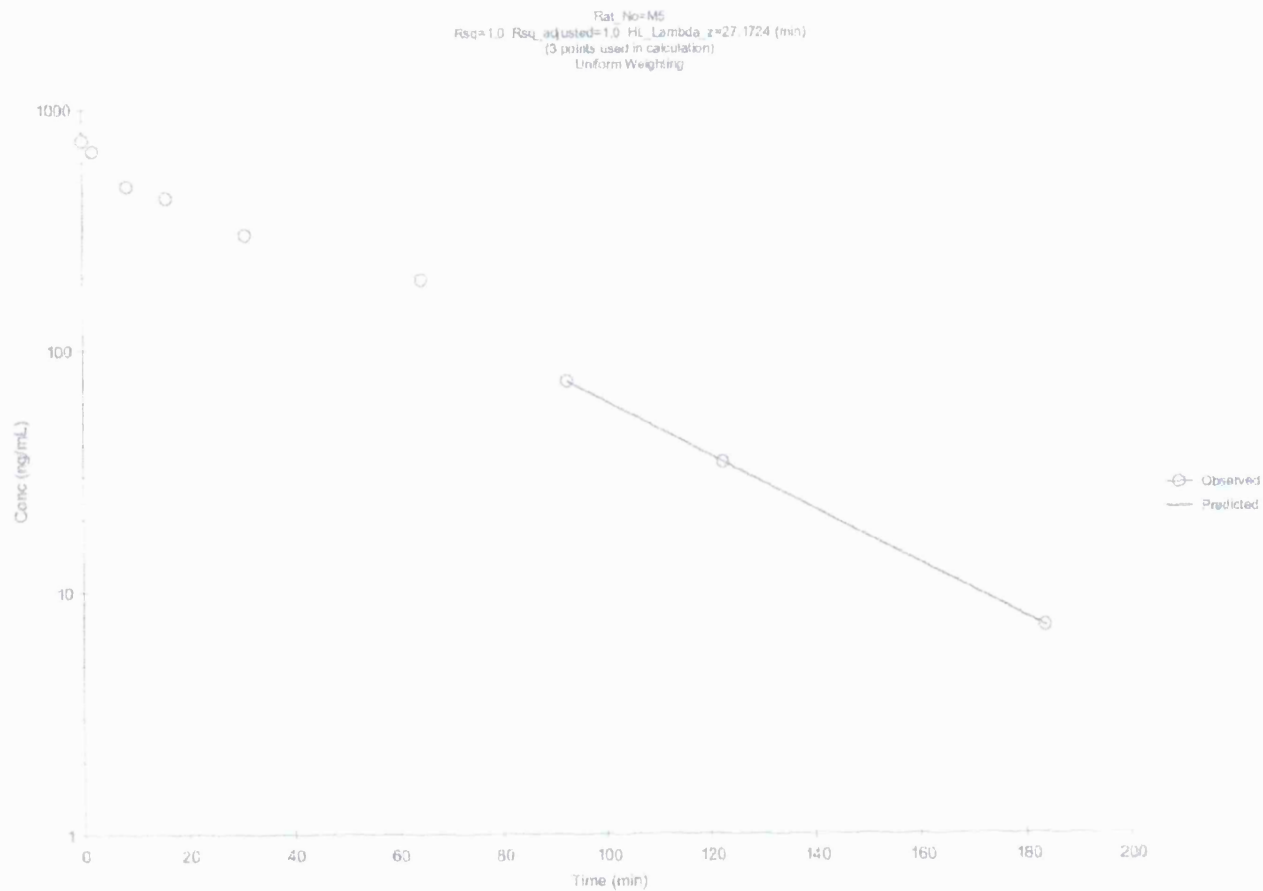


Figure 5.12: Example of fitting of metoprolol intravenous plasma concentration-time profile to a non-compartmental model by WinNonlin[®] (rat M5).

Table 5.8: WinNonlin[®] generated pharmacokinetic parameters from the non-compartmental analysis of plasma concentration-time profiles obtained following an intravenous bolus dose of 1 mg alprenolol to rats.

Rat no.	A2	A3	A4	A5	A7	A9	A10	Geometric mean
<i>AUC</i>_(0-inf) (min.ng/mL)	83746	61484	47497	93414	67234	133212	58743	73885
<i>t</i>_{1/2} (min)	142	115	54	34	130	205	63	91
<i>CL</i> (mL/min)	12	16	21	11	15	8	17	14
<i>V</i>_{SS} (mL)	2481	2903	1254	322	2886	1284	1665	1510

Table 5.9: WinNonlin[®] generated pharmacokinetic parameters from the non-compartmental analysis of plasma concentration-time profiles obtained following an intravenous bolus dose of 1 mg metoprolol to rats.

Rat no.	M2	M3	M4	M5	Geometric mean
<i>AUC</i>_(0-inf) (min.ng/mL)	4667	5099	10504	29043	9231
<i>t</i>_{1/2} (min)	15	21	20	27	20
<i>CL</i> (mL/min)	214	196	95	34	108
<i>V</i>_{SS} (mL)	6064	9996	3740	1434	4246

5.4.2.2 Subcutaneous Injection of Alprenolol and Metoprolol HIPs in Aqueous Solution

Weight normalised drug plasma concentrations for subcutaneously administered solutions of alprenolol and metoprolol hydrophobic ion pairs are reported in Tables 5.10 and 5.11 respectively. Rat A1 was excluded from further calculations as it was deemed to be an outlier (i.e. ± 2 SD). Semi-log plots of these data are illustrated in Figures 5.13 and 5.14. Concentration values of 0.01 ng/mL were assigned at $t = 0$ and when the measured plasma drug concentration was below the LLOQ to enable graphical representation of these zero values on a logarithmic ordinate scale (however, 0 ng/mL was used in calculations). The plasma concentration-time profiles follow the expected pattern for extravascularly administered compounds, with a rapid absorption phase and the attainment of C_{max} , followed by the elimination phase characterised by the gradual decline in drug plasma concentration. Non-compartmental analysis using WinNonlin[®] was then carried out and the mean terminal elimination rate constants (k_{el}) for alprenolol and metoprolol were calculated as 0.008 ± 0.002 and 0.026 ± 0.005 min⁻¹ respectively. An independent-samples t -Test was conducted to compare these elimination rate constants to those obtained following intravenous administration of each compound. There was no significant difference at the 0.05 level, indicating that route of administration had no significant effect on elimination rate. It can be inferred that absorption of the ion pairs from the subcutaneous site was not, therefore, dissolution rate limited, which can be of concern when administering poorly soluble compounds subcutaneously.

Partial AUC values from $t = 0$ to time t ($AUC_{(0-t)}$) were calculated using the linear trapezoidal rule and are reported in Tables 5.12 and 5.13. Wagner-Nelson deconvolution was then applied as described in Section 5.3.8, and a plot of fraction of drug absorbed versus time was constructed (Fig. 5.15). Mixed between-within subjects analysis of variance, (or split-plot ANOVA, SPANOVA) was conducted to explore the impact of nature of the drug on absorption rate and fraction absorbed from this site. Alprenolol was absorbed to a statistically significantly greater extent ($F(1,6) = 26.1, p = 0.02$) at the $p < 0.05$ level. The effect size, calculated using eta squared, was very large (0.8). This observation can be explained by the more extensive partitioning of the lipophilic alprenolol from the aqueous injection vehicle, into and across the epithelial wall.

Table 5.10 : Weight normalised alprenolol plasma concentrations following a 1 mg (free base equivalent) subcutaneous dose. Rat A1 was deemed an outlier and was therefore excluded from further calculations.

Rat weight (g)	230		184		208		260		230	
Rat no.	A1		A2		A3		A4		A5	
Approx. time (min)	Time (min)	Conc. (ng/mL)	Time (min)	Conc. (ng/mL)	Time (min)	Conc. (ng/mL)	Time (min)	Conc. (ng/mL)	Time (min)	Conc. (ng/mL)
0	0	0.010	0	0.010	0	0.010	0	0.010	0	0.010
5	7.5	42.162	7.5	166.860	6	150.060	5.5	95.507	6	115.720
15	17.5	*	16.5	223.400	22.5	374.920	16	129.940	17.5	113.740
30	34	61.890	32	251.800	32	437.330	32.5	164.800	31	187.560
60	63	38.060	61.5	282.590	63.5	315.030	61.5	186.860	62	206.000
90	93	33.214	96	249.720	93.5	248.940	91.5	190.420	94.5	203.710
120	123	26.416	121.5	203.820	123	178.420	123.5	178.840	123.5	178.530
240	242	9.436	245	51.964	250	37.214	248	50.894	248.5	62.745
360	402	3.440	368	11.126	369	50.326	362.5	27.950	363.5	45.420

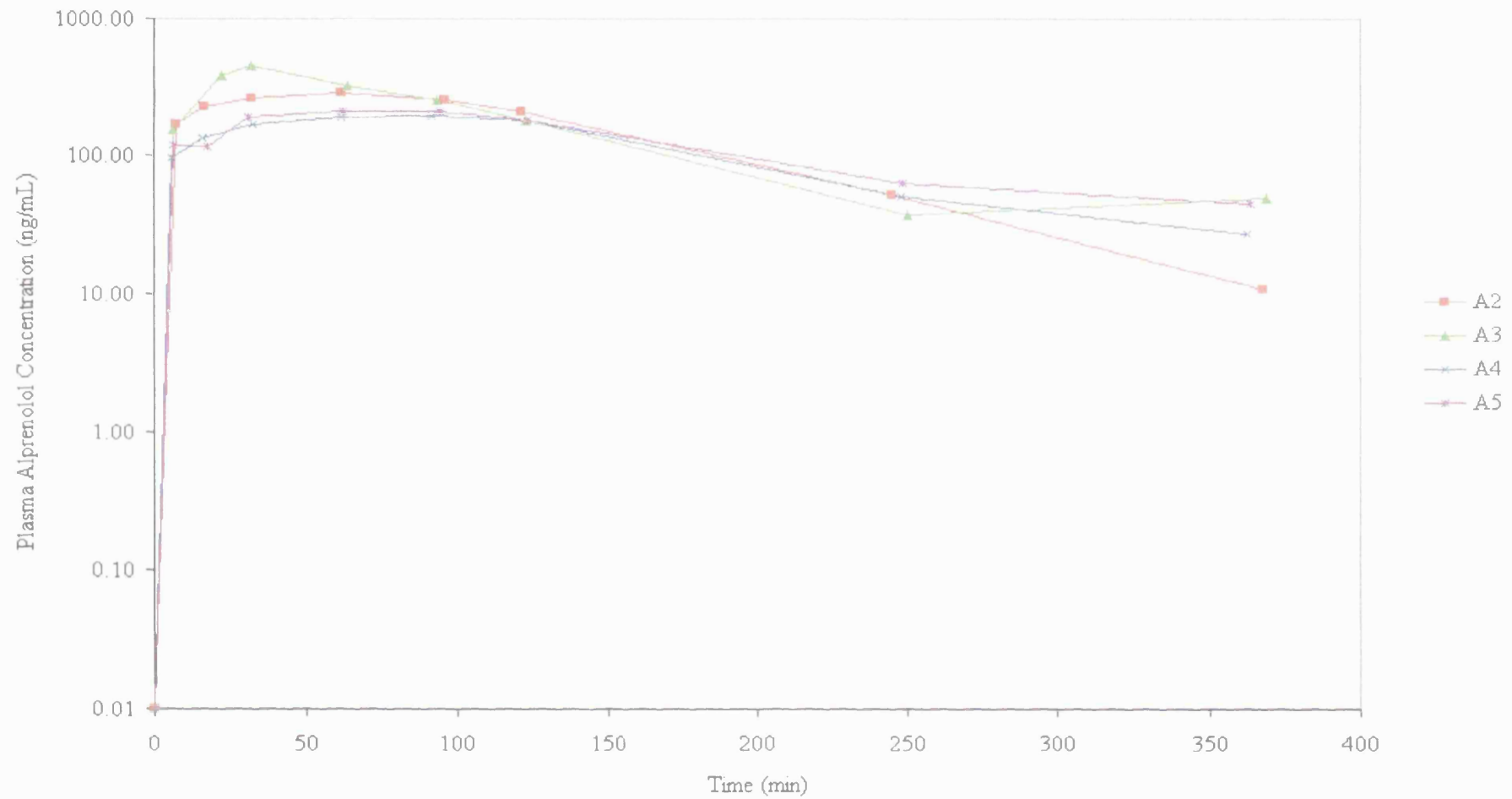


Figure 5.13: Weight normalised alprenolol plasma concentration-time curves following a 1 mg (free base equivalent) subcutaneous dose of alprenolol HIP in aqueous solution.

Table 5.11: Weight normalised metoprolol plasma concentrations following a 1 mg (free base equivalent) subcutaneous dose. *Denotes insufficient sample volume.

Rat weight (g)	205		190		185		190		183	
Rat no.	M1		M2		M3		M4		M5	
Approx. time (min)	Time (min)	Conc. (ng/mL)	Time (min)	Conc. (ng/mL)	Time (min)	Conc. (ng/mL)	Time (min)	Conc. (ng/mL)	Time (min)	Conc. (ng/mL)
0	0	0.010	0	0.010	0	0.010	0	0.010	0	0.010
5	6.5	14.994	8	21.428	8	30.612	7.5	13.257	8	17.905
15	17	21.650	17	18.175	22	23.613	17.5	26.490	16	17.287
30	31.5	16.243	31.5	16.361	34	23.604	32.5	30.554	32	21.350
60	65	20.145	61.5	16.452	65.5	21.277	*		64	22.347
90	91.5	10.396	93	12.054	92.5	13.924	93	23.427	97.5	9.809
120	121.5	3.842	121	3.649	124	5.988	*		121	4.800
240	245	0.010	246.5	0.303	253.5	0.221	254	0.010	241	0.010
360	363	0.010	361.5	0.010	363.5	0.010	*		365	0.010

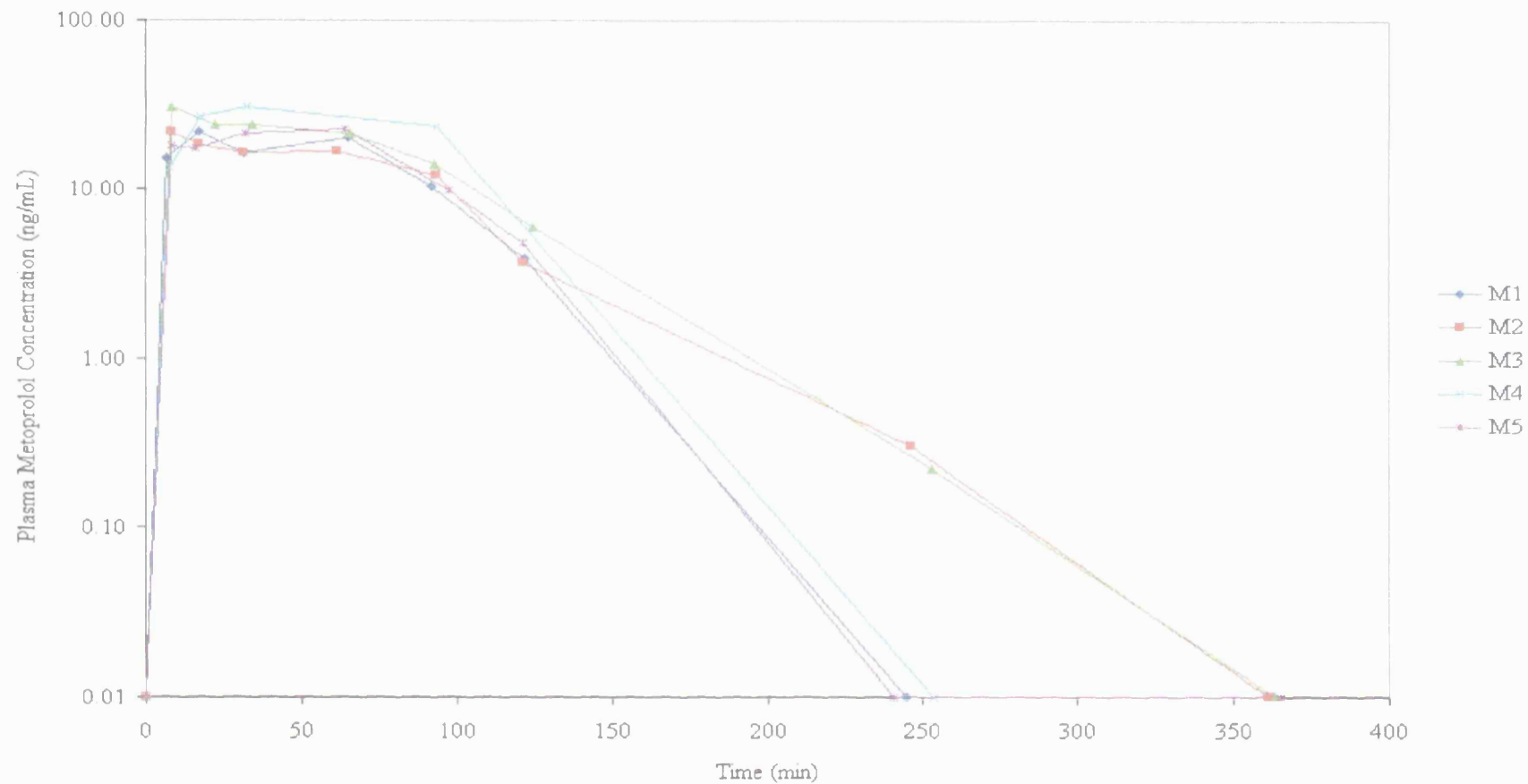


Figure 5.14: Weight normalised metoprolol plasma concentration-time curves following a 1 mg (free base equivalent) subcutaneous dose of metoprolol HIP in aqueous solution.

Table 5.12 : Area under the plasma alprenolol concentration-time curve (*AUC*) following a 1 mg (free base equivalent) subcutaneous dose from 0 to time *t*, calculated using the linear trapezoidal rule.

A2		A3		A4		A5	
Time (min)	$AUC_{(0-t)}$ (min.ng/mL)	Time (min)	$AUC_{(0-t)}$ (min.ng/mL)	Time (min)	$AUC_{(0-t)}$ (min.ng/mL)	Time (min)	$AUC_{(0-t)}$ (min.ng/mL)
0	0	0	0	0	0	0	0
7.5	626	6	450	5.5	263	6	347
16.5	2382	22.5	4781	16	1446	17.5	1667
32	6065	32	8639	32.5	3878	31	3700
61.5	13947	63.5	20489	61.5	8977	62	9801
96	23129	93.5	28949	91.5	14636	94.5	16458
121.5	28912	123	35252	123.5	20544	123.5	22001
245	44707	250	48945	248	34845	248.5	37080
368	48587	369	54154	362.5	39359	363.5	43300

Table 5.13: Area under the plasma metoprolol concentration-time curve (*AUC*) following a 1 mg (free base equivalent) subcutaneous dose from 0 to time *t*, calculated using the linear trapezoidal rule.

M1		M2		M3		M4		M5	
Time (min)	<i>AUC</i> _(0-t) (min.ng/mL)	Time (min)	<i>AUC</i> _(0-t) (min.ng/mL)	Time (min)	<i>AUC</i> _(0-t) (min.ng/mL)	Time (min)	<i>AUC</i> _(0-t) (min.ng/mL)	Time (min)	<i>AUC</i> _(0-t) (min.ng/mL)
0	0	0	0	0	0	0	0	0	0
6.5	49	8	86	8	122	7.5	50	8	72
17	241	17	264	22	502	17.5	248	16	212
31.5	516	31.5	514	34	785	32.5	676	32	521
65	1125	61.5	1007	65.5	1492			64	1221
91.5	1530	93	1455	92.5	1967	93	2309	97.5	1759
121.5	1744	121	1675	124	2281			121	1931
245	1981	246.5	1923	253.5	2683	254	4195	241	2219
363	1981	361.5	1941	363.5	2695			365	2219

Table 5.14: Wagner-Nelson deconvolution of alprenolol subcutaneous data.

A2		A3		A4		A5		Geometric mean time (min)	Geometric mean <i>F</i>	SD
Time (min)	Fraction absorbed (<i>F</i>)	Time (min)	Fraction absorbed (<i>F</i>)	Time (min)	Fraction absorbed (<i>F</i>)	Time (min)	Fraction absorbed (<i>F</i>)			
0	0.000	0	0.000	0	0.000	0	0.000	0.0	0.000	0.000
7.5	0.261	6	0.233	5.5	0.148	6	0.179	6.2	0.200	0.051
16.5	0.370	22.5	0.631	16	0.216	17.5	0.194	18.0	0.315	0.201
32	0.462	32	0.777	32.5	0.301	31	0.333	31.9	0.436	0.217
61.5	0.616	63.5	0.753	61.5	0.404	62	0.444	62.1	0.537	0.161
96	0.690	93.5	0.768	91.5	0.486	94.5	0.530	93.9	0.608	0.133
121.5	0.699	123	0.746	123.5	0.548	123.5	0.567	122.9	0.635	0.098
245	0.683	250	0.718	248	0.548	248.5	0.596	247.9	0.633	0.078
368	0.674	369	0.809	362.5	0.575	363.5	0.654	365.7	0.673	0.097

Table 5.15 : Wagner-Nelson deconvolution of metoprolol subcutaneous data.

M1		M2		M3		M4		M5		Geometric mean time (min)	Geometric mean <i>F</i>	SD
Time (min)	Fraction absorbed (<i>F</i>)	Time (min)	Fraction absorbed (<i>F</i>)	Time (min)	Fraction absorbed (<i>F</i>)	Time (min)	Fraction absorbed (<i>F</i>)	Time (min)	Fraction absorbed (<i>F</i>)			
0	0.000	0	0.000	0	0.000	0	0.000	0	0.000	0.0	0.000	0.000
6.5	0.069	8	0.100	8	0.143	7.5	0.062	8	0.084	7.6	0.087	0.032
17	0.118	17	0.106	22	0.155	17.5	0.139	16	0.096	17.8	0.121	0.024
31.5	0.125	31.5	0.125	34	0.185	32.5	0.203	32	0.147	32.3	0.154	0.036
65	0.207	61.5	0.179	65.5	0.252			64	0.227	64.0	0.215	0.031
91.5	0.210	93	0.209	92.5	0.272	93	0.350	97.5	0.232	93.5	0.250	0.059
121.5	0.205	121	0.197	124	0.273			121	0.230	121.9	0.224	0.034
245	0.215	246.5	0.210	253.5	0.292	254	0.455	241	0.240	247.9	0.270	0.102
363	0.215	361.5	0.210	363.5	0.292			365	0.240	363.2	0.237	0.038

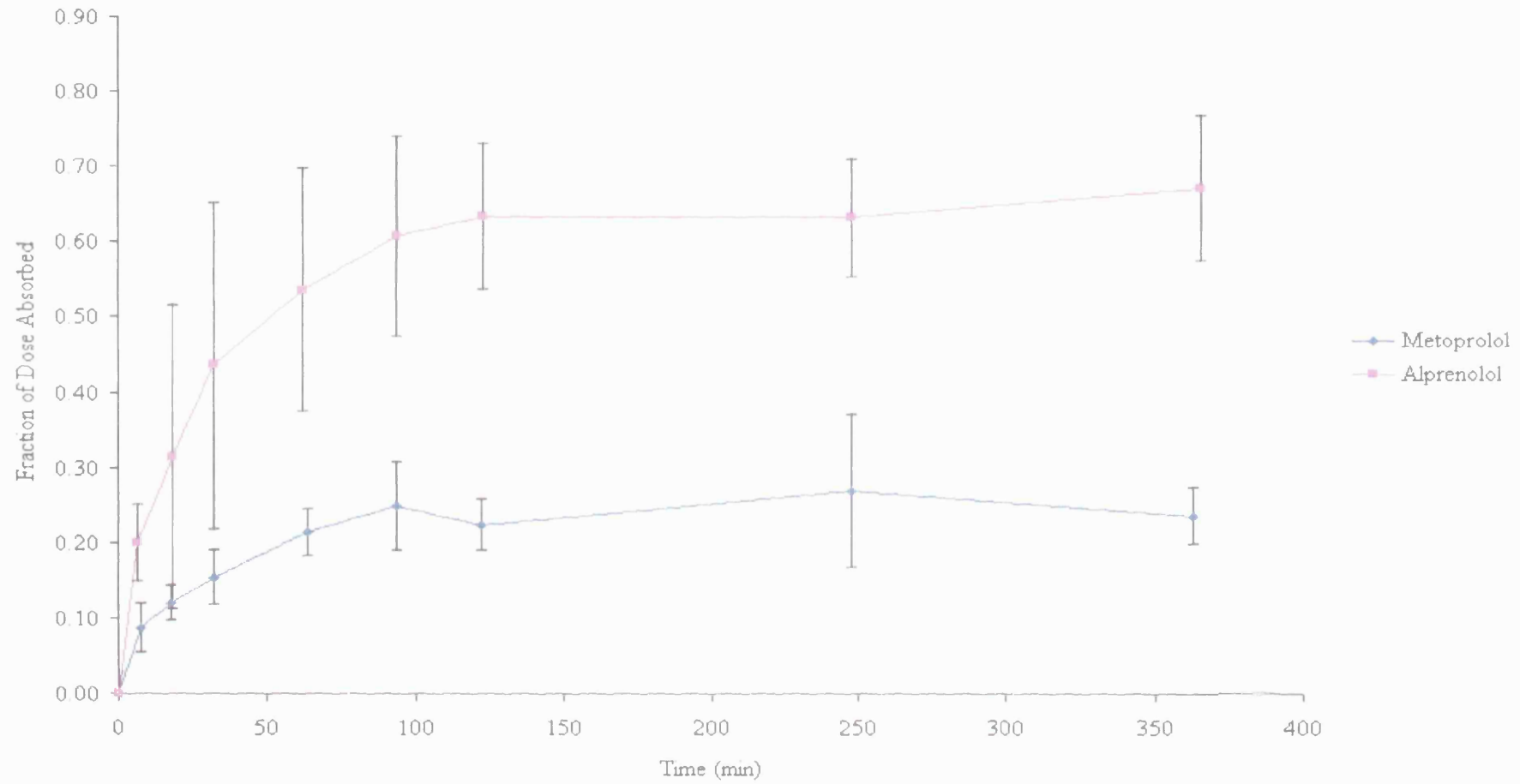


Figure 5.15 : Fraction absorbed vs time curves of aqueous alprenolol and metoprolol subcutaneous injection.

The slope of the fraction absorbed-time curve represents the absorption rate with respect to time. Approximate absorption rates between various time intervals (0 - 5, 5 - 90 and 90 - 360 minutes) were calculated from the gradient of the straight line drawn between these points and are reported in Table 5.16. An independent-samples *t*-Test was conducted to compare the absorption rates for the different drugs (also reported in Table 5.16). Alprenolol absorption rates were significantly higher than for metoprolol ($p < 0.05$), until 90 minutes where absorption rates for both compounds were approximately equal to zero, indicating no further absorption during this time interval.

Table 5.16: Mean absorption rate from subcutaneous solution of alprenolol and metoprolol HIPs. ^a $n=4$, ^b $n=5$. *significant at the 0.05 level.

Time interval (min)	Mean absorption rate (min ⁻¹) ± SD		
	0 - 5	5 - 90	90 - 360
Alprenolol HIP^a	0.0326 ± 0.0053	0.0047 ± 0.0010	-0.0004 ± 0.0011
Metoprolol HIP^b	0.0119 ± 0.0036	0.0019 ± 0.0008	0.0002 ± 0.0003
<i>p</i> (<i>t</i> -Test)	0.000*	0.003*	0.304

The more lipophilic alprenolol HIP was absorbed at a faster rate and more extensively from this site than metoprolol HIP. This can be explained by the more rapid partitioning of a lipophilic drug from the aqueous injection vehicle into and across the epithelial wall, and into the systemic circulation.

5.4.2.3 Microspheres

The microsphere formulations were freely injectable through a 25 G needle *in vitro* i.e. when injected into buffer or expelled into an empty vial. However, needle clogging was encountered on a number of occasions during the *in vivo* investigations. This may have been as a result of 'coring' of tissue within the needle bore, or due to changes in fluid dynamics as reported by Dickinson et al. (2003). For the purposes of this study, the needle was withdrawn and replaced with a new needle and the injection recommenced when clogging occurred. Had time been less of a constraint, optimisation of the formulation in terms of suspending agents, microsphere size and morphology could have helped to circumvent this issue. Development of injection systems for the injection of viscous solutions and particulate formulations is underway (Imprint Pharmaceuticals Ltd. 2006).

Weight normalised plasma concentration-time data are shown in Tables 5.17 and 5.18, and represented graphically in Figures 5.16 and 5.17. For alprenolol HIP loaded microspheres (10 mg free base equivalent), the geometric mean peak plasma concentration (C_{max}) of 115.4 ± 31.3 ng/mL occurred 2 hr post dose compared with 242 ± 61.1 ng/mL at 60 min after a subcutaneous injection of 1 mg of the non-depot aqueous solution. With metoprolol microspheres, the mean C_{max} of 32 ± 18 ng/mL occurred more rapidly (0 - 30 min post administration). This compares with the C_{max} of 21 ± 4 ng/mL achieved 15 min following the subcutaneous injection of 1 mg of the non-depot formulation. The initial burst from the microspheres, defined here as the percentage of drug released in the first 24 hours, compared with the total amount released over the 10

day study period, was $34 \pm 7\%$ and $53 \pm 13\%$ from alprenolol and metoprolol loaded microspheres respectively. This burst effect is a phenomenon common to PLGA microsphere formulations, and is attributed to the release of surface associated drug from the polymeric microspheres (Ravivarapu et al. 2000a). Provided the C_{max} is non-toxic, and the remaining payload is sufficient to achieve therapeutic plasma levels over the desired time-period, the burst effect is not necessarily problematic. The initial burst was followed by low level but sustained drug release over the next seven days, with plasma drug concentrations maintained within the ranges of 0.5 - 16 ng/mL and 0.0 - 1.5 ng/mL for alprenolol and metoprolol respectively. In fact, the rise in plasma concentration at day 10 indicates the possible start of the polymer degradation phase and resultant increased release rate of entrapped drug. Extending the study would have given more information on this phase of the absorption profile. The alprenolol and metoprolol HIP loaded microspheres tracked the classic triphasic profile often associated with PLGA microspheres (Okada and Toguchi 1995).

Wagner-Nelson deconvolution was used to calculate the fraction of drug absorbed with time (see Tables 5.19 and 5.20) and represented graphically in Figure 5.18. Approximate absorption rates were calculated from the slope of this curve over three time intervals (0 - 8 h, 8 h - 7 days and 7 - 10 days), and are reported in Table 5.21. The statistical significance and a discussion of these observations are given in Section 5.4.2.5 in context with the assessment of the *in situ*-forming depot formulations.

Table 5.17 : Weight normalised alprenolol plasma concentrations following subcutaneous dosing of microspheres.

Rat weight (g)	230		222		257		218		240	
Rat No.	A1		A2		A3		A4		A5	
Approx. time (min)	Time (min)	Conc. (ng/mL)	Time (min)	Conc. (ng/mL)	Time (min)	Conc. (ng/mL)	Time (min)	Conc. (ng/mL)	Time (min)	Conc. (ng/mL)
0	0	0.000	0	0.000	0	0.000	0	0.000	0	0.000
30	30	96.407	30	157.798	40	176.384	31	78.551	31.5	75.779
120	128	116.214	119	104.704	125	99.862	124	97.472	121.5	172.656
240	243	42.232	240	43.548	248	28.593	244.5	37.898	247.5	44.850
480	484	11.978	474	11.970	486	10.165	476	10.660	508	20.144
1440	1459	3.165	1452	3.937	1437	2.498	1428	7.295	1449	9.219
2880	3005	1.065	2999	1.509	2965	1.158	2960	1.521	2910	5.601
4320	4298	1.762	4290	2.139	4325	3.496	4323	1.085	4260	4.017
5760	5772	0.820	5781	0.640	5763	1.229	5753	5.249	6090	6.705
7200	7241	0.476	7257	1.852	7240	0.916	7225	1.347	7219	11.712
8640	8661	1.995	8681	1.658	8745	16.474	8703	2.146	8642	13.796
10080	10098	7.666	10143	2.751	10120	3.257	10151	3.430	10084	11.285
14400	14408	21.758	14398	32.284	14360	2.258	14351	4.163	12965	17.556

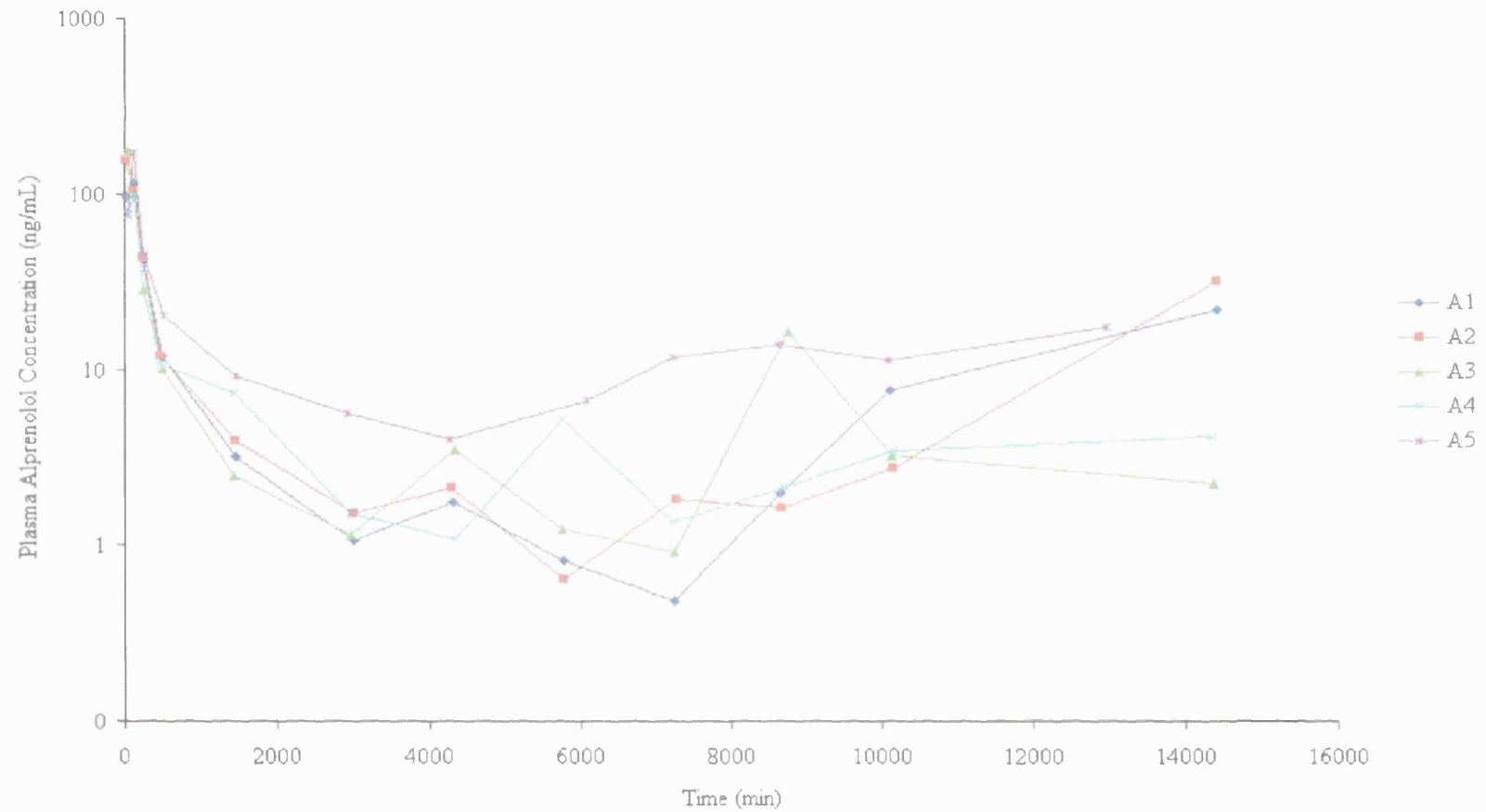


Figure 5.16 : Weight normalised alprenolol plasma concentration vs time curves following subcutaneous dosing of microspheres (containing approximately 10 mg alprenolol, free base equivalent).

Table 5.18: Weight normalised metoprolol plasma concentrations following subcutaneous dosing of microspheres.

Rat weight (g)	200		250		217		265		205	
Rat no.	M1		M2		M3		M4		M5	
Approx. time (min)	Time (min)	Conc. (ng/mL)	Time (min)	Conc. (ng/mL)	Time (min)	Conc. (ng/mL)	Time (min)	Conc. (ng/mL)	Time (min)	Conc. (ng/mL)
0	0	0.010	0	0.010	0	0.010	0	0.010	0	0.010
30	37	9.832	37	49.147	30	28.702	31.5	43.375	35	54.851
120	121	8.619	124	12.031	125	7.695	131	13.777	133	8.398
240	250	1.079	247	1.380	248	0.718	257	0.504	259	0.731
480	490	0.145	490	0.381	493	0.072	487	0.791	486	1.050
1440	1455	0.634	1450	1.085	1468	0.138	1441	0.171	1441	0.228
2880	2933	0.082	2930	0.167	2943	0.435	2915	1.460	2912	0.049
4320	4353	0.010	4348	0.089	4373	0.010	4355	0.036	4361	0.107
5760	5791	0.010	5792	0.402	5821	0.041	5797	0.267	5836	0.010
7200	7475	0.048	7411	0.082	7475	0.010	7452	0.090	7456	0.010
8640	8683	0.351	8688	0.278	8688	0.943	8652	0.157	8656	0.102
10080	10128	0.166	10124	0.077	10134	0.172	10100	0.206	10108	0.102
14400	14715	0.065	14710	0.322	14751	0.632	14712	1.549	14707	0.605

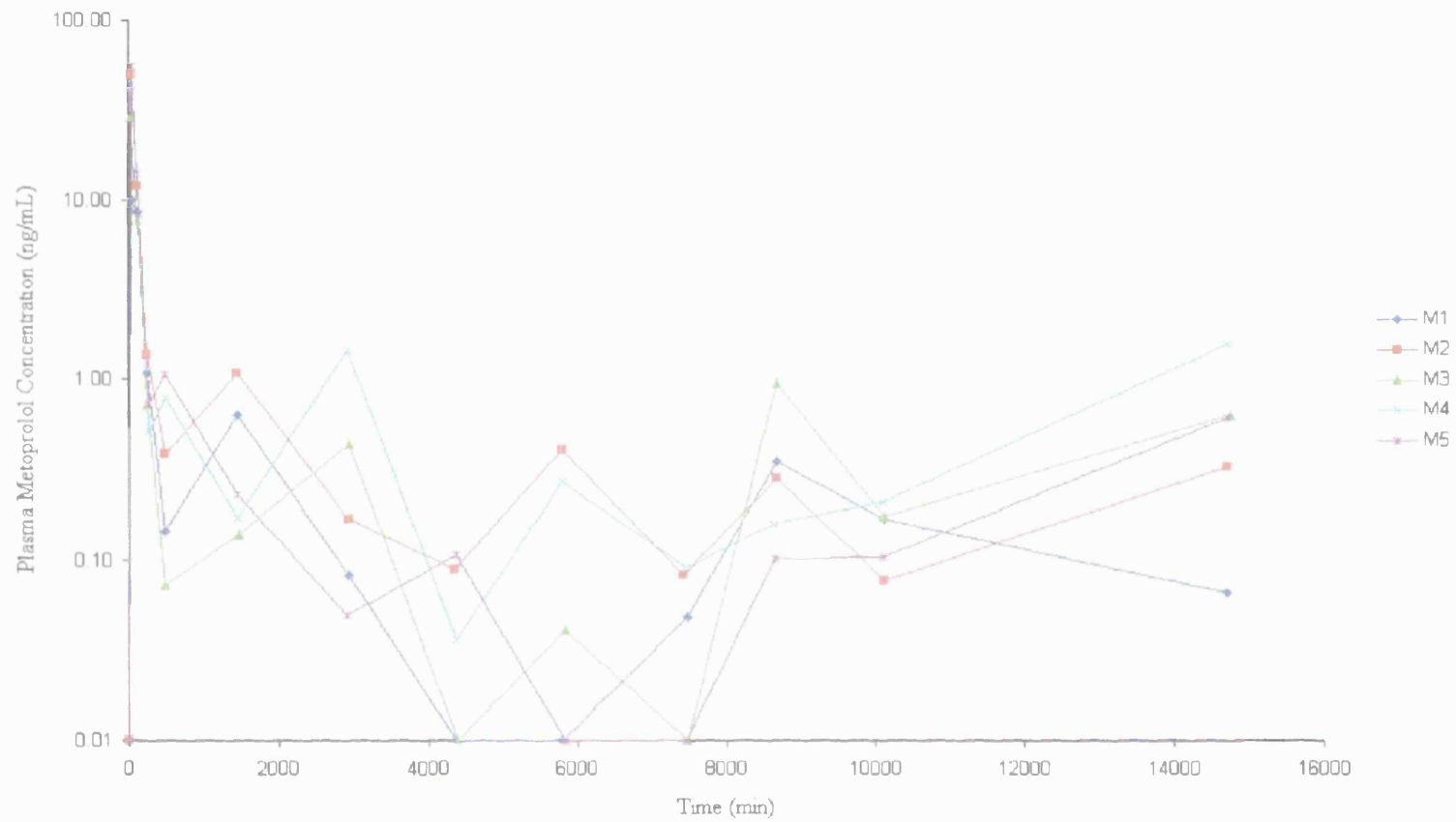


Figure 5.17 : Weight normalised metoprolol plasma concentration-time curves following subcutaneous dosing of microspheres (containing approximately 10 mg metoprolol, free base equivalent).

Table 5.19: Wagner-Nelson deconvolution of alprenolol microsphere data.

A1		A2		A3		A4		A5		Geometric mean time (min)	Geometric Mean <i>F</i>	SD
Time (min)	Fraction absorbed (<i>F</i>)	Time (min)	Fraction absorbed (<i>F</i>)	Time (min)	Fraction absorbed (<i>F</i>)	Time (min)	Fraction absorbed (<i>F</i>)	Time (min)	Fraction absorbed (<i>F</i>)			
0	0.000	0	0.000	0	0.000	0	0.000	0	0.000	0.0	0.000	0.000
30	0.017	30	0.027	40	0.031	31	0.014	31.5	0.013	32.3	0.019	0.008
128	0.034	119	0.035	125	0.036	124	0.027	121.5	0.043	123.5	0.035	0.005
243	0.035	240	0.038	248	0.036	244.5	0.029	247.5	0.042	244.6	0.036	0.005
484	0.039	474	0.042	486	0.039	476	0.033	508	0.050	485.5	0.040	0.006
1459	0.048	1452	0.051	1437	0.046	1428	0.044	1449	0.067	1445.0	0.051	0.009
3005	0.052	2999	0.056	2965	0.050	2960	0.052	2910	0.081	2967.6	0.057	0.013
4298	0.054	4290	0.060	4325	0.054	4323	0.055	4260	0.089	4299.1	0.061	0.015
5772	0.057	5781	0.062	5763	0.059	5753	0.061	6090	0.103	5830.4	0.067	0.020
7241	0.058	7257	0.065	7240	0.061	7225	0.067	7219	0.118	7236.4	0.071	0.025
8661	0.061	8681	0.068	8745	0.081	8703	0.071	8642	0.143	8686.4	0.081	0.033
10098	0.071	10143	0.073	10120	0.097	10151	0.077	10084	0.167	10119.2	0.091	0.041
14408	0.159	14398	0.178	14360	0.113	14351	0.098	12965	0.224	14084.5	0.148	0.051

Table 5.20: Wagner-Nelson deconvolution of metoprolol microsphere data.

M1		M2		M3		M4		M5		Geometric mean time (min)	Geometric Mean <i>F</i>	SD
Time (min)	Fraction absorbed (<i>F</i>)	Time (min)	Fraction absorbed (<i>F</i>)	Time (min)	Fraction absorbed (<i>F</i>)	Time (min)	Fraction absorbed (<i>F</i>)	Time (min)	Fraction absorbed (<i>F</i>)			
0	0.000	0	0.000	0	0.000	0	0.000	0	0.000	0.0	0.000	0.000
37	0.006	37	0.031	30	0.017	31.5	0.026	35	0.034	34.0	0.019	0.011
121	0.014	124	0.044	125	0.027	131	0.044	133	0.048	126.7	0.032	0.014
250	0.018	247	0.048	248	0.029	257	0.048	259	0.051	252.2	0.036	0.015
490	0.019	490	0.050	493	0.030	487	0.050	486	0.053	489.7	0.035	0.015
1455	0.023	1450	0.058	1468	0.031	1441	0.055	1441	0.059	1451.0	0.042	0.017
2933	0.029	2930	0.068	2943	0.036	2915	0.068	2912	0.061	2929.5	0.045	0.019
4353	0.029	4348	0.070	4373	0.039	4355	0.079	4361	0.062	4358.0	0.052	0.021
5791	0.029	5792	0.074	5821	0.039	5797	0.082	5836	0.063	5807.4	0.054	0.022
7475	0.030	7411	0.078	7475	0.040	7452	0.085	7456	0.063	7454.2	0.049	0.024
8683	0.032	8688	0.080	8688	0.046	8652	0.086	8656	0.064	8673.4	0.058	0.023
10128	0.036	10124	0.083	10134	0.055	10100	0.089	10108	0.066	10118.8	0.063	0.021
14715	0.042	14710	0.093	14751	0.075	14712	0.134	14707	0.083	14720.7	0.070	0.033

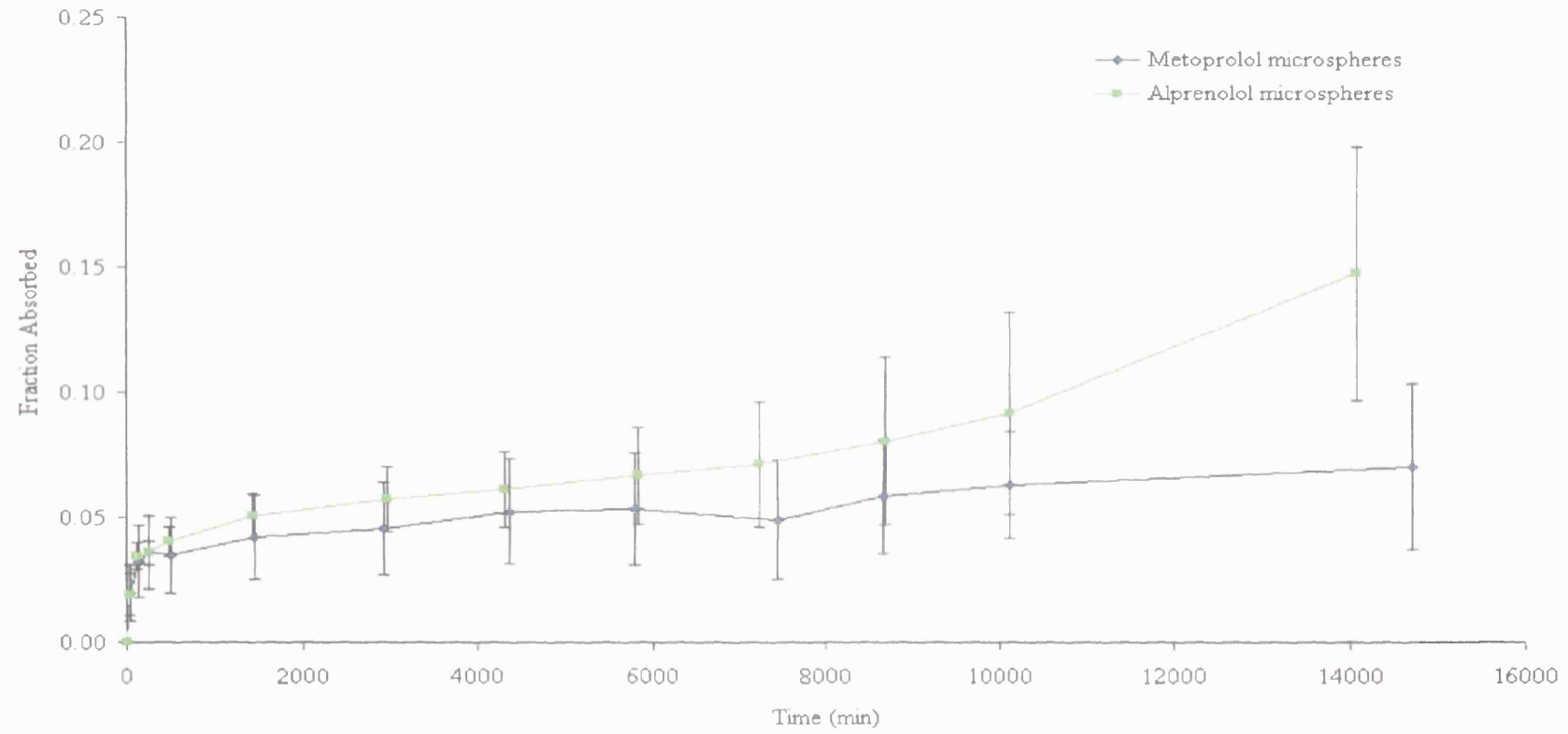


Figure 5.18: Absorption profiles of metoprolol and alprenolol from subcutaneously injected HIP loaded microspheres, generated using the Wagner-Nelson method of deconvolution.

Table 5.21: Absorption rate constants over three time intervals of alprenolol and metoprolol HIPs from subcutaneously injected microspheres.

Time interval	Absorption rate ($\text{min}^{-1} \times 10^{-6}$)				
	A1	A2	A3	A4	A5
0 - 8 h	80.6	88.1	80.5	69.3	98.0
8 h - 7 days	3.3	3.2	6.0	4.5	12.2
7 - 10 days	20.4	24.7	3.7	5.2	19.8
	M1	M2	M3	M4	M5
0 - 8 h	38.4	102.2	61.0	102.5	108.7
8 h - 7 days	1.8	3.4	2.6	4.1	1.3
7 - 10 days	1.3	2.2	4.4	9.6	3.9

5.4.2.4 *In Situ*-Forming Depots

Weight normalised plasma concentration data obtained following the subcutaneous administration of alprenolol and metoprolol HIPs (10 mg free base equivalent) are shown in Tables 5.22 and 5.23, and illustrated graphically in Figures 5.19 and 5.20. The plasma concentration-time curves reveal an initial burst followed by low level but sustained drug release over the duration of the study.

Mean alprenolol levels in plasma peaked at 368 ± 38 ng/mL within 2 hours following administration while the peak metoprolol level was 41 ± 30 ng/mL 30 min post dose. The initial burst release from these formulations (calculated as the fraction absorbed in

the first 24 hours as a percentage of the fraction absorbed over the 10 day study period) was $41.2 \pm 12.1\%$ and $59.9 \pm 19.1\%$ for alprenolol and metoprolol respectively. Upon injection, the organic solvent (NMP) dissipates and the polymer precipitates entrapping the drug within the depot, from where it is released by a combination of diffusion and matrix degradation. However, the rapid dissipation of NMP results in some drug release by solvent drag and leads to the observed initial burst (Ravivarapu et al. 2000a). Following the initial burst, drug levels declined gradually, but remained in the range of 0 - 48 ng/mL and 0 - 7 ng/mL for alprenolol and metoprolol respectively, for the duration of the study. The fraction of drug absorbed with respect to time, calculated using Wagner-Nelson deconvolution, is reported in Tables 5.24 and 5.25 and illustrated in Figure 5.21. Absorption rate constants were calculated as previously described and are reported in Table 5.26. The statistical significance of these data is discussed in the following section (Section 5.4.2.5).

Table 5.22: Weight normalised alprenolol plasma concentrations following subcutaneous dosing of *in situ*-forming depots.

Rat weight (g)	228		230		242		226		235	
Rat no.	A1		A2		A3		A4		A5	
Approx. time (min)	Time (min)	Conc. (ng/mL)	Time (min)	Conc. (ng/mL)	Time (min)	Conc. (ng/mL)	Time (min)	Conc. (ng/mL)	Time (min)	Conc. (ng/mL)
0	0	0.010	0	0.010	0	0.010	0	0.010	0	0.010
30	30	182.810	40	569.848	35	341.781	29	276.064	33	325.456
120	178	400.268	126	399.326	125	319.943	118	336.595	135	390.899
240	264	215.706	236	202.796	227	189.418	243	90.888	246	168.439
480	486	100.329	*		480	34.527	477	22.205	479	56.167
1440	1431	55.043	1444	28.677	1487	20.737	1477	26.088	1465	9.410
2880	2904	28.525	2885	21.447	2885	8.474	2880	9.327	2885	2.851
4320	4322	14.221	4325	3.060	4320	47.618	4321	27.901	4326	1.469
5760	5763	6.165	5775	2.169	5765	22.865	5761	4.353	5791	2.477
7200	7220	4.739	7209	9.486	7200	1.251	7193	3.692	7242	4.690
8640	8678	0.762	8629	4.477	8621	3.386	8609	0.491	8659	0.893
10080	10097	3.598	10075	6.545	10079	2.313	10076	0.010	10712	0.010
14400	14568	1.237	14464	1.531	14454	0.041	14445	0.010	14402	5.062

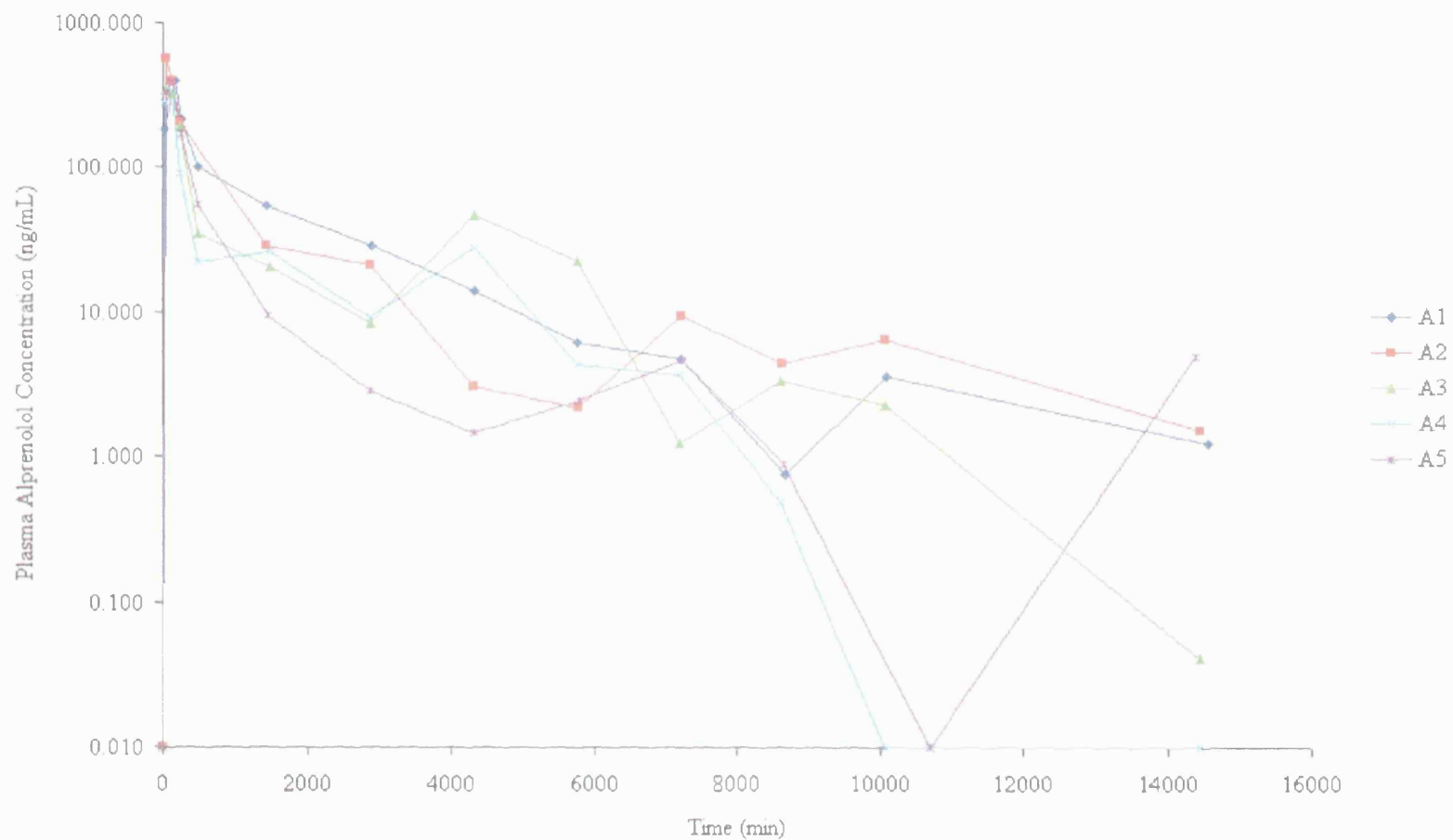


Figure 5.19: Weight normalised alprenolol plasma concentration vs time curves following subcutaneous dosing of *in situ*-forming depots (containing approximately 10 mg alprenolol, free base equivalent).

Table 5.23: Weight normalised metoprolol plasma concentrations following subcutaneous dosing of *in situ*-forming depots.

Rat weight (g)	224		223		228		234		214	
Rat no.	M1		M2		M3		M4		M5	
Approx. time (Min)	Time (min)	Conc. (ng/mL)	Time (min)	Conc. (ng/mL)	Time (min)	Conc. (ng/mL)	Time (min)	Conc. (ng/mL)	Time (min)	Conc. (ng/mL)
0	0	0.010	0	0.010	0	0.010	0	0.010	0	0.010
30	28	89.958	37	18.257	34	24.636	42	43.809	37	67.479
120	138	44.253	138	50.840	130	35.651	129	33.410	124	36.558
240	261	13.625	257	26.728	250	11.468	240	16.677	240	106.966
480	482	2.628	480	3.968	476	1.415	482	3.471	473	7.506
1440	1473	1.401	1469	0.776	1470	0.406	1437	1.875	1437	1.192
2880	2886	0.862	2886	0.375	2883	0.167	2892	0.448	2890	0.405
4320	4327	0.162	4325	0.042	4322	0.042	4334	0.818	4332	1.154
5760	5795	2.440	5795	0.435	5812	0.307	5783	1.568	5776	0.856
7200	7254	1.352	7251	0.165	7303	0.059	7237	2.102	7222	0.267
8640	8743	0.036	8694	0.279	7303	0.010	8651	0.070	8644	0.409
10080	10712	0.010	10706	6.967	8693	0.010	10661	1.020	10653	2.016
14400	14403	0.021	14402	0.704	14403	0.120	14398	0.553	14394	0.275

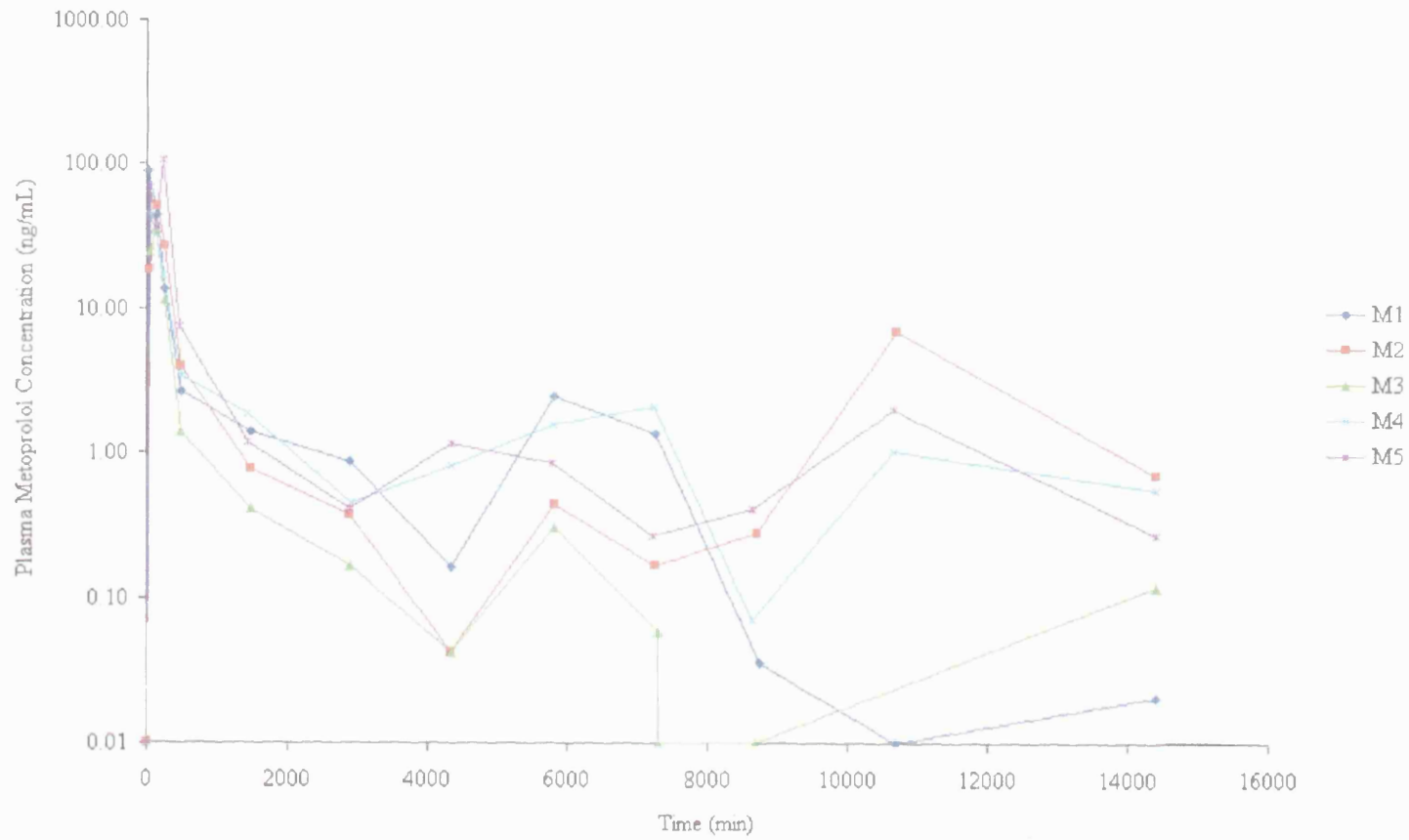


Figure 5.20: Weight normalised metoprolol plasma concentration vs time curves following subcutaneous dosing of *in situ*-forming depots (containing approximately 10 mg metoprolol, free base equivalent).

Table 5.24: Wagner-Nelson deconvolution of alprenolol *in situ*-forming depot data.

A1		A2		A3		A4		A5		Geometric mean time (min)	Geometric mean <i>F</i>	SD
Time (min)	Fraction absorbed (<i>F</i>)	Time (min)	Fraction absorbed (<i>F</i>)	Time (min)	Fraction absorbed (<i>F</i>)	Time (min)	Fraction absorbed (<i>F</i>)	Time (min)	Fraction absorbed (<i>F</i>)			
0	0.000	0	0.000	0	0.000	0	0.000	0	0.000	0.0	0.000	0.000
30	0.031	40	0.101	35	0.060	29	0.047	33	0.056	33.2	0.055	0.026
178	0.123	126	0.132	125	0.097	118	0.093	135	0.116	134.9	0.111	0.017
264	0.131	236	0.147	227	0.112	243	0.092	246	0.124	242.9	0.120	0.021
486	0.161			480	0.127	477	0.100	479	0.143	481.7	0.143	0.026
1431	0.253	1444	0.310	1487	0.163	1477	0.133	1465	0.179	1460.7	0.198	0.072
2904	0.332	2885	0.358	2885	0.188	2880	0.164	2885	0.190	2889.7	0.255	0.091
4322	0.371	4325	0.379	4320	0.249	4321	0.203	4326	0.194	4322.8	0.268	0.090
5763	0.390	5775	0.384	5765	0.314	5761	0.231	5791	0.198	5771.0	0.293	0.087
7220	0.400	7209	0.396	7200	0.334	7193	0.239	7242	0.205	7217.7	0.323	0.090
8678	0.405	8629	0.409	8621	0.339	8609	0.242	8659	0.210	8639.2	0.310	0.092
10097	0.410	10075	0.420	10079	0.344	10076	0.243	10712	0.211	10204.8	0.314	0.095
14568	0.424	14464	0.443	14454	0.351	14445	0.243	14402	0.225	14471.9	0.325	0.101

Table 5.25: Wagner-Nelson deconvolution of metoprolol *in situ*-forming depot data.

M1		M2		M3		M4		M5		Geometric mean time (min)	Geometric mean <i>F</i>	SD
Time (min)	Fraction absorbed (<i>F</i>)	Time (min)	Fraction absorbed (<i>F</i>)	Time (min)	Fraction absorbed (<i>F</i>)	Time (min)	Fraction absorbed (<i>F</i>)	Time (min)	Fraction absorbed (<i>F</i>)			
0	0.00	0	0.00	0	0.00	0	0.00	0	0.00	0.0	0.000	0.000
28	0.05	37	0.01	34	0.01	42	0.03	37	0.04	35.3	0.025	0.017
138	0.11	138	0.06	130	0.05	129	0.06	124	0.08	131.7	0.070	0.024
261	0.14	257	0.10	250	0.07	240	0.08	240	0.20	249.5	0.111	0.051
482	0.15	480	0.13	476	0.08	482	0.10	473	0.30	477.7	0.149	0.086
1473	0.17	1469	0.15	1470	0.09	1437	0.13	1437	0.34	1457.1	0.162	0.097
2886	0.19	2886	0.16	2883	0.10	2892	0.15	2890	0.36	2886.2	0.181	0.098
4327	0.20	4325	0.17	4322	0.10	4334	0.16	4332	0.37	4328.0	0.180	0.102
5795	0.22	5795	0.17	5812	0.10	5783	0.18	5776	0.38	5792.2	0.192	0.106
7254	0.25	7251	0.17	7303	0.10	7237	0.21	7222	0.39	7253.3	0.206	0.107
8743	0.26	8694	0.18	7303	0.10	8651	0.22	8644	0.40	8387.5	0.212	0.109
10712	0.26	10706	0.26	8693	0.10	10661	0.24	10653	0.42	10251.5	0.234	0.114
14403	0.26	14402	0.41	14403	0.11	14398	0.27	14394	0.47	14400.0	0.271	0.142

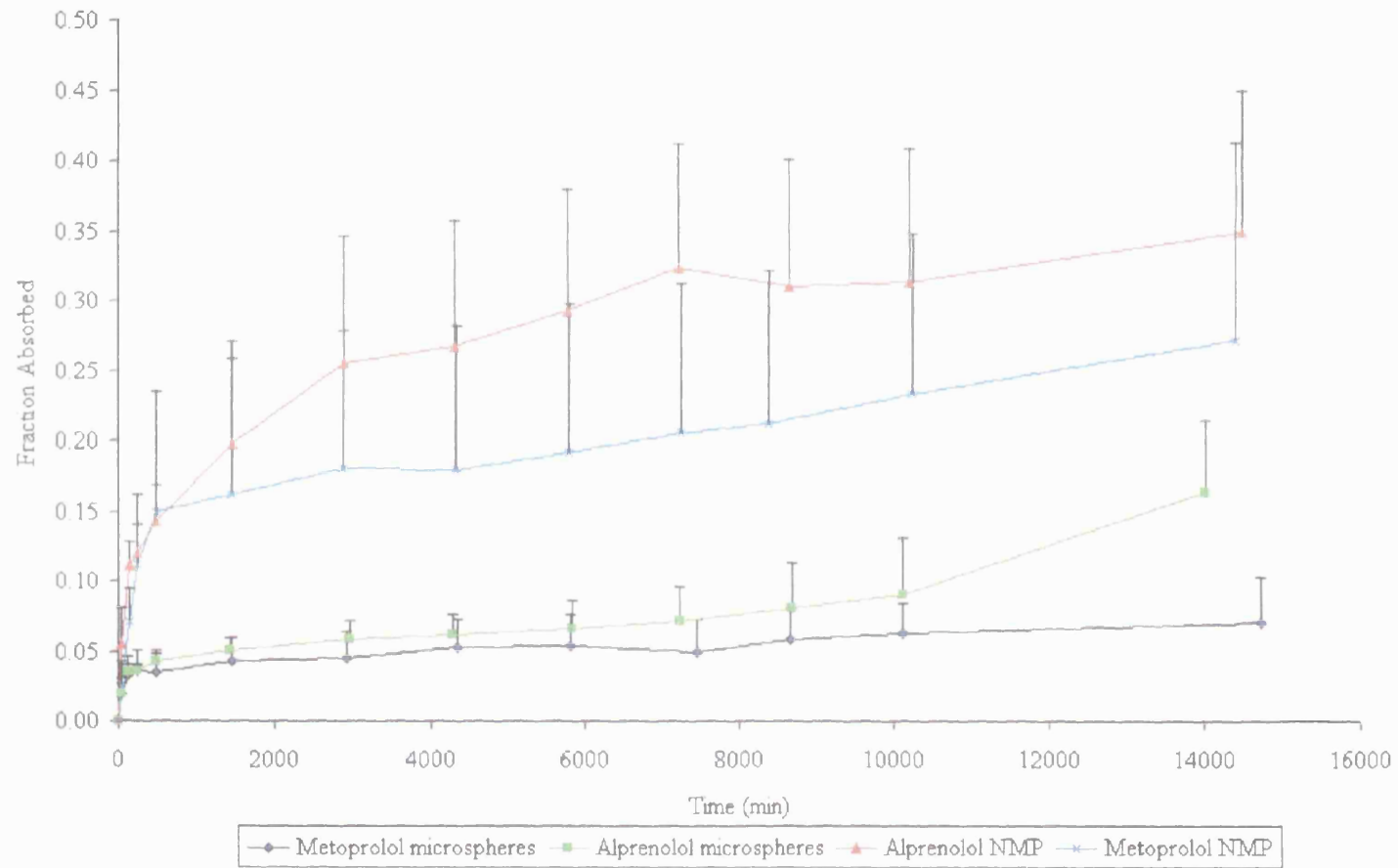


Figure 5.21: Absorption profiles generated using the Wagner-Nelson method of deconvolution.

Table 5.26: Absorption rate constants over three time intervals of alprenolol and metoprolol HIPs from subcutaneously injected *in situ*-forming depots.

Absorption rate ($\text{min}^{-1} \times 10^{-6}$)					
Time interval	A1	A2	A3	A4	A5
0 - 8 h	316.9	271.3	174.1	216.5	635.1
8 h - 7 days	10.6	12.7	2.6	12.9	12.2
7 - 10 days	0.1	40.8	0.7	8.5	12.2
M1 M2 M3 M4 M5					
0 - 8 h	330.3	623.9	264.7	209.0	297.7
8 h - 7 days	25.9	12.7	22.6	14.9	6.7
7 - 10 days	3.2	5.3	1.5	0.0	3.6

5.4.2.5 Statistical Comparisons of Drug Release from Microspheres and *In Situ*-Forming Depots

Both the microsphere and *in situ*-forming depot formulations exhibited a high initial burst release of drug within the first 24 hours following subcutaneous administration. The geometric mean % burst release from *in situ*-forming depots was higher for both alprenolol and metoprolol, although this difference did not prove significant (*t*-Test, $p > 0.05$).

Mixed between-within subjects analysis of variance (SPANOVA) was conducted to explore the impact of the nature of drug and of the formulation type on the fraction of dose absorbed over time after subcutaneous administration. There was a statistically

significant difference ($F(3,16) = 13.3, p = 0.00$) at the $p < 0.05$ level between the four groups. The effect size, calculated using eta squared, was very large (0.714). Post-hoc comparisons using the Tukey HSD test indicated that the significant differences could be found between the formulation types, but not between different drugs incorporated within them (see Table 5.27).

Table 5.27: Tukey HSD test of fraction absorbed. * significant at the 0.05 level

Formulation	Alprenolol microspheres	Metoprolol microspheres	Alprenolol <i>in Situ</i>-forming depot
Metoprolol microspheres	0.978		
Alprenolol <i>in situ</i>-forming depot	0.001*		
Metoprolol <i>in situ</i>-forming depot		0.008*	0.476

The larger error bars associated with the *in situ*-forming depot data illustrated in Figure 5.21 indicates higher variability from this formulation compared with the pre-formed microspheres. This effect has been reported in the literature, and is attributed to the irregular and variable size and shape of the depot formed following administration of the drug/polymer solution.

One way analysis of variance (ANOVA) of absorption rates calculated from the slopes of the fraction of dose absorbed versus time curves revealed significant differences. Tukey HSD post hoc comparisons were performed to identify the source of these differences (see Table 5.28).

Table 5.28: Tukey HSD post hoc comparison of mean absorption rate where Rate1 = 0 - 8h, Rate 2 = 8 h - 7 days and Rate 3 = 7 - 10 days. Values of *p* are shown and * indicates significance at the *p* < 0.05 level.

		Alprenolol microspheres			Metoprolol microspheres			Alprenolol <i>in situ</i> -forming depot		
		Rate 1	Rate 2	Rate 3	Rate 1	Rate 2	Rate 3	Rate 1	Rate 2	Rate 3
Metoprolol microspheres	Rate 1	1.00								
	Rate 2		0.726							
	Rate 3			0.359						
Alprenolol <i>in situ</i> -forming depot	Rate 1	0.019*			0.018*					
	Rate 2		0.014*			0.002*				
	Rate 3			0.251			0.994			
Metoprolol <i>in situ</i> -forming depot	Rate 1	0.033*			0.033*			0.991		
	Rate 2		0.503			0.104			0.202	
	Rate 3			0.982			0.563			0.422

No statistically significant difference was found between rates of absorption of alprenolol and metoprolol from the microsphere formulations over any of the 3 time intervals. Drug lipophilicity therefore had little impact on the absorption rate from microspheres. Equally, there were no differences between alprenolol and metoprolol absorption rates from *in situ*-forming depots. Comparisons between formulation types reveal significantly faster initial rates from *in situ*-forming depots than from microspheres for both compounds, reflecting the higher initial burst previously reported. This may be due to the fact that the drug:polymer ratio is doubled in the *in situ* formulation compared with the microspheres, thereby doubling % loading, or an inherent property of the formulation itself. The literature supports the latter explanation. A previous comparison between PLGA microspheres and *in situ*-forming depots loaded with 6% w/w leuprolide acetate also showed higher initial drug levels from the *in situ*-forming depots (Ravivarapu et al. 2000a).

From these findings I would surmise that, provided the initial burst release does not result in toxic levels, and the remaining payload is released over a suitable time course, *in situ*-forming depot systems are superior to microspheres in terms of ease of manufacture (a solution vs microspheres) and administration (no clogging). The higher variability in release is tolerable if the concentrations remain within the therapeutic range. The main concern with these delivery systems is the potential toxicity of the organic solvent used (NMP). This issue is investigated in the following section.

5.4.3 Histopathology

Within a few hours of subcutaneous injection of the polymeric dosage forms, a number of the animals were seen to persistently scratch the injections site, resulting in hair loss and scabbing (see Fig. 5.22). This reaction may have been caused by either chemical irritation caused by the formulation, or the physical presence of the foreign body beneath the skin. This was observed in both the microsphere and *in situ*-forming depot groups, for both drugs. No such reaction was observed following administration of aqueous solutions of the HIPs at the same site.



Figure 5.22: Digital photograph illustrating the superficial wound caused by scratching of the injection site (circled in red).

At the end of the study period i.e. 10 days post dose, the animals were sacrificed. The skin was cut away from the scruff to allow macroscopic evaluation of the injection site (see Figures 5.23a and b). The solid polymeric masses are clearly visible. The morphology of the depot formed varied from animal to animal, and no particular trends in size or shape were noted.

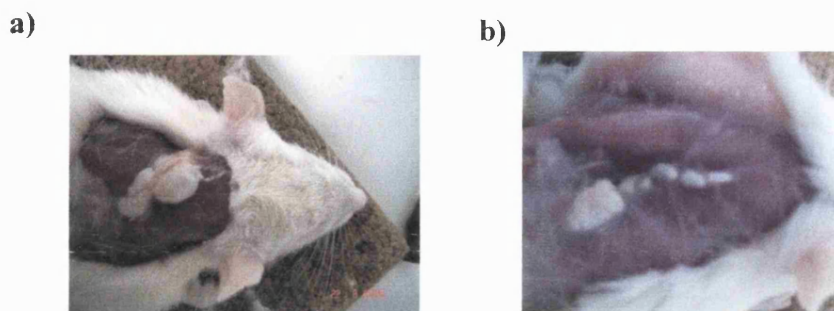


Figure 5.23: Digital photograph of the injection site with the skin removed revealing the polymeric mass of (a) microspheres and (b) *in situ*-forming depot.

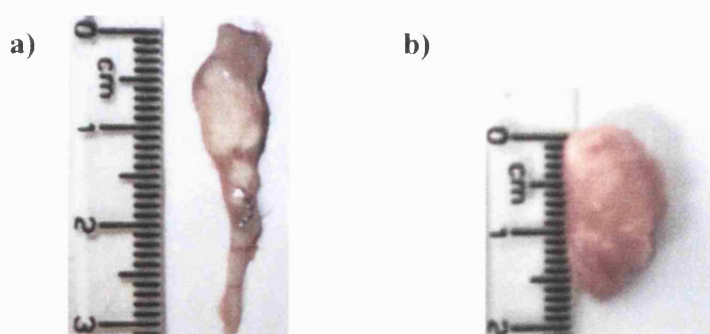


Figure 5.24: Digital photographs of the excised mass of a) *in situ*-forming depot and b) microspheres at 10 days post administration.

The polymeric masses were excised from the injection site of a selection of the animals, along with some of the surrounding tissue (Fig. 5.24). The tissues were fixed in formaldehyde, and H&E stained slides of cross sections were prepared, and examined under a light microscope (Fig. 5.25).

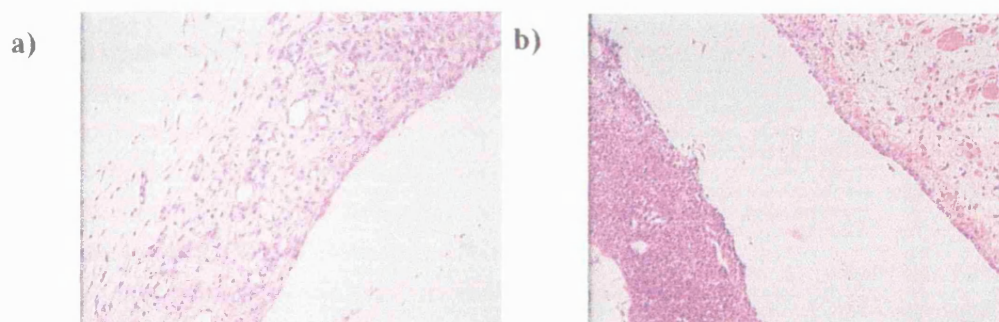


Figure 5.25: Light microscope images of H&E stained sections of a) alprenolol *in situ*-forming depot and b) alprenolol microspheres following 10 days at the injection site.

Haematoxylin is a basic dye, and stains acidic structures purple/blue. Nuclei and rough endoplasmic reticulum have a strong affinity for this dye due to the high content of DNA and RNA respectively (Wheater et al. 1993). The purple/blue elements seen lining the polymer depots in Figure 5.25 therefore represent the invading nucleated white blood cells, characteristic of the acute and chronic inflammatory responses.

The dosage forms remained at the injection site for 10 days. This is insufficient time for formation of the fibrous capsule, which takes a few weeks to develop. There is a visible accumulation of nucleated cells at the depot surface, but nothing over and above the expected inflammatory response, and no discernible difference between microspheres and *in situ*-forming depots.

5.5 Conclusions

In terms of formulation, preparation of *in situ*-forming depots is significantly simpler and less time consuming than spray dried microspheres. *In vivo* injectability of the solution was also much easier in contrast to microsphere suspensions where the presence of particulates led to needle clogging.

Both the microspheres and *in situ*-forming depots provided a low level but sustained drug release over the 10-day study period, compared to a subcutaneously injected aqueous solution of each compound, which was cleared from the circulation within a matter of hours. No significant difference was found between release rates of alprenolol and metoprolol HIP from these delivery systems, indicating that drug lipophilicity is not a particularly influential factor in the release rate of drugs from such systems. Formulation type had a much greater effect on release rate. The *in situ*-forming depot formulations exhibited a higher burst release than their microspheric counterparts, and standard deviations were larger, reflecting the variability in surface area of the depots formed. The burst may be improved by optimisation of the formulation, by adjusting loading, polymer composition and organic solvent employed. In my opinion, the ease of manufacture and ease of administration give *in situ*-forming depots significant advantages over microspheres as parenteral slow release drug delivery systems.

Chapter 6

General Discussion and Future Directions

6 General Discussion and Future Directions

Despite the disadvantages of drug administration by injection, injectable formulations are still desirable, particularly in the field of slow release drug delivery where drugs (including peptides/proteins) can be administered as long-term depots, greatly increasing patient acceptability and compliance. The focus of the work described in this thesis was investigating the effects of drug lipophilicity on release rates from subcutaneously injected slow release PLGA microspheres. Another aspect of the study was to compare the drug release characteristics from these preformed microspheres with those of a similar, but much simpler to formulate dosage form, the *in situ*-forming depot. The beta-blockers were deemed suitable model drugs for use in the study, as they had suitable physicochemical properties and adequate stability in the dissolution medium (Chapter 2). Atenolol, metoprolol and alprenolol were chosen as suitable candidates based on their experimentally determined apparent partition coefficients (P_{app}) which were -1.14, 0.04 and 1.20 respectively.

Incorporation of the beta-blockers into polymeric microspheres for sustained drug release proved challenging (Chapter 3). Burst release was very high (61.9, 76.0 and 87.5% of the encapsulated metoprolol, alprenolol and atenolol respectively were released in the first 6 minutes) and near-total release of the payload was effected within the first four hours of the *in vitro* dissolution studies. Formulation approaches to improve the release profiles included emulsion spray drying and incorporation of competing surfactants (Span 60) and stabilising agents (PVA), all of which proved futile. Alternative strategies to reduce burst release such as changing the spray drying solvent, incorporating additives such as glucose and milling (as reported by Bain et al.

1999; Wang et al. 2004; Geze et al. 1999 respectively) were not investigated due to the limited time frame available.

The beta-blockers are known to be surface active in nature, as exemplified by their membrane stabilising actions and local anaesthetic effects (Attwood and Agarwal 1979). It was hypothesised that their amphiphilic structure may have resulted in the orientation of the active at the solvent/air interface during spray drying, causing drug accumulation at the droplet surface. Subsequently, drug would be concentrated at the dried microsphere surface which would be responsible for the immediate drug release seen. Techniques to investigate the distribution of drug within the matrix of microspheres of this size would have been useful to confirm the hypothesis. Infra Red spectroscopy has been used successfully to scan microsphere cross sections (Clarke et al. 2005) but was unsuitable in this instance owing to the small size of the spray dried microspheres (volume median diameter $\sim 6 \mu\text{m}$). Attachment of a fluorescent probe to the active drug substance could allow the study of its distribution within the polymer matrix by confocal microscopy, and is a possible future direction for this investigation.

Hydrophobic ion pairing has been identified as a simple but effective strategy for reducing burst release from polymeric microspheres (Choi and Park 2000), and thus was attempted herein (Chapter 4). Hydrophobic ion pairs of alprenolol octanoate and metoprolol octanoate were successfully prepared and characterised. The differences in aqueous solubility and melting point between the parent compounds and the HIPs confirmed their formation. An ion pair of atenolol could not be made and was therefore dropped from the study. It was apparently not energetically favourable for ion pair formation between atenolol and octanoic acid to occur under these conditions.

Microspheres containing the ion pairs of alprenolol and metoprolol, of suitable size and morphology, were prepared by spray drying at a theoretical drug loading of 9.1% w/w. Significantly reduced *in vitro* burst release was observed ($15.0 \pm 1.7\%$ and $14.9 \pm 1.3\%$ released within the first hour for alprenolol and metoprolol respectively) compared with microspheres loaded with the original drug salts (Mann-Whitney U test, $p < 0.05$), and release was prolonged over 7 days. This improved dissolution profile was thought to arise from the alteration of the drug solubility in the polymer matrix and reduced surface activity of the encapsulated drugs, resulting in a more even distribution of drug throughout the microsphere particles. *In vitro* release studies were conducted and repeated measures analysis of variance revealed no significant difference between the rate and extent of release from the alprenolol HIP and metoprolol HIP loaded microspheres at the $p < 0.05$ level. This suggests that the difference in lipophilicity of the two compounds had no significant effect on release profile. However, caution must be exercised when making assumptions based on such a small sample set. The inclusion of a third compound (i.e. atenolol) would have given the findings more credence. Further work to formulate atenolol HIP loaded microspheres is therefore warranted.

Because of the complexities of microspheres as drug delivery systems and their injection, simpler *in situ*-forming depots which are easier to formulate and administer, and which have been shown to be successful slow release drug delivery systems (Dunn et al. 1990) were also formulated. The injections were prepared by dissolving the HIP and polymer in *N*-methyl-2-pyrrolidone (NMP). Upon subcutaneous injection, the solvent dissipates and the aqueous tissue fluids penetrate into the organic phase. This leads to phase separation and precipitation of the polymer and concurrent entrapment of the drug, leaving a semi-solid bolus at the injection site from which drug is gradually released.

In vivo testing of the two injectable formulations (microspheres and *in situ*-forming depots) was performed in rats (Chapter 5). Both the microspheres and *in situ*-forming depots provided a low level but sustained drug release over the 10-day study period, compared with subcutaneously injected aqueous solutions of each compound, when the drugs were cleared from the circulation within a matter of hours. The more lipophilic alprenolol HIP was absorbed at a faster rate and more extensively from the subcutaneously injected aqueous solution than metoprolol HIP. This can be explained by the more rapid partitioning of a lipophilic drug from the aqueous injection vehicle into and across the epithelial wall, and into the systemic circulation. Conversely, no significant difference was found between release rates of alprenolol and metoprolol HIP from either microspheres or *in situ*-forming depots, indicating that drug lipophilicity was not a particularly influential factor in the release rate of drugs from such systems *in vivo*.

In terms of comparison of the two formulation types, the *in situ*-forming depots exhibited a higher burst release than their microspheric counterparts. This effect has also been reported in the literature: a previous comparison between PLGA microspheres and *in situ*-forming depots loaded with 6% w/w leuprolide acetate also showed higher initial drug levels from the *in situ*-forming depots (Ravivarapu et al. 2000a). Alteration of formulation variables such as solvent and polymer content have been shown to reduce this burst effect (Kranz et al. 2001), but the latter is likely to remain problematic due to the lag period between subcutaneous injection and solidification of the depot. Standard deviations were also larger with the *in situ*-forming depots than with the microspheres, reflecting the variability in surface area of the depots formed upon solvent efflux.

While the drug release profiles are better from the pre-formed microspheres, the manufacture of *in situ*-forming depots is significantly simpler and less time consuming than spray dried microspheres. *In vivo* injectability of the solution was also much easier in contrast to microsphere suspensions where the presence of particulates led to needle clogging. The main disadvantage of these systems is the myotoxicity of the solvents used (Kranz et al. 2001), although less toxic alternatives such as benzyl alcohol and benzyl benzoate have shown promise. The local anaesthetic effects of benzyl alcohol may also attenuate the pain associated with the subcutaneous injection of an organic solvent (Packhaeuser et al. 2004), which is a further drawback of these systems.

The problems encountered with the formulation of the beta-blocker loaded microspheres with suitable slow release profiles was circumvented by the successful formulation of ion pairs of two of the model compounds. Hydrophobic ion pairing proved to be a simple and effective method for improving drug release profiles from such devices, and enabled the conduct of investigation to answer the thesis question of: How does drug lipophilicity affect drug release from subcutaneous polymeric dosage forms. The outcome was that formulation type (pre-formed microspheres vs *in situ*-forming depot) had a great influence on release rate while lipophilicity of the entrapped drug did not influence drug release. Slow release polymeric drug delivery systems have shown great potential in the field of drug delivery technology and any studies that lead to an improved understanding of the complex processes governing release rates from such devices are invaluable.

Appendix

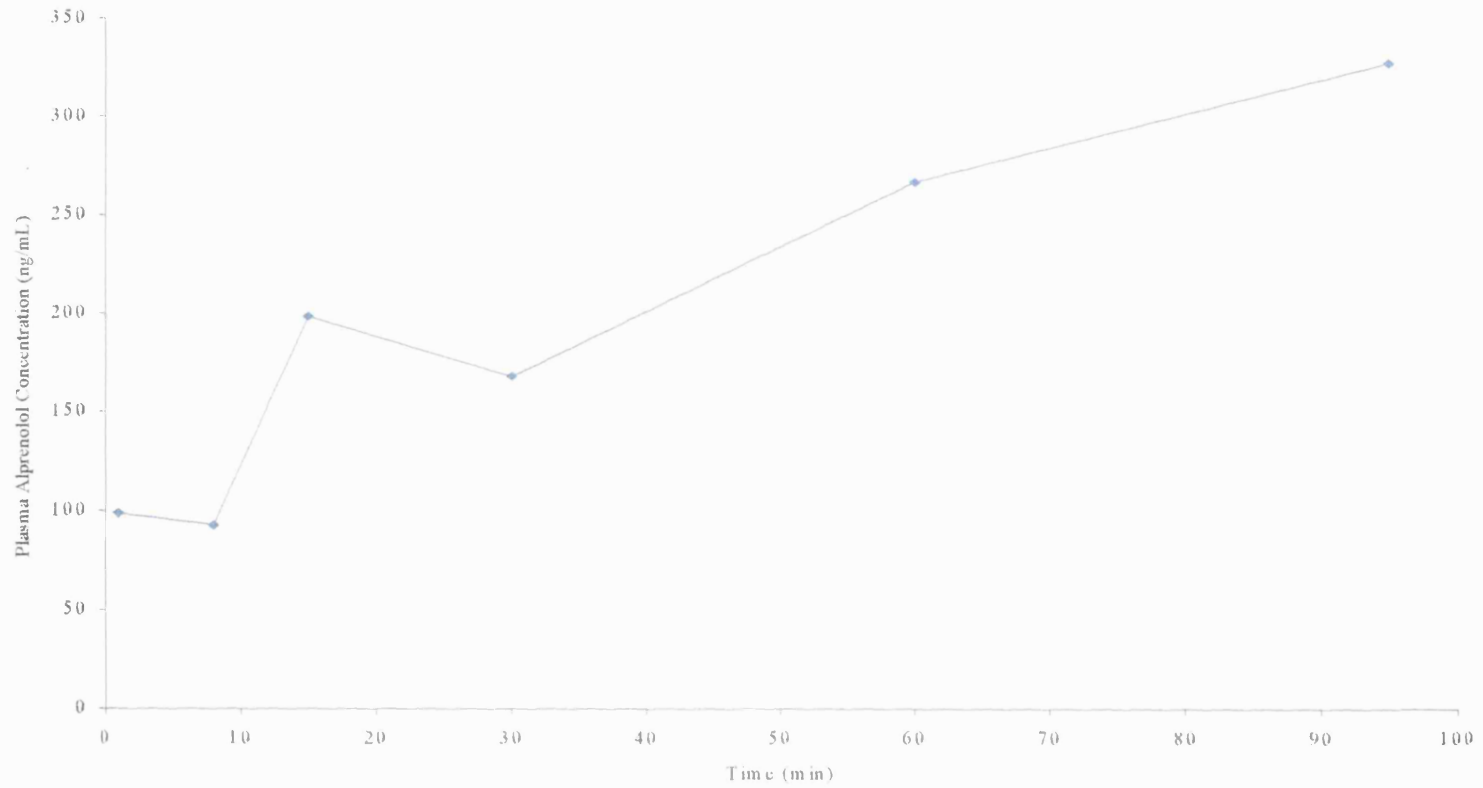


Figure A1: Plasma alprenolol concentration-time profile for rat A8, illustrating an unsuccessful IV injection i.e. inadvertent extravascular administration. Data from this animal was therefore excluded from calculations.

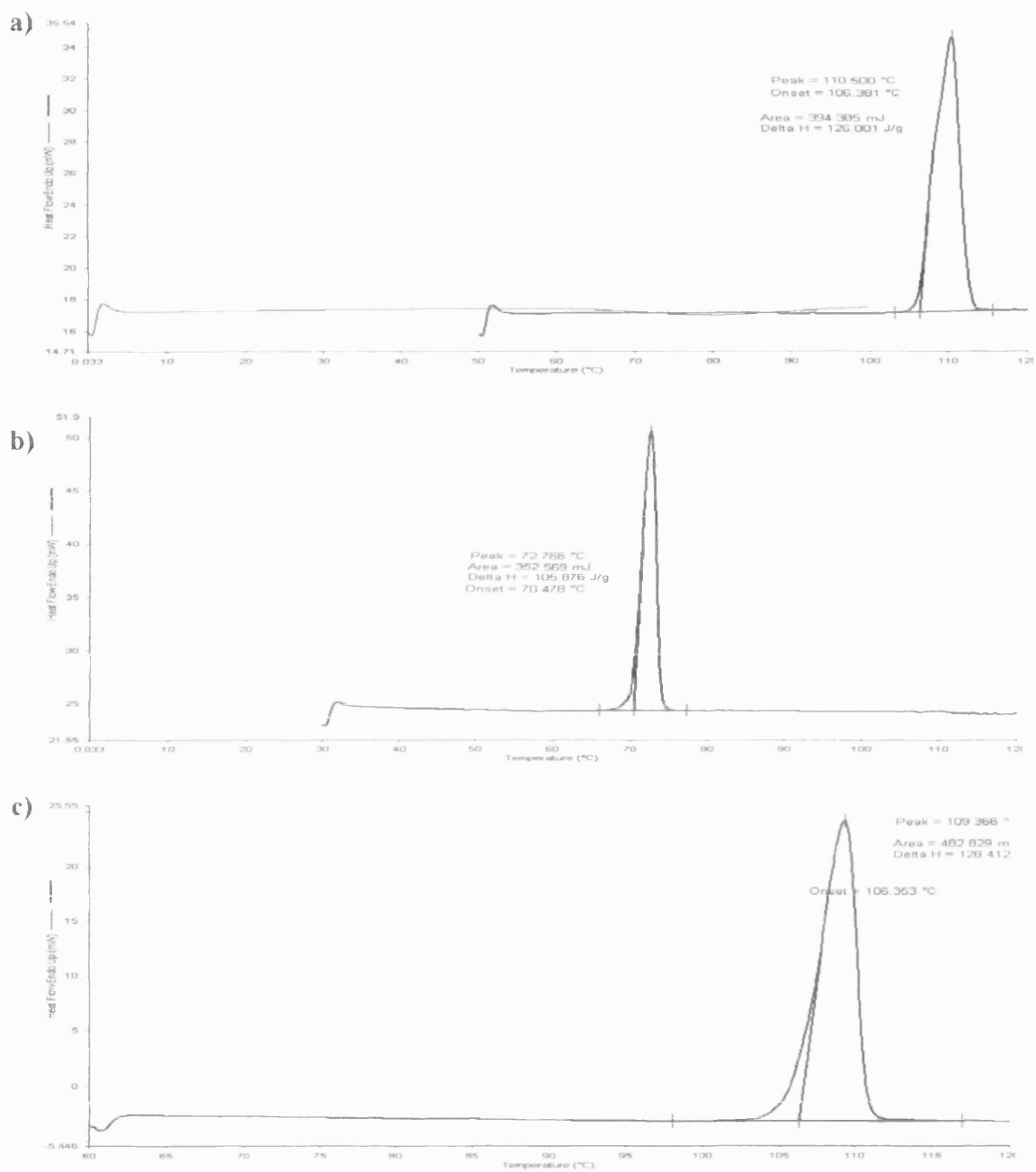


Figure A2: Representative DSC traces of a) alprenolol HCl, b) alprenolol HIP and c) freeze dried alprenolol HCl.

References

- Akers MJ. 1985. Parenteral quality control: Sterility, pyrogen, particulate and package integrity testing. New York: Marcel Dekker.
- Akers MJ. 2005. Parenteral Preparations. In: Lippincott, Williams, Wilkiss, editors. Remington: The Science and Practice of Pharmacy. Maryland:p 802-836.
- Alcock R, Blair JA, O'Mahony DJ, Raoof A, Quirk AV. 2002. Modifying the release of leuprolide from spray dried OED microparticles. *J Controlled Release* 82:429-440.
- Alkermes. 2001. Medisorb polymer products. Available from <http://www.alkermes.com/polymer/products.html>, last accessed 27-1-2003.
- Anderson JM, Shive MS. 1997. Biodegradation and Biocompatibility of PLA and PLGA microspheres. *Advanced Drug Delivery Reviews* 28:5-24.
- Athanasiou KA, Niederauer GG, Agrawal CM. 1996. Sterilization, toxicity, biocompatibility and clinical applications of polylactic acid/polyglycolic acid copolymers. *Biomaterials* 17:93-102.
- Attwood D, Agarwal SP. 1979. The surface activity and self-association of some beta-adrenoceptor blocking agents in aqueous solution. *J Pharm Pharmacol* 31:392-395.
- Avis KE, Morris BG. 1984. The dosage form and its historical development - Pharmaceutical dosage forms: Parenteral medications. New York: Marcel Dekker Inc.
- Bain DF, Munday DL, Smith A. 1999. Solvent influence on spray-dried biodegradable microspheres. *J Microencapsul* 16:453-474.
- Ballard BE. 1968. Biopharmaceutical considerations in subcutaneous and intramuscular drug administration. *J Pharm Sci* 57:357-377.
- Baras B, Benoit M, Poulain-Godefroy O, Schacht A, Capron A, Gillard J, Riveau G. 2000. Vaccine properties of antigens entrapped in microparticles produced by spray-drying technique and using various polyester polymers. *Vaccine* 18:1495-1505.
- Basci NE, Temizer A, Bozkurt A, Isimer A. 1998. Optimization of mobile phase in the separation of β -blockers by HPLC. *J Pharm Biomed Anal* 18:745-750.

Belpaire FM, De Smet F, Vynckier LJ, Vermeulen AM, Rosseel MT, Bogaert MG, Chauvelot-Moachon L. 1990. Effect of Ageing on the Pharmacokinetics of Atenolol, Metoprolol and Propranolol in the Rat. *The Journal of Pharmacology and Experimental Therapeutics* 254:116-122.

Benoit JP, Benita S, Puisieux F, Theis C. 1984. Stability and release kinetics of drugs incorporated within microspheres. In: Davis SS, Illum L, McVie JG, Tomlinson E, editors. *Microspheres and drug therapy. Pharmaceutical, immunological and medical aspects*. Amsterdam: Elsevier Science. p 91-102.

Bitz C, Doelker E. 1996. Influence of the preparation method on residual solvents in biodegradable microspheres. *Int J Pharm* 131:171-181.

Blanco-Prieto MJ, Besseghir K, Zerbe O, Andris D, Orsolini P, Heimgartner F, Merkle HP, Gander B. 2000. In vitro and in vivo evaluation of a somatostatin analogue released from PLGA microspheres. *J Controlled Release* 67:19-28.

BNF. 2006. *British National Formulary 51*. British Medical Association and Royal Pharmaceutical Society of Great Britain.

Borchard U. 1998. Pharmacological properties of beta-adrenoceptor blocking drugs. *J Clin Bas Cardiol* 1:5-9.

BP. 2003. *British Pharmacopoeia*. London: The Stationary Office.

Brandenberger, H. 2003. Development of a novel high-performance cyclone to increase the yield in a mini spray dryer. *Buchi Labortechnik AG 27*. Available from http://www.buchi-analytical.com/uploads/media/BestBuchi27_EVA_01.pdf last accessed 30-8-2006.

Braza AJ, Modamio P, Mariño EL. 2000. Two reproducible and sensitive liquid chromatographic methods to quantify atenolol and propranolol in human plasma and determination of their associated analytical error functions. *J Chromatogr* 738:225-231.

Brem H, Gabikian P. 2001. Biodegradable polymer implants to treat brain tumors. *J Controlled Release* 74:63-67.

Brodbeck KJ, Pushpala S, McHugh AJ. 1999. Sustained release of human growth hormone from PLGA solution depots. *Pharm Res* 16:1825-1829.

Buchi. 2002. Training Papers: Spray Drying. Buchi Labortechnik AG , 1-14.. Available from <http://www.buchi.com/Products.176.0.html>, last accessed 30-8-2006.

Burgess DJ, Hussain AS, Ingallinera TS, Chen M-L. 2002. Assuring Quality and Performance of Sustained and Controlled Release Parenterals: Workshop Report. AAPS Pharmsci 4:1-11.

Burgess, DJ, Crommelin, D. J. A, Hussain, A. S, and Chen M-L. 2004. Assuring Quality and Performance of Sustained and Controlled Release Parenterals: EUFEPS Workshop Report. AAPS Pharmsci 6[1], 1-13.

Chandrashekar G, Udupa N. 1996. Biodegradable injectable implant systems for long term drug delivery using poly (lactic-co-glycolic) acid copolymers. J Pharm Pharmacol 48:669-674.

Choi SH, Park TG. 2000. Hydrophobic ion pair formation between leuprolide and sodium oleate for sustained release from biodegradable polymeric microspheres. Int J Pharm 203:193-202.

Clarke BC, Dickinson PA, Pyrah IT. 2005. Case Study-In Vitro/In Vivo Release. Unpublished manuscript.

Clas S, Dalton CR, Hancock BC. 1999. Differential scanning calorimetry: applications in drug development. PSTT 2:311-320.

Clinical Pharmacokinetics: Drug Data Handbook. 1998. 3rd Ed. Adis International, Auckland.

Cruickshank JM. 1980. The clinical importance of cardioselectivity and lipophilicity in beta blockers. American Heart Journal 100:160-178.

Dang W, Daviau T, Brem H. 1996. Morphological characterization of polyanhydride biodegradable implants of gliadel during in vitro and in vivo erosion using scanning electron microscopy. Pharmaceutical Research 13:683-691.

Davies C. 1990. Chromatography of β -adrenergic blocking agents. J Chromatogr 531:131-180.

Davies B, Morris T. 1993. Physiological Parameters in Laboratory Animals and Humans. Pharmaceutical Research 10(7):1093-1097.

Dickinson PA, Pyrah IT, Deadman CM. 2003. The Physiology of Different Parenteral Routes of Administration: Preclinical Models and Implications for Product Performance. Groundbreaking Workshop on Assuring Quality and Performance of Sustained and Controlled Release Parenterals, Basel, Switzerland, February 17-18, 2003.

Diehl K-H, Hull R, Morton D, Pfister R, Rabemampianina Y, Smith D, Vidal J-M, Vorstenbosch C. 2001. A good practice guide to the administration of substances and removal of blood, including routes and volumes. *Journal of Applied Toxicology* 21:15-23.

Dunn RL. 2003. The Atrigel Drug Delivery System. In: Rathbone MJ, Hadgraft J, Roberts M, editors. *Modified-Release Drug Delivery Technology*. p 647-655.

Dunn, R. L., English, J. P., Cowsar, D. R., and Vanderbilt, D. P. Biodegradable in-situ forming implants and methods of producing the same. 252645[4938763], 1-12. 3-7-1990.

Eliaz RE, Wallach D, Kost J. 2000. Delivery of soluble tumor necrosis factor receptor from in-situ forming PLGA implants: in-vivo. *Pharm Res* 17:1546-1550.

Falk R, Randolph TW, Meyer JD, Kelly RM, Manning MC. 1997. Controlled release of ionic compounds from poly(L-lactide) microspheres produced by precipitation with a compressed antisolvent. *J Controlled Release* 44:77-85.

Florence AT, Attwood D. 2005. *Physicochemical Principles of Pharmacy*. London: Pharmaceutical Press.

Geze A, Venier-Julienne MC, Mathieu D, Filmon R, Phan-Tan-Luu R, Benoit JP. 1999. Development of 5-iodo-2'-deoxyuridine milling process to reduce initial burst release from PLGA microparticles. *Int J Pharm* 178:257-268.

Giunchedi, P, Conti, B, Scalia, S, and Conte, U. 1998. In vitro degradation study of polyester microspheres by a new HPLC method for monomer release determination. *Journal of Controlled Release* 56, 53-62.

Gulyaeva N, Zaslavsky A, Lechner P, Chlenov M, Chait A, Zaslavsky B. 2002. Relative hydrophobicity and lipophilicity of β -blockers and related compounds as measured by aqueous two-phase partitioning, octanol-buffer partitioning, and HPLC. *Eur J Pharm Sci* 17:81-93.

Hasirci V, Lewandrowski K, Gresser JD, Wise DL, Trantolo DJ. 2001. Versatility of biodegradable biopolymers: degradability and an in vivo application. *J Biotechnol* 86:135-150.

Hausberger, A. G and DeLuca, P. P. Characterization of biodegradable poly(D,L-lactide-co-glycolide) polymers and microspheres. *Journal of Pharmaceutical and Biomedical Analysis* 13[6], 747-760. 1995.

Imprint Pharmaceuticals Ltd. 2006. Particulate Injections Made Easy Using Imprint Technology. Imprint Pharmaceuticals Ltd. 1[1]. available from http://www.imprintpharma.com/build.php?tt_page=article&article=13, last accessed 30-8-2006.

ISO 13320-1. 1999. Particle size analysis - Laser diffraction methods part 1: General principles.

Jain RA, Rhodes CT, Railkar AM, Malick AW, Shah NH. 2000a. Controlled delivery of drugs from a novel injectable in situ formed biodegradable PLGA microsphere system. *J Microencapsul* 17:343-362.

Jain RA. 2000. The manufacturing techniques of various drug loaded biodegradable poly(lactide-co-glycolide) (PLGA) devices. *Biomaterials* 21:2475-2490.

Jain RA, Rhodes CT, Railkar AM, Malick AW, Shah NH. 2000b. Comparison of various injectable protein-loaded biodegradable poly(lactide-co-glycolide) (PLGA) devices: in-situ-formed implant versus in-situ-formed microspheres versus isolated microspheres. *Pharm Dev Technol* 5:201-207.

Kadir, F. 1990. Intramuscular and subcutaneous drug delivery: Encapsulation in liposomes and other methods to manipulate drug availability. Thesis, University of Utrecht.

Kim H, Burgess DJ. 2002. Effect of drug stability on the analysis of release data from controlled release microspheres. *J Microencapsul* 19:631-640.

Kim HK, Hong JH, Park MS, Kang JS, Lee MH. 2001. Determination of propranolol concentration in small volume of rat plasma by HPLC with fluorometric detection. *Biomed Chromatogr* 15:539-545.

Kranz H, Brazeau GA, Napaporn J, Martin RL, Millard W, Bodmeier R. 2001. Myotoxicity studies of injectable biodegradable in-situ forming drug delivery systems. *Int J Pharm* 212:11-18.

Lambert WJ, Peck KD. 1995. Development of an in situ forming biodegradable poly-lactide-co-glycolide system for the controlled release of proteins. *J Controlled Release* 33:189-195.

Lee, Robinson. 1978. *Sustained and Controlled Release Drug Delivery Systems*. New York: Marcel Dekker Inc.

Leo A, Hansch C, Elkins D. 1971. Partition coefficients and their uses. *Chem Rev* 71:525-553.

Luan X, Bodmeier R. 2006. In situ forming microparticle system for controlled delivery of leuprolide acetate: Influence of the formulation and processing parameters. *Eur J Pharm Sci* 27:143-149.

MacDiarmid SC. 1983. The Absorption of Drugs from Subcutaneous and Intramuscular Injection Sites. *Veterinary Bulletin* 53:9-23.

Martindale. 2004. *Martindale: The complete drug reference*. London. The Pharmaceutical Press.

Masters K. 1991. *Spray Drying Handbook*. New York: Longman Scientific and Technical.

Matschke C, Isele U, van Hoogevest P, Fahr A. 2002. Sustained-release injectables formed in situ and their potential use for veterinary products. *J Control Release* 85:1-15.

Meyer JD, Manning MC. 1998. Hydrophobic ion pairing: Altering the solubility properties of biomolecules. *Pharmaceutical Research* 15:188-193.

Meylan WM, Howard PH. 1995. Atom/fragment contribution method for estimating octanol-water partition coefficients. *J Pharm Sci* 84:83-91.

Miller-Chou BA, Koenig JL. 2003. A review of polymer dissolution. *Progress in Polymer Science* 28:1223-1270.

Mitruka BM, Rawnsley HM. 1977. *Clinical Biochemical and Hematological Reference Values in Normal Experimental Animals*. New York: Masson Publishing USA.

Modamio P, Lastra CF, Montejo O, Mariño EL. 1996. Development and validation of liquid chromatography methods for the quantitation of propranolol, metoprolol, atenolol and bisoprolol: application in solution solubility studies. *Int J Pharm* 130:137-140.

Murdan S, Florence AT. 2000. Non-aqueous solutions and suspensions as sustained-release injectable formulations. In: Senior J, Radomsky M, editors. *Sustained-release injectable products*. Denver, Colorado: Interpharm Press.p 71-107.

Nakano M, Wakiyama N, Kojima T, Juni K, Iwaoku R, Inoue S, Yoshida Y. 1984. Biodegradable microspheres for prolonged local anaesthesia. In: Davis SS, Illum L, McVie JG, Tomlinson E, editors. *Microspheres and drug therapy*. Pharmaceutical, immunological and medical aspects. Amsterdam: Elsevier Science.p 327-335.

Nebendahl K. 2000. Procedures - Routes of Administration. In: Krinke GJ, editor. *The Laboratory Rat (Handbook of Experimental Animals)*. London: Academic Press.p 463-479.

Negrin CM, Delgado A, Llabrés M, Évora C. 2001. In vivo-in vitro study of biodegradable methadone delivery systems. *Biomaterials* 22:563-570.

O'Donnell PB, McGinity JW. 1997. Preparation of microspheres by the solvent evaporation technique. *Advanced Drug Delivery Reviews* 28:25-42.

Okada H. 1997. One- and three-month release injectable microspheres of the LH-RH superagonist leuprorelin acetate. *Advanced Drug Delivery Reviews* 28:43-70.

Okada H, Inoue Y, Heya T, Ueno H, Ogawa Y, Toguchi H. 1991. Pharmacokinetics of once-a-month injectable microspheres of leuprolide acetate. *Pharmaceutical Research* 8:787-791.

Okada H, Doken Y, Ogawa Y, Toguchi H. 1994. Preparation of three-month depot injectable microspheres of leuprorelin acetate using biodegradable polymers. *Pharm Res* 11:1143-1147.

Okada H, Toguchi H. 1995. Biodegradable microspheres in drug delivery. *Crit Rev Ther Drug Carrier Syst* 12:1-99.

Packhaeuser CB, Schnieders J, Oster CG, Kissel T. 2004. In situ forming parenteral drug delivery systems: an overview. *Eur J Pharm Biopharm* 58:445-455.

Palm K, Luthman K, Ungell A, Strandlund G, Artursson P. 1996. Correlation of drug absorption with molecular surface properties. *J Pharm Sci* 85:32-39.

Panchagnula R, Thomas NS. 2000. Biopharmaceutics and pharmacokinetics in drug research. *Int J Pharm* 201:131-150.

Patel BR, Kirschbaum JJ, Poet RB. 1981. High pressure liquid chromatography of nadolol and other β -adrenergic blocking drugs. *J Pharm Sci* 70:336-338.

Pavanetto F, Conti B, Genta I, Giunchedi P. 1992. Solvent evaporation, solvent extraction and spray drying for polylactide microsphere preparation. *Int J Pharm* 84:151-159.

PC. 1979. *The Pharmaceutical Codex*. London: The Pharmaceutical Press.

Purcell WP, Bass GE, Clayton JM. 1973. Experimental Determination of Partition Coefficients. In: Purcell WP, Bass GE, Clayton JM, editors. *Strategy of Drug Design: A Guide to Biological Activity*. New York: Wiley-Interscience.p 126-143.

Radomsky M, Liu L, Iwamoto T. 2000. Synthetic polymers for nanosphere and microsphere products. In: Senior J, Radomsky M, editors. *Sustained release injectable products*. Denver: Interpharm Press.p 181-202.

Ravivarapu HB, Moyer KL, Dunn RL. 2000a. Sustained activity and release of leuprolide acetate from an in situ forming polymeric implant. *AAPS Pharmsci* 1.

Ravivarapu HB, Moyer KL, Dunn RL. 2000b. Parameters affecting the efficacy of a sustained release polymeric implant of leuprolide. *Int J Pharm* 194:181-191.

Rowland M, Tozer TN. 1995. *Clinical Pharmacokinetics: Concepts and Applications*. Pennsylvania, USA: Lippincott Williams and Wilkins.

Royals MA, Fujita SM, Yewey GL, Rodriguez J, Schultheiss PC, Dunn RL. 1999. Biocompatibility of a biodegradable in-situ forming implant system in rhesus monkeys. *Journal of Biomedical Materials Research* 45:231-239.

RxList. Goserelin. Last updated 2-8-2004. Available from http://www.rxlist.com/cgi/generic/goserel_cp.htm, last accessed 10-8-2006.

Sah H, Chien YW. 2001. Rate Control in Drug Delivery and Targeting. Fundamentals and Applications to Implantable Systems. In: Hillery AM, Lloyd AW, Swarbrick J, editors. *Drug Delivery and Targeting for Pharmacists and Pharmaceutical Scientists*. London and New York: Taylor and Francis.

Sanofi-Aventis. 2005. Eligard prescribing information. Available from http://products.sanofi-aventis.us/eligard/eligard_30.html, last accessed 30-08-2006.

Senior J, Radomsky M. 2000. Sustained Release Injectable Products. Colorado: Interpharm Press.

Sherwood L. 1996. Human Physiology: From Cells to Systems. Belmont, CA: Wadsworth.

Soltés L. 1989. High-performance liquid chromatographic determination of beta-adrenoceptor blocking agents in body fluids. *Biomed Chromatogr* 3:139-152.

Sturesson, C, Carlfors, J, Edsman, K, and Andersson, M. Preparation of biodegradable poly(lactic-co-glycolic) acid microspheres and their in vitro release of timolol maleate. *International Journal of Pharmaceutics* 89, 235-244. 1993.

Takács-Novák K, Avdeef A. 1996. Interlaboratory study of log P determination by shake flask and potentiometric methods. *J Pharm Biomed Anal* 14:1405-1413.

Tipton AJ. 2003. SAIB. In: Rathbone MJ, Hadgraft J, Roberts M, editors. *Modified Release Drug Delivery Technology*. New York: Marcel Dekker Inc. p 679-687.

Tracy MA, Ward KL, Firouzabadian L, Wang Y, Dong N, Qian R, Zhang Y. 1999. Factors affecting the degradation of poly(lactide-co-glycolide) microspheres in vivo and in vitro. *Biomaterials* 20:1057-1062.

USP. 2000. *The United States Pharmacopoeia*. Maryland.

Wang FJ, Wang C. 2002a. Sustained release of etanidazole from spray dried microspheres prepared by non-halogenated solvents. *J Controlled Release* 81:263-280.

Wang, F. J and Wang, C. H. 2002b. Effects of fabrication conditions on the characteristics of etanidazole spray-dried microspheres. *Journal of Microencapsulation* 19[4], 495-510.

Wang J, Wang BM, Schwendeman SP. 2004. Mechanistic evaluation of the glucose-induced reduction in initial burst release of octreotide acetate from poly(D,L-lactide-co-glycolide) microspheres. *Biomaterials* 25:1919-1927.

Ward-Smith, R. S, Gummery, N, and Rawle, A. F. 2002. Validation of wet and dry laser diffraction particle characterisation methods.

Weiss J, Taylor G, Zimmermann F, Nebendahl K. 2000. Procedures - Collection of Body Fluids. In: Krinke GJ, editor. The Laboratory Rat (Handbook of Experimental Animals). London: Academic Press.p 485-506.

Whateley TL. 1993. Biodegradable microspheres for controlled drug delivery. In: Karson DR, Stephenson RA, editors. Encapsulation and Controlled Release. Cambridge: Royal Society of Chemistry.

Wheater P, Burkitt G, Lancaster P. 1993. Colour Atlas of Histology. Essex: Longman.

Zuidema J, Kadir F, Titulaer HAC, Oussoren C. 1994. Release and absorption rates of intramuscularly and subcutaneously injected pharmaceuticals (II). Int J Pharm 105:189-207.

Zuidema J, Pieters FAJM, Duchateau GSMJE. 1988. Release and absorption rate aspects of intramuscularly injected pharmaceuticals. Int J Pharm 47:1-12.